Synthesis of Thiohistidines and its Metabolic Pathway Precursors

Lutete Peguy Khonde

UNIVERSITY OF CAPE TOWN

2017

Synthesis of Thiohistidines and its Metabolic Pathway Precursors

Lutete Peguy Khonde

Dissertation presented for the degree of Doctor of Philosophy

in the Department of Chemistry

University of Cape Town

Department of Chemistry, University of Cape Town

Supervisor: Dr Anwar Jardine

February 2017

Declaration

I declare that the thesis titled "**Synthesis of Thiohistidines and its Metabolic Pathway Precursors**" is my own work and has not been previously submitted for any degree or examination at this or any other university. All the relevant sources of information and support have been fully referenced and acknowledged.

Lutete Peguy Khonde

Signature…….. Date……

Acknowledgements

I would like to express my esteemed gratitude and appreciation to the following individuals for their contribution to make this thesis successful, without their support this PhD research project would not have been possible. I am forever grateful:

First and foremost, my Almighty Lord and my Shepherd God for His unconditional love and for His grace sufficient for each day that carried me through the course of this unforgettable journey. All praise, honour and glory be unto Him!

My supervisor, Dr Anwar Jardine, for his guidance, enthusiasm, patience, encouragement, support and invaluable training throughout the course of my PhD studies. Thank you for this opportunity to join his research group which It has truly been a pleasure to be a member.

My special appreciation goes to Dr Carine Sao, Dr Bienyameen Baker (Tygerberg Stellenbosch University, Cape Town, South Africa) our collaborators for valuable discussions and their assistance working with *Mycobacterium smegmatis*.

Mr Pete Roberts for recording of NMR spectra and for the training to use Bruker (400 MHz) and Varian (300 MHz) NMR spectrometers. Mr Piero Benincasa for EI-MS, Dr. Zac Mcdonald (Molecular and Cell biology, University of Cape Town, South Africa) for LCMS studies.

I would also like to gratefully acknowledge the financial support from the Sciences faculty of the University of Cape Town, Bill and Melinda Gates Foundation (Keystones Global travel award) and the UCT Postgraduate Funding Office (International Travel Grant).

My colleagues in the UCT Chemistry Department; particularly the former and current Jardine research group members, Dr James Sehata, Dr Dorothy Semenya, Shakeela Sayed, Marwaan Rylands, the Gammon research group, Dr Denis Ngumbu Muhunga, Mathew Williams and the Chibale research group for their helpful discussions while contributing to an enjoyable research environment.

Lastly but not least, I dedicate this PhD thesis to my son Lutumba Jesse Khonde (*dad loves you so much*), Nsombi Lutumba Lydie (*my lovely wife*), and my family, Tsimba Khonde Joseph (*father*), Ngoma Yezi Hortence (*mother*), Fanny, Rebecca, Josue, Rachel, Priscille (*siblings*), Precieux, Yohan, Ethan (*nephews*), Eunice, Ara, Amrel, Benel (*nieces*), Samuella Lutete (*my love*), words cannot express how much I appreciate your unconditional love and support throughout my life. I am so blessed to have you all in my life.

Abstract

Natural thiohistidines such as ergothioneine and ovothiols are biosynthesized by actinomycetes, fungi and many parasitic protozoa, respectively.

Actinomycetes such as *Mycobacterium tuberculosis* produce mycothiol and ergothioneine as their principal low molecular mass thiols. It is only very recently that the link between ergothioneine and tuberculosis disease has started to emerge, these studies suggested that ergothioneine is essential for the survival of *Mycobacterium tuberculosis*, the causal agent of tuberculosis. The biosynthesis of ergothioneine involved five enzymes encoded by the genes *egtA, egtB, egtC, egtD* and *egtE*. Because of the essentiality of these enzymes, in particular EgtD, could be considered as a potential tuberculosis drug target.

Ergothioneine is a newly discovered vitamin and is widely used in cosmetics as an antioxidant, whereas ovothiol biosynthesis has received interest for the synthetic design of potential trypanosomal drugs. However, the commercial availability of these thiohistidines is limited, mainly due to multiple challenges associated to their synthesis or isolation from natural sources.

This study describes the improved total synthesis of the super-antioxidant, ergothioneine and all its biosynthetic pathway intermediates, including deuterated versions thereof. A simple, short and high yielding novel process of the synthesis of ergothioneine was developed. Additionally, enzymatic methods were also considered for the desulfurisation step. The *C-S* lyase experiments mediated by *Mycobacterium smegmatis* cell-free lysate provided small scale transformations by the C-S lyase, EgtE, acting on its substrate, hercynylcysteine

sulfoxide. Overoxidation of the latter substrate provided a sulfone that inhibited ergothioneine biosynthesis. While hercynylcysteine sulfoxide is known to be the substrate in *Neurospora crassa*, the EgtC enzyme in mycobacteria prefer γ-glutamyl hercynylcysteinesulfoxide as its precursor to ergothioneine. Hence, the need for sufficient quantity of this important metabolite has motivated the development of the first total synthesis of EgtC enzyme substrate, γ-glutamylhercynylcysteine sulfoxide.

Finally, interesting synthetic challenges toward the synthesis of the most powerful natural related ovothiol, completes this study.

List of Abbreviations

µL	microliter
AcOH	Acetic acid glacial
aq.	Aqueous
Ar	Aromatic
Bn	Benzyl
BnBr	Benzyl bromide
Boc	*Tert-butyl* dicarbonate
br.	Broad
br. s	Broad singlet
BSH	Bacillithiol
BzCl	Benzoyl chloride
c	Concentration (g/100 mL)
cat.	Catalytic
Cs_2CO_3	Cesium carbonate
CF_3COOH	Trifluoroacetic acid
CH_2Cl_2	Dichloromethane / Methylene chloride
CH_3CN	Acetonitrile
CH_3I	Iodomethane
Conc	Concentrated
C=O	Carbonyl
°	Degree
°C	Degree Celcius
δ	Chemical shift in ppm

d	Doublet
D_2O	Deuterated water
DCM	Dichloromethane
dec	Decomposition
DIC	*N*, *N*-Diisopropyl carbodiimide
DIPEA	*N*, *N*-Diisopropylethylamine
dd	Doublet of doublet
dt	Doublet of triplet
DMSO	Dimethyl sulfoxide
DMF	Dimethyl formamide
DNA	Deoxyribonucleic acid
EDC	*N*-(3-Dimethylaminopropyl)-*N*'-ethylcarbodiimide hydrochloride
EDTA	Ethylene diamine tetracetic acid
EI^+	Electron impact (positive mode)
EIC	Extract ion chromatogram
ESH	Ergothioneine
ESI^+	Electro spray ionization (positive mode)
Et_3N	Triethylamine
Et_2O	Diethyl ether
EtOAc	Ethyl acetate
EtOH	Ethanol
eq.	Equivalent
FTIR	Fourier Transform Infrared
g	Gram(s)

GSH	Glutathione
H_2O_2	Hydrogen peroxide
HCl	Hydrochloric acid
HIV	Human immunodeficiency virus
HMBC	Heteronuclear multiple-bond correlation spectroscopy
HPLC	High pressure liquid chromatography
hr.	Hour
HRMS	High Resolution Mass Spectrometry
HOBt	*N*-Hydroxybenzotriazole
Hz	Hertz
IR	Infrared
J	Coupling constant
KSCN	Potassium thiocyanate
m	Meta
m	Multiplet
*m*CPBA	Meta-chloroperoxybenzoic acid
Mtb	*Mycobacterium tuberculosis*
MeOH	Methanol
Me_2SO_4	Dimethyl sulfate
mg	Milligram(s)
$MgSO_4$	Magnesium sulphate
$[M]^+$	Molecular ion
MHz	Mega Hertz

MIC	Minimum inhibitory concentration at which no growth is observed
min	Minute
mL	Milliliter(s)
mmol	Millimole(s)
Mp	Melting point
MS	Mass spectrum
MSH	Mycothiol
m/z	Mass to charge ratio
NBS	N-bromo succinimide
NMR	Nuclear magnetic resonance
$NaBH_4$	Sodium borohydride
$NaBH(OAc)_3$	Sodium triacetoxyborohydride
NaCl	Sodium chloride / salt / brine
NaH	Sodium hydride
NaOH	Sodium hydroxide
Na_2SO_4	Sodium sulphate
Lit	Literature
LRMS	Low Resolution Mass Spectrometry
o	Ortho
p	Para
PCTF	Phenylchlorothionoformate
PDB	Protein data bank
PG	Protecting group

Pd/C	Palladium-on-carbon
Pet Ether	Petroleum ether
Ph	Phenyl
PLP	Pyridoxal 5'-phosphate
p-TsOH	*p*-Toluenesulfonic acid
%	Percentage
RNA	Ribonucleic acid
rt	Room temperature
RT	Retention time
s	Singlet
SAH	*S*-adenosylhomocysteine
SAM	*S*-adenosylmethionine
SiO_2	Silica
S_N1	Unimolecular nucleophilic substitution
S_N2	Bimolecular nucleophilic substitution
t	Triplet
TB	Tuberculosis
TCT	2, 4, 6-Trichloro-[1, 3, 5]triazine
td	Triplet of doublets
TEA	Triethylamine
THF	Tetrahydrofuran
TIC	Total ion chromatogram
TFA	Trifluoroacetic acid
TLC	Thin layer chromatography

TSH	Trypanothione
q	Quartet
QTOF	Quadrupole Time Of Flight
UV	Ultra violet
WHO	World Health organization
w/v	Weight by volume
v/v	Volume by volume

Outputs

The work reported in this thesis has contributed to the following outputs:

Paper articles:

1. **Peguy Lutete Khonde** and Anwar Jardine**,** ***Improved synthesis of the super antioxidant, ergothioneine, and its biosynthetic pathway intermediates*****;** Org. Biomol. Chem.; **2015**, **13**, 1415 – 1419; DOI: 10.1039/c4ob02023e**.** Impact factor 3.562**.** Citations: 5

2. **Peguy Lutete Khonde** and Anwar Jardine**,** ***Biomimetic Synthesis of Ergothioneine Biosynthesis Precursor, γ-glutamylcysteinylhercynine sulfoxide*****;** Paper drafted

Patent:

1. Anwar Jardine and **Lutete Peguy Khonde;** *Process for synthesizing Ergorthioneine and related compounds***; WO 2016046618 A1**, Patent published on the 31st March **2016**.

Conference contributions:

Oral presentations:

1. Ergothioneine, the super antioxidant produced by *Mycobacterium tuberculosis*. PhD progress lecture presented at Science PhD Fellowship Symposium at University of Cape Town, South Africa, on the 13th June **2016**.

2. Ergothioneine, a lesser-known vitamin. PhD progress lecture presented at Science PhD Fellowship Symposium at University of Cape Town, South Africa, on the 22nd October **2014**.

Poster presentations:

1. L. P. Khonde and A. Jardine. "**Evaluation of EgtE as a potential anti-TB drug target"**. Poster presented at Gordon Research Seminar (GRS) and Gordon Research Conference (GRC) on Tuberculosis Drug Discovery & Development, Spain, 11 – 19th July **2015**.

2. L. P. Khonde and A. Jardine. **"S-(β-amino-β-carboxyethyl)ergothioneine sulfone inhibits the reconstituted cell-free biosynthesis of ergothioneine in *Mycobacterium smegmatis*".** Poster presented at Young Chemist's Symposium, University of Cape Town, South Africa, on the 23rd October **2014**.

3. L. P. Khonde and A. Jardine. **"S-(β-amino-β-carboxyethyl)ergothioneine sulfone inhibits the reconstituted cell-free biosynthesis of ergothioneine in *Mycobacterium smegmatis*".** Poster presented at prestigious EMBO practical course: Solution and solid-state NMR of paramagnetic molecules, Sesto Fiorentino, Italy, 13 - 19th July **2014**.

4. L. P. Khonde and A. Jardine. **"Synthesis of Mycobacterial Ergothioneine biosynthetic pathway metabolites"**. Poster presented at Keystone symposium on Novel Therapeutic Approaches to Tuberculosis, Keystone Resort, Colorado, USA, 30th March to 4th April **2014**.

Table of contents

Declaration i
Acknowledgements ii
Abstract iv
List of Abbreviations vi
Outputs xii
Table of contents xiv
List of Figures xviii
List of Schemes xxi
Chapter 1 Ergothioneine, a low molecular weight thiol of the Actinomycetes 1
1.1. Naturally occurring Low Molecular Weight (LMW) thiols 1
1.2. Ergothioneine 4
1.2.1. Ergothioneine physical properties and distribution in living organisms 4
1.2.2. Reconstitution of ergothioneine biosynthesis pathways 8
1.2.3. Enzymes of the ergothioneine biosynthesis pathway 13
1.2.4. Involvement of ergothioneine in the biosynthesis pathways of natural products 18
1.3. *Mycobacterium tuberculosis* and anti-tuberculosis drugs 21
1.3.1. Mycobacterium tuberculosis, a causative agent of tuberculosis 21
1.3.2. Global tuberculosis burden and tuberculosis drugs 23
1.3.3. Drug-resistant tuberculosis 28
1.3.4. Tuberculosis biological drug targets. 30
1.4. Redox homeostasis in mycobacteria 32
1.5. Unveiling the physiological role of ergothioneine in mycobacteria 34
1.6. Aims and objectives of this study 37
1.7. References 39
Chapter 2 Synthesis of the newly discovered vitamin, ergothioneine 47
2.1. Background 47
2.2. Ergothioneine chemical synthesis. 49

2.2.1. Synthesis of L-ergothioneine using phenylchlorothionoformate (PCTF) as the sulfur source.[4,7] 49
2.2.2. Synthesis of L-ergothioneine using potassium thiocyanate (KSCN) as the sulfur source.[5] 51
2.2.3. Biomimetic synthesis of L-ergothioneine using cysteine as the sulfur source.[8] 53
2.3. Improved synthesis of L-ergothioneine 59
2.3.1. Retrosynthetic analysis 59
2.3.2. Alternative sulfur sources to cysteine 60
2.3.3. Improved synthesis of L-ergothioneine using cysteine as the sulfur source. 72
2.4. References 89
Chapter 3 Synthesis and biotransformation of 2-cysteinylhercynine by EgtE (C-S lyase enzyme) 92
3.1. Synthesis of hercynine and its stable isotope labelled versions, hercynine-d_3 as well as ESH-d_3 92
3.1.1. Synthesis of hercynine and hercynine-d_3 93
3.2. Total synthesis of 2-cysteinylhercynine sulfoxide and 2-cysteinylhercynine sulfone 102
3.2.1. Synthesis of 2-cysteinylhercynine sulfoxide (EgtE enzyme substrate) 102
3.2.2. Synthesis of 2-cysteinylhercynine sulfone 106
3.3. In vitro reconstitution of ergothioneine biosynthesis in Mycobacterium smegmatis. 108
3.3.1. Total protein quantitation 110
3.3.2. Ergothioneine quantitation 110
3.3.3. Biotransformation of EgtE substrates to ergothioneine using crude M. smegmatis enzyme preparations. 112
3.3.4. Non-enzymatic cleavage of the C-S bond catalyzed by PLP 116
3.3.5. Mycobacterium smegmatis EgtE inhibition by 2-cysteinylhercynine sulfone 117
3.3.6. Minimum Inhibitory Concentration (MIC) of 2-cysteinylhercynine sulfone, ESH-inhibitor. 120
3.3.7. Proposed mechanism of C-S lyase of sulfide (2.19), sulfoxide (3.8) and sulfone (3.16) catalysed by PLP.[15] 121
3.3.8. Summary of major findings 127
3.4. Derivatization and detection of thiols 130
3.4.1. Rationale 130

3.4.2. Propiolic acid, a reagent for thiol detection, tagging and derivatization.....131
3.5. References.....138
Chapter 4 Synthesis of γ-glutamylcysteinylhercynine sulfoxide, the glutamine amidohydrolase enzyme (EgtC) substrate.....142
4.1 Introduction.....142
4.2. Retrosynthetic strategies of EgtC enzyme substrate.....144
4.3. Synthesis of EgtC enzyme substrate through S-alkylation of ergothioneine. (Method 1).....145
4.3.1. Retrosynthetic analysis.....145
4.3.2. Synthesis of benzyl N^5-((S)-1-(benzyloxy)-3-chloro-1-oxopropan-2-yl)-N^2-(tert-butoxycarbonyl)-L-glutaminate.....146
4.3.2. Synthesis of γ-glutamylserine (N^5-((S)-1-carboxy-2-hydroxyethyl)-L-glutamine) 152
4.4. Biomimetic synthesis of (2S)-3-(2-(((R)-2-((S)-4-amino-4-carboxybutanamido)-2-carboxyethyl)sulfinyl)-1H-imidazol-4-yl)-2-(trimethylammonio) propanoate. (Method 2).....154
4.4.1. Synthesis of O, S-dibenzyl-L-cysteinate.....155
4.4.2. Synthesis of γ-glutamylcysteine (N^5-((R)-1-carboxy-2-mercaptoethyl)-L-glutamine).....158
4.4.3. Synthesis and characterization of (S)-3-(2-(((R)-2-((S)-4-amino-4-carboxybutanamido)-2-carboxyethyl)thio)-1H-imidazol-4-yl)-2-(trimethylammonio) propanoate.....161
4.4.4. UV-vis spectroscopic study of the oxidation of γ-GluCys as a competing side reaction during sulfurization.....163
4.5. Synthesis of (2S)-3-(2-(((R)-2-((S)-4-amino-4-carboxybutanamido)-2-carboxyethyl)sulfinyl)-1H-imidazol-4-yl)-2-(trimethylammonio) propanoate. (Method 3).....168
4.5.1. Synthesis of (2S)-3-(2-(((R)-2-((S)-4-amino-4-carboxybutanamido)-2-carboxyethyl)sulfinyl)-1H-imidazol-4-yl)-2-(trimethylammonio)propanoate.....169
4.6. Conclusion.....177
4.7. References.....180
Chapter 5 Advances toward the synthesis of ovothiols.....183
5.1. Introduction.....183
5. 2. Biosynthesis of Ovothiols.....184
5.3. Ovothiol synthesis.....186

5.4. Design and synthesis of ovothiol A using L-histidine as a starting material 188
5.4.1. Retrosynthetic analysis 188
5.4.2. Regioselective methylation at N-3 position of the imidazole heterocyclic ring ..189
5.4.3. Bromination at the 5-position of the imidazole ring 206
5.4.4. Summary 209
5.5. References 211
Chapter 6 Conclusion 213
6.1. References 216
Chapter 7 Experimental section 218
7.1. Synthesis and Characterisation of Compounds 218
7.1.1. General Procedures 218
7.1.2. Synthesis and characterization of Compounds 220
7.2. Total Protein extraction and Purification from Mycobacterium smegmatis.[1] 262
7.2.1. Mc^{2}155 (M. smegmatis) growth conditions. 262
7.2.2. Total protein extraction 262
7.2.3. Total protein purification. 263
7.2.4. Protein calibration curve 263
7.3. HPLC –ESI/MS (QTOF) analysis. 263
7.4. In vitro reconstituted biosynthesis of ergothioneine in Mycobacterium smegmatis.[1,21] 264
7.4.1. Enzymatic reactions using M. smegmatis cell-free lysate enzyme preparation ..264
7.4.2. Non-enzymatic cleavage of the C-S bond catalysed by PLP 265
7.5. Mycobacterium smegmatis Ergothioneine enzymes inhibition by S-(β-amino-β-carboxyethyl)ergothioneine sulfone (3.16). 265
7.6. Determination of the Minimum Inhibitory Concentration (MIC) (Broth micro-dilution method)[22] 265
7.7. UV-vis spectroscopy monitoring of the oxidation of thiols in presence of NBS/DMF 266
7.7.1. Preparation of solutions 266
7.7.2. Detection of free thiols 267
7.7.3. Reduction of disulfides by DTT subsequently followed by free thiols detection. 267
7.8. References 268

List of Figures

Figure 1.1. Chemical structures of Low Molecular Weight Thiols (LMW). 2
Figure 1.2. Chemical structures of Low Molecular Weight Thiols (LMW) (Thio-histidine-based thiol) 3
Figure 1.3. Tautomeric forms of ergothioneine 5
Figure 1.4. ESH uptake chain 7
Figure 1.5. Proposed ergothioneine biosynthesis sequence by Askari *et al*.[26] 10
Figure 1.6. Structure of S-(β-amino-β-carboxyethyl)ergothioneine sulfoxide 11
Figure 1.7. ESH biosynthesis pathway structures in *Mycobacterium smegmatis* (EgtA- EgtE enzyme catalysis) and ESH biosynthesis pathway in the Fungal *N. crassa* (Egt1) 12
Figure 1.8. Structure of ergothioneine and selenoneine. 12
Figure 1.9. Crystal structure of methyltransferase EgtD (PDB 4PIM) isolated from Mycobacterium smegmatis. 14
Figure 1.10. Crystal structure of sulfoxide synthetase EgtB (PDB 4X8B) isolated from *Mycobacterium thermoresistible*. 15
Figure 1.11. Apo enzyme crystal structure of EgtC (PDB 4ZFL).[37] 17
Figure 1.12. Superposition of EgtC apo form (in red), EgtC in complex with glutamate/glutamine (in light blue) and $EgtC_{C2A}$ in complex with γ-glutamyl cysteine hercynine sulfoxide (in green).[37] 17
Figure 1.13. The ESH (blue) and MSH (red) programmed biosynthetic pathway of lincomycin A. The recycling of ESH and the regeneration of MSH are shown as dashed lines. (Figure adapted from Zhao et al.[47]) 19
Figure 1.14. Spithioneines A and B, two new bohemamine-type pyrrolizidine alkaloids possessing an ergothioneine moiety isolated from a marine-derived streptomyces spinoverrucosus.[48] 20
Figure 1.15. Structure of Gastrolatathioneine isolated from ‘‘tian ma’’ (the Gastrodia elata rhizomes).[49] 20
Figure 1.16. Simplified depiction of phases of *Mycobacterium tuberculosis* infection 23
Figure 1.17. Estimated tuberculosis incidence top-10 countries in 2014.[52] 24
Figure 1.18. Estimated tuberculosis rates, 2014.[52] 25
Figure 1.19. Estimated HIV prevalence and relapse TB cases, 2014.[52] 26
Figure 1.20. Chemical structure of first line TB drugs. 27
Figure 1.21. Chemical structure of some second line TB drugs. 27
Figure 1.22. Chemical structure of some third line TB drugs. 28
Figure 1.23. Pipeline of new tuberculosis drugs. MDR-TB: multidrug-resistant tuberculosis OBR-optimised background regimen; DS-TB: drug-susceptible tuberculosis; LTBI: latent tuberculosis infection.[58] 30
Figure 2.1. Ergothioneine-related publications over the last 55 years. Graph exported from www.scifinder.cas.org.[1] (accessed on 02/12/2016) 47
Figure 2.2. *L*-(+)-ergothioneine chemical structure highlighting chemical synthetic challenges. 49

Figure 2.3. Bamberger-type cleavage: an AN-RORC process (addition of nucleophile, ring opening, ring closure).[7] 50
Figure 2.4. Retrosynthesis strategy of *L*-ergothioneine 2.10. 60
Figure 2.5. ^{1}H NMR spectrum of 2.38 vs 2.39 showing successful deacetylation. 63
Figure 2.6. ^{1}H NMR spectrum confirming the oxidation of (2-nitrophenyl)methanethiol 2.39 to the disulfide 2.41. 65
Figure 2.7. ^{1}H NMR spectrum in D_2O at 300 MHz (aromatic region from 9.1 to 6.4 ppm) comparison between 2.30 & 2.10 obtained after sulfurization using thioacetic acid as the sulfur source. 68
Figure 2.8. Reaction yield based upon ^{1}H NMR integration of the isolated L-ergothioneine 2.10 (aromatic region from 9.4 to 6.5 ppm) from the reaction using thioacetic acid as a sulfur source. 69
Figure 2.9. HRMS spectrum of the desulfurized product, hercynine. Retention time of 9.62 min. 69
Figure 2.10. Model explaining the presence of the desulfurized product, hercynine. 70
Figure 2.11. EI^{+} mass spectrum of purified L-ergothioneine 2.10. 71
Figure 2.12. ^{1}H NMR spectrum of N^{c}-benzyl-N^{α},N^{α}-dimethyl-*L*-histidine 2.29 in D_2O at 300 MHz. 74
Figure 2.13. Structures of ring-bromohistidine/histamine. 77
Figure 2.14. Proposed mechanism of the formation of 2-cysteinylhercynine thioether 2.19 NBS-mediated using N-benzyl hercynine 2.30 as substrate. 80
Figure 2.15. ^{1}H NMR spectrum of 2-cysteinylhercynine 2.19 in D_2O at 400 MHz. 82
Figure 2.16. ESI/QTOF mass spectra of 2-cysteinylhercynine thioether 2.19 in positive ion mode 83
Figure 2.17. Non-enzymatic production of ESH catalysed by PLP. 84
Figure 2.18. Portion of ^{1}H NMR spectrum in D_20 at 300 MHz (7.9-6.0 ppm) of PLP, 2-cysteinylhercynine thioether 2.19 and ESH 2.10. 86
Figure 3.1. ^{1}H NMR of N^{α},N^{α}-dimethyl-*L*-histidine 3.2 at 300 MHz. 96
Figure 3.2. ^{13}C NMR of N^{α},N^{α}-dimethyl-*L*-histidine 3.2 at 101 MHz. 97
Figure 3.3. Top. Theoretical HRMS isotopic pattern calculated for $C_9H_{13}D_3N_3O_2^{+}$ $[M]^{+}$. Bottom. Experimental ESI/QTOF mass spectra of hercynine-d_3 3.4 in positive ion mode. 99
Figure 3.4. Top. Theoretical HRMS isotopic pattern calculated for $C_9H_{13}D_3N_3O_2S^{+}$ $[M]^{+}$. Bottom. Experimental ESI/QTOF mass spectra of ergothioneine-d_3 (3.7) in positive ion mode. 102
Figure 3.5. Top. Theoretical HRMS isotopic pattern calculated for $C_{12}H_{22}N_4O_5S^{+}$ 334.1311 $[MH]^{+}$. Bottom. Experimental ESI/QTOF mass spectra of 2-cysteinylhercynine sulfoxide 3.8 in positive ion mode. 106
Figure 3.6. Top. Theoretical HRMS isotopic pattern calculated for $C_{12}H_{21}N_4O_6S^{+}$ $[M]^{+}$. Bottom. Experimental ESI/QTOF mass spectra of 2-cysteinylhercynine sulfone 3.16 in positive ion mode. 108
Figure 3.7. Simplified flow chart of the biotransformation mediated by EgtE crude enzyme preparations. 109
Figure 3.8. Overlaid TIC of ergothioneine (Top 25 ng mL^{-1}, bottom 12.5 ng mL^{-1} concentrations). Retention time of 1.5 min. (Positive ionization mode) (ESI^{+}) and column (Eclipse + C18 RRHD 1.8 µm.2.1 X 50, Agilent 1290 infinity, Germany) 111

Figure 3.9. ESI/QTOF mass spectra of ESH standard in positive ion mode. 111
Figure 3.10. Calibration curve of ESH. 112
Figure 3.11. LCMS spectrum of ESH-d_3 (3.7) *in vitro* reconstititued experiment using hercynine-d_3 (3.4) as substrate.....114
Figure 3.12. In vitro reconstitution of ESH;.....115
Figure 3.13. TIC extracted for ESH in-vitro reconstititued experiment using substrate: (a) 2-cysteinylhercynine thioether (2.19) as substrate, (b) 2-cysteinylhercynine sulfoxide (3.8) as substrate. 116
Figure 3.14. Non enzymatic production of ESH catalysed by PLP. TIC extracted for ESH and PLP using 2-cysteinylhercynine thioether (2.19), 2-cysteinylhercynine sulfoxide (3.8) and 2-cysteinylhercynine sulfone (3.16).....117
Figure 3.15. LCMS spectrum of *M. smegmatis*. ESH enzymes inhibition. (a) TIC extracted for ESH in enzymatic reaction using sulfoxide (3.8) as a substrate. (b) TIC extracted for ESH in the enzymatic reaction using sulfoxide (3.8) and sulfone (3.16) as an inhibitor. 118
Figure 3.16. LCMS spectrum of M. smegmatis. ESH enzymes inhibition. (a) TIC extracted for ESH in enzymatic reaction using sulfide (2.19) as a substrate (b) TIC extracted for ESH in the enzymatic reaction using sulfide (2.19) and sulfone (3.16) as an inhibitor.....118
Figure 3.17. Ergothioneine biosynthesis inhibition studies contain;.....119
Figure 3.18. Broth dilution method. 120
Figure 3.19. β-Elimination of the sulfide (2.19).[15] 123
Figure 3.20. β-Elimination of the sulfoxide (3.8).[15].....124
Figure 3.21. Sulfenic acid 3.18 conversion to ESH. 125
Figure 3.22. Proposed model explaining EgtE reaction using sulfoxide (3.8) as a substrate. (Adapted from song *et al*.[12]) 126
Figure 3.23. Stabilisation of the sulfone (3.16).....127
Figure 3.24. UV-vis spectrum monitoring the formation of thioacrylate formed from the reaction between L-cysteine 2.20 and propiolic acid 3.23 (at 25°C).....132
Figure 3.25. ^{1}H NMR spectrum of crude reaction of cysteine (2.20) and propiolic acid (3.23) in D_2O at 300 MHz from 8.4 to 5.6 ppm.....133
Figure 3.26. UV-vis spectrum of the reaction of propiolic acid 3.23 with *N*-acetyl cysteine (at 25°C).....134
Figure 3.27. UV-vis spectrum of the reaction of propiolic acid 3.23 with thiophenol (at 25°C). 135
Figure 3.28. UV-vis spectrum of the reaction of propiolic acid (3.23) with L-ESH (2.10) produced *in situ* during the PLP-mediated C-S lysis of 2-cysteinylhercynine (2.19) (at 25°C). 137
Figure 4.1. EgtC substrate retrosynthetic strategies. 144
Figure 4.2. Biomimetic retrosynthetic strategy of EgtC enzyme substrate.....155
Figure 4.3. ^{1}H NMR spectrum of *O,S*-dibenzyl-L-cysteinate 4.23 in $CDCl_3$ at 300 MHz. 157
Figure 4.4. ^{13}C NMR spectrum of *O,S*-dibenzyl-L-cysteinate 4.23 in $CDCl_3$ at 101 MHz. 158
Figure 4.5. ^{13}C NMR spectrum of γ-glutamylcysteine (4.18) in DMSO-d_6 at 101 MHz.....160
Figure 4.6. UV-vis spectroscopy monitoring of the oxidation of γ-GluCys 4.18 (1 mM) in presence of NBS/DMF (at 25°C).....166
Figure 4.7. UV-vis spectroscopy monitoring of the oxidation of cysteine (1 mM) in a presence of NBS/DMF (at 25°C). 167

Figure 4.8. Retrosynthetic analysis of (2S)-3-(2-(((R)-2-((S)-4-amino-4-carboxybutanamido)-2-carboxyethyl)sulfinyl)-1H-imidazol-4-yl)-2-(trimethylammonio) propanoate proceeding through amide coupling of the protected hercynylcysteine thioether 4.39 (EgtE enzyme substrate). 168
Figure 4.9. Portion of ^{1}H NMR spectrum of the sulfoxide 4.43 (between δ_H 4.7-3.8 ppm) illustrating the diastereotopicity. 173
Figure 4.10. COSY ^{1}H - ^{1}H NMR spectrum of (2S)-3-(2-(((R)-2-((S)-4-amino-4-carboxybutanamido)-2-carboxyethyl)sulfinyl)-1H-imidazol-4-yl)-2-(trimethylammonio)propanoate or γ-glutamylcysteinylhercynine sulfoxide (4.1) in D_2O. 177
Figure 5.1. Structure of ovothiols (A, B & C). 183
Figure 5.2. Previous ovothiols total synthesis routes proposed by Ohba et al.[11] (right) and Holler et al.[10] (left) Reactant a is (R)-2,5-dihydro-3,6-diethoxy-2-isopropylpyrazine, n-butyllithium. (Scheme adapted from Mirzahosseini et al.[12]) 187
Figure 5.3. Ovothiol A retrosynthetic analysis. 189
Figure 5.4. pK_a of histidine ionisable functions (left), imidazole tautomeric conformations (right). 190
Figure 5.5. ^{1}H NMR spectrum of methyl N^{α},N^{C}-dibenzyl-*L*-histidinate 5.16 in $CDCl_3$ at 400 MHz. 199
Figure 5.6. Expanded ^{1}H NMR spectrum showing successful regioselective methylation of 5.16 to yield 5.17 in $CDCl_3$ at 400 MHz. 202
Figure 5.7. ^{13}C NMR spectrum of (S)-1-benzyl-4-(2-(benzylamino)-3-methoxy-3-oxopropyl)-3-methyl-1H-imidazol-3-ium 5.17 in $CDCl_3$ at 101 MHz. 203
Figure 5.8. COSY-NMR spectrum of (S)-1-benzyl-4-(2-(benzylamino)-3-methoxy-3-oxopropyl)-3-methyl-1H-imidazol-3-ium 5.17 in $CDCl_3$. 204
Figure 5.9. A portion expanded HMBC-NMR spectrum of (S)-1-benzyl-4-(2-(benzylamino)-3-methoxy-3-oxopropyl)-3-methyl-1H-imidazol-3-ium 5.17 in $CDCl_3$. 205

List of Schemes

Scheme 1.1. Reactions catalysed by $EgtB_{wild\ type}$, $EgtB_{Y377F}$ and cysteine dioxygenase (CDO) enzymes. (Scheme adapted from Goncharenko *et al.* [42]) 16
Scheme 2.1. *L*-ergothioneine synthesis according to Yadan.[4,7] 50
Scheme 2.2. *L*-ergothioneine synthesis according to Trampota.[5] 52
Scheme 2.3. Biomimetic *L*-ergothioneine synthesis according to Erdelmeier *et al.*[6,8] 54
Scheme 2.4. Synthesis of 2-S-cysteinyl histidine 2.21 according to Ito.[10] 55
Scheme 2.5. Removal of the excess of cysteine.[8] 56
Scheme 2.6. Proposed mechanism of cysteine oxidative introduction. [8] 56
Scheme 2.7. Pyrolytic cleavage of 2-cysteinylhercynine thioether 2.19 scavenged by 3-mercaptopropionic acid 2.22. 57
Scheme 2.8. Synthesis of (2-nitrophenyl)methanethiol 2.39. 62
Scheme 2.9. Attempted synthesis of L-ergothioniene 2.10 using (2-nitrophenyl)methanethiol 2.39 as a sulfur source. 64

Scheme 2.10. *L*-ergothioneine 2.10 synthesis using thioacetic acid 2.42 as a sulfur donor. ..67
Scheme 2.11. Synthesis of (S)-3-(1-benzyl-1H-imidazol-4-yl)-2-(trimethylammonio) propanoate (N^c-benzyl hercynine 2.30).....73
Scheme 2.12. NBS/DMF mediated synthesis of 2-cysteinylhercynine thioether 2.19. 77
Scheme 2.13. Selective and mild bromination of the imidazole ring.[25,26].....79
Scheme 2.14. Enzymatic-free cleavage of C-S bond in 2-cysteinylhercynine thioether 2.19 catalysed by PLP. 85
Scheme 2.15. Improved biomimetic *L*-ergothioneine synthesis. 87
Scheme 3.1. Two steps synthesis strategy of hercynine 3.3 and hercynine-d_3 3.4. 93
Scheme 3.2. One-pot synthesis of hercynine 3.3. 94
Scheme 3.3. Synthesis of hercynine 3.3 and hercynine-d_3 3.4 via improved synthesis of N^{α},N^{α}-dimethyl histidine 3.2. 95
Scheme 3.4. Synthesis of hercynine 3.3 or hercynine-d_3 3.4. 98
Scheme 3.5. Synthesis of ESH-d_3 (3.7). 101
Scheme 3.6. Synthesis of 2-cysteinylhercynine sulfoxide 3.8. 103
Scheme 3.7. Proposed mechanism of sulfoxidation using H_2O_2 and p-TsOH acting as a proton source. 104
Scheme 3.8. Proposed mechanism of sulfoxidation proceeding through pertolylsulfonic acid 3.9 (reactive intermediate) 104
Scheme 3.9. Synthesis of 2-cysteinylhercynine sulfone 3.16. 107
Scheme 3.10. Enzymatic biotransformation of hercynine-d_3 (3.4). 114
Scheme 3.11. Synthesis of cysteinylhercynine thioether 2.19, sulfoxide 3.8 and sulfone 3.16.[15] 128
Scheme 3.12. Biotransformation and non enzymatic PLP-mediated reactions of cysteinylhercynine thioether (2.19), sulfoxide 3.8 and sulfone (3.16). 129
Scheme 3.13. Synthesis of thioacrylates 3.20 and 3.21 obtained from the reaction of propiolic acid 3.23 and *L*-cysteine 2.20 132
Scheme 3.14. In situ derivatization of L-ergothioneine (2.10) by using propiolic acid (3.23) during the enzymatic-free cleavage of 2-cysteinylhercynine thioether (2.19). 136
Scheme 4.1. Retrosynthetic strategy of EgtC substrate 4.1 involving *S*-alkykation of ergothioneine 2.10. 146
Scheme 4.2. Synthesis of benzyl N^5-((S)-1-(benzyloxy)-3-chloro-1-oxopropan-2-yl)-N^2-(*tert*-butoxycarbonyl)-*L*-glutaminate 4.13. 147
Scheme 4.3. Attempted S-alkylation of ergothioneine 2.10 by benzyl N^5-((*S*)-1-(benzyloxy)-3-chloro-1-oxopropan-2-yl)-N^2-(*tert*-butoxycarbonyl)-*L*-glutaminate 4.13. 150
Scheme 4.4. Proposed mechanism of formation of thioether 4.15 similarly to the one suggested by Ishikawa *et al.*[8] 151
Scheme 4.5. Synthesis of N^5-((*S*)-1-carboxy-2-hydroxyethyl)-*L*-glutamine 4.14. 153
Scheme 4.6. Synthesis of *O,S*-dibenzyl-*L*-cysteinate 4.23.. 156
Scheme 4.7. Synthesis of γ-glutamylcysteine 4.18. Reagents and conditions. 159
Scheme 4.8. Synthesis of (S)-3-(2-(((R)-2-((S)-4-amino-4-carboxybutanamido)-2-carboxyethyl)thio)-1H-imidazol-4-yl)-2-(trimethylammonio) propanoate 4.2. 161
Scheme 4.9. Putative mechanism of the sulfurization of the protected hercynine derivative 2.30 by γ-glutamylcysteine 4.18. 163

Scheme 4.10. Oxidation of γ-GluCys 4.18 in NBS/DMF to form its disulfide derivative 4.30 which can be reduced by DTT. 164
Scheme 4.11. Disulfide does not react with 5,5'-Dithio-bis-(2-nitrobenzoic acid) (DTNB) [Ellman's reagent] 165
Scheme 4.12. Reduction of disulfide to free thiol by DTT (1,4-Dithiothreitol, Cleland's reagent) and derivatization of free thiol compounds (RSH) by 5,5'-Dithio-bis-(2-nitrobenzoic acid) (DTNB) generating TNBA adduct detected at λ_{max} 412 – 420 nm. 165
Scheme 4.13.Total synthesis of (2*S*)-3-(2-(((*R*)-2-((*S*)-4-amino-4-carboxybutanamido)-2 carboxyethyl)sulfinyl)-1*H*-imidazol-4-yl)-2-(trimethylammonio) propanoate 4.1. 169
Scheme 4.14. Synthesis of (2*S*)-1-(benzyloxy)-3-(2-(((*R*)-3-(benzyloxy)-2-((*S*)-5-(benzyloxy)-4-((*tert*-butoxycarbonyl)amino)-5-oxopentanamido)-3-oxopropyl)sulfinyl)-1H-imidazol-4-yl)-N,N,N-trimethyl-1-oxopropan-2-aminium 4.43..... 172
Scheme 5.1. Ovothiols biosynthesis pathway. 185
Scheme 5.2. Van Den Berge *et al.*[14] *N*-methylation strategy. 190
Scheme 5.3. Steric hindrance directs N-alkylation on the imidazole ring. 191
Scheme 5.4. Synthesis of *tert*-butyl (S)-4-(3-(benzyloxy)-2-((*tert*-butoxycarbonyl)amino)-3-oxopropyl)-1H-imidazole-1-carboxylate.. 192
Scheme 5.5. Methylation of *tert*-butyl (*S*)-4-(3-(benzyloxy)-2-((*tert*-butoxycarbonyl)amino)-3-oxopropyl)-1*H*-imidazole-1-carboxylate 5.7. 195
Scheme 5.6. Methylation of *tert*-butyl (S)-4-(2-((*tert*-butoxycarbonyl)amino)-3-methoxy-3-oxopropyl)-1H-imidazole-1-carboxylate 5.12. 197
Scheme 5.7. Synthesis of methyl N^{α},N^{c}-dibenzyl-L-histidinate 5.16. 198
Scheme 5.8. Attempted N-3 regioselective methylation of methyl N^{α},N^{c}-dibenzyl-*L*-histidinate 5.16. 200
Scheme 5.9. Synthesis of (S)-1-benzyl-4-(2-(benzylamino)-3-methoxy-3-oxopropyl)-3-methyl-1H-imidazol-3-ium 5.17. 201
Scheme 5.10. Regioselective sulfurization at the 5-position of imidazole ring using thioacetic acid according to Daunay *et al.*[18] 208
Scheme 5.11. Proposed ovothiol A synthesis route. 210

Chapter 1 Ergothioneine, a low molecular weight thiol of the Actinomycetes

1.1. Naturally occurring Low Molecular Weight (LMW) thiols

Naturally occurring low molecular weight thiols are essential for the maintenance of cellular redox potential in living organisms, hence they play a key role in the survival of the species. These natural thiols preserve the protein thiol-disulfide balance and protect the cells from various toxic reactive intermediates such as reactive oxygen (ROS) and nitrogen species (RNI).[1,2]

Low molecular weight thiols including bacillithiol (BSH), mycothiol (MSH), glutathione (GSH) and trypanothione (TSH) are cysteine-based thiols. Coenzyme A (CoA) is a cysteamine-based thiol. It is noteworthy that cysteine is in fact the sulfur source in the biosynthesis of most naturally occurring thiols.[3] (Figure 1.1)

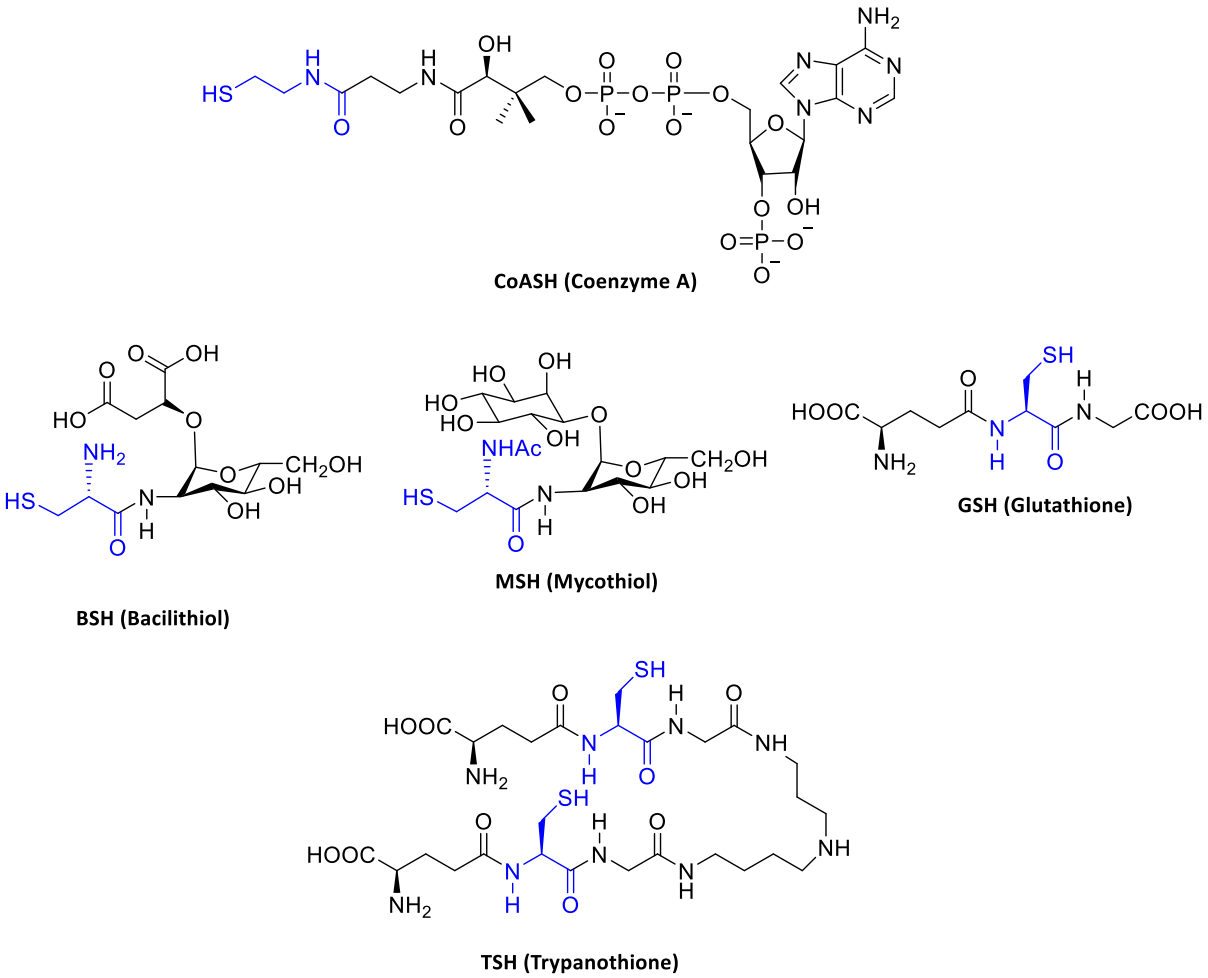

Figure 1.1. Chemical structures of Low Molecular Weight Thiols (LMW).

Glutathione is present in many organisms including humans. Almost all eukaryotes contain GSH except some species such as *Giardia duodenalis, Entamoeba histolytica, Tritrichomonas foetus* and *Trichomonas vaginalis*. In these organisms GSH has been detected in millimolar levels making it the most common thiol in the cell.[3] *Trypanosoma* and *Leishmania* produce ovothiols ($OSH_{A, B \& C}$) and trypanothione (TSH) which consist of two molecules of GSH linked together by a spermidine molecule or moiety.[3] (Figure 1.1 & Figure 1.2)

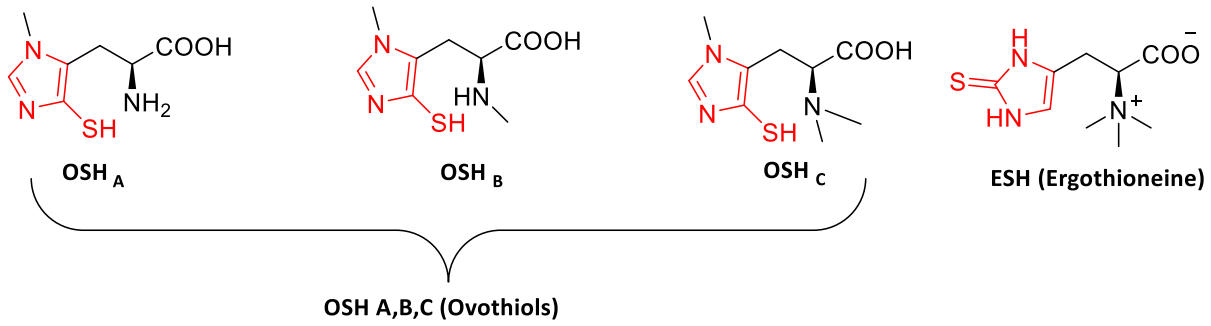

Figure 1.2. Chemical structures of Low Molecular Weight Thiols (LMW) (Thio-histidine-based thiol)

However, most Gram positive bacteria lack GSH, but rely on alternate thiols for their protection against oxidative stress. *Staphylococcus aureus*, a Gram positive bacterium does not produce GSH; instead it produce millimolar quantities of the reduced coenzyme A (CoASH), acting as their principal protective thiol.[2] Bacilithiol (BSH) is produced by several microorganisms including many *Bacillus* and *Staphylococcus* species such as *Bacillus anthracis*, *Bacillus cereus*, *Staphylococcus agalactiae*, and *Streptococcus saprophyticus*. The latter species do not produce GSH or MSH, they rely on BSH which is suggested to play an important role in the metabolic regulation process including detoxification of fosfomycin, an electrophilic xenobiotic.[4]

Mycobacteria also lack GSH, however, they produce mycothiol (MSH) and ergothioneine (thio-histidine-based thiol) as their protective thiols. (Figure 1.1 & Figure 1.2) Extensive efforts have been conducted to shed more light on their essentiality toward the survival of *Mtb*. While quite substantial studies have been conducted on mycothiol, very little is known about the role played by ergothioneine as a protective thiol in mycobacteria. The next section will be dedicated to an extensive review of this valuable low molecular weight thiol, ergothioneine.

1.2. Ergothioneine

Ergothioneine (ESH) was first isolated by a French pharmacist, Charles Tanret in 1909 from ergot (*Claviceps purpurea*), the fungal infection of rye grain.[5] Since that discovery was made numerous studies has been conducted by the scientific community to understand its physiological role as protective thiol in humans and various organisms, mostly mycobacteria.

Very recently, ESH has been advocated to be a new vitamin due to its beneficial role in human health as it acts as a very important physiological cytoprotectant.[6]

1.2.1. Ergothioneine physical properties and distribution in living organisms

Ergothioneine (ESH) is a natural thio-histidine betaine derivative (*N,N,N*-α-trimethylammonium 2-mercaptohistidine) with a thiol group attached at the C-2 position of the imidazole ring. ESH is an unique natural C2-thio-imidazole containing amino acid.[7]

1.2.1.1. Ergothioneine physical properties

In aqueous solution and in solid state, the carboxyl group of ergothioneine is deprotonated. ESH exists in two tautomeric forms as thiol or and as a thione predominantly as illustrated in the Figure 1.3. The thione form is almost exclusively present under physiological conditions (pH 7.4).[7,8]

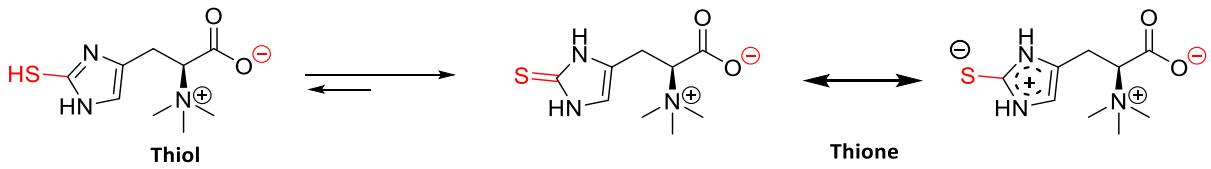

Figure 1.3. Tautomeric forms of ergothioneine.

The fact that ESH is present in solution predominantly in the thione form explains its stability, therefore ESH is not easily auto-oxidized unlike alkylmercaptans, and this characteristic differentiates ESH from other biological LMW thiols.[7]

Ergothioneine's reduction potential ($E^0 = -60$ mV) is significantly greater than glutathione ($E^0 = -0.240$ mV), thus making ESH extremely difficult to oxidize.[2,9] ESH is very stable even when aerated in aqueous solution. It has been proven that ergothioneine can be oxidized in very strong acidic solutions, but these forms (reduced/oxidized) happen to be present in solution simultaneously.[10]

Furthermore, the X-ray structure of *L*-ESH-dihydrate confirmed the thione form of ESH, it revealed an uncommon *S-C* bond length of 1.69 Å, which is a value in-between the *S-C* single and double bond lengths of 1.82 and 1.56 Å, respectively. That unusual *S-C* bond length is due to the resonance thiol-thione form (thione form predominantly).[11]

The pKa of ergothioneine was calculated according to Henderson-Hasselbalch equation from the data generated experimentally by ^{13}C NMR chemical shift values and pH profiles and it was found to be 11.5.[8]

1.2.1.2. Ergothioneine distribution in living organisms

Ergothioneine is synthesized by bacteria, specifically mycobacteria as revealed by exhaustive analyses of 101 mycobacterial strains from various sources. All these strains exhibited a high concentration of ergothioneine, about 1.4 µmol per gram on average.[12] Similar ergothioneine concentrations were detected in many strains of Actinomycetes including *Actinoplanes philippinensis, Nocardia asteroides* strains and in three classes of *Streptomycetes.*[13] Ergothioneine is synthesized by cyanobacteria; both ergothioneine (up to 0.8 mg per gram of dry mass) and its biosynthetic precursor, hercynine were detected in *Cyanobacterium phormidium*, thus supporting that cyanobacteria produces high levels of ergothioneine.[14]

Ergothioneine is synthesized by the fungus *Neurospora crassa* and higher comestible fungi like mushrooms.[15,16] Very recently, it was discovered that the fission yeast, *Schizosaccharomyces pombe* synthesize ergothioneine as well.[17]

ESH has been detected in millimolar concentrations in fungi, bacteria, plants and mammals. Plants, animals and humans do not synthesize ESH, but exclusively acquire it from their environment. Plants take up ESH from soil through their roots while animals as well as humans acquire it from their nutrition. Food such as mushrooms, red and black beans, corn, garlic, oats and meat (liver and kidney) are extremely rich in ergothioneine.[18] (Figure 1.4)

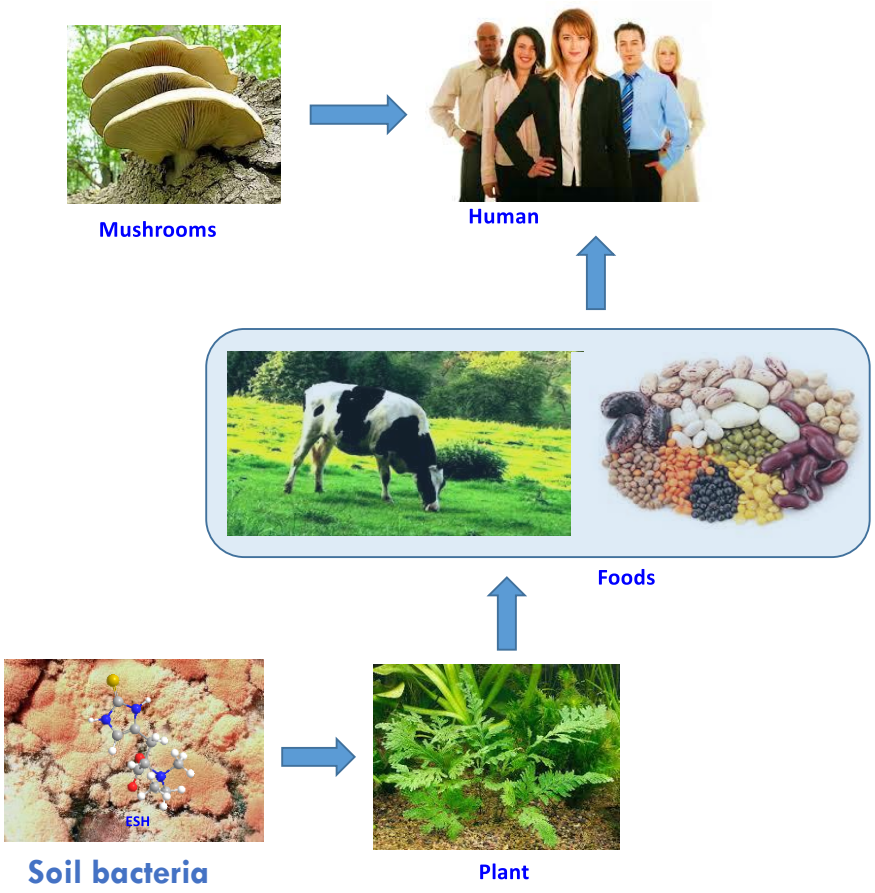

Figure 1.4. ESH uptake chain

In humans, ESH is present at millimolar level in specific cells and tissues believed to be exposed to oxidative stress including liver, kidney, heart, red bloods, semen and ocular lens tissues. ESH exists in the brain at slightly lower levels, thought to be in micromolar quantities. Studies showed that human red cells contain about 1.5-3.7 mg ESH/100 mL of blood, although the human lens contains up to 68-115 mg ESH/100g of lens.[2]

1.2.1.3. Ergothioneine specific transporter

In 2005, Gründemann *et al.* discovered the ergothioneine specific transporter, OCTN1, which is responsible for the distribution and accumulation of ergothioneine across cells.[19]

Previously, it was assumed that OCTN1 is involved in the transport of tetraethylammonium cation through the plasma membrane, though Gründemann *et al.* demonstrated that ergothioneine is in fact the key substrate transported, as ergothioneine was more than 100 times more efficiently transported than tetraethylammonium and carnitine altogether.[19] Furthermore, OCTN1 transporter was expressed in over 293 human cells lines and its efficiency of transporting ergothioneine was established to be 195 µL per min per mg of protein.[19] This discovery has motivated the scientific community to unveil ergothioneine's role.

Very recently, Frigeni *et al.* demonstrated that the OCTN1 transporter is in fact broadly tolerant to amino acid substitution whereas the OCTN2 transporter is exclusively carnitine specific.[20] These results suggested that the *SLC22A4* gene (OCTN1 encoding gene) could be derived from a duplication of *SLC22A5* (OCTN2 encoding gene), hence OCTN1 transporter physiological role might not have been well-defined as yet.[20]

1.2.2. Reconstitution of ergothioneine biosynthesis pathways

The beneficial role of ergothioneine to human health has motivated biochemists to attempt the elucidation of its biosynthesis. The elucidation of ergothioneine biosynthesis started many decades ago, around the mid-20th century.[15,21-25]

In 1957, Wildy and Heath investigated the biosynthesis of ergothioneine in *Claviceps purpurea*. Their research revealed that when growing *Claviceps purpurea* cultures on media supplemented with either radio-labelled [α-^{14}C] histidine or [2(ring-imidazole)-^{14}C] histidine, radiolabelled, ergothioneine was isolated thus suggesting that the imidazole ring and the amino acid side chain of ergothioneine is biosynthetically derived from histidine. Therefore establishing that histidine or a closely related analogue could indeed be an ergothioneine biosynthetic precursor, and not histamine or 2-thiohistidine as initially believed.[21,22]

The same year Melville *et al*. confirmed these findings by performing the study on a different organism, *Neurospora crassa*.[25] This fungus was selected for the study because of its high concentration in ergothioneine (estimated to be in millimolar level). The authors used the classical radio isotopic labelling (^{14}C and ^{35}S) method and provided strong evidence that histidine is in fact the biosynthetic precursor of ergothioneine. The introduction of a sulfhydryl group at 2-position of the imidazole ring is provided by cysteine, and at least one of the three methyl groups of ergothioneine is derived from methionine.[25]

In 1962, Askari *et al.* proposed the possible straightforward ergothioneine biosynthetic sequence in *Neurospora crassa*, which involved histidine, hercynine and thiol histidine as precursor intermediates, whereby cysteine is responsible for the introduction of sulfur at the 2-position of the imidazole ring and three methyl groups of the betaine moiety derived from methionine.[26] (Figure 1.5)

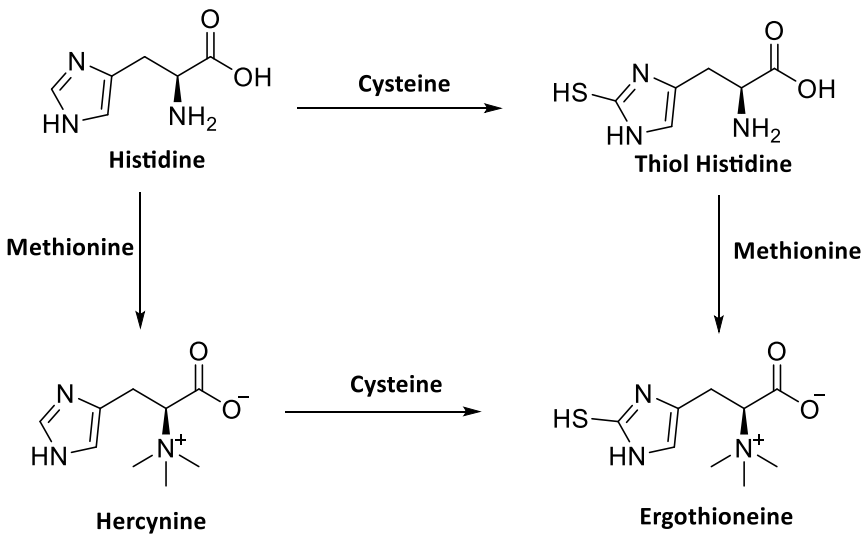

Figure 1.5. Proposed ergothioneine biosynthesis sequence by Askari *et al.*[26]

Five years after Askari's study, Genghof *et al.* confirmed that endogenous hercynine is the ESH biosynthetic precursor in *Mycobacterium smegmatis*.[15,23] They also discovered that growing *M. smegmatis* cells supplemented with low concentration of cysteine and high concentration of histidine in the culture medium, resulted in the production of 100 to 200 µg of ESH per g of dry cells after only 2.5 to 3 hr of incubation, thus supporting that cysteine is the direct source of sulfur in ESH biosynthesis in *M. smegmatis.*[23]

In 1974, Ishikawa *et al.* explored in depth the transfer of the sulfur atom from cysteine to the imidazole ring using cell-free extracts of *Neurospora crassa*. Sulfur was transferred onto histidine ring of hercynine by incubating cysteine and histidine in the presence of O_2 and Fe^{2+}. The sulfoxide intermediate, *S*-(β-amino-β-carboxyethyl)ergothioneine sulfoxide (Figure 1.6) was isolated and the latter was subsequently cleaved to ergothioneine and pyruvate by a PLP-dependent enzyme.[27] These authors attempted the chemical synthesis of the sulfoxide intermediate, without affording enough chemical structural evidence.[27]

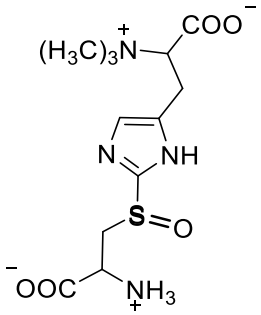

Figure 1.6. Structure of *S*-(β-amino-β-carboxyethyl)ergothioneine sulfoxide

Recently, two different ESH biosynthesis pathways have been discovered. Seebeck was the first to publish the gene cluster (*egtABCDE*) encoding for ESH biosynthesis in *Mycobacterium smegmatis*.[28] In *Mycobacterium smegmatis,* ESH is synthesized by the sequential action of five enzymes encoded by the genes *egtA, egtB, egtC, egtD* and *egtE.*[28]

The mycobacterial ESH pathway involves five steps, EgtD catalyses the *N,N,N*-α-trimethylation of histidine to form hercynine; EgtA condenses glutamate and cysteine to form γ-glutamylcysteine (γ-Glu-Cys). Subsequently, EgtB, a FGE (Formylglycine Generating Enzyme) like enzyme catalyzes the oxidative *S-C* bond coupling between hercynine and γ-Glu-Cys to form γ-glutamyl cysteinyl hercynine sulfoxide, which become hydrolysed by the catalytic action of EgtC to form hercynylcysteine sulfoxide. The last step involves the *C-S* lyase of hercynylcysteine sulfoxide to yield ergothioneine. (Figure 1.7) [28-30]

In *Mycobacterium smegmatis*, γ-glutamylcysteine is the source of sulfur whereas in the fungus *Neurospora crassa*, cysteine is the source of sulfur. *Neurospora crassa* Egt1 enzyme catalyses the direct biotransformation of hercynine to hercynylcysteine sulfoxide. (Figure 1.7)[31,32]

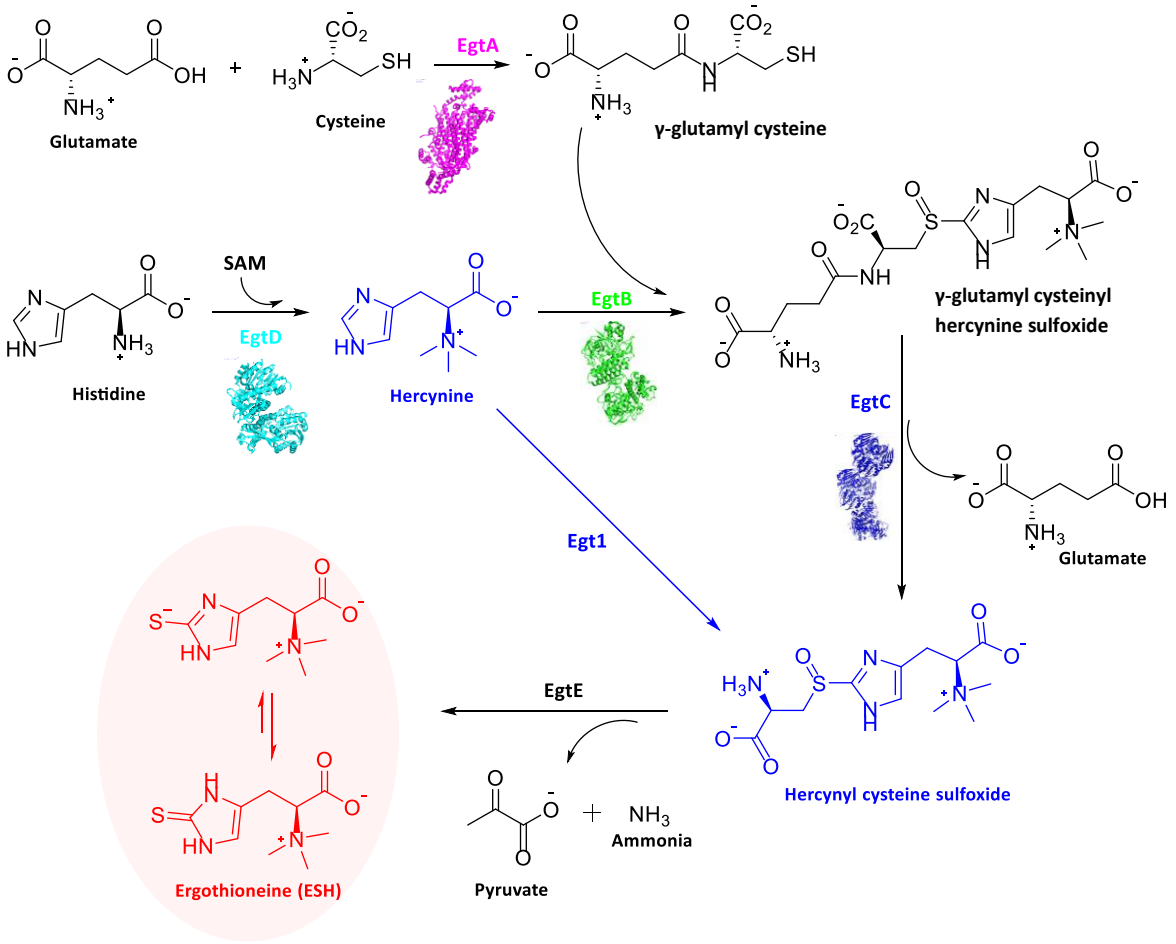

Figure 1.7. ESH biosynthesis pathway structures in *Mycobacterium smegmatis* (EgtA- EgtE enzyme catalysis) and ESH biosynthesis pathway in the Fungal *N. crassa* (Egt1)

In 2014, ergothioneine and selenoneine (a selenium-containing derivative of ergothioneine) biosynthesis was reconstituted in fission yeast, *Schizosaccharomyces pombe*, the genes encoding the pathway were also discovered. (Figure 1.8)

Figure 1.8. Structure of ergothioneine and selenoneine.

The selenoneine biosynthesis pathway in yeast is similar to the one found in *Neurospora crassa* and *Mycobacterium smegmatis*. It was furthermore demonstrated that ergothioneine pathways can produce selenoneine by simply supplementing culture medium with selenium during growth.[17]

Actinobacteria including mycobacteria prefer γ-glutamylcysteine over cysteine as sulfur source as depicted in the Figure 1.7. Studies suggested that mycobacteria avoid the "cysteine problem".[33] Cysteine is readily auto-oxidized and its terminal 1,2-aminothiol group complexes with redox active transition metals such as iron and copper, that making free cysteine less available. Consequently, mycobacteria do not use cysteine but they turn to γ-glutamylcysteine as their sufur source. γ-Glutamylcysteine possesses 1,2-amide thiol instead which is unable to complex with transition metals, therefore γ-glutamylcysteine is more available than cysteine within the cell.[34]

1.2.3. Enzymes of the ergothioneine biosynthesis pathway

All the enzymes implicated in the ESH biosynthesis have recently been recombinantly expressed and purified.[29,35-38] An overview of these enzymes will be provided.

1.2.3.1. Methyltransferase EgtD

EgtD is an *S*-adenosyl *L*-methionine (SAM)-dependent methyltransferase enzyme which catalyses the *N,N,N*-trimethylation of the α-amino group of histidine to form hercynine in the initial step of the mycobacterial ergothioneine biosynthesis process.[28]

The crystal structure coordinates of purified EgtD has been recently solved illustrating the binding pocket and supporting the catalytic mechanism.[35,36] Intriguingly, the EgtD enzyme possesses an unique substrate binding domain dissimilar to any known methyltransferase.[35] EgtD contains a Rossman-like fold and belong to class I methyltransferases (MTases).[39] It consists of two distinct domains: the catalytic MTase domain (a typical methyltransferase) which shares the highest sequence similarities with the histamine *N*-methyltransferase HNMT (PDB ID 1JQD; RMSD, 3.4 Å for 208 residues)[40] and the substrate binding domain (unique to EgtD). (Figure 1.9)[35]

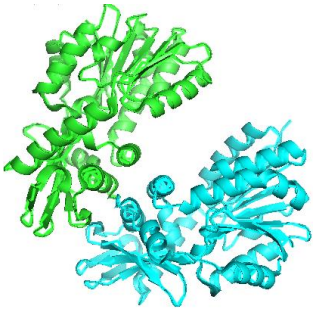

Figure 1.9. Crystal structure of methyltransferase EgtD (PDB 4PIM) isolated from *Mycobacterium smegmatis.*

Moreover, EgtD shares 16% sequence identity with the human methyltransferase Ad-003 (PDB 2EX4), which is believed to catalyze the N-terminal proline dimethylation.[36]

1.2.3.2. Sulfoxide Synthetase EgtB

The enzyme responsible for the second step in ESH biosynthesis is EgtB (EC 1.14.99.50) which is a non-heme iron enzyme sulfoxide synthetase that catalyses the central step in the ergothioneine biosynthesis pathway. EgtB is responsible for an O_2-dependent oxidative *C-S* bond formation between γ-glutamylcysteine and hercynine.[28]

EgtB shares a common DUF323 domain with FGEs (formylglycine-generating enzymes), which catalytically mediates the generation of a formylglycine residue by posttranslational oxidation of the cysteine precursor.[28,41] EgtB consists of residues 7–150 that folds to a DinB-like four-helix bundle with long linkers between helices 1 and 2 (18 residues), 2 and 3 (34 residues), and 3 and 4 (7 residues). (Figure 1.10)

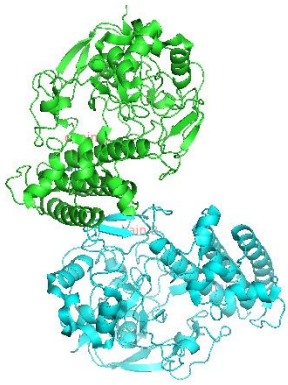

Figure 1.10. Crystal structure of sulfoxide synthetase EgtB (PDB 4X8B) isolated from *Mycobacterium thermoresistible.*

The EgtB crystal structure in the apo form as well as in complex with its natural substrate, along with its mechanistic and enzyme binding studies were also established.[38] The same research group also demonstrates that a simple mutation of Tyr377 in the EgtB active site by Phe completely changes its catalytic activity.[42] EgtB catalyses the oxidative *C-S* coupling between γ-glutamylcysteine and hercynine to form γ-glutamylcysteine hercynine sulfoxide. Mutation of Tyr377 by Phe in the active site of EgtB results in the formation of $EgtB_{Y377F}$ enzyme which instead catalyses the dioxygenation of γ-glutamylcysteine to form of γ-glutamylcysteine sulfinic acid.[42] The latter enzyme exhibited a strong similarity with the natural evolved cysteine dioxygenases (CDO, EC 1.13.11.20) which produces cysteine sulfinic

acid. CDOs and EgtB share no evolutionary relationship and their overall structure is quite different. [43] (Scheme 1.1)

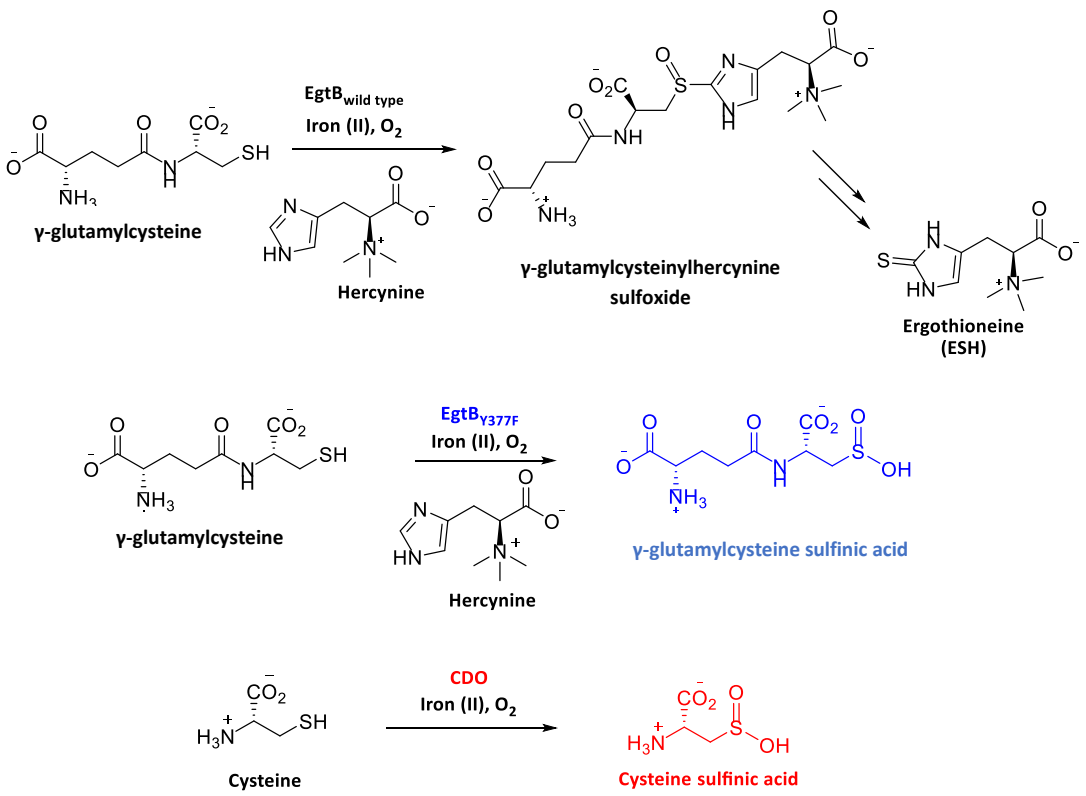

Scheme 1.1. Reactions catalysed by EgtB$_{wild\ type}$, EgtB$_{Y377F}$ and cysteine dioxygenase (CDO) enzymes. (Scheme adapted from Goncharenko *et al*. [42])

1.2.3.3. Amidohydrolase EgtC

EgtC is an amidotransamidase enzyme catalysing the hydrolysis of the glutamate from γ-glutamylcysteinylhercynine sulfoxide to produce hercynylcysteine sulfoxide in the mycobacterial ergothioneine pathway.

Crystal structure coordinates of EgtC enzyme in the apo form (Figure 1.12)[37], in complex with glutamine/glutamate and in complex with its natural substrate, γ-glutamylcysteinyl hercynine

sulfoxide were solved, thus shedding light on the enzyme substrate binding pocket in support of the enzymatic catalytic mechanism. (Figure 1.11)[37] Crystal structure of EgtC in complex with substrates (glutamine/glutamate and γ-glutamylcysteinyl hercynine) revealed an "open" conformation of the Ala90–Pro95 loop for hydrogen bonding and a large hydrophobic pocket with negative charge required for betaine recognition. The substrate-binding site is localised at the interface of the EgtC enzyme dimer.[37]

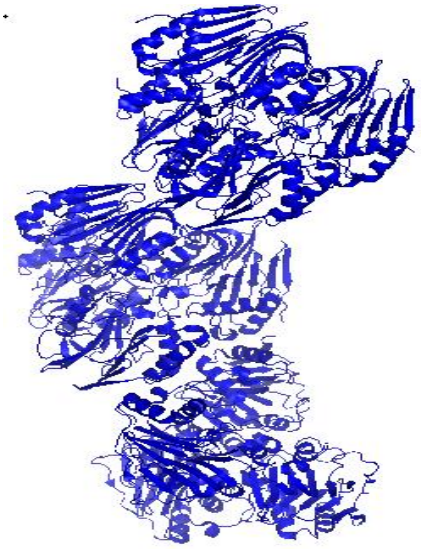

Figure 1.11. Apo enzyme crystal structure of EgtC (PDB 4ZFL).[37]

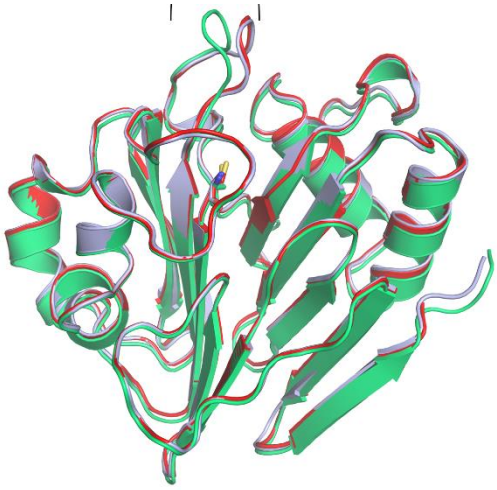

Figure 1.12. Superposition of EgtC apo form (in red), EgtC in complex with glutamate/glutamine (in light blue) and $EgtC_{C2A}$ in complex with γ-glutamyl cysteine hercynine sulfoxide (in green).[37]

1.2.3.4. PLP-dependent C-S lyase EgtE

PLP-dependent EgtE catalyses the last step in the mycobacterial ergothioneine biosynthetic pathway. Thus, the cleavage of the *C-S* bond of hercynylcysteine sulfoxide produces ergothioneine, while releasing pyruvate and ammonia.

Its catalytic activity was proposed by Seebeck but not demonstrated *in vitro* due to common difficulties in the overexpression of the PLP-dependent enzyme of *Mycobacterium*

smegmatis. Due to that failure, Seebeck substituted EgtE enzyme by an unrelated β-lyase from *Erwinia tasmaniensis*, which successfully cleaved hercynylcysteine sulfoxide to yield ergothioneine.[28]

Khonde *et al.* studied the EgtE *C-S* lyase activity of *Mycobacterium smegmatis* using cell lysate, which was later confirmed by Song *et al.*[29,30] The latter authors successfully overexpressed and purified *Mycobacterium smegmatis* EgtE. However, to date the crystal structure coordinates of EgtE has still not been solved.

Therefore, the elucidation of the crystal structure coordinates of these enzymes implicated in the mycobacterial ergothioneine biosynthesis pathway could help in designing ergothioneine biosynthesis inhibitors that could represent a novel class of anti-mycobacterial drugs candidates.

1.2.4. Involvement of ergothioneine in the biosynthesis pathways of natural products

It has emerged that ESH alongside cysteine, mycothiol (MSH) and glutathione (GSH) are involved in the biosynthesis pathways of natural products in many organisms illustrating an unique specificity.

For example, MSH and ESH are involved in the biosynthesis of Lincomycin A, which has been widely used for half a century to treat Gram-positive bacterial infections.[44] (Figure 1.13)

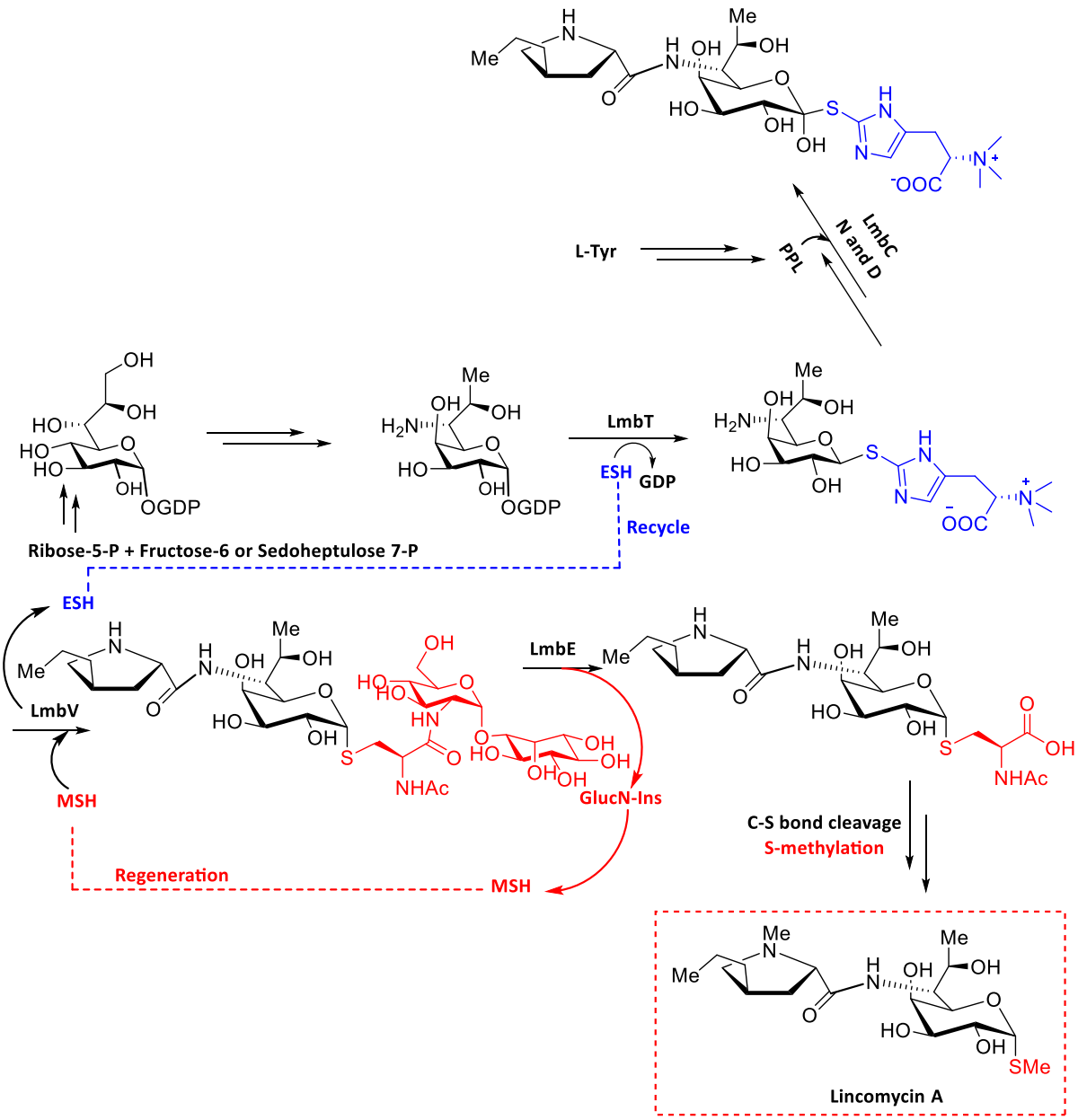

Figure 1.13. The ESH (blue) and MSH (red) programmed biosynthetic pathway of lincomycin A. The recycling of ESH and the regeneration of MSH are shown as dashed lines. (Figure adapted from *Zhao et al.*[44])

Furthermore, two new bohemamine-type pyrrolizidine alkaloids (Spithioneines A and B) possessing an unusual ESH moiety, were isolated from a marine derived *Streptomyces spinoverrucosus*.[45] (Figure 1.14)

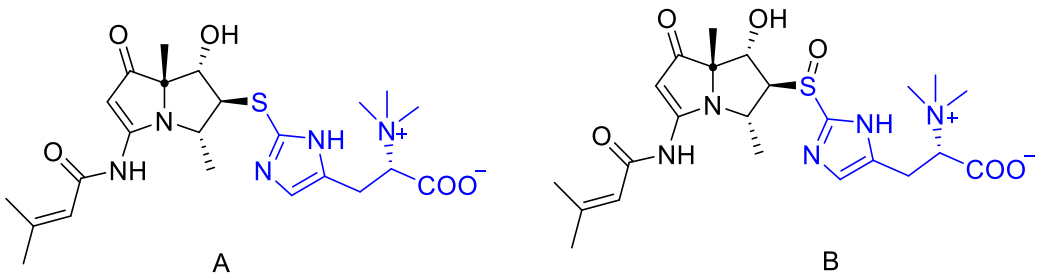

Figure 1.14. Spithioneines A and B, two new bohemamine-type pyrrolizidine alkaloids possessing an ergothioneine moiety isolated from a marine-derived *streptomyces spinoverrucosus*.[45]

Very recently, a *Chinese group* have isolated an unusual ergothioneine containing natural product, from an aqueous extract of ‘‘tian ma’’ (the *Gastrodia elata* rhizomes). This latter compound was named gastrolatathioneine and it is in fact an *N-1',N-3',* bis [4 –hydroxybenzyl] ergothioneine.[46] (Figure 1.15)

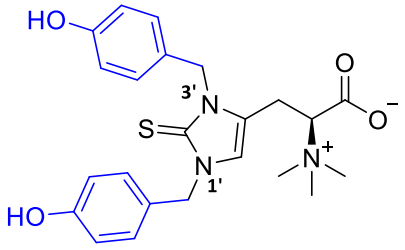

Figure 1.15. Structure of Gastrolatathioneine isolated from ‘‘tian ma’’ (the *Gastrodia elata* rhizomes).[46]

However, the genes encoding for ESH were absent in the plant that suggested that the gastrolatathioneine is co-produced by this higher eukaryote. Moreover, the plant enzyme that catalyses the transfer of the 4-hydroxybenzyl to ergothioneine is unknown to date.

Recent knowledge suggests that ergothioneine could be vital for the survival of *Mycobacterium tuberculosis*, therefore link between ergothioneine and tuberculosis is worth an in-depth discussion.

1.3. *Mycobacterium tuberculosis* and anti-tuberculosis drugs

1.3.1. *Mycobacterium tuberculosis*, a causative agent of tuberculosis

Mycobacterium tuberculosis (*Mtb*) is the causative microbe of tuberculosis (TB), a worldwide infectious disease. *Mycobacterium tuberculosis* is capable of persisting in a dormant state in human host for many years before causing active disease in approximately 10% of people infected. The very long duration of TB treatment (up to 9 months) and the emergence of *Mtb* drug resistance strains are the main reason making the treatment of tuberculosis extremely challenging.[47,48] As a result TB is the leading cause of mortality worldwide alongside the Human Immunodeficiency Virus (HIV) as it affects millions of people every year.[49]

Mycobacterium tuberculosis typically affects lungs hence cause pulmonary TB, but can also affect other parts of the human body to cause extra pulmonary TB. TB infection spreads by inhalation of micro-droplets of 2.5 µm of diameter having 1-3 bacilli. The bacteria get phagocytosed by macrophages as soon as they reach the alveola of the pulmonary system. The host reacts by apoptosis of the infected macrophages, but virulent strains may escape apoptosis by subversion of the immune system, hence resulting in dormant bacteria in the macrophages.[50]

The World Health Organization (WHO) declared TB a global public health emergency in 1993, since then impressive progress were made thus resulting in the decrease of TB mortality by 45%.[49] However, TB remains a global health problem despite the availability of various

antibiotics for many decades and the emergence of novel drugs. Almost one third of the world's population asymptomatically still possess a dormant or latent form of *Mycobacterium tuberculosis*. Many factors such as poverty, malnutrition, immune system suppression, poor hygiene, tobacco smoking, excessive alcohol consumption, as well as co-infection with other diseases such as HIV, diabetes usually lead to the reactivation of the latent TB to active TB disease.[50,51] About 95% of patients suffering from drug susceptible (DS) TB recovered after an adequate treatment, even though a minority of 5% may relapsed. However, if the TB patient does not get treated it will unavoidably lead to death. A simplified depiction of the phases of *Mycobacterium tuberculosis* infection is shown in the Figure 1.16.

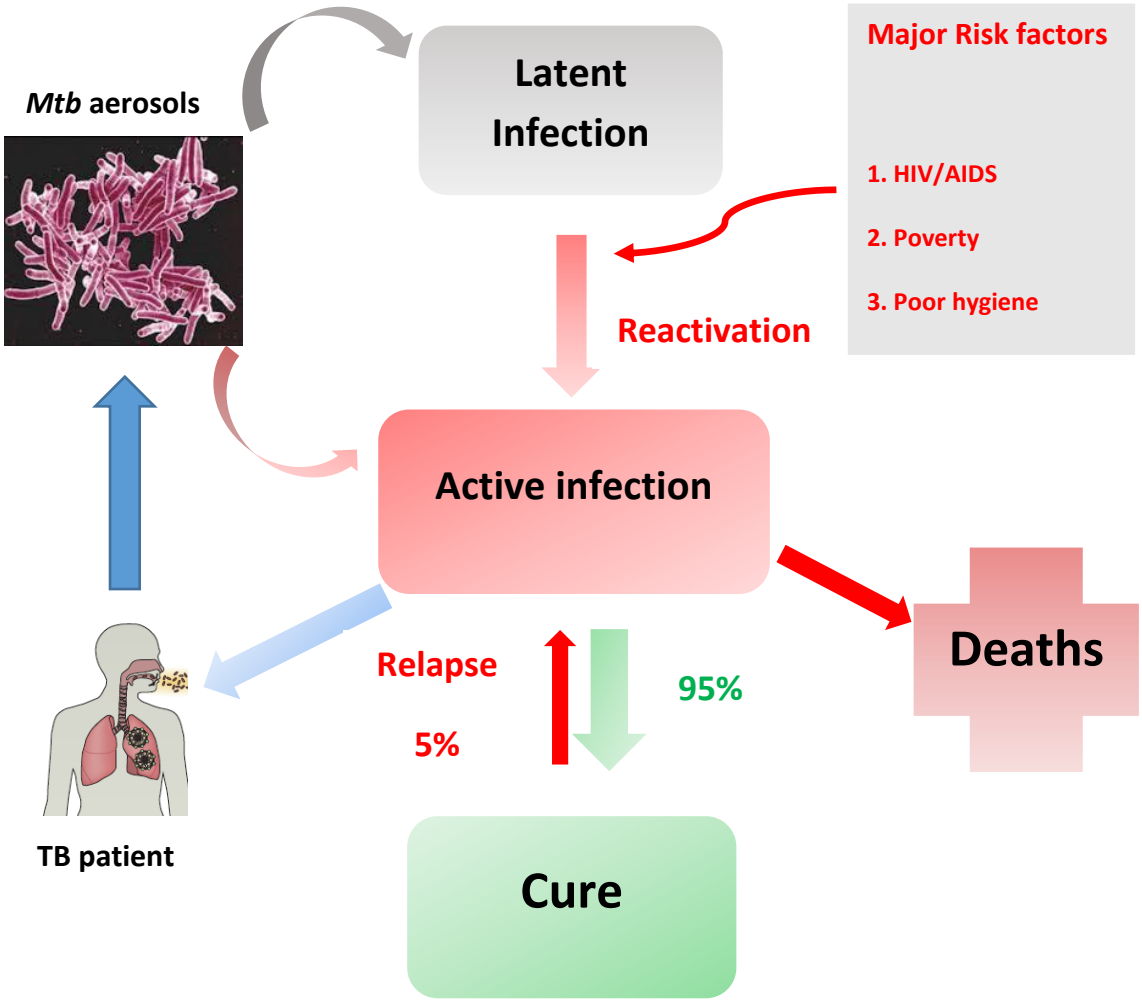

Figure 1.16. Simplified depiction of phases of *Mycobacterium tuberculosis* infection.

1.3.2. Global tuberculosis burden and tuberculosis drugs

1.3.2.1. Tuberculosis burden

Tuberculosis is spread through air and normally affects the lungs (pulmonary TB) but can also affect other sites as well (extrapulmonary TB). An overall of 5-15% of the estimated 3 billion people infected with *Mtb* will develop active TB during their lifetime, and this probability increases drastically among HIV positive patients.[49]

In 2014, there were an estimated 9.6 million new TB cases worldwide, with approximately 1.5 million deaths. The TB incidence rate has been dropping in the last decade, the cumulative decrease was 18% from 2000 to 2014.[49] Asia (58%) and Africa (28%) recorded the most of the estimated number of TB cases occurred in 2014, whereas Eastern Mediterranean (8%), Europe (3%) and America (3%) registered a smaller proportion. India, Indonesia and China accounted for 48% of TB case globally, alongside Nigeria, Pakistan, South Africa, Bangladesh, Philippines, Democratic Republic of Congo, and Ethiopia making the top 10 countries with higher TB incidence in 2014.[49] (Figure 1.17)

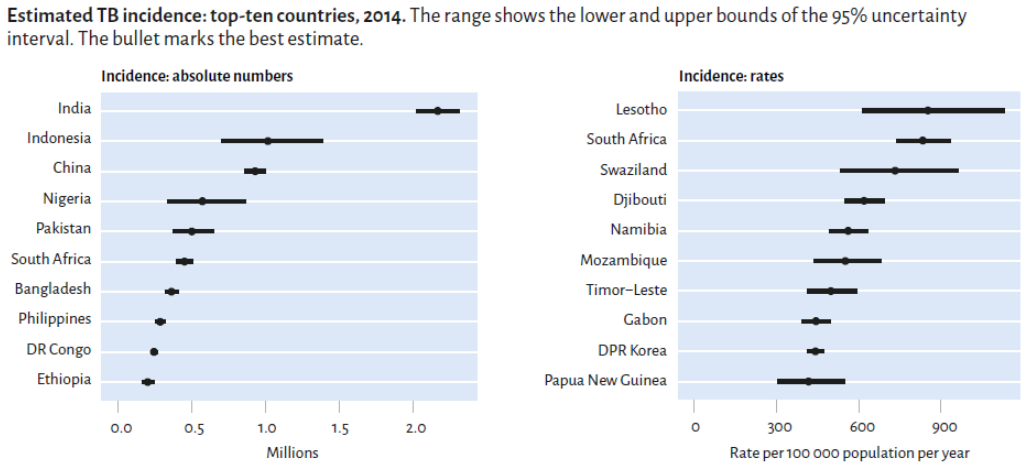

Figure 1.17. Estimated tuberculosis incidence top-10 countries in 2014.[49]

The countries with high-income such as USA, Canada, Australia, New Zealand, Western Europe exhibited a lower TB incidence rate of less than 10 cases per 100000 population per year, while Southern Africa, India, Russia and China displayed the highest TB incidence, 300 or more cases per 100000 in 2014. (Figure 1.18)

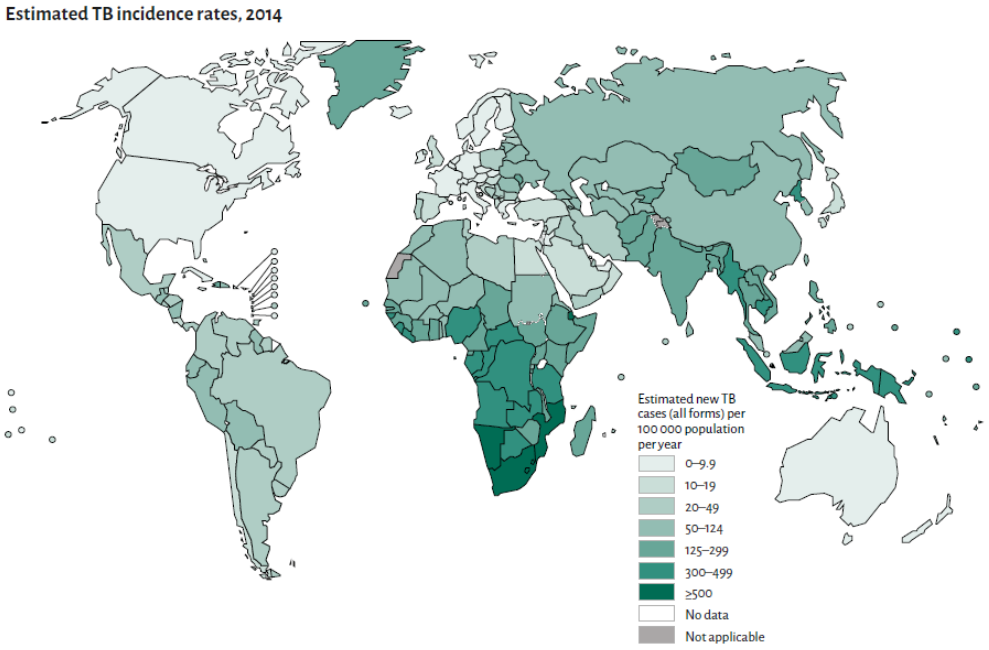

Figure 1.18. Estimated tuberculosis rates, 2014.[49]

1.3.2.2. HIV and Tuberculosis

The Human Immunodeficiency Virus (HIV) weakens the human immune system, hence increases the chance of developing active TB especially when a patient is infected by *Mycobacterium tuberculosis*, the causative agent of TB disease. Amongst 9.6 million of TB cases reported in 2014, an estimated 1.2 million (12%) were living with HIV. The rate of TB-HIV co-infection was higher in Africa which represents 74% of TB cases among people living with HIV worldwide. (Figure 1.19)

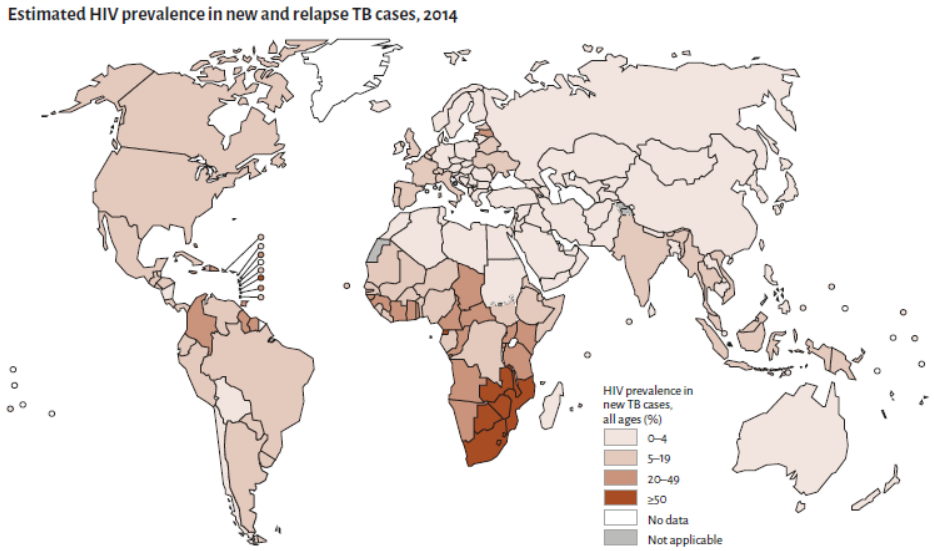

Figure 1.19. Estimated HIV prevalence and relapse TB cases, 2014.[49]

Despite, the number of deaths related to HIV associated to TB has drastically decreased by 32% from 570000 deaths in 2004 to 390000 deaths in 2014, but TB infection amongst HIV patients remains a major concern as an estimated one-third of 1.2 million deaths among HIV/AIDS population were due to TB co-infection.[49]

1.3.2.3. Current tuberculosis drugs

The treatment of tuberculosis is difficult due to some major factors, such as persistence (survival of *M. tuberculosis* despite the use of TB drugs), complete drug resistance as well as relapse. Therefore, the management of TB disease requires lengthy drug treatment regiments of six to nine months. The treatment of drug-susceptible (DS)-TB involves a four-drug regimen of first-line anti TB drugs. An intensive phase includes the use of isoniazid, pyrazinamide, rifampicin, and ethambutol for a period of two months. The intensive phase is followed by a

continuation phase which includes the use of two drugs rifampicin and isoniazid for an additional 4 months period.[50] (Figure 1.20)

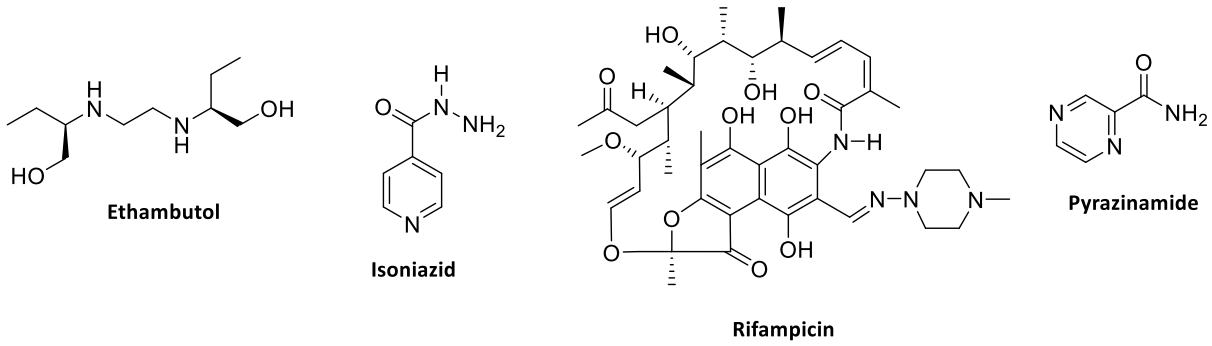

Figure 1.20. Chemical structure of first line TB drugs.

However, the second line TB drugs and third line TB drugs are either more expensive, or less effective (e.g. *p*-aminosalicylic acid), and have toxic side-effects (e.g cycloserine) than the first line drugs. (Figure 1.21 & Figure 1.22)

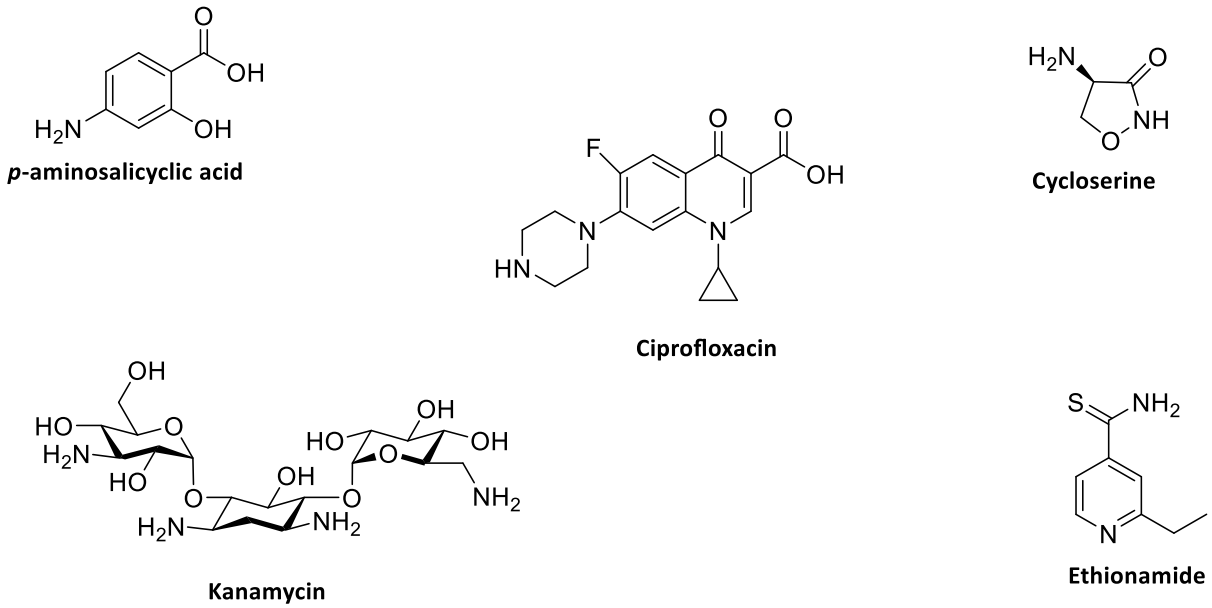

Figure 1.21. Chemical structure of some second line TB drugs.

The second line TB drugs belong to several chemical classes including polypeptides (e.g. capreomycin), thioamides (e.g. ethionamide), aminoglycosides (e.g. kanamycin), fluoroquinolones (e.g. ciprofloxacin), and thioamides (e.g. ethionamide).

It is noteworthy that the second line TB drugs are only mandatory in the extreme case, when the TB patient either does not tolerate the first line TB drugs or the treatment does not respond.

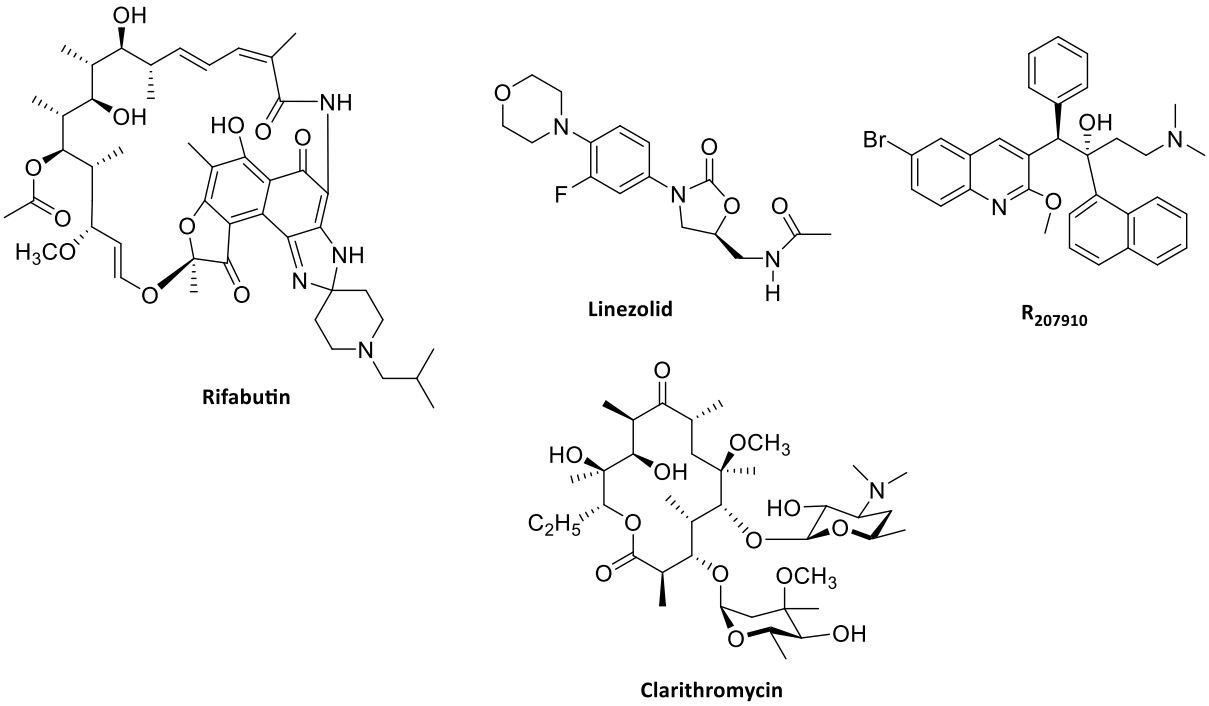

Figure 1.22. Chemical structure of some third line TB drugs.

1.3.3. Drug-resistant tuberculosis

Drug-resistant *Mycobacterium tuberculosis* strains were first reported in 1944 after the discovery of streptomycin. Later, resistance to others TB drugs were also established. TB drug resistance is due to genetic mutation which alter the affinity of either the target or the activator of the drug.[48]

Multidrug-resistant (MDR-TB) are strains resistant to at least one of the first list drugs, mostly isoniazid (INH) and rifampicin, the most effective anti-TB drugs. Extremely-drug resistant (XDR-TB) are *Mtb* strains resistant to isoniazid, rifampicin and to second line anti-TB drugs belonging to the fluoroquinolone family and resistant to at least one of aminoglycoside injectable drugs (kanamycin, capreomycin, or amikacin).[48] MDR-TB is difficult to treat compared to susceptible TB, since less than 70% cure-rates are more often achieved.[50] MDR-TB has been surveyed worldwide, an estimated half a million cases was reported in 2011 and this rate remains almost unchanged to date. XDR-TB on the other hand has been reported in 105 countries, in average 9.7% of people with MDR-TB possess XDR-TB.[49,52]

More recently, totally-drug resistant (TDR) *Mtb* strains which exhibit resistance to all first-line and second anti-TB drugs have been reported, thus posing a huge threat for TB therapy. TDR-TB is practically incurable and was reported in several countries such as India, South Africa, Italy and Iran.[53,54]

Therefore, the development of new tools for prevention, diagnostics and new antitubercular drugs are urgently needed in order to bring TB disease under control. The development of novel chemotherapeutics which are effective against drug-resistant *Mtb* strains, less toxic and acting on new biological targets is of foremost importance.

However, several drug candidates with novel modes of action are either in the late-stage clinical development or have been approved for TB chemotherapy. (Figure 1.23) Amongst

them bedaquiline (a diarylquinoline) and delamanid (a nitroimidazo-oxazole) have been successful examples of the TB drug discovery in a modern era.[55]

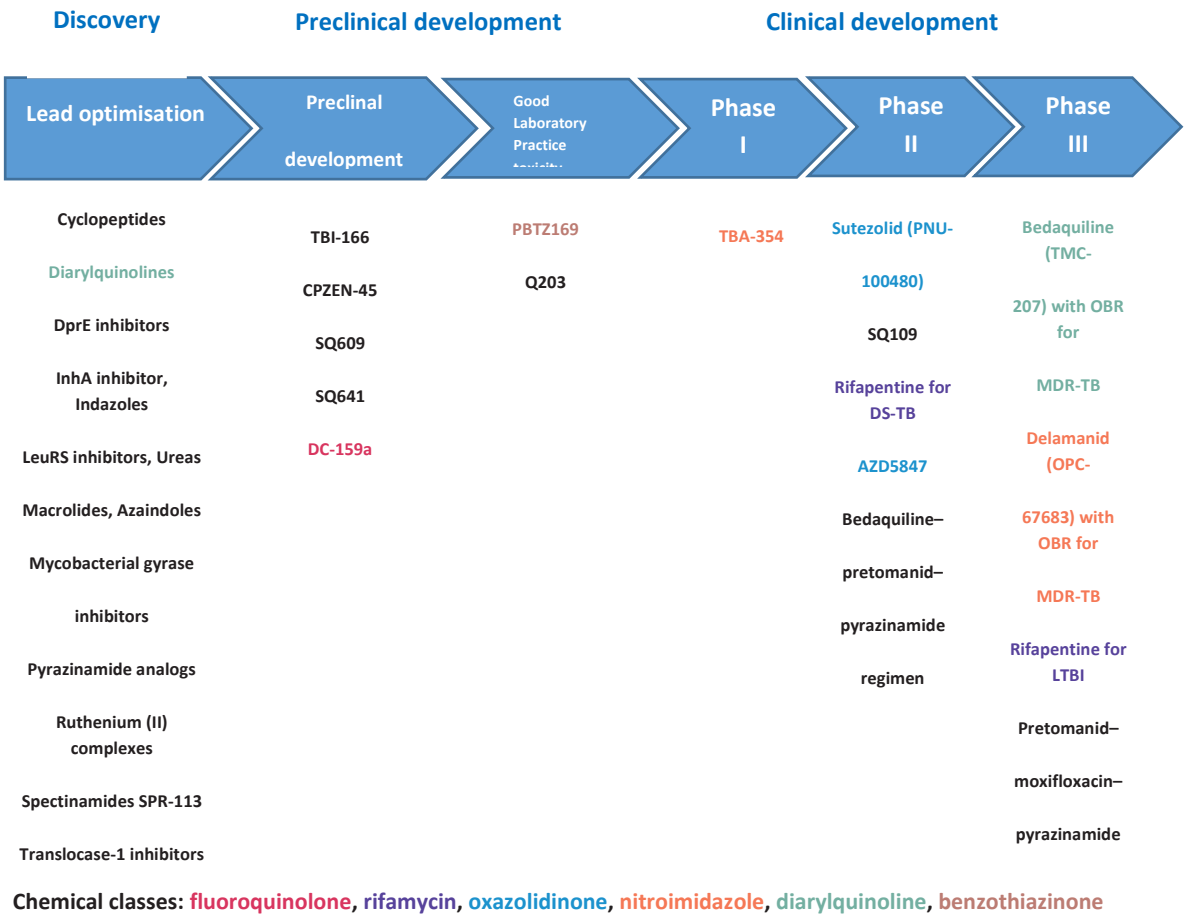

Figure 1.23. Pipeline of new tuberculosis drugs. MDR-TB: multidrug-resistant tuberculosis OBR-optimised background regimen; DS-TB: drug-susceptible tuberculosis; LTBI: latent tuberculosis infection.[55]

1.3.4. Tuberculosis biological drug targets.

Existing TB drugs have diverse mechanisms of action. First line-TB drug targets the mycobacterial cell wall biosynthesis with Isoniazid as well as ethambutol blocking the synthesis of mycolic acid, an essential component of the mycobacterial cell wall.

Two newly approved TB drugs have quite dissimilar modes of action. Delamanid, inhibits the synthesis of mycolic acid, hence destroying the bacterial cell wall,[56] while Bedaquinine targets the proton pump of ATP synthesis.[57] Pyrazinamide, structurally similar to INH, is a prodrug readily transformed into pyrazinoic acid (its active form) by nicotinamidase/pyrazinamidase (PZase) enzyme.[58] However, its mode of action has been debated, it is suggested that this drug inhibits the fatty acid synthase I (FAS),[59] an enzyme implicating in the biosynthesis of mycobacterial fatty acid by depleting ATP reserves and by binding to the ribosomal protein S1.[60-62] Rifampicin, acts on replicating and non-replicating mycobacteria by inhibiting the bacterial RNA-dependent polymerase.[60] Cycloserine inhibits the mycobacterial cell wall by acting on the mycolylarabinogalactan-peptidoglycan complex.[63] The aminoglycosides inhibit the protein synthesis by disturbing the translocation of peptidyl transfer RNA, while the thioamide TB drug inhibits the mycolid acid biosynthesis, even though the detailed mechanism remain unclear.[64,65] Fluoroquinolone TB drugs are the first choice for the treatment of patient with multidrug-resistant (MDR-TB) and extensively drug resistant tuberculosis. Fluoroquinolone TB drugs act on Type II topoisomerase (DNA gyrase), which result on the inhibition of DNA replication and transcription.[66-68]

Most existing drugs target the cell wall and is susceptible to the development of resistance. It is therefore important that future TB drugs also target essential metabolites, hence introducing novel mode of actions and reducing resistance or/and cross resistance with existing TB-drugs. Mycothiol and ergothioneine are the principal low molecular weight thiols produced by *Mtb*, and these metabolites play a key role in maintaining redox homeostasis which is essential for the *in vitro* and *in vivo* survival of *Mtb*. Therefore, enzymes of the

mycothiol and ergothioneine biosynthesis pathway appeared to be potential anti-TB drug targets.[51,69,70]

1.4. Redox homeostasis in mycobacteria

Homeostasis can be defined as a 'relatively stable state of equilibrium or a tendency towards such a state between the different but interdependent elements or groups of elements of an organism, population, or group' (Merriam-Webster).

For many years, it has been known that *Mtb* is an obligate aerobe, although research has shown that *Mtb* can survive *in vitro* under anaerobic conditions for more than a decade. *Mtb* is exposed to various extreme and stressful environmental conditions during infection, which triggered an as yet uncharacterized response by the bacteria in order to maintain a normal redox state.[51]

The bacterial host provides nutrients (carbon sources), gas and pathological conditions such as hypoxic granulomas, which allow the *Mtb*, through unknown mechanisms, to subvert the immune system and to cause TB proliferation. An intracellular redox imbalance state can affect the efficacy of TB drugs which require a bioreductive activation, these drugs include isoniazid (INH), ethionamide (ETA) and pretomanid (nitro-imidazole drug).[51] Furthermore, it was established that INH resistance could be directly due to the increase in the ratio of $NADH/NAD^+$, while mycobacteria with deletion mutations in the MSH biosynthesis pathway demonstrated resistance to INH and ETA.[71] Nevertheless, the mechanism used by *Mtb* to maintain the *in vivo* redox homeostasis and their role in drug susceptibly and efficiency remain poorly understood.

The GSH redox couple (GSSG/2GSH) is lacking in *Mtb*, instead they possess millimolar quantities of the mycothiol redox couple (MSSM/2MSH) as major redox buffer. Recently, Bhaskar *et al.* developed a genetically encoded biosensor method to quantify the redox potential of mycothiol E_{MSH} in real time for diverse *Mycobacterium tuberculosis* strains and mutants inside macrophages.[72] Intriguingly, these studies revealed that the heterogeneity in the mycothiol redox potential E_{MSH} of the *Mtb* population is induced by the intravacuoles and intramacrophage environment. Consequently, treatment with anti-TB drugs oxidatively affects this mycothiol redox potential E_{MSH} which results in the disruption of the MSH homeostasis that contributes to the killing of *Mtb*.[72]

Mycobacteria contain many other redox couples such as $NADH/NAD^+$, $NADPH/NADP^+$ and thioredoxin (TrxSS/Trs $(SH)_2$).[51] The reduction of the mycothiol disulfide is catalysed by a special enzyme, the FAD-binding mycothiol reductase using NADPH as a cofactor as depicted in the equation below:

$$NADPH + H^+ + MSSM \longrightarrow 2\,MSH + NADP^+$$

It was reported that MSH deletion mutants are sensitive to oxidative stress caused by cumene hydroperoxide, H_2O_2, and superoxide radical ($O_2^{\cdot -}$).[73] While the redox potential of ESH_{ox}/ESH_{red} couple for mycobacteria is established ($E^O = -60$ mV), its role as protective thiol is not well-known.

The understanding of the redox homeostasis in mycobacteria and how it influences drug efficacy remains the key to control tuberculosis disease. However, recent findings suggest

that ESH could be essential for the *in vitro* and *in vivo* survival of *Mtb*. Hence, enzymes implicated in its biosynthesis could be valuable TB drug targets.

1.5. Unveiling the physiological role of ergothioneine in mycobacteria

The role of mycothiol in *Mycobacterium (smegmatis and tuberculosis)* have been extensively studied in the last decade, whereas ESH's natural function in *Mycobacteria* has recently been under the spot light. Various research groups have focused on the validation of ergothioneine biosynthesis as a potential tuberculosis drug target. Despite these recent efforts, the direct link between ESH and tuberculosis remains a topic for further investigation.

Studies conducted by Ta *et al.* have revealed that a *Mycobacterium smegmatis* mutant (*ΔmshA*) lacking mycothiol, overproduced ergothioneine and organic hydroperoxide resistance protein (Ohr), thus suggesting that ESH as well as Ohr act as an alternative antioxidant to compensate for any mycothiol loss.[74] Sao Emani *et al.* confirmed these findings, moreover they attempted to quantify ESH in *Mycobacterium smegmatis* while comparing its intracellular versus extracellular concentration.[70] The percentage of ergothioneine appeared to be higher extracellularly than intracellularly in either *M. smegmatis* wild type as well as *M. smegmatis* mutants (*ΔmshA, ΔegtD*$_c^a$), hence confirmed that *M. smegmatis* produce and secrete ESH.[70] The presence of ESH extracellularly suggestes a possible existence of an ESH specific transporter in mycobacteria similar to the human ESH transporter OCTN1, which

could be responsible for the active diffusion of ESH outside the *M. smegmatis* cells, although these suggestions still have to be confirmed.[70]

The same research group discovered that *M. smegmatis* egtD deletion mutants do not produce ergothioneine. More importantly it has been found that double *M. smegmatis* mutants (*ΔmshA ΔegtD*), lacking mycothiol and ESH were significantly more sensitive to peroxide than either of the single mutants lacking ESH or MSH, thus suggesting that MSH as well as ESH play a crucial role in protecting *M. smegmatis* against oxidative stress while compensating each other. These findings suggested that the EgtD enzyme could be a potential mycobacterial drug target. Amongst all the other ESH enzymes evaluated in their study, only EgtD enzyme knockout results in *M. smegmatis* mutants sensitive to peroxide.[70]

Richard-Greenblatt *et al.* have extended studies to better understand the role of ESH in *Mycobacterium tuberculosis*. They have identified a *rv3701c* gene from *Mtb* which encode for EgtD, the enzyme implicated in the first step of ESH biosynthesis.[75] They have demonstrated that EgtD is essential for ESH biosynthesis but not required for the growth of *Mycobacterium tuberculosis*.[75] In *Mycobacterium tuberculosis*, EgtD was discovered to be a substrate for either *in vitro* and cell base phosphorylation by a serine/threonine kinase enzyme, PknD. It was shown that this competitive reaction down-regulates ESH biosynthesis as 20% reduction in EgtD methyltransferase activity was observed.[75]

More importantly, this group showed that ESH is indeed required for the survival of *Mtb* during long starvation conditions as well as inside the murine macrophage as a rise in intracellular ESH was observed during late logarithmic growth.[75]

Very recently Saini *et al.* have shown that specific *Mtb WhiB3* redox sensor controls the production of ESH while maintaining bioenergetic homeostasis.[47] *Mtb ΔegtA, ΔegtD* deletion mutants lacking ESH exhibited higher sensitivity to anti-TB drugs such as rifampin (RIF), isoniazid (INH), bedaquiline (BDQ), and clofazimine (CFZ) compared to *Mtb* wild type. Molecular biology studies suggested that ESH and MSH have distinct but overlapping physiological function in *Mtb*. Furthermore they showed that ESH is vital for *Mtb* survival *in vivo* in a mouse model of *Mtb*.[47]

Unpublished research conducted at the University of Stellenbosch by Sao Emani (post doc fellow in Bienyameen Baker research group) have provided evidence of ESH being essential for the survival of *Mtb* cell cultures. This group claimed that the depletion of ESH in *Mtb* weakens the mycobacteria which eventually died. The same trend was still observed when *Mtb* ergothioneine deletion mutants (Δegt) were assayed *in vitro* either under mimicking human latent or active tuberculosis conditions. Nevertheless, still more research has to be conducted to establish that if the same feature can be replicated *in vivo* and inside the human host cells.

1.6. Aims and objectives of this study

It is now emerging that ergothioneine is required for the survival of *Mtb* as demonstrated independently by two research groups (Baker B., University of Stellenbosch, Tygerberg, South Africa[70] and Steyn, J.C., KwaZulu-Natal Research Institute for Tuberculosis and HIV, Durban, South Africa[47,75]).

The reconstitution of ergothioneine biosynthesis pathway in mycobacteria will aid the understanding of the essentiality of ESH in mycobacteria. Designing potential mechanism based inhibitors targeting ergothioneine is mandatory for the development of future drugs against tuberculosis.

Ergothioneine is commercially available but expensive due to the challenge associated with its synthesis. The biosynthetic pathway intermediates of ergothioneine are not commercially available.

Ovothiol is structurally similar to ergothioneine and is the most powerful natural antioxidant. It has been suggested that ovothiols protect *trypanosomatid* parasites from oxidative stress.[76] Recent knowledge suggested that ovothiol A could be active against the proliferation of Hep-G2, human liver cancer cells.[77] Therefore developing a better process for the synthesis of this important thiol is of valuable interest.

The research reported in this thesis aims to:

(i) Develop improved synthetic methods to produce ergothioneine in a better yield.

(ii) Synthesize stable isotopically labelled substrates, essential tools for metabolomic studies and drug discovery.

(iii) To perform the biotransformation of EgtE enzyme (PLP-dependent) *substrates to ESH using cell-free lysate preparation from M. smegmatis monitored by LCMS technique, in order to shed light on the mechanism of C-S lyase as well as enzyme-substrate specificity.*

(iv) Design and develop a strategy for the first total synthesis of the EgtC enzyme substrate. Previously, this enzyme substrate was enzymatically synthesized in a very low amount. A viable synthesis protocol will provide the scientific community with valuable tools for further investigation of ESH and the TB link.

(v) Design and develop a scalable synthetic process for ergothioneine as well as ovothiols.

1.7. References

1 Claus Bornemann, C., Jardine, M. A., Spies, H. S. C. & Steenkamp, D. J. Biosynthesis of mycothiol: elucidation of the sequence of steps in Mycobacterium smegmatis. *Biochemistry* **325**, 623–629 (1997).

2 Hand, C. E. & Honek, J. F. Biological Chemistry of Naturally Occurring Thiols of Microbial and Marine Origin. *Journal of Natural Products* **68**, 293-308 (2005).

3 Fahey, R. C. Novel Thiols of Prokaryotes *Annual Review of Microbiology.* **55**, 333-356 (2001).

4 Sharma, S. V. *et al.* Chemical and Chemoenzymatic syntheses of bacillithiol: a unique low-molecular-weight thiol amongst low G + C Gram-positive bacteria. *Angewandte Chemie* **50**, 7101-7104, doi:10.1002/anie.201100196 (2011).

5 Tanret, C. New base obtained from ergot of rye. Ergothioneine. *Comptes Rendus hebdomadaires des séances de l'Académie des sciences* **199**, 222-224 (1909).

6 Paul, B. D. & Snyder, S. H. The unusual amino acid L-ergothioneine is a physiologic cytoprotectant. *Cell Death & Differentiation* **17 (7)**, 1134-1140, doi:10.1038/cdd.2009.163 (2010).

7 Fahey, R. C. Novel thiols of Prokaryote *Annual Reviews Microbiology* **55**, 333-356 (2001).

8 Motohashi, N., Mori, I. & Sugiura, Y. ^{13}C-Nuclear Magnetic Resonance and Raman Spectroscopic Studies on Ionisation and Mercury Complex of Ergothioneine. *Chemical and Pharmaceutical Bulletin* **28**, 1737-1741 (1976).

9 Scott, E. M., Duncan, I. W. & Ekstrand, V. Purification and Properties of Glutathione Reductase of Human Erythrocytes. *Journal of Biological Chemistry* **238**, 3928-3933 (1963).

10 Heath, H. & Toennies, G. The Preparation and Properties of Ergothioneine Disulphide. *Journal of Biochemistry* **68**, 204-2010 (1958).

11 Sugihara, A. *et al.* The Crystal Structure of L-Ergothioneine Dihydrate, $C_9H_{15}N_3O_2S.2H_2O$. *Acta Crystallographica* **B32**, 181-185 (1976).

12 Genghof, D. S. & Van Damme, O. Biosynthesis of Ergothioneine and Hercynine by Mycobacteria. *Journal of bacteriology* **87**, 852-862 (1964).

13 Genghof, D. S. Biosynthesis of Ergothioneine and Hercynine by Fungi and Actinomycetales. *Journal of bacteriology* **103**, 475-478 (1970).

14 Pfeiffer, C., Bauer, T., Surek, B., Schömig, E. & Gründemann, D. Cyanobacteria produce high levels of ergothioneine. *Food chemistry* **129**, 1766-1769, doi:10.1016/j.foodchem.2011.06.047 (2011).

15 Genghof, D. S. Biosynthesis of Ergothioneine and Hercynine by Fungi and Actinomycetales. *Journal of bacteriology* **103** (1970).

16 Tepwong, P., Giri, A., Sasaki, F., Fukui, R. & Ohshima, T. Mycobial enhancement of ergothioneine by submerged cultivation of edible mushroom mycelia and its application as an antioxidative compound. *Food chemistry* **131**, 247-258, doi:10.1016/j.foodchem.2011.08.070 (2012).

17 Pluskal, T., Ueno, M. & Yanagida, M. Genetic and metabolomic dissection of the ergothioneine and selenoneine biosynthetic pathway in the fission yeast, S. pombe, and construction of an overproduction system. *PloS one* **9**, e97774, doi:10.1371/journal.pone.0097774 (2014).

18 EY, J., Schomig, E. & Taubert, D. Dietary Sources and Antioxidant Effects of Ergothioneine. *Journal of Agricultural and Food Chemistry* **55**, 6466−6474 (2007).

19 Grundemann, D. *et al.* Discovery of the ergothioneine transporter. *Proceedings of the National Academy of Sciences of the United States of America* **102, No 14**, 5256–5261, doi:10.1073/pnas.0408624102 (2005).

20 Frigeni, M., Iacobazzi, F., Yin, X. & Longo, N. Wide tolerance to amino acids substitutions in the OCTN1 ergothioneine transporter. *Biochimica et biophysica acta* **1860**, 1334-1342, doi:10.1016/j.bbagen.2016.03.021 (2016).

21 Heath, H. & Wildy, J. Biosynthesis of Ergothioneine by Claviceps purpurea: The incorporation of labelled histidine. *Journal of Biological Chemistry* **68** (1958).

22 Wildy, J. & Heath, H. Biosynthesis of Ergothioneine by Claviceps purpurea. *Journal of Biological Chemistry* **65**, 220 (1957).

23 Genghof, S. D. & Van Damme, O. Biosynthesis of Ergothioneine from Endogenous Hercynine in *Mycobacterium smegmatis*. *Journal of bacteriology* **95** (1968).

24 Reinhold, V. N., Ishikawa, Y. & Melville, D. B. Conversion of Histidine to Hercynine by *Neurospora crassa*. *Journal of bacteriology* **101** (1970).

25 Melville, D. B., Eich, S. & Ludwig, M. L. The biosynthesis of ergothioneine. *Journal of Biological Chemistry* **224**, 871-877 (1957).

26 Askari, A. & Melville, D. B. The Reaction Sequence in Ergothioneine Biosynthesis: Hercynine as an Intermediate. *Journal of Biological Chemistry* **237, No 5**, 1615-1618 (1962).

27 Ishikawa, Y., Israel, S. E. & Melville, D. B. Participation of an Intermediate Sulfoxide in the Enzymatic Thiolation of the Imidazole Ring of Hercynine to Form Ergothioneine. *Journal of Biological Chemistry* **249, 14**, 4420 (1974).

28 Seebeck, F. P. In Vitro Reconstitution of Mycobacterial Ergothioneine Biosynthesis. *Journal of American Chemical Society* **132**, 6632 (2010).

29 Song, H. *et al.* Mechanistic studies of a novel C-S lyase in ergothioneine biosynthesis: the involvement of a sulfenic acid intermediate. *Scientific reports* **5**, 11870, doi:10.1038/srep11870 (2015).

30 Khonde, P. L. & Jardine, A. Improved synthesis of the super antioxidant, ergothioneine, and its biosynthetic pathway intermediates. *Organic & biomolecular chemistry* **13**, 1415-1419, doi:10.1039/c4ob02023e (2015).

31 Hu, W. *et al.* Bioinformatic and biochemical characterizations of C-S bond formation and cleavage enzymes in the fungus *Neurospora crassa* ergothioneine biosynthetic pathway. *Organic letters* **16**, 5382-5385, doi:10.1021/ol502596z (2014).

32 Bello, M. H., Barrera-Perez, V., Morin, D. & Epstein, L. The Neurospora crassa mutant NcDeltaEgt-1 identifies an ergothioneine biosynthetic gene and demonstrates that ergothioneine enhances conidial survival and protects against peroxide toxicity during conidial germination. *Fungal genetics and biology : FG & B* **49**, 160-172, doi:10.1016/j.fgb.2011.12.007 (2012).

33 Vit, A., Mashabela, G. T., Blankenfeldt, W. & Seebeck, F. P. Structure of the Ergothioneine-Biosynthesis Amidohydrolase EgtC. *Chembiochem* **16**, 1490-1496, doi:10.1002/cbic.201500168 (2015).

34 Fahey, R. C. Glutathione analogs in prokaryotes. *Biochimica et biophysica acta* **1830**, 3182-3198, doi:10.1016/j.bbagen.2012.10.006 (2013).

35 Jeong, J. H., Cha, H. J., Ha, S. C., Rojviriya, C. & Kim, Y. G. Structural insights into the histidine trimethylation activity of EgtD from *Mycobacterium smegmatis*. *Biochemical and biophysical research communications* **452**, 1098-1103, doi:10.1016/j.bbrc.2014.09.058 (2014).

36 Vit, A., Misson, L., Blankenfeldt, W. & Seebeck, F. P. Crystallization and preliminary X-ray analysis of the ergothioneine-biosynthetic methyltransferase EgtD. *Acta crystallographica. Section F, Structural biology communications* **70**, 676-680, doi:10.1107/S2053230X1400805X (2014).

37 Allegra Vit, Gabriel T. Mashabela, Wulf Blankenfeldt & Seebeck, F. P. Structure of the Ergothioneine-Biosynthesis Amidohydrolase EgtC. *ChemBioChem* **16**, 1490 (2015).

38 Goncharenko, K. V., Vit, A., Blankenfeldt, W. & Seebeck, F. P. Structure of the sulfoxide synthase EgtB from the ergothioneine biosynthetic pathway. *Angewandte Chemie* **54**, 2821-2824, doi:10.1002/anie.201410045 (2015).

39 Gana, R., Rao, S., Huang, H., Wu, C. & Sona Vasudevan, S. Structural and functional studies of S-adenosyl-L-methionine binding proteins: a ligand-centric approach. *BMC Structural Biology* **13**, 6 (2013).

40 Horton, J. R., Sawada, K., Nishibori, M., Zhang, X. & Cheng, X. Two Polymorphic Forms of Human Histamine Methyltransferase: Structural, Thermal, and Kinetic Comparisons. *Structure* **9**, 837–849 (2001).

41 Dierks, T. *et al.* Molecular basis for multiple sulfatase deficiency and mechanism for formylglycine generation of the human formylglycine-generating enzyme. *Cell* **121**, 541-552, doi:10.1016/j.cell.2005.03.001 (2005).

42 Goncharenko, K. V. & Seebeck, F. P. Conversion of a non-heme iron-dependent sulfoxide synthase into a thiol dioxygenase by a single point mutation. *Chemical communications* **52**, 1945-1948, doi:10.1039/c5cc07772a (2016).

43 Li, W. & Pierce, B. S. Steady-state substrate specificity and O(2)-coupling efficiency of mouse cysteine dioxygenase. *Archives of biochemistry and biophysics* **565**, 49-56, doi:10.1016/j.abb.2014.11.004 (2015).

44 Zhao, Q., Wang, M., Xu, D., Zhang, Q. & Liu, W. Metabolic coupling of two small-molecule thiols programs the biosynthesis of lincomycin A. *Nature* **518**, 115-119, doi:10.1038/nature14137 (2015).

45 Fu, P. & MacMillan, J. B. Spithioneines A and B, Two New Bohemamine Derivatives Possessing Ergothioneine Moiety from a Marine-Derived Streptomyces spinoverrucosus. *Organic letters* **17**, 3046-3049, doi:10.1021/acs.orglett.5b01328 (2015).

46 Guo, Q.-L. *et al.* Gastrolatathioneine, an unusual ergothioneine derivative from an aqueous extract of "tian ma": A natural product co-produced by plant and symbiotic fungus. *Chinese Chemical Letters* **In press**, doi:10.1016/j.cclet.2016.06.040 (2016).

47 Saini, V. *et al.* Ergothioneine Maintains Redox and Bioenergetic Homeostasis Essential for Drug Susceptibility and Virulence of *Mycobacterium tuberculosis*. *Cell Reports* **14**, 572–585, doi:10.1016/j.celrep.2015.12.056 (2016).

48 Sacchettini, J. C., Rubin, E. J. & Freundlich, J. S. Drugs versus bugs: in pursuit of the persistent predator *Mycobacterium tuberculosis*. *Nature reviews. Microbiology* **6**, 41-52, doi:10.1038/nrmicro1816 (2008).

49 http://www.who.int/tb/publications/global_report/en. Global tuberculosis report 2015. Report No. ISBN 978 92 4 156505 9, (World Health Organization 2015, Geneva, Switzerland, **2015**, Accessed 22/02/2016).

50 Koul, A., Arnoult, E., Lounis, N., Guillemont, J. & Andries, K. The challenge of new drug discovery for tuberculosis. *Review Research Nature* **469**, 483-490, doi:10.1038/nature09657 (2011).

51 Kumar, A. *et al.* Redox homeostasis in mycobacteria: the key to tuberculosis control? *Expert reviews in molecular medicine* **13**, e39, doi:10.1017/S1462399411002079 (2011).

52 Zumla, A., Nahid, P. & Cole, S. T. Advances in the development of new tuberculosis drugs and treatment regimens. *Nat Rev Drug Discov* **12**, 388-404, doi:10.1038/nrd4001 (2013).

53 Velayati, A. A., Farnia, P. & Masjedi, M. R. Letter to Editor:The totally drug resistant tuberculosis (TDR-TB). *International journal of clinical and experimental medicine* **6**, 307-309 (2013).

54 Parida, S. K. *et al.* Totally drug-resistant tuberculosis and adjunct therapies. *J Intern Med* **277**, 388-405, doi:10.1111/joim.12264 (2015).

55 Pontali, E., Sotgiu, G., Lia D'Ambrosio, Rosella Centis, R. & Migliori, G. B. Bedaquiline and multidrug-resistant tuberculosis: a systematic and critical analysis of the evidence. *Eur Respir J* **47**, 394–402, doi:10.1183/13993003.01891-2015 (2016).

56 Lienhardt, C. *et al.* New Drugs for the Treatment of Tuberculosis: Needs, Challenges, Promise, and Prospects for the Future. *Journal of Infectious Diseases* **205**, S241-S249, doi:10.1093/infdis/jis034 (2012).

57 Dunn, E. A. *et al.* Incorporation of triphenylphosphonium functionality improves the inhibitory properties of phenothiazine derivatives in *Mycobacterium tuberculosis*. *Bioorganic & medicinal chemistry* **22**, 5320-5328, doi:10.1016/j.bmc.2014.07.050 (2014).

58 Zhang, Y. & Mitchison, D. The curious characteristics of pyrazinamide: a review. *The International Journal of Tuberculosis and Lung Disease* **7, No 1**, 6-21 (2003).

59 Zimhony, O., Vilcheze, C., Arai, M., Welch, J. T. & Jacobs, W. R., Jr. Pyrazinoic acid and its n-propyl ester inhibit fatty acid synthase type I in replicating tubercle bacilli. *Antimicrobial agents and chemotherapy* **51**, 752-754, doi:10.1128/AAC.01369-06 (2007).

60 Villemagne, B. *et al.* Tuberculosis: the drug development pipeline at a glance. *European journal of medicinal chemistry* **51**, 1-16, doi:10.1016/j.ejmech.2012.02.033 (2012).

61 Shi, W. *et al.* Pyrazinamide Inhibits Trans-Translation in *Mycobacterium tuberculosis*. *Science* **333**, 630-1632 (2011).

62 Lu, P. *et al.* Pyrazinoic Acid Decreases the Proton Motive Force, Respiratory ATP Synthesis Activity, and Cellular ATP Levels. *Antimicrobial agents and chemotherapy* **55**, 5354-5357, doi:10.1128/aac.00507-11 (2011).

63 Neuhaus, F. C. & Lynch, J. L. The Enzymatic Synthesis of D-Alanyl-malanine. 111. On the Inhibition of D-Alanyl-D-alanine Synthetase by the Antibiotic D-Cycloserine*. *Biochemistry* **3, No 4**, 471-480 (1964).

64 Almeida Da Silva, P. E. & Palomino, J. C. Molecular basis and mechanisms of drug resistance in *Mycobacterium tuberculosis*: classical and new drugs. *J Antimicrob Chemother* **66**, 1417-1430, doi:10.1093/jac/dkr173 (2011).

65 Caminero, J. A., Sotgiu, G., Zumla, A. & Migliori, G. B. Best drug treatment for multidrug-resistant and extensively drug-resistant tuberculosis. *The Lancet Infectious Diseases* **10**, 621–629, doi:doi.org/10.1016/S1473-3099(10)70139-0 (2010).

66 Chan, E. D. *et al.* Treatment and outcome analysis of 205 patients with multidrug-resistant tuberculosis. *Am J Respir Crit Care Med* **169**, 1103-1109, doi:10.1164/rccm.200308-1159OC (2004).

67 Caminero, J. A. Treatment of multidrug-resistant tuberculosis: evidence and controversies. *The International Journal of Tuberculosis and Lung Disease* **10, No. 8**, 829-837 (2006).

68 Drlica, K. Mechanism of fluoroquinolone action. *Current opinion in microbiology* **2**, 504–508 (1999).

69 Nilewar, S. S. & Kathiravan, M. K. Mycothiol: a promising antitubercular target. *Bioorganic chemistry* **52**, 62-68, doi:10.1016/j.bioorg.2013.11.004 (2014).

70 Emani, C. S. *et al.* Ergothioneine Is a Secreted Antioxidant in *mycobacterium smegmatis*. *Antimicrobial agents and chemotherapy* **57**, 3202 (2013).

71 Vilcheze, C. *et al.* Coresistance to isoniazid and ethionamide maps to mycothiol biosynthetic genes in Mycobacterium bovis. *Antimicrobial agents and chemotherapy* **55**, 4422-4423, doi:10.1128/AAC.00564-11 (2011).

72 Bhaskar, A. *et al.* Reengineering redox sensitive GFP to measure mycothiol redox potential of Mycobacterium tuberculosis during infection. *PLoS Pathog* **10**, e1003902, doi:10.1371/journal.ppat.1003902 (2014).

73 Rawat, M. *et al.* Mycothiol-Deficient *Mycobacterium smegmatis* Mutants Are Hypersensitive to Alkylating Agents, Free Radicals, and Antibiotics. *Antimicrobial agents and chemotherapy* **46**, 3348-3355, doi:10.1128/aac.46.11.3348-3355.2002 (2002).

74 Ta, P., Buchmeier, N., Newton, G. L., Rawat, M. & Fahey, R. C. Organic hydroperoxide resistance protein and ergothioneine compensate for loss of mycothiol in *Mycobacterium smegmatis* mutants. *Journal of bacteriology* **193**, 1981-1990, doi:10.1128/JB.01402-10 (2011).

75 Richard-Greenblatt, M. *et al.* Regulation of Ergothioneine Biosynthesis and Its Effect on *Mycobacterium tuberculosis* Growth and Infectivity. *The Journal of biological chemistry* **290**, 23064-23076, doi:10.1074/jbc.M115.648642 (2015).

76 Castellano, I. *et al.* Shedding light on ovothiol biosynthesis in marine metazoans. *Scientific reports* **6** 21506, doi:10.1038/srep21506 (2016).

77 Russo, G. L., Russo, M., Castellano, I., Napolitano, A. & Palumbo, A. Ovothiol isolated from sea urchin oocytes induces autophagy in the Hep-G2 cell line. *Marine drugs* **12**, 4069-4085, doi:10.3390/md12074069 (2014).

Chapter 2 Synthesis of the newly discovered vitamin, ergothioneine

2.1. Background

Ergothioneine is the newly discovered vitamin therefore huge interest worldwide in the molecule has been unveiled. Ergothioneine's beneficial role has encouraged the scientific community to study this unique molecule in depth. Since its discovery in 1909, every year an average of 14 ergothioneine-related papers were per annum published. However, since 2006 this number has increased drastically. In 2013 alone there were about 88 publications while in 2016 around 103 publications were published, thus demonstrating growing interest in ergothioneine over the last decade. (Figure 2.1)

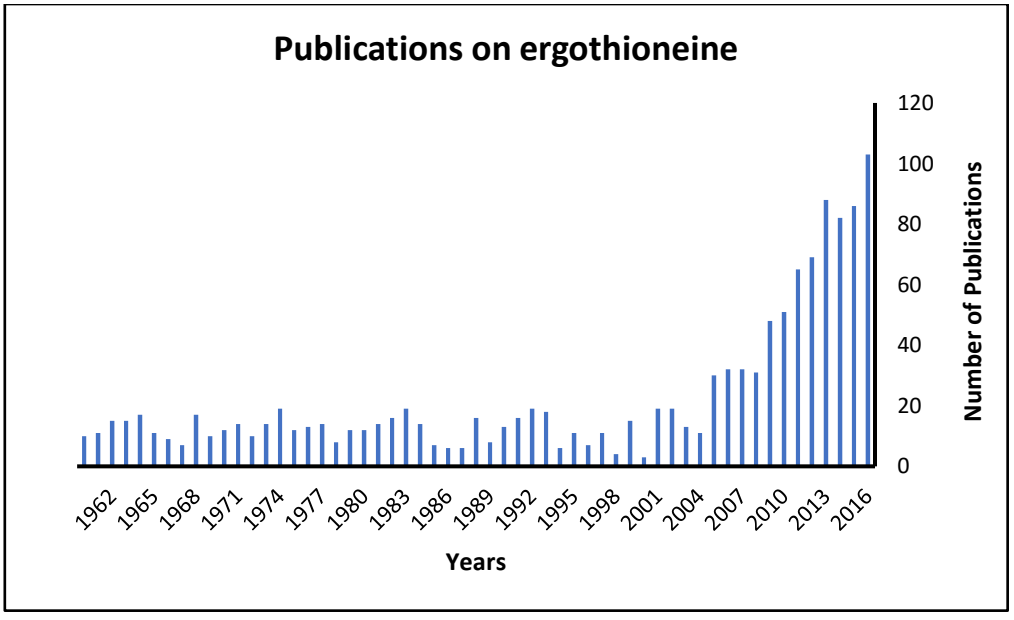

Figure 2.1. Ergothioneine-related publications over the last 55 years. Graph exported from www.scifinder.cas.org.[1] (accessed on 02/12/2016)

Ergothioneine is a powerful antioxidant thought to protect human skin, therefore it is extensively used as principal ingredient in the formulation of skin care products.[2] The cosmetic industry uses the majority of the worldwide ergothioneine production. L'Oreal, a French cosmetic company, includes ergothioneine in its list of antioxidants in many of their patents for cosmetic and hair care application. Ergothioneine has also been administrated as a dietary supplement known to boost immunity.

Ergothioneine can be isolated from organisms such as bacteria, though it is mostly isolated from mushrooms. Very recently, Wenxia *et al.* isolated *L*-ergothioneine from mushroom mycelium in a very low yield of 0.01-0.32% after hot water treatment, ultracentrifugation and chromatography using a mobile phase consisting of a mixture of acetonitrile-water (ratio 80:20 to 88:12).[3] This extremely low yielding effort is common for natural ergothioneine extracts. Hence, it is not economically viable to achieve a considerable scale of ergothioneine (Kg) production by isolating ergothioneine from natural sources.

Commercial interest in ergothioneine has led chemists to embark on developing more efficient synthetic processes. Despite ergothioneine's apparent simple structure, it's synthesis is found to be very challenging. To date only few total chemical synthetic methods for *L*-(+)-ergothioneine have been published.[4-6] Five major challenges can be considered when attempting the synthesis of *L*-(+)-ergothioneine (Figure 2.2):

1. Orthogonal selective protection of the α-amino and carboxylic acid groups of histidine.

2. Complete *N*-trimethylation of the *N*-α amino group.

3. Regioselective thionation of the imidazole moiety.

4. Preservation of the natural stereochemistry, avoiding or limiting any possible racemization throughout the process.

5. Global deprotection.

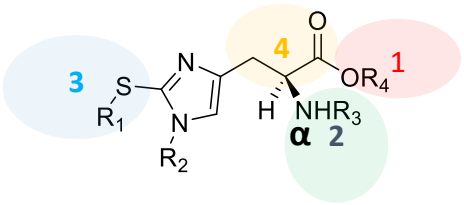

Figure 2.2. *L*-(+)-ergothioneine chemical structure highlighting chemical synthetic challenges.

2.2. Ergothioneine chemical synthesis.

2.2.1. Synthesis of *L*-ergothioneine using phenylchlorothionoformate (PCTF) as the sulfur source.[4,7]

2.2.1.1. Synthesis of *L*-ergothioneine according to Yadan.

In the latter part of the 20th century, French chemists Yadan *et al.* published a patent of *L*-ergothioneine chemical synthesis starting from *L*-histidine, the natural precursor.[4] This process involved multiple steps, starting by the protection of the carboxylic group followed by methylation of the *N*-α amino moiety.

The key step was the thionation, *via* a Bamberger type imidazole cleavage. The sequential cleavage and reformation of imidazole ring **2.4** allow the introduction of a thiol functionality at the 2-position using phenylchlorothionoformate (PCTF) as sulfur donor.[7] (Figure 2.3)

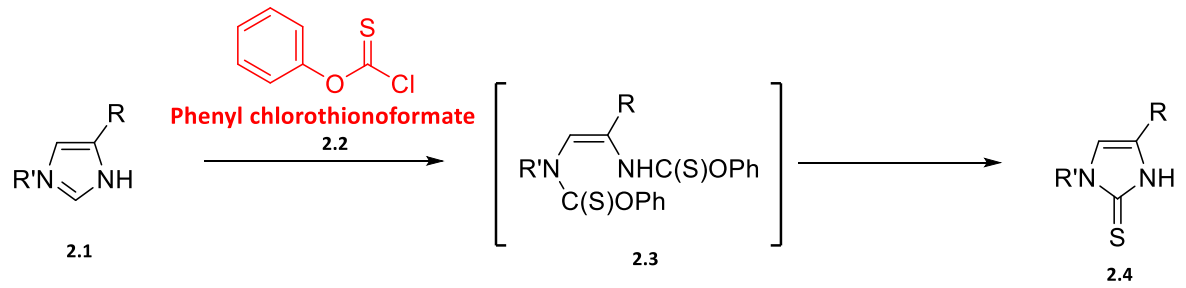

Figure 2.3. Bamberger-type cleavage: an AN-RORC process (addition of nucleophile, ring opening, ring closure).[7]

The thiol group and the nitrogen at the C-3 position of the mercapto ring were protected as an ethyl carbamate. Quartenarization and deprotection yield *L*-ergothioneine **2.10** in an overall yield of 34%. (Scheme 2.1)

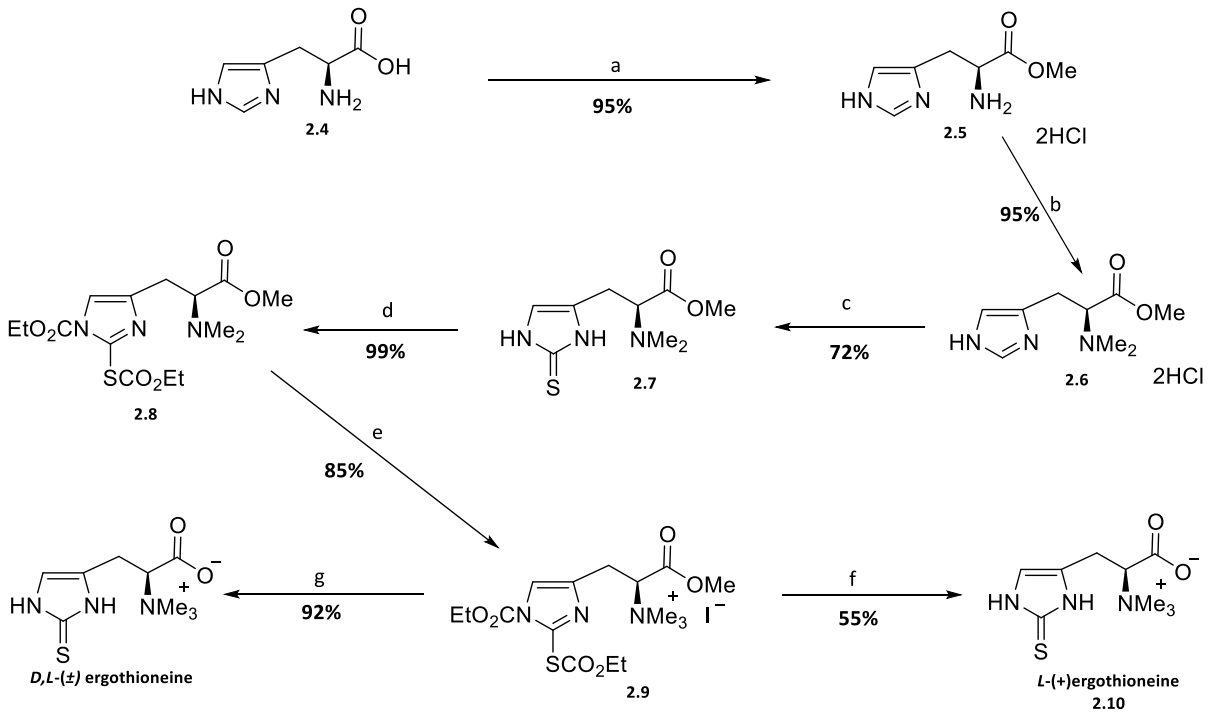

Scheme 2.1. *L*-ergothioneine synthesis according to Yadan.[4,7] Reagents and conditions. (a) MeOH, gaseous HCl; (b) 37% aqueous CH_2O, H_2, 10% Pd/C , rt; (c) (i). PCTF, $NaHCO_3$, H_2O/Et_2O, (ii) TEA, MeOH, rt (d) $ClCO_2Et$, TEA,

CH_2Cl_2, 10 °C; (e) MeI, THF , rt; (f) Conc HCl, 75 equiv $HSCH_2CH_2CO_2H$; (g) TEA, H_2O/MeOH, 60°C. **Overall yield 34%.**[4,7]

2.2.1.2. Drawbacks

Despite the fact that this method was one of the earliest breakthroughs, it has many drawbacks. Beside numerous of steps, this approach uses toxic and hazardous phenylchlorothionoformate in the key step. Moreover, this method involved tedious chromatographic purifications. Hydrolysis under basic conditions (TEA) in the final step yields ergothioneine as a racemate (*D,L*- (±)). This process was difficult to reproduce in our laboratory.

2.2.2. Synthesis of *L*-ergothioneine using potassium thiocyanate (KSCN) as the sulfur source.[5]

2.2.2.1. Synthesis of *L*-ergothioneine according to Trampota.

Fifteen years later (in 2010) Trampota published a patent very similar to that of Yadan.[5] This method successfully utilised the Bamberger cleavage reaction without any noticeable racemisation. The inorganic salt KSCN was used as the sulfur source and thionation was conducted prior to methylation, in contrast to the Yadan process. The mercaptohistidine **2.14** was first *S*-protected by a readily removable *t*-butyl group.

One of the critical steps was the methylation of the *N*-α amino group. The author utilised the mild reductive amination method using sodium triacetoxyborohydride as a reducing reagent.

Quaternarization and deprotection afforded *L*-ergothioneine in an overall yield of 21%. (Scheme 2.2)

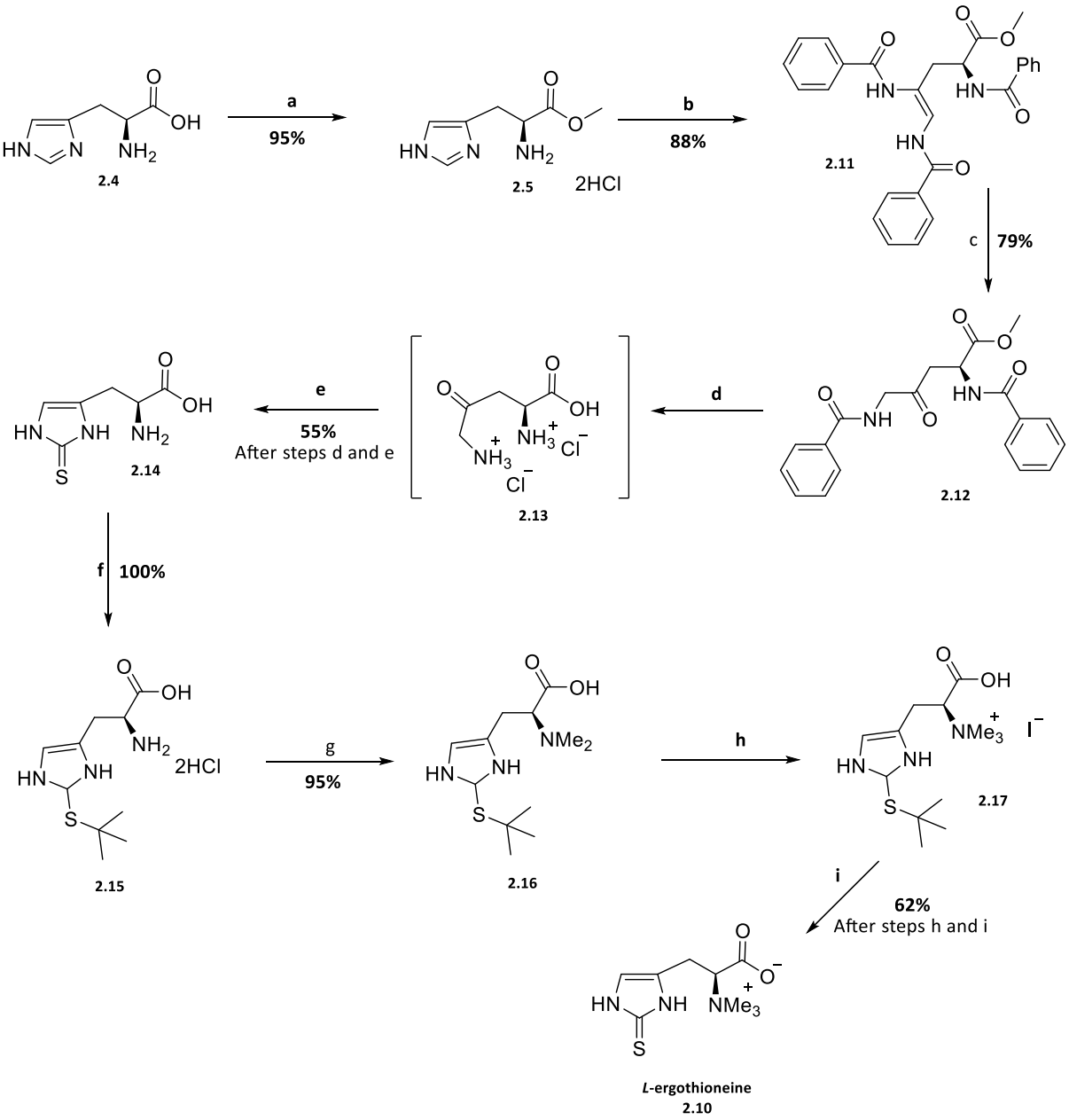

Scheme 2.2. *L*-ergothioneine synthesis according to Trampota.[5] Reagents and conditions. a) MeOH, gaseous HCl b) (i) H_2O/THF, $NaHCO_3$, BzCl (ii) Et_2O/TEA c) MeOH, gaseous HCl d) concentrated HCl, 90°C, 15hr e) H_2O, KSCN, 90°C, 3hr f) (i) H_2O, *t*-butanol, concentrated HCl, 90°C, 3hr (ii) Sodium Acetate, 2-propanol; g) THF, 37% aqueous CH_2O, $NaBH(OAc)_3$, 10°C h) MeOH, NH_4OH, MeI, rt i) 40 mol equivalents concentrated HCl, 20 mol equivalents $CH_3CHSHCO_2H$, 110°C, 18hr. **Overall yield 21%.**[5]

The author claimed to have developed a simple process as a limited amount of chromatographic purifications were performed, scalable, short and efficient to synthesize an optically pure *L*-(+)-ergothioneine after crystallisation and recrystallization.

2.2.2.2. Drawbacks

Despite these improvements, the overall yield remains around 20 - 30 % similar to Yadan's process probably due to multiple steps. Moreover, this process still uses a toxic sulfur source (KSCN) as well as a considerable amount of concentrated inorganic acid (e.g up to 40 mol equivalent of concentrated HCl in the last step) which drastically increases the waste stream. (Scheme 2.2)

2.2.3. Biomimetic synthesis of *L*-ergothioneine using cysteine as the sulfur source.[8]

In 2012, Erdelmeier *et al.* published a biomimetic synthesis of *L*-ergothioneine.[6,8] The first two steps involved the *N*-quaternarization of histidine **2.4** to afford hercynine **2.18** in a good yield of 70-80% according to the published method by Reinhold *et al*.[9] The key step was the synthesis of 2-cysteinylhercynine thioether intermediate **2.19** using cysteine, a natural and non-toxic sulfur donor in aqueous solvent. The last step was a pyrolytic *C-S* cleavage of the thioether **2.19** scavenged by 3-mercaptopropionic acid to yield *L*-ergothioneine **2.10**. (Scheme 2.3)

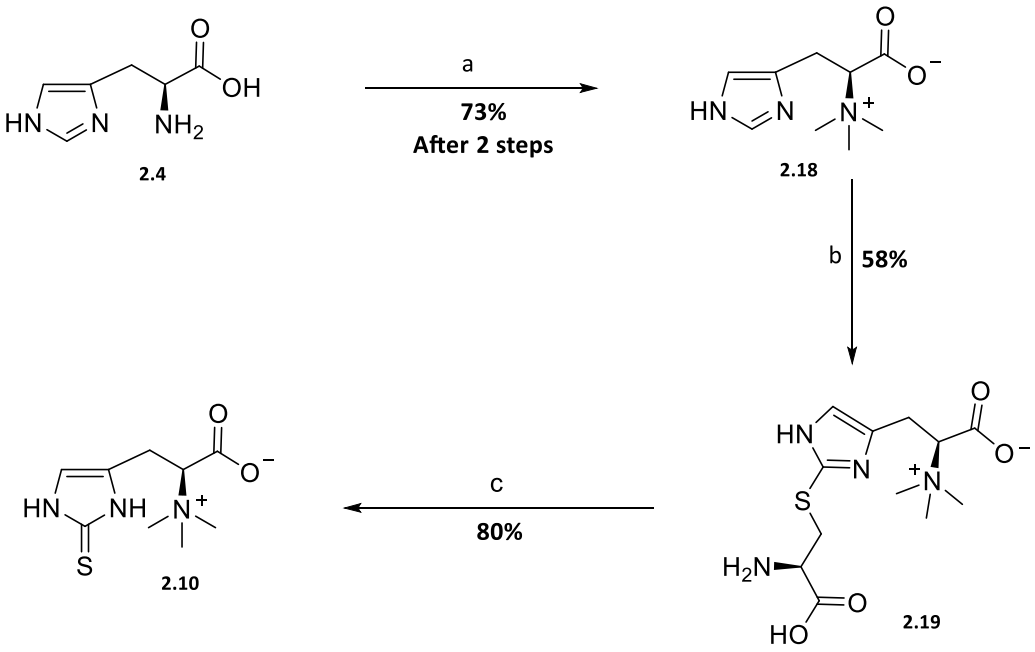

Scheme 2.3. Biomimetic *L*-ergothioneine synthesis according to Erdelmeier *et al*.[6,8] Reagents and conditions**.** a) 2 steps according to Reinhold *et al.* method,[9] 73% b) (i) HCl/Br_2 (1.3 mol equivalents), (ii) cysteine (3-5 mol equivalents), H_2O, 1 hr at 0°C, 58% optimum yield, c) 3-mercaptopropionic acid, 18 hr at 90-100°C, 80%, **Overall yield 34%.**

2.2.3.1. Biomimetic synthesis of the key intermediate, 2-cysteinylhercynine thioether

The biomimetic reaction was inspired by Ito who discovered the formation of an unusual thioether bond at the 2-position of imidazole ring after reacting bromine with histidine **2.4** to generate a bromo-activated histidine. This subsequently reacts with cysteine **2.20** to form 2-*S*-cysteinyl histidine **2.21** in a very low yield of 19%. (Scheme 2.4)[10]

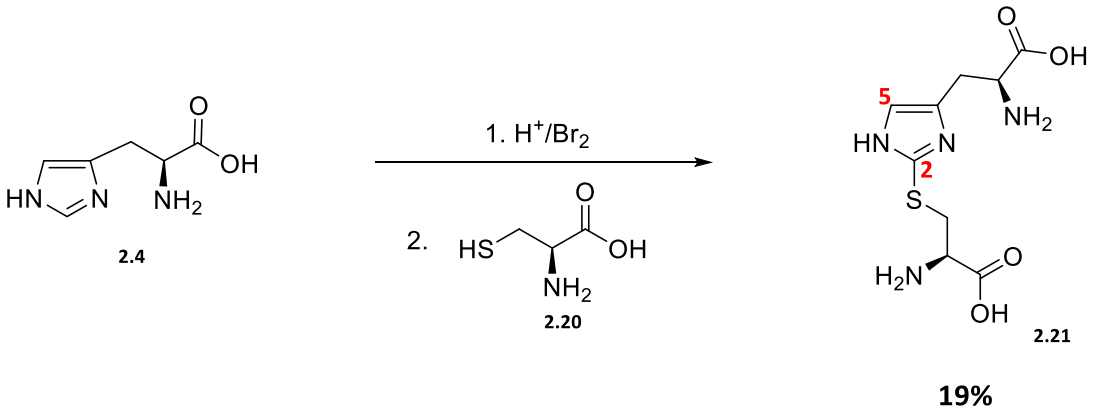

Scheme 2.4. Synthesis of 2-*S*-cysteinyl histidine 2.21 according to Ito.[10]

Histidine **2.4** is the biosynthetic precursor of hercynine **2.18**,[11] hence the same methodology as depicted in the Scheme 2.4 was optimized using hercynine **2.18** as a starting material. The large excess of cysteine (3-5 mol equivalents), bromination in an aqueous acidic medium (0.5 M) in an ice bath 0-5 °C. These conditions were optimal to afford 2-cysteinylhercynine thioether **2.19** in a moderate yield of 46-58%.

However, the excess cysteine can be removed by Dowex-H^+ ionic exchange chromatography or by reacting the reaction mixture with benzaldehyde to yield the readily removable phenylthiazolidine-carboxylic acid.[12] (Scheme 2.5) Alternatively the excess cysteine can be oxidised to cystine which is easy removed by filtration.[13]

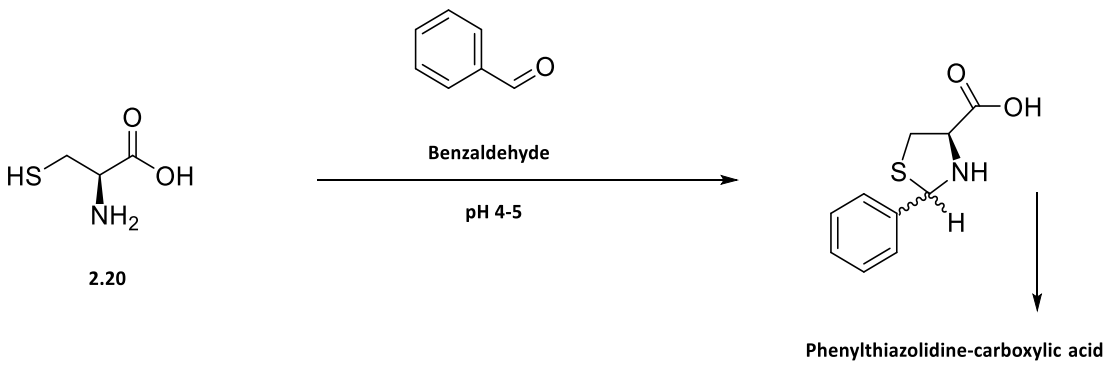

Scheme 2.5. Removal of the excess of cysteine.[8]

Mechanistically, the reaction proceeds *via* a reactive bromolactone intermediate, produced by the reaction of bromine with hercynine, which is followed by cysteine introduction to afford the target sulfide compound, 2-cysteinylhercynine thioether **2.19**. (Scheme 2.6)

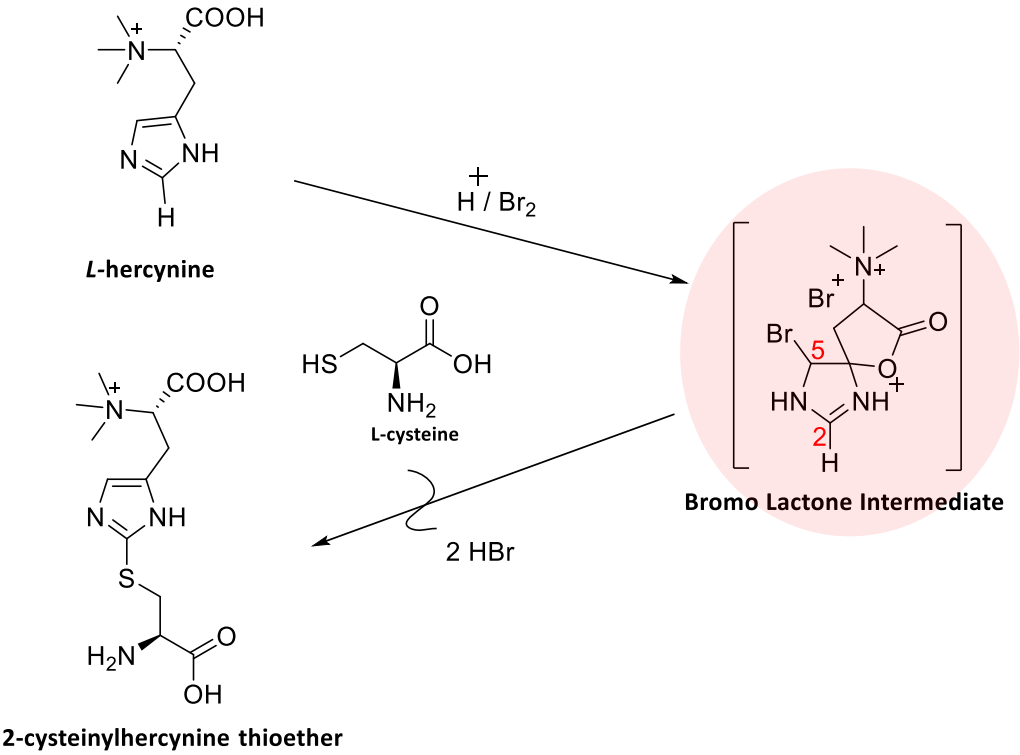

Scheme 2.6. Proposed mechanism of cysteine oxidative introduction. [8]

2.2.3.2. Pyrolytic cleavage of 2-cysteinylhercynine thioether yields *L*-ergothioneine

The last step is the pyrolytic cleavage of thioether **2.19** in a presence of large excess of the 3-mercaptopropionic acid scavenger. 3-Mercaptopropionic acid selectively reacts *in situ* with pyruvate **2.23** (by-product) to form the corresponding dithioketal **2.24**, which is readily extracted alongside the unreacted 3-mercaptopropionic acid **2.22** in ethyl acetate. This facilitates the isolation of the desired product, *L*-ergothioneine **2.10** in 80% yield after crystallization without any chromatographic purification. (Scheme 2.7)

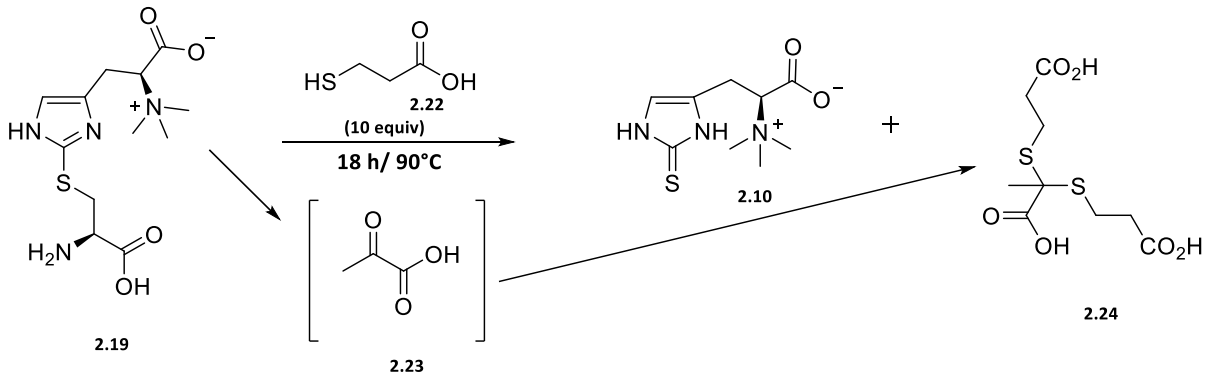

Scheme 2.7. Pyrolytic cleavage of 2-cysteinylhercynine thioether 2.19 scavenged by 3- mercaptopropionic acid 2.22.

Although alternative *C-S* cleavage methods exist, such as heating at 100 °C for 18 h using a large excess of red phosphorus in hydroiodic acid medium, the latter was unacceptable due to the toxic waste that would be generated and tedious chromatographic purifications required.[10]

Even though the mechanism of thermal cleavage of aryl-alkyl-sulfoxides are well known,[14] the mechanism of pyrolysis of the thioether on the other hand remains unclear. Nevertheless,

the reaction still progresses smoothly even under anaerobic conditions, thus suggesting that the reactive intermediate is not the sulfoxide (oxidation product of thioether).

2.2.3.3. Drawbacks

Despite the fact that this process has implemented many improvements, it is noteworthy to highlight some of the drawbacks such as the use of highly hazardous and toxic liquid bromine. Even though greener bromination methods are well documented,[15] Erdelmeier *et al.* evaluated four alternative bromination methods which produced bromine *in situ*.[8]

It is noteworthy that this process was hampered by huge amounts of inorganics salts (by product) which required ion exchange chromatography and reverse osmosis to allow isolation of the target product, *L*-ergothioneine.

Finally, the reproducibility of this process was poor in our hands. This method required strict temperature control, stoichiometry of reactants and concentration of the reaction mixture, that provided much lower yields than the 46-58% reported.[8]

In order to obtain a scalable, reproducible and high yielding ergothioneine chemical synthesis many drawbacks from previously reported process have to be addressed. The ideal process must also be shorter (fewer steps), allow simple purification, greener (using less or not toxic reagent or solvent) and more importantly affords an optically pure product for human consumption.

2.3. Improved synthesis of *L*-ergothioneine

During the course of this research, the strive toward developing a novel ergothioneine synthesis was attempted by addressing some of the drawbacks of past processes.

2.3.1. Retrosynthetic analysis

The retrosynthesis leads to a simple commercially available protected histidine **2.26**, that affords hercynine derivative **2.15** through *Nα*-methylation as well as thionation using different approaches depending on the nature of the sulfur sources utilised. (Figure 2.4) According to this strategy, thionation requires the imidazole ring to be activated *via* bromination.

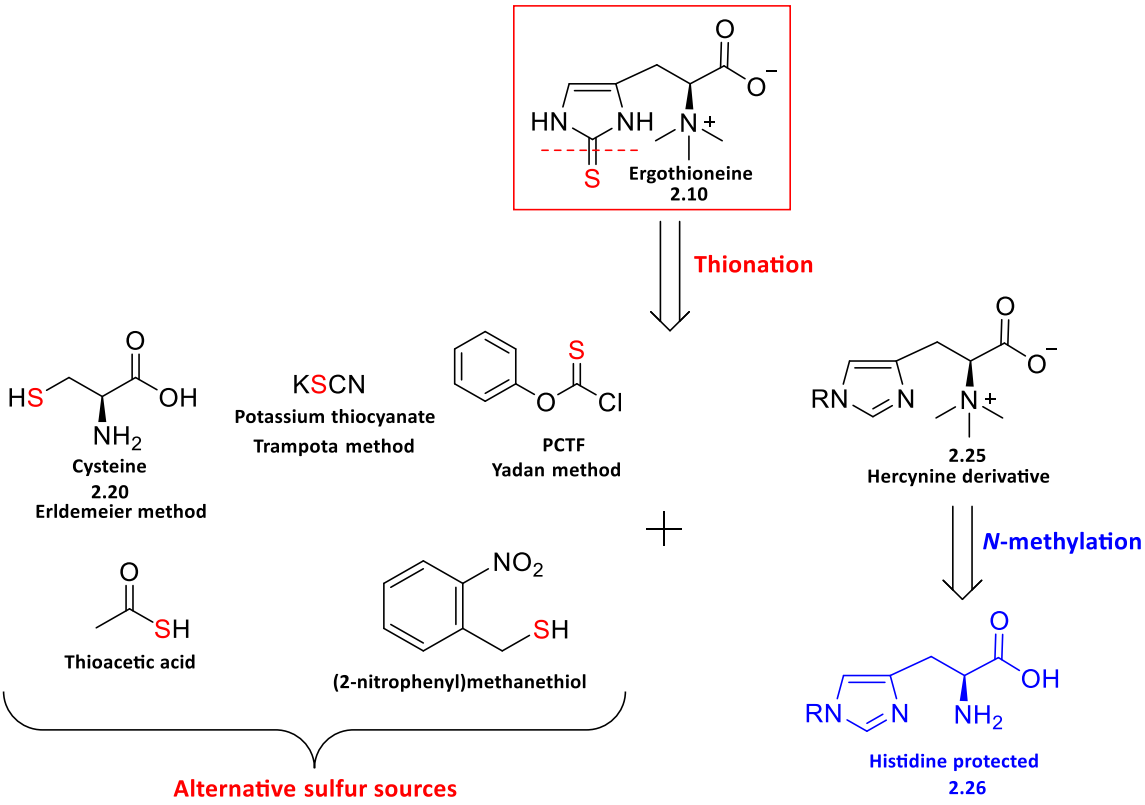

Figure 2.4. Retrosynthesis strategy of *L*-ergothioneine 2.10.

To date only few sulfur sources have been explored such as KSCN, PCTF (phenylchlorothionoformate), Na_2S, as well as cysteine. The ideal sulfur source must be easy to introduce and any unwanted moiety (protecting group) must be facile to remove.

2.3.2. Alternative sulfur sources to cysteine

Even though cysteine was successfully introduced, many efforts were conducted to find an alternative sulfur source, that is simple to introduce and which allow for easy subsequent removal of the unwanted protecting group.

Ito used Na_2S as sulfur to synthesize 2-thiohistidine in 12%, while Erdelmeier *et al.* claimed they detected only traces of *L*-ergothioneine (2-4%) when they reacted Na_2S as sulfur source on a bromine-activated hercynine (5 mmol-scale).[8,10] For industrial production, Na_2S is transformed to H_2S (direct sulfur source) in acidic medium. H_2S is toxic and hazardous gas thus the use of both Na_2S and H_2S reagents were found to be unattractive. Therefore, alternative sulfur sources were investigated.

2.3.2.1. (2-nitrophenyl)methanethiol

(2-Nitrophenyl)methanethiol **2.39** was the first alternative sulfur source investigated as the removal of the unwanted 2-nitrobenzyl moiety is facile and well documented.[16] Using UV lamp irradiation, an inexpensive photo-technology would efficiently remove the 2-nitrobenzyl unwanted moiety.

(2-Nitrophenyl)methanethiol **2.39** was synthesized in two consecutive steps in a good overall yield of 73% without the need of any chromatographic purification according to the literature.[17] In a S_N2 reaction 2-nitrobenzyl bromide **2.37** was transformed quantitatively into *S*-(2-nitrobenzyl) ethanethioate **2.38**, followed by *S*-deacetylation to yield the target product, (2-nitrophenyl)methanethiol **2.39**. (Scheme 2.8)

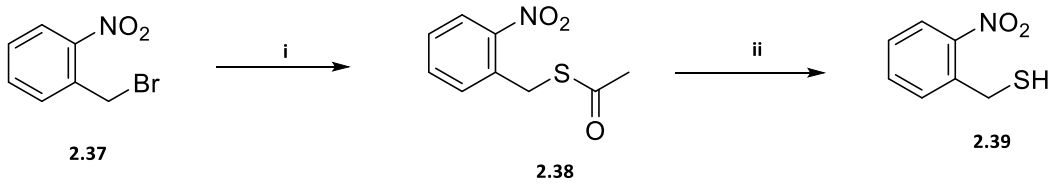

2.37 2.38 2.39

Scheme 2.8. Synthesis of (2-nitrophenyl)methanethiol 2.39. Reagents and conditions. (i) KSAc (potassium thioacetate) (5.3 mol equivalents), THF, overnight at rt, quantitative; (ii) MeOH/HCl, overnight at 60 °C, 73%.[17]

A key diagnostic in the ^{1}H NMR spectrum of *S*-(2-nitrobenzyl) ethanethioate **2.38** was the slightly deshielded proton signal resonated as a singlet at δ_H 2.31 ppm integrating for 3 protons thus confirming the presence of acetate group. While the ^{1}H NMR spectrum of **2.39** showed disappearance of acetate group present in **2.38** at δ_H 2.31 ppm and the appearance of a characteristic SH proton resonating as a triplet at δ_H 2.13 ppm (J = 8.4 Hz) suggesting a coupling with the methylene proton resonating as a doublet at δ_H 4.02 ppm (J = 8.4 Hz) (expended in the spectrum) in its neighbourhood. This confirmed the successful synthesis of (2-nitrophenyl)methanethiol **2.39**. (Figure 2.5)

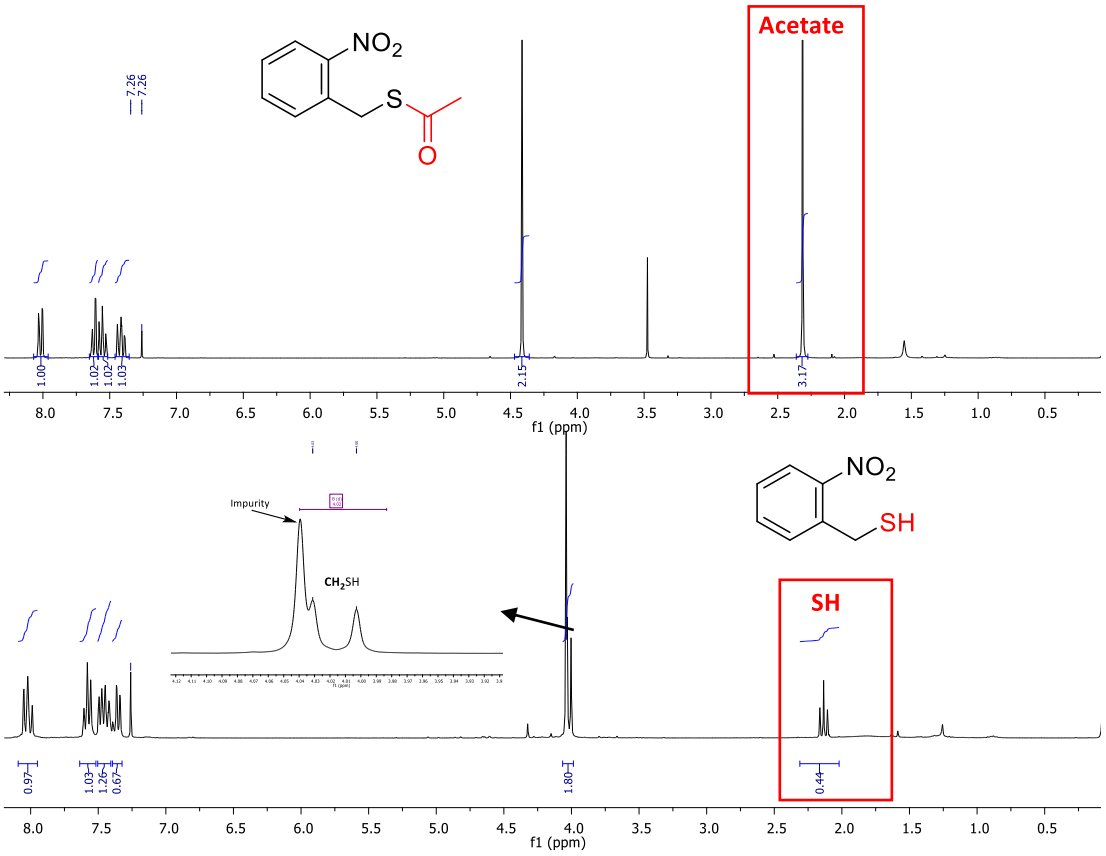

Figure 2.5. ^{1}**H NMR spectrum of 2.38 vs 2.39 showing successful deacetylation.**

Having (2-nitrophenyl)methanethiol **2.39** in our possession, it was utilised as a sulfur source. *N*-benzyl hercynine **2.30** was brominated by NBS followed by thiol addition using 1.5 mol equivalents of (2-nitrophenyl)methanethiol **2.39**. (Scheme 2.9)

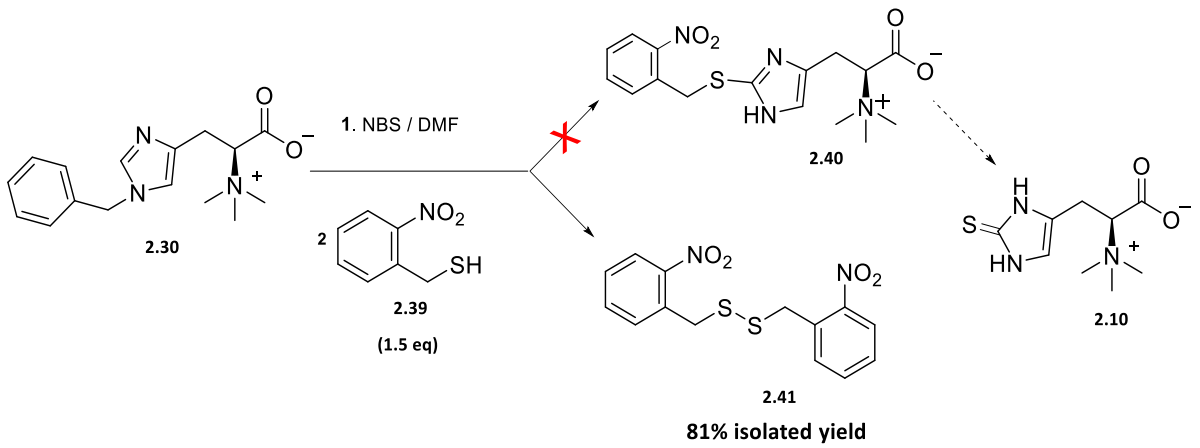

Scheme 2.9. Attempted synthesis of *L*-ergothioniene 2.10 using (2-nitrophenyl)methanethiol 2.39 as a sulfur source.

This reaction did not afford the desired product **2.40**, instead, the disulfide, 1,2-bis(2-nitrobenzyl)disulfane **2.41** was isolated in high yield of 81%. The evidence of this disulfide **2.41** was provided by the ^{1}H NMR spectrum which revealed the disappearance of the characteristic SH protons resonated at δ_H 2.13 ppm in proton NMR of **2.39**. (Figure 2.6)

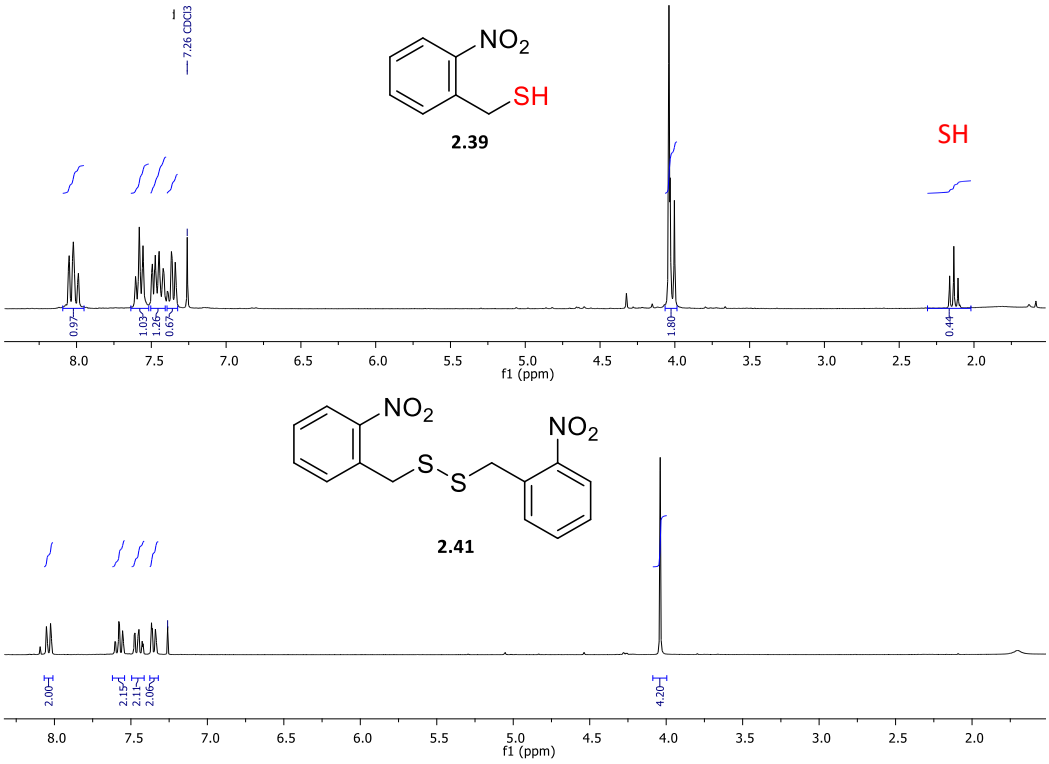

Figure 2.6. ^{1}H NMR spectrum confirming the oxidation of (2-nitrophenyl)methanethiol 2.39 to the disulfide 2.41.

Furthermore, EI$^+$ mass spectrum of **2.41** showed the molecular ion at *m/z* 336.0 $[M]^+$ calculated for $C_{14}H_{12}N_2O_4S_2$ 336.0, hence confirming the structure of the disulfide **2.41**.

These results suggested that (2-nitrophenyl)methanethiol **2.39** was easily oxidized to its disulfide form **2.41** under the reaction conditions (side reaction). That high isolated yield of 81% of disulfide recovery does not mean that the adduct **2.40** was not formed; it might have been produced at very low (< 5%) could not have been detected. It is noteworthy that this thiol (2-nitrophenyl)methanethiol **2.40** appeared to be malodorous with a very bad smell even at lower concentration, this does not make it a favoured sulfur source especially for

industrial scale. Therefore the investigation of (2-nitrophenyl)methanethiol **2.39** as a sulfur source for the synthesis of *L*-ergothioneine **2.10** was not pursued any further.

2.3.2.2. Thioacetic acid

Thioacetic acid **2.42** was also investigated as sulfur donor due to its facile deacetylation under basic conditions. We suggested to use an excess of thoacetic acid to compensate for potential side reactions hence 4 mol equivalents were utilized. One possible side reaction is the hydrolyse of thioacetic acid to acetic acid that could possibly occurred under the reaction conditions, therefore more than one mol equivalents are required to accomplish the sulfurization reaction.

N-benzyl hercynine **2.30** was brominated using NBS (2.0-2.5 mol equivalents) in DMF solvent, subsequently followed by the sulfurization using 4 mol equivalents of thioacetic acid **2.42**. Several attempts to isolate the pure (*S*)-3-(2-(acetylthio)-1*H*-imidazol-4-yl)-2-(trimethylammonio)propanoate **2.43** were unsuccessful due to its degradation, thus suggesting that this intermediate was unstable upon purification. Therefore, the crude residue **2.43** obtained after removal of solvent to dryness was immediately deacetylated under basic conditions (NaOMe) in methanol without any prior purification. Reverse phase chromatography afforded the target compound *L*-ergothioneine **2.10** which was contaminated by traces of desulfurized and acetylated products (Scheme 2.10).

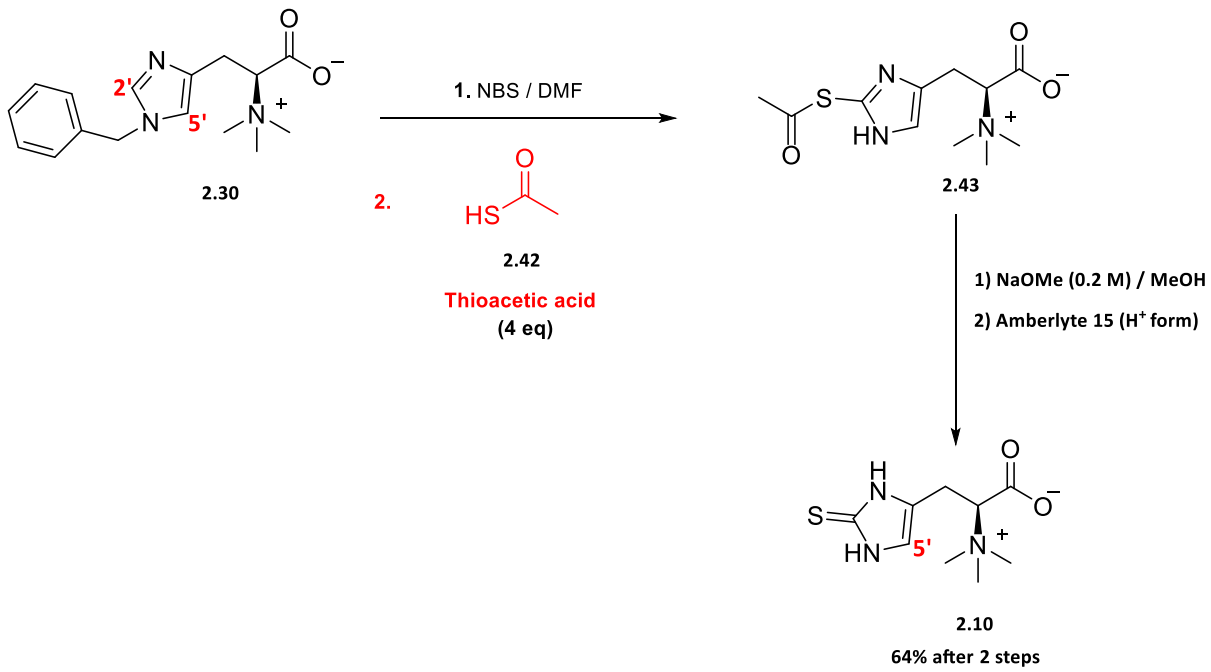

Scheme 2.10. *L*-ergothioneine 2.10 synthesis using thioacetic acid 2.42 as a sulfur donor.

The proton NMR analysis of the aromatic region (9.1-6.4 ppm) was consistent with the successful synthesis of the target compound, *L*-ergothioneine **2.10** as the major product of the reaction. (Scheme 2.10)

A key diagnostic signal was the disappearance of the imidazole proton H-2' which resonated as a singlet around δ_H 8.2 ppm in the ^{1}H NMR spectrum of (*S*)-3-(1-benzyl-1*H*-imidazol-4-yl)-2-(trimethylammonio)propanoate **2.30,** thus clearly confirmed the regioselective thionation at the 2-position of the imidazole ring. (Figure 2.7)

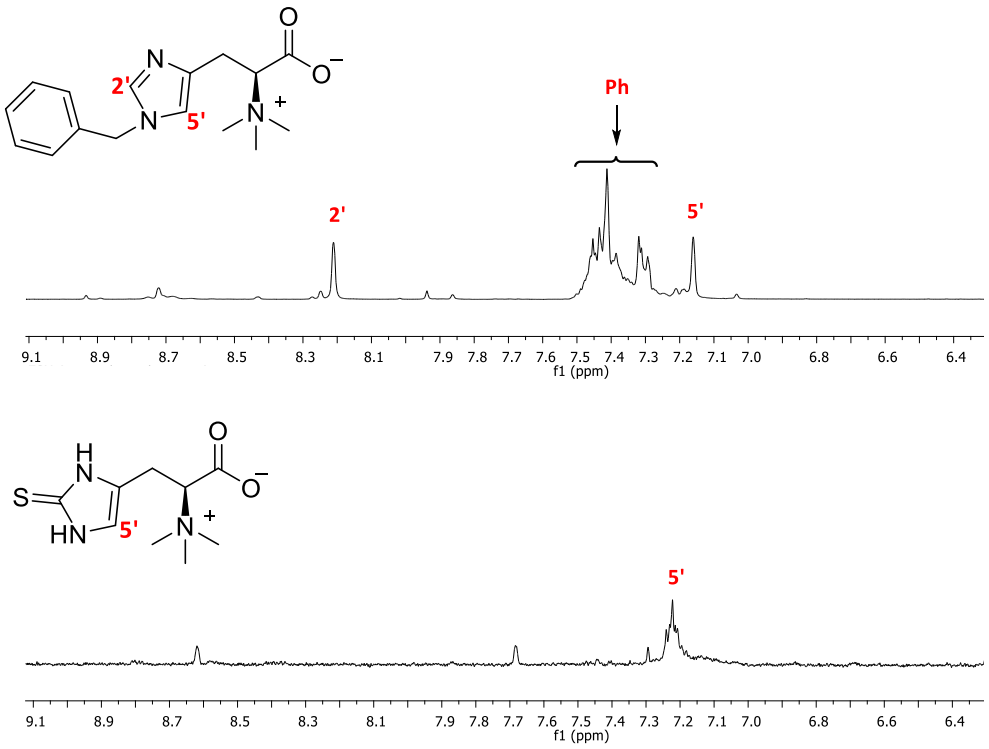

Figure 2.7. ^{1}**H NMR spectrum in** D_2O **at 300 MHz (aromatic region from 9.1 to 6.4 ppm) comparison between 2.30 & 2.10 obtained after sulfurization using thioacetic acid as the sulfur source.**

The reaction yield was calculated by integration of the aromatic region between 9.4 and 6.5 ppm assuming that the desired product formed are characterized by one aromatic H-5' proton. The desired product, *L*-ergothioneine **2.10** was obtained in a crude estimate yield of 64% based on ^{1}H NMR after two steps. Close ^{1}H NMR spectrum inspection revealed the presence of impurities as by-products of the reaction, including the desulfurized product, hercynine (14%) as depicted in the Figure 2.8.

The presence of the desulfurized product, hercynine was further confirmed by LCMS analysis which displayed the molecular ion at *m/z* 199.1239 as $[M+2H]^+$ (positive mode) calculated $C_9H_{17}N_3O_2^+$ (199.1315) at the retention time of 9.62 min. (Figure 2.9)

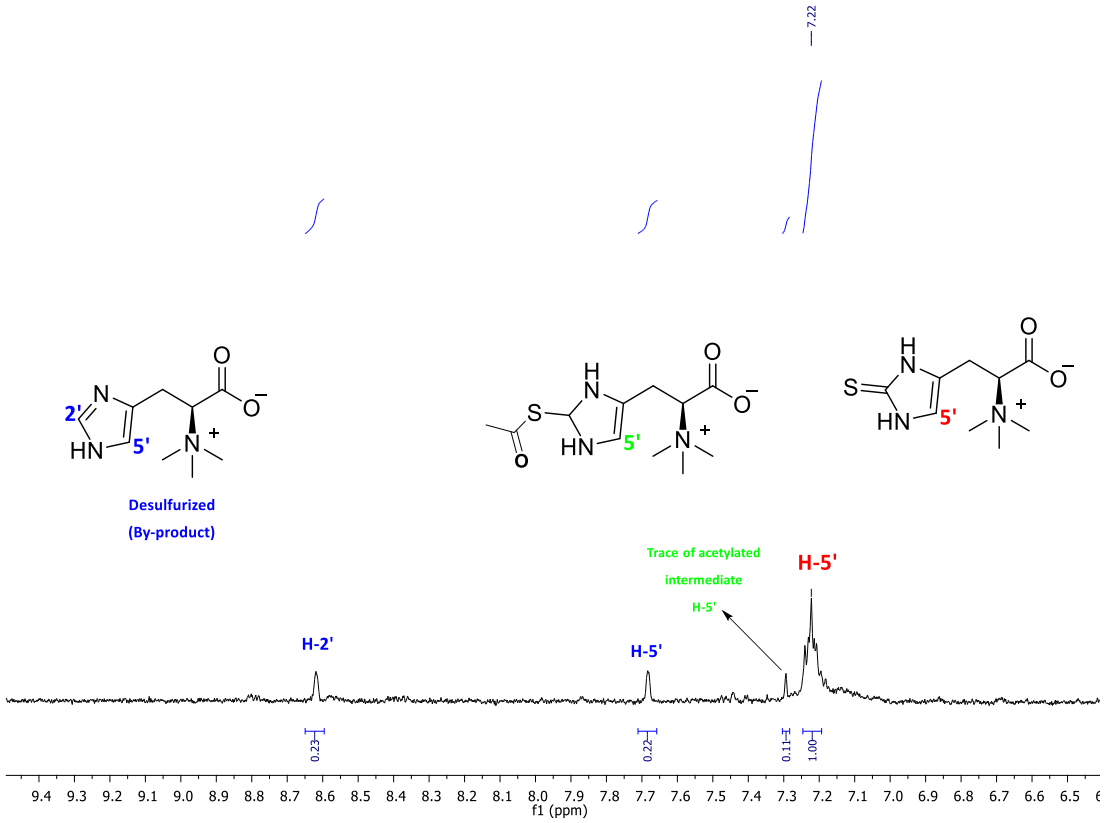

Figure 2.8. Reaction yield based upon ^{1}H NMR integration of the isolated *L*-ergothioneine 2.10 (aromatic region from 9.4 to 6.5 ppm) from the reaction using thioacetic acid as a sulfur source.

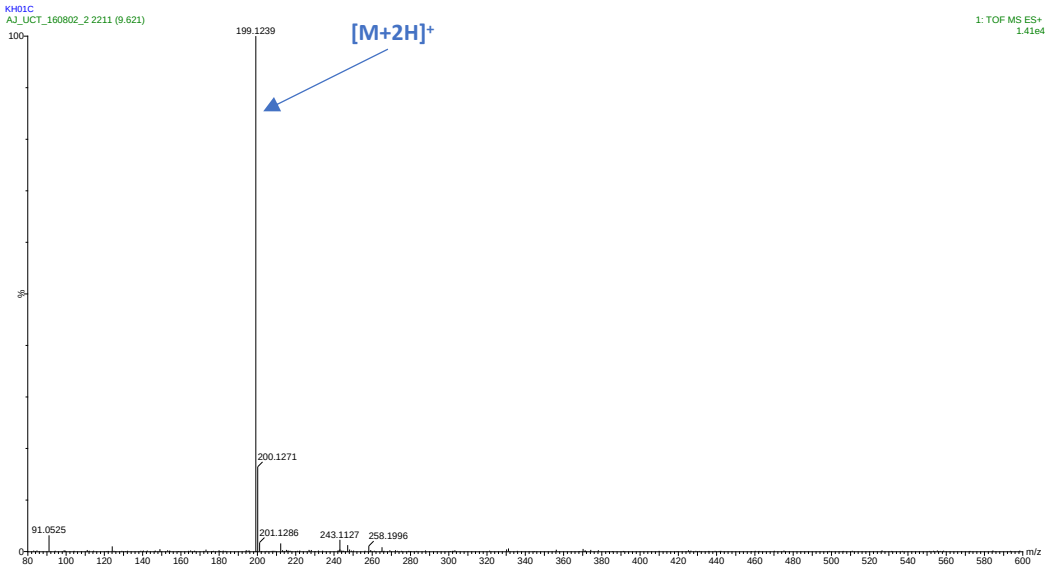

Figure 2.9. HRMS spectrum of the desulfurized product, hercynine. Retention time of 9.62 min. (Positive ionization mode) (ESI^{+}) and column (Waters BEH Amide, 2.1x100mm, Waters Synapt G2, Cone Voltage 15 V)

It is suggested that the *L*-ergothioneine **2.10** major product of the reaction could get oxidized under these strong oxidative and alkaline conditions (NBS/DMF, NaOMe) to form an highly unstable sulfinic acid derivative which degraded during the isolation process to form hercynine after elimination of sulfur dioxide. (Figure 2.10)[18,19] That could explain the presence of hercynine revealed in the ^{1}H NMR spectrum and confirmed by LCMS studies. (Figure 2.8 & Figure 2.9)

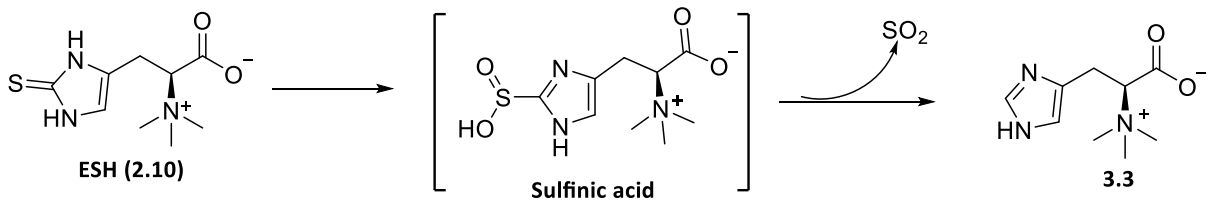

Figure 2.10. Model explaining the presence of the desulfurized product, hercynine.

Furthermore, the EI^+ mass spectrum (direct injection) analysis revealed the molecular ion of *L*-ergothioneine sodium adduct at *m/z* 253.7 calculated for $C_9H_{16}N_3NaO_2S^+$ (253.1) and the characteristic fragment at *m/z* 127.8 calculated for $C_5H_7N_2S^+$ 127.0 corresponding to a loss of $N(CH_3)_3$ and carbonyl groups, a similar fragmentation pattern with the one reported by Wang *et al.*[20] (Figure 2.11)

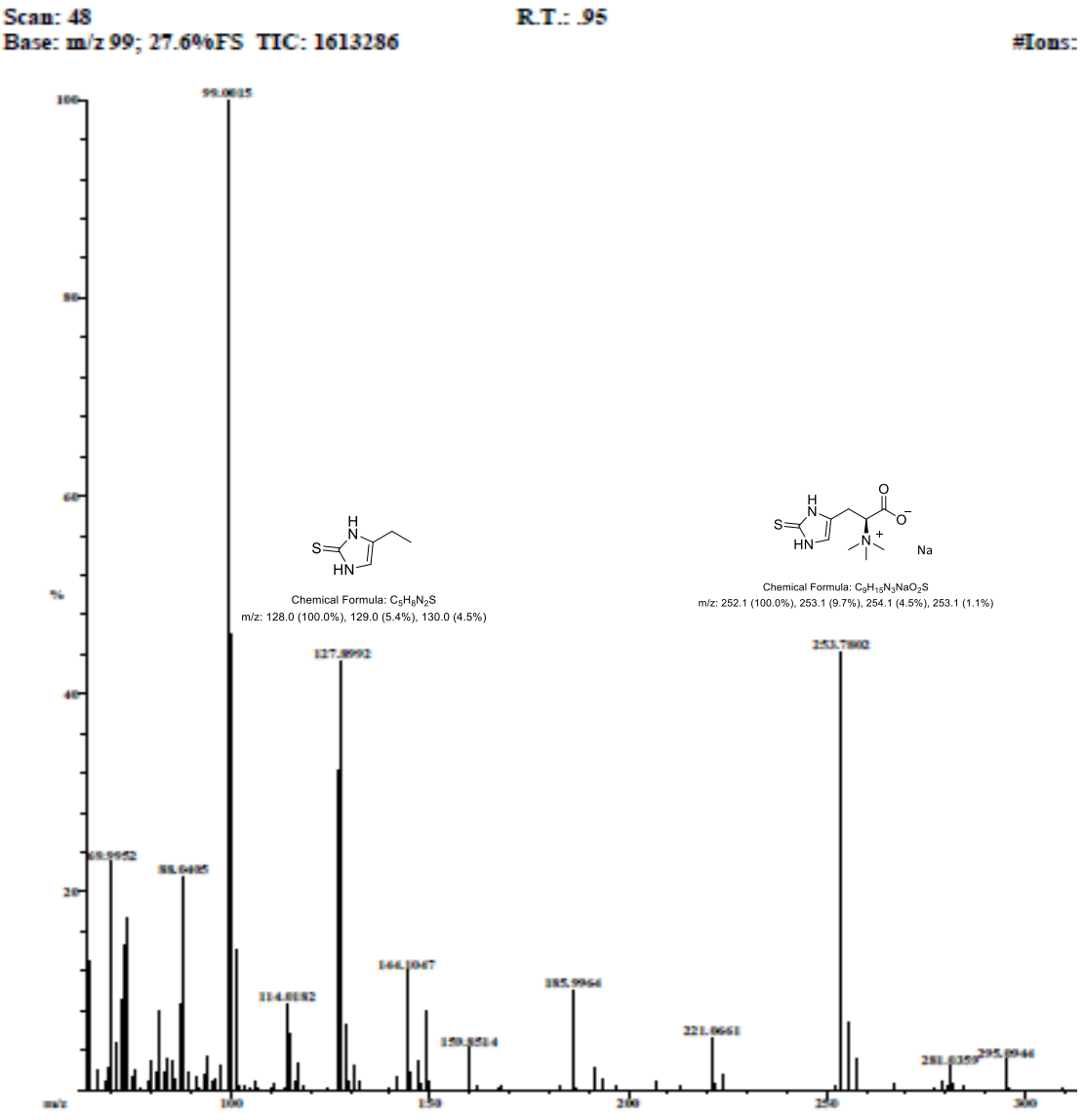

Figure 2.11. EI^+ mass spectrum of purified *L*-ergothioneine 2.10.

2.3.3. Improved synthesis of *L*-ergothioneine using cysteine as the sulfur source.

Early research conducted by Erdelmeier *et al.* have demonstrated the instability of hercynine upon bromination.[6,8] It was suggested that liquid bromine was consumed rapidly by hercynine, leading to the formation of a bromolactone hercynine intermediate (very unstable) which reacts with cysteine to form the desired sulfide.

Therefore, if the reaction mixture is not maintained at a low temperature (below 2 °C), it will lead to multiple decomposition products. Controlling the temperature and time of this reaction appeared to be very crucial. However, to date, attempts to isolate this bromolactone intermediate has been unsuccessful.

Ito has already proven the existence of bromolactone intermediate as the reaction only proceeded with the histidine derivative having a free carboxylate moiety. In other words, histidine esters did not provide the lactone intermediate, hence no sulfurization reaction had occurred.[10]

The first challenge was to select a starting material which will give rise to a more stable bromolactone derivative. The *N*-benzyl protected histidine seemed more attractive as a starting material. The benzyl group would also impart greater lipophilicity useful for C18 or silica purification. The presence of benzyl group attached to the imidazole group possibly exert a mesomeric effect which stabilises the heterocyclic ring.

2.3.3.1. Synthesis and characterisation of (*S*)-3-(1-benzyl-1*H*-imidazol-4-yl)-2-(trimethylammonio) propanoate (*N*-benzyl hercynine)

N^c-benzyl hercynine **2.30** was synthesized in three consecutive steps starting from the commercially available N^c-benzyl-N^α-(*tert*-butoxycarbonyl)-*L*-histidine **2.27**. Standard acid deprotection yielded N^c-benzyl-*L*-histidine **2.28** in an excellent yield of 90%. Direct reductive amination of N^c-benzyl-*L*-histidine using formaldehyde and sodium triacetoxyborohydride afforded the dimethyl product, N^c-benzyl-N^α,N^α-dimethyl-*L*-histidine **2.29** quantitatively. The last step entailed the quartenarization using iodomethane as an alkylating reagent to yield the protected hercynine, (*S*)-3-(1-benzyl-1*H*-imidazol-4-yl)-2-(trimethylammonio) propanoate **2.30** in an excellent yield of 93% (Scheme 2.11).

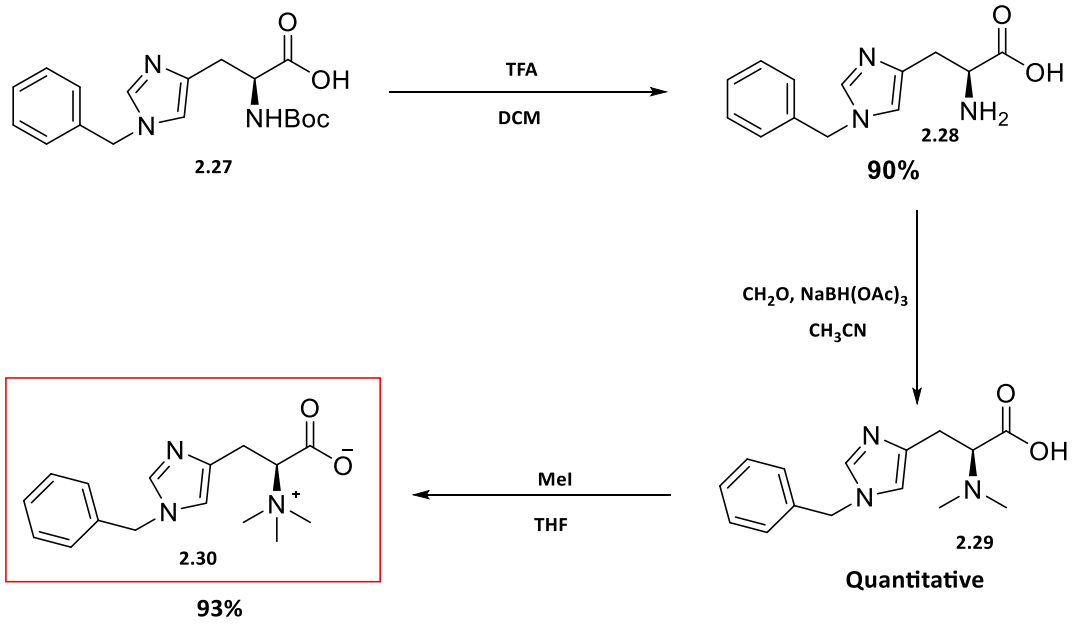

Scheme 2.11. Synthesis of (*S*)-3-(1-benzyl-1*H*-imidazol-4-yl)-2-(trimethylammonio) propanoate (N^c-benzyl hercynine 2.30).

The ^{1}H NMR spectrum of *N*-benzyl histidine **2.28** revealed the disappearance of Boc resonance around 1.5 ppm confirming the successful Boc removal. The successful synthesis of N^{c}-benzyl-N^{α},N^{α}-dimethyl-*L*-histidine **2.29** was confirmed by the ^{1}H NMR spectrum which displayed a characteristic deshielded singlet resonating at δ_H 2.69 ppm integrating for six protons confirming the successful introduction of two equivalent methyl groups. (Figure 2.12)

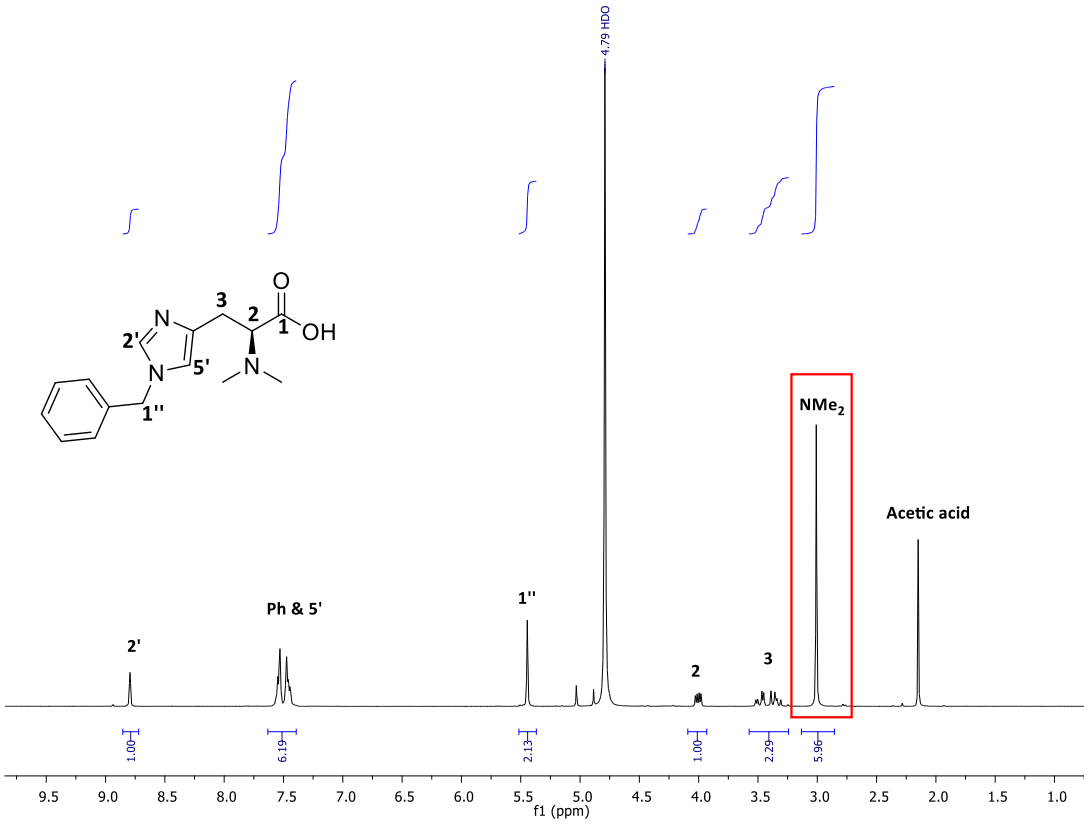

Figure 2.12. ^{1}H NMR spectrum of N^{c}-benzyl-N^{α},N^{α}-dimethyl-*L*-histidine 2.29 in D_2O at 300 MHz.

The ^{13}C NMR spectrum of N^{c}-benzyl-N^{α},N^{α}-dimethyl-*L*-histidine **2.29** displayed a carbonyl signal at δ_C 168.7 ppm, seven aromatic carbon signals resonated at δ_C 135.2, 135.1, 133.6, 129.4, 128.5, 127.6, 121.0 ppm, and four aliphatic carbon resonances at δ_C 66.0, 65.9, 52.9,

21.9 ppm, thus confirming the carbon skeleton identity of N^{c}-benzyl-N^{α},N^{α}-dimethyl-*L*-histidine **2.29**.

Furthermore, the EI^{+} mass spectrum displayed the molecular ion $[M]^{+}$ at *m/z* 273.1 calculated for $C_{15}H_{19}N_3O_2$ (273.1) as well as the molecular ion of a fragment corresponding to a loss of carbonyl group $[M\text{-}CO_2]^{+}$ at 229.1 calculated $C_{14}H_{19}N_3$ (229.2) $[M\text{-}CO_2]^{+}$ thus confirming the assigned structure of N^{c}-benzyl-N^{α},N^{α}-dimethyl-*L*-histidine **2.29.**

The last step entailed the quaternarization of N^{c}-benzyl-N^{α},N^{α}-dimethyl-*L*-histidine **2.29.** It is noteworthy, that the quaternarization reaction is usually a very difficult step as it often required the longest reaction time, suffered from low yield as the reaction barely reach completion and gave rise to certain degree of racemization.[21] In our case the racemization was not investigated but it was feared that prolonged treatment under basic conditions may lead to racemization.

The reaction was conducted in a dry tetrahydrofuran with iodomethane as an alkylating reagent for 1-2 days at room temperature, crystallization in absolute ethanol afforded (S)-3-(1-benzyl-1*H*-imidazol-4-yl)-2-(trimethylammonio) propanoate **2.30** as a yellow solid isolated in the iodide salt in a very high yield of 93%.

The ^{1}H NMR spectrum of (*S*)-3-(1-benzyl-1*H*-imidazol-4-yl)-2-(trimethylammonio) propanoate **2.30** revealed the disappearance of singlet resonance at δ_H 2.69 ppm belonging to dimethyl group and the appearance of a characteristic deshielded singlet at δ_H 3.33 ppm integrating for 9 protons which was attributed to *N,N,N*-trimethyl (betaine) group, thus confirming the successful quaternarization.

The ^{13}C NMR spectrum, corroborated by a mass spectrum confirmed the structure of the target compound, (*S*)-3-(1-benzyl-1*H*-imidazol-4-yl)-2-(trimethylammonio) propanoate **2.30.** The ESI^+ mass spectrum revealed the molecular ion $[MH]^+$ at *m/z* 288.2 calculated for $C_{16}H_{22}N_3O_2^+$ (288.2) $[MH]^+$, two characteristic fragments at *m/z* 244.2 calculated for $C_{15}H_{22}N_3^+$ (244.2) $[M\text{-}CO_2]^+$ corresponding to a loss of carbonyl and at *m/z* 199.2 calculated for $C_{12}H_{13}N_3$ (199.1) $[M\text{-}CO_2\text{–}CH_3)_3]^+$ corresponding to a loss of carbonyl and trimethyl group, hence supporting the structure of (*S*)-3-(1-benzyl-1*H*-imidazol-4-yl)-2-(trimethylammonio) propanoate **2.30**.

2.3.3.2. Synthesis and characterisation of (*S*)-3-(2-(((*R*)-2-amino-2-carboxyethyl)thio)-1*H*-imidazol-4-yl)-2-(trimethylammonio) propanoate (2-cysteinylhercynine thioether)

Having successfully synthesized *N*-benzyl hercynine **2.30**, the next challenge was to attempt the synthesis of 2-cysteinylhercynine thioether **2.19**. The synthesis of (*S*)-3-(2-(((*R*)-2-amino-2-carboxyethyl)thio)-1*H*-imidazol-4-yl)-2-(trimethylammonio) propanoate **2.19** was conducted in 2 consecutive steps. First *N*-benzyl hercynine **2.30** was brominated with 2.5 mol equivalents of *N*-bromosuccinimide (NBS) in DMF in the dark. Subsequent thionation using excess of *L*-cysteine (2-2.5 mol equivalents) as a sulfur donor afforded the 2-cysteinylhercynine thioether acetate salt **2.19** in a good yield of 76% after C18 reverse phase chromatography. (Scheme 2.12)

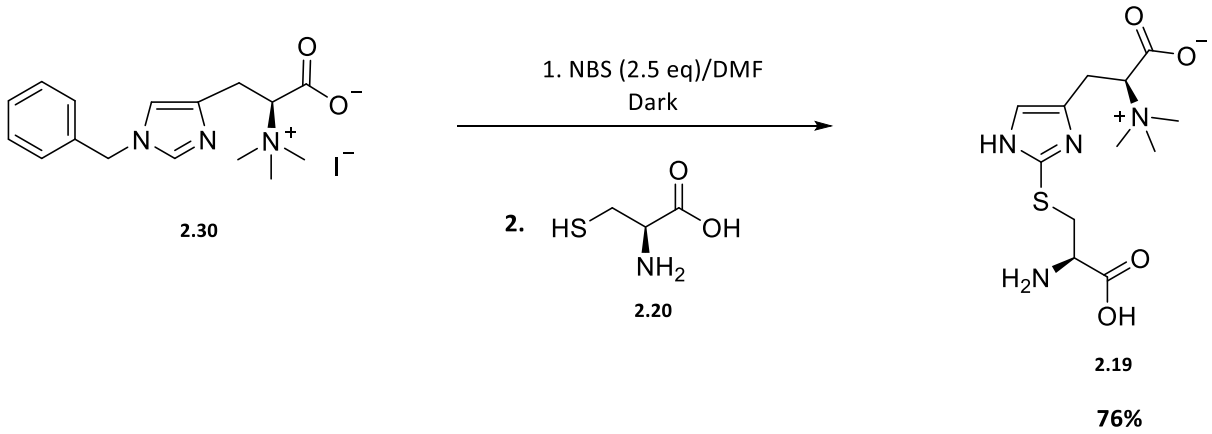

Scheme 2.12. NBS/DMF mediated synthesis of 2-cysteinylhercynine thioether 2.19.

2.3.3.2.1. Selective and mild bromination of the imidazole ring

Previously bromination utilised liquid bromine,[8] therefore developing milder bromination conditions were of interest especially on industrial scale.

NBS was the preferred milder bromine source as it easy to handle than dense fuming liquid bromine. It is noteworthy that NBS was already successfully used as a brominating reagent by Jain *et al.* to synthesize ring-bromohistidines and histamines.[22] (Figure 2.13)

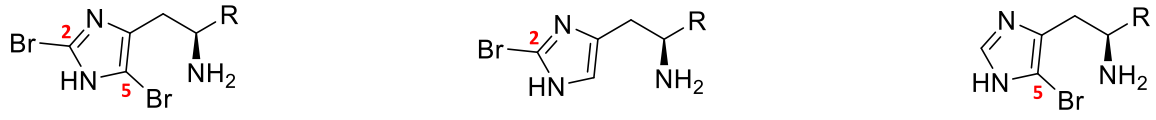

R= CO_2H **Histidine**

R= H **Histamine**

Figure 2.13. Structures of ring-bromohistidine/histamine.

These authors demonstrated that using one mol equivalent of NBS in the absence of light afforded readily separable mixtures of 2,5-dibromohistidines/histamines derivatives (10-25%) and 5-bromohistidines derivatives (70-75%), while 2 mol equivalents afforded 2,5-dibromohistidines/histamines in a rather higher yield (65-75%). Electrophilic halogenation performed on *N*-Boc protected histidine/histamine methyl ester as a starting material led to better yield, whereas the unprotected histidine/histamine resulted to over consumption of NBS. Incomplete reactions thus gave rise to a multitude of inseparable products.[22]

The early reports by Jain *et al.* encouraged the use of NBS to halogenate the imidazole ring of N^c-benzyl hercynine **2.30** prior to cysteine **2.20** introduction.[22] Firstly, only one mol equivalent of NBS in acetonitrile gave multiple products on TLC suggesting incomplete reaction and probably multiply brominated and/or decomposition products.

Schmir *et al.* have shown that the reaction of bromine or NBS with imidazole in aqueous media might also lead to oxidative degradation of the heterocycle ring, thus causing the imidazole ring to decompose into ammonia, glyoxal and formamide. However the authors did not provide any evidence of the labile lactone intermediate.[23]

Secondly, using 2 to 2.5 mol equivalents of NBS in dry DMF as a solvent gave a much cleaner reaction on TLC, hence these conditions were found to be optimal. Regina *et al*. previously utilised NBS-DMF to selectively monobrominate electron rich aromatic compounds.[24]

Isolation of the brominated intermediates were attempted to shed light on the reaction mechanism. Delightfully, two *N*-debenzylated bromohistidines were found, stable enough to be isolated by reverse phase C18 column chromatography. The monobrominated

intermediate, 5-bromohercynine **2.31** was isolated in very high yield (90%), while 2,5 dibromohercynine intermediate **2.32** was isolated in a low yield of 10%. Bearing in mind that bromination of histidine derivatives having a free carboxylic acid results in the formation of the labile bromolactone derivative, it is believed that brominated products (**2.32** and **2.33**) isolated from this reaction could be derived from their related bromolactones. (Scheme 2.13)

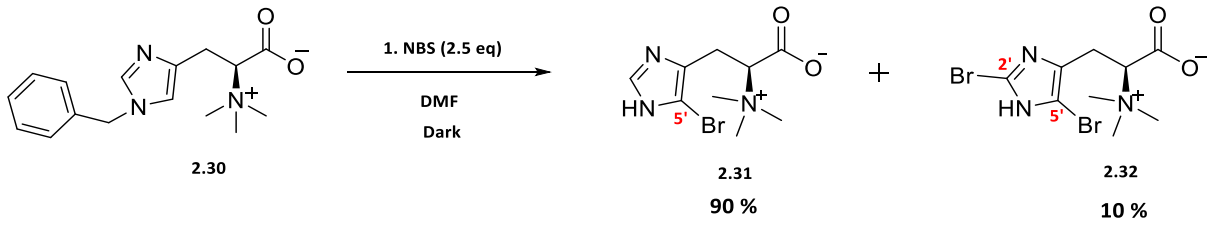

Scheme 2.13. Selective and mild bromination of the imidazole ring.[25,26]

A key diagnostic resonance in the proton NMR spectrum of **2.31** was the presence of one aromatic proton resonating at δ_H 7.4 ppm assigned for the H-2' in the imidazole ring, thus supporting the structure of mono 5-brominated product **2.31**. There was no proton signal in the aromatic region of the proton NMR spectrum of **2.32**, hence supporting the presence of the 2,5-dibrominated product **2.32**.

Moreover, NBS-mediated *N*-debenzylation is not novel as it was extensively studied in *N*-benzylamide substrates by Wang *et al*., where the authors proposed a plausible mechanism.[27] Baker *et al*. on the other hand proposed a free radical mechanism. However, NBS-mediated *N*-debenzylation of *N*-benzyl imidazole is not well known.[28]

2.3.3.2.2. Mechanism of NBS-mediated synthesis of 2-cysteinylhercynine thioether.

Based on the reaction outcome, it can be envisaged that the 2-cysteinylhercynine thioether **2.19** formation proceeds *via* a stepwise mechanism. Hence, bromination followed by lactonisation and subsequent debenzylation and finally cysteine introduction gave the target product as depicted in the Figure 2.14.

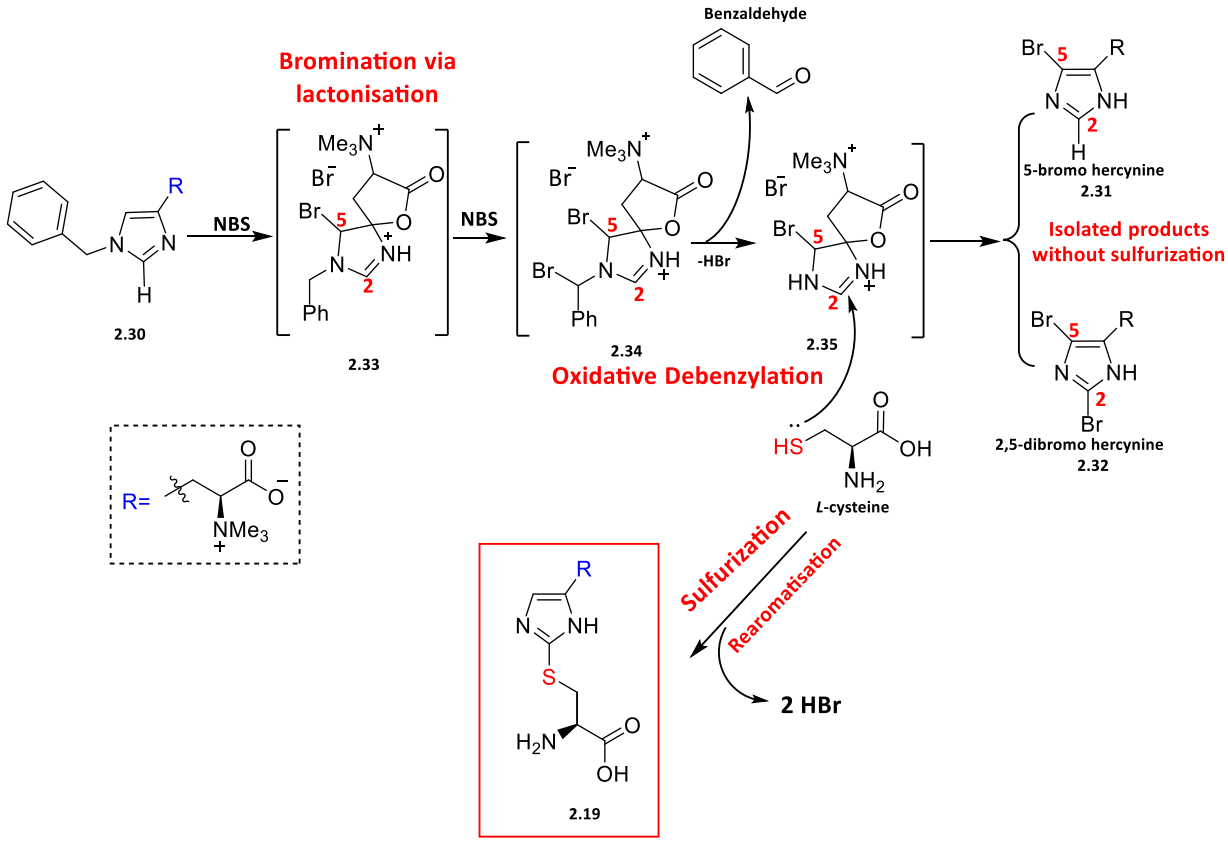

Figure 2.14. Proposed mechanism of the formation of 2-cysteinylhercynine thioether 2.19 NBS-mediated using *N*-benzyl hercynine 2.30 as substrate.

Mechanistically, it is suggested that the first mol equivalent of NBS produces the brominium cation which results in a S_NAr to form the bromolactone hercynine *N*-benzyl derivative **2.33**. The second mol equivalent reacts with the lactone intermediate **2.33** to form the

debenzylated bromolactone hercynine **2.35** and benzaldehyde as a by-product. This putative mechanism suggested the need for an excess of NBS (2.0-2.5 mol equivalents) to subsequently brominate and debenzylate the substrate. The last step is the cysteine introduction through sulfurization to afford the desired product, 2-cysteinylhercynine thioether **2.19** after rearomatisation. (Figure 2.14)

The evidence of the bromolactone being the reactive intermediate was provided by Ito in his earlier research.[10] However, 5-bromohercynine and 2,5-dibromohercynine were the only isolated intermediates prior to the oxidative cysteine introduction. It is likely that these isolated intermediates are derived from their related bromolactones, which are highly unstable intermediates that may have been decomposed during the isolation process. (Figure 2.14)

2.3.3.2.3. Cysteine oxidative introduction and characterization of the 2-cysteinylhercynine thioether

Thionation was accomplished by oxidative addition of excess (2-2.5 mol equivalents) of cysteine to yield 2-cysteinylhercynine thioether **2.19** in a yield of 76%. It is noteworthy that this yield is better than any previously reported synthesis while using a relatively moderate amount of cysteine (2-2.5 mol equivalents). Erdelmeier *et al* achieved 46-58% yield using 3-5 mol equivalents of cysteine.[8]

The ^{1}H NMR spectrum of 2-cysteinylhercynine thioether **2.19** revealed one aromatic resonance at δ_H 7.41 ppm assigned to be proton at H-5' of the imidazole, thus confirming a successful thionation at 2-position of the imidazole ring. Two deshielded protons resonated

at δ_H 4.54 ppm (doublet of doublets, *J* = 7.7, 4.4 Hz) and 4.42 ppm (triplet, *J* = 5.0 Hz) respectively, characteristic of α-amino protons confirming the presence of the two amino acid moieties, cysteine and histidine. (Figure 2.15)

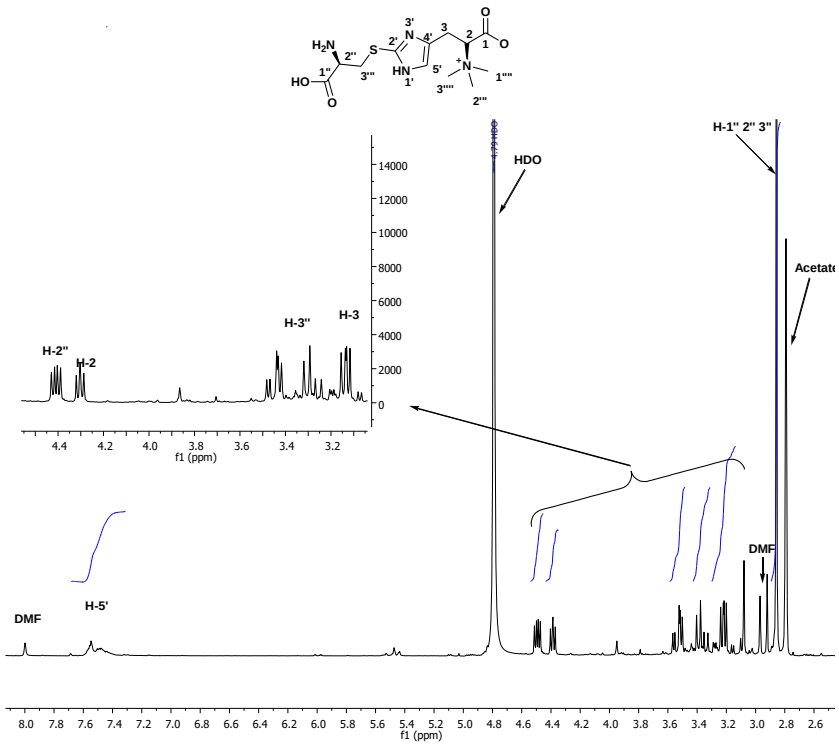

Figure 2.15. ^{1}H NMR spectrum of 2-cysteinylhercynine 2.19 in D_2O at 400 MHz.

The ^{13}C NMR spectrum 2-cysteinylhercynine thioether **2.19** displayed ten carbon signals resonating at δ_C 170.3, 170.0, 129.4, 128.9, 120.9, 61.0, 54.4, 51.7 (for *N,N,N*-trimethyl group), 36.3 and 23.9 ppm; thus confirming the carbon skeleton identity of 2-cysteinylhercynine thioether **2.19**.

Furthermore, high-resolution mass spectrum (ESI$^+$) displayed the molecular ion at *m/z* 317.1277 $[M]^+$ calculated for $C_{12}H_{21}N_4O_4S^+$ 317.1284 $[M]^+$ supporting the structure of 2-cysteinylhercynine thioether **2.19** as shown in the Figure 2.16.

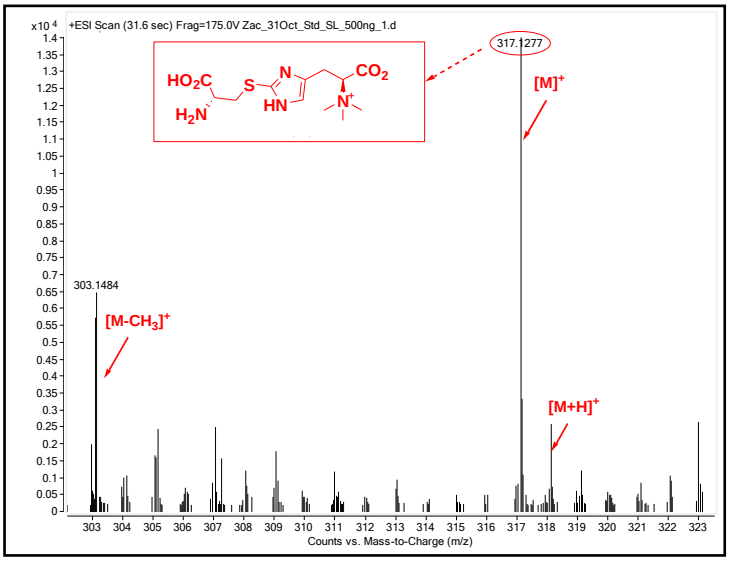

Figure 2.16. **ESI/QTOF mass spectra of 2-cysteinylhercynine thioether 2.19 in positive ion mode**

2.3.3.3. *C-S* bond cleavage of 2-cysteinylhercynine thioether affords *L*-ergothioneine

After successfully synthesizing 2-cysteinylhercynine thioether **2.19**, the last challenge was to cleave *C-S* bond to yield the target compound, *L*-ergothioneine **2.10**.

Thermal cleavage of 2-cysteinylhercynine thioether scavenged by an excess of 3-mercaptopropionic acid (10 mol equivalents) was utilised by Erdelmeier *et al* to yield *L*-ergothioneine in good yield of 80%.[6] Therefore in the course of this research, we investigated alternative cleavage methods that are milder.

In an earlier publication, it was demonstrated that hercynylcysteine sulfoxide can be cleaved by either a β-lyase from *Erwinia tasmaniensia* (PLP-enzyme) or PLP itself to produce *L*-ergothioneine.[11] Most *C-S* lyase enzymes in the literature utilise thioether as substrates, but only fewer catalyse sulfoxides C-S bond lysis.[18] Thus inspired the investigation of the enzymatic or the non-enzymatic cleavage of 2-cysteinylhercynine thioether **2.19** instead.

2.3.3.3.1. Enzymatic *C-S* bond cleavage of 2-cysteinylhercynine thioether: Biomimetic synthesis of *L*-ergothioneine

Due to lack of pure EgtE enzyme, 50 mM of 2-cysteinylhercynine thioether **2.19** was incubated at 37°C with *M. smegmatis* cell-free lysate enzymatic preparation for 24 hr. LCMS analysis indicated conversion of 2-cysteinylhercynine thioether **2.19** to *L*-ergothioneine **2.10**, about 19.2 (±0.2) ng/mL of *L*-ergothioneine was detected.

2.3.3.3.2. Enzyme-free, PLP mediated C-S lyase of 2-cysteinylhercynine thioether

The same assay was performed using 50 mM of PLP alone, and 50 mM of 2-cysteinylhercynine thioether **2.19** was cleaved to *L*-ergothioneine **2.10**, about 96 ±2 ng/mL was detected by LCMS. (Figure 2.17)

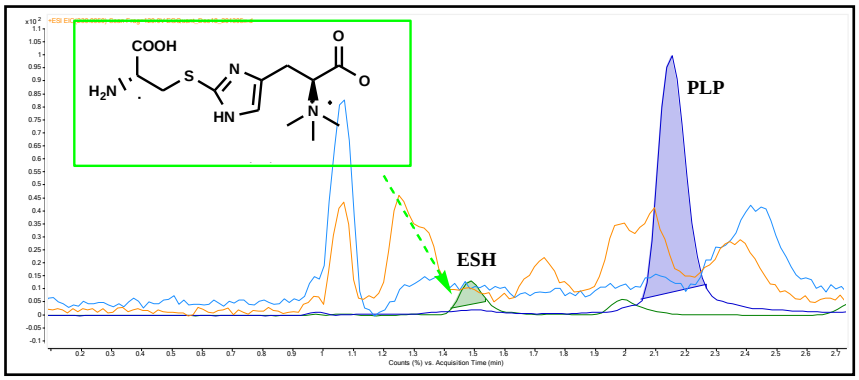

Figure 2.17. Non-enzymatic production of ESH catalysed by PLP. TIC extracted for ESH and PLP using 2-cysteinylhercynine thioether 2.19 produced 96 ±2 ng/mL of ESH.

2.3.3.3.3. Enzyme-free, PLP mediated *C-S* lyase of 2-cysteinylhercynine thioether: NMR experiment and attempted ergothioneine isolation

LCMS technique showed successful *C-S* lyase of 2-cysteinylhercynine thioether **2.19** as *L*-ergothioneine was detected and quantified at retention time of 15 min. Therefore, the enzyme-free PLP experiment were conducted on mg scale. 2-Cysteinylhercynine thioether **2.19** was cleaved by pyridoxal-5-phosphate at 37-40 °C. Dowex-H^+ ion exchange and C18 reverse phase column chromatography were utilised to isolate *L*-ergothioneine **2.10** in a good yield of 76%. (Scheme 2.14)

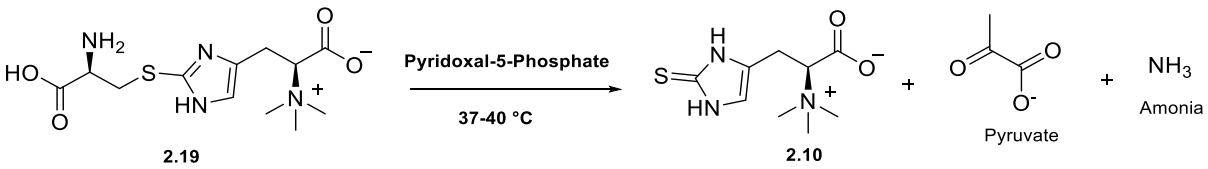

Scheme 2.14. Enzymatic-free cleavage of *C-S* bond in 2-cysteinylhercynine thioether 2.19 catalysed by PLP.

Key diagnostics in the ^{1}H NMR spectrum of the isolated *L*-ergothioneine **2.10** was the characteristic aromatic proton resonating at δ_H 6.85 ppm shifted from δ_H 7.41 ppm in 2-cysteinylhercynine thioether in **2.19** as well as the disappearance of one α-amino proton belonging to the cysteine moiety, which resonated as a doublet of doublets (*J* = 7.7, 4.4 Hz) at δ_H 4.54 ppm in 2-cysteinylhercynine thioether **2.19** thus confirming the successful *C-S* cleavage of 2-cysteinylhercynine thioether **2.31**. (Figure 2.18)

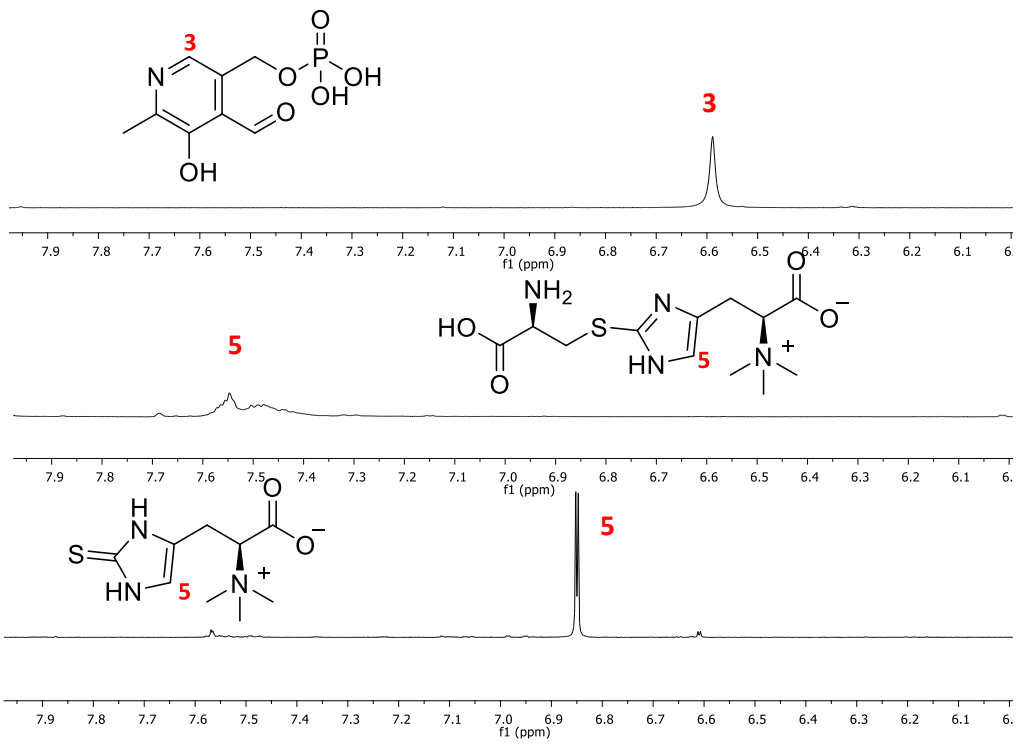

Figure 2.18. Portion of ^{1}H NMR spectrum in D_20 at 300 MHz (7.9-6.0 ppm) of PLP, 2-cysteinylhercynine thioether 2.19 and ESH 2.10.

This result was encouraging, however for industrial scale preparations it would be better to design a process that allows an easy purification method. Supporting PLP (cheap and recyclable) on a solid support would be a viable option for large scale synthesis of ESH compared to the expensive enzymatic process. PLP solid supported would afford the desired product of the reaction, *L*-ESH **2.10** in greater yield by simple filtration and easier purification as the filtrate containing *L*-ESH would only be contaminated by pyruvate.

2.3.3.4. Summary of the improved synthesis of *L*-ergothioneine using cysteine as the sulfur source.

L-ergothioneine **2.10** was successfully synthesized in fewer steps, two steps starting from N^{ζ}-benzyl hercynine **2.30** or four steps starting from *N*-benzyl histidine **2.28** as starting material. (Scheme 2.15)

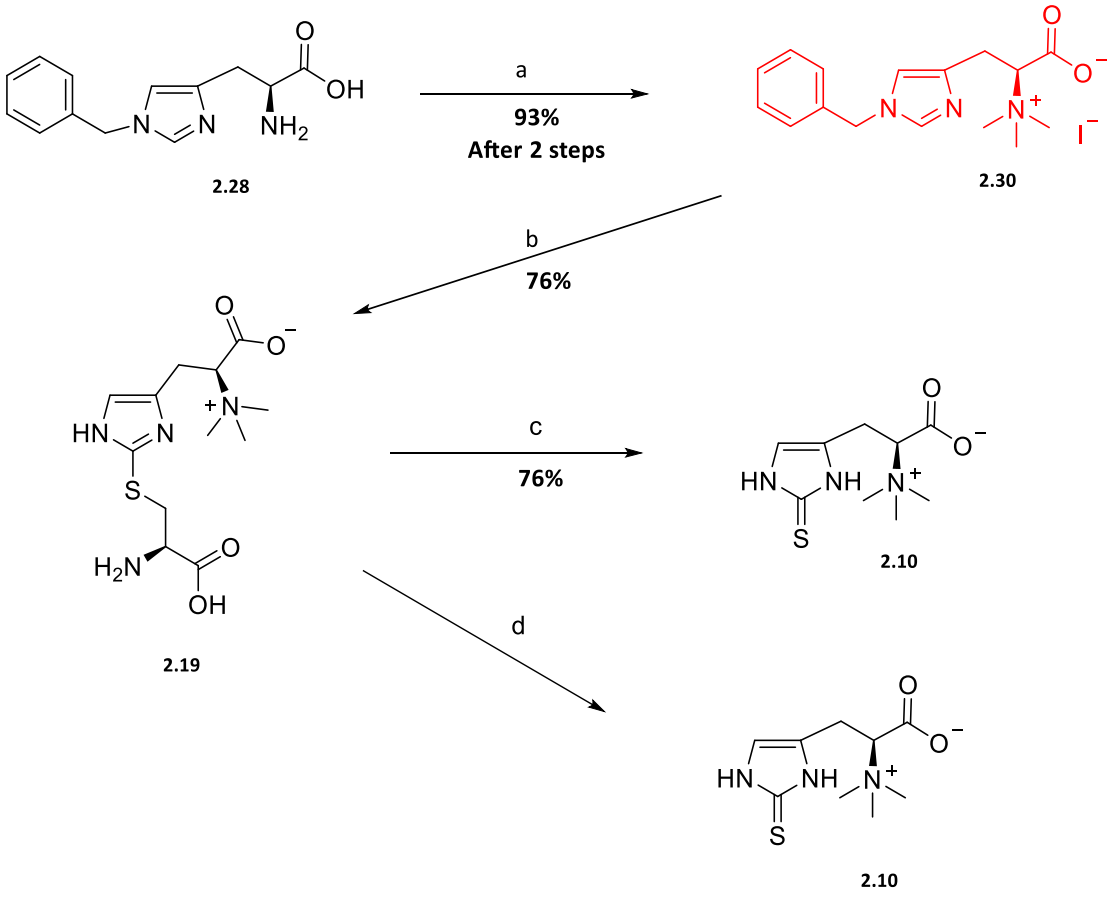

Scheme 2.15. Improved biomimetic *L*-ergothioneine synthesis. Reagents and conditions. a) (i) CHO, $NaBH(OAc)_3$, acetonitrile, 24 hr at rt, quantitative, (ii) CH_3I, dry THF, 1-2 days dark at rt, 93%; (b) (i) NBS (2.5 mol equivalents)/DMF, (ii) cysteine, rt, 76%; c) PLP, 37-40°C, 76%; d) *M.smegmatis*. cell free lysate extract. Overall yield of sequential steps a, b and c is 54%. Overall yield of sequential steps a, b and d is at least 70%

Many improvements were implemented to efficiently introduce cysteine in a one pot synthesis, *N*-benzyl hercynine **2.30** was first brominated and subsequently coupled with cysteine to afford 2-cysteinylhercynine thioether **2.19** in a very good yield of 76%.

The last step was achieved by a *C*-*S* lyase of 2-cysteinylhercynine thioether **2.19** which could be performed either quantitatively by *M. smegmatis* cell-free lysate enzymatic preparation or by PLP to yield *L*-ergothioneine **2.10** in a good yield of 76%.

This method allows the synthesis of *L*-ergothioneine **2.10** in fewer steps. This process is relatively simplified, shortened, all reactions were performed at ambient temperatures of 25-40 °C (energy saving) and in good overall yield of 54-70%. Thus, a greater overall yield has been achieved than any prior patented or published process.

2.4. References

1 https://scifinder.cas.org/scifinder/view/scifinder/scifinderExplore.jsf *(Accessed on 02/12/2016)*.

2 Powell, C. Skincare formulations and regimens US 2016/0120781 Al (**2016**).

3 Wenxia, J. *et al.* 1. Manufacture of L-ergothioneine with mushroom and isolation of the chemical from mycelium. WO 2015103974-A1 (2015).

4 Yadan, J. C. & Jinzhu Xu, J. Process for the preparation of ergothioneine US005438151A (**1995**).

5 Miroslav Trampota. Process for the synthesis of L-(+)-ergothioneine US 7,767,826 B2 (**2010**).

6 Erdelmeier, I. Method of synthesizing ergothioneine and analogs US 8,399,500 B2 (**2013**).

7 Xu, J. & Yadan, J. C. Synthesis of L-(+)-Ergothioneine. *Journal of Organic Chemistry* **60**, 6296-6301 (1995).

8 Erdelmeier, I., Daunay, S., Lebel, R., Farescour, L. & Yadan, J.-C. Cysteine as a sustainable sulfur reagent for the protecting-group-free synthesis of sulfur-containing amino acids: biomimetic synthesis of l-ergothioneine in water. *Green Chemistry* **14**, 2256, doi:10.1039/c2gc35367a (2012).

9 Reinhold, V. N., Ishikawa, Y. & Melville, D. B. Synthesis of α-N-methylated histidines. *Journal of medicinal chemistry* **11**, 258 (1968).

10 Ito, S. Synthesis of 2-S-Cysteinylhistidine and 2-Mercaptohistidine via Bromo Lactone Derivative of Histidine. *Journal of Organic Chemistry* **50**, 3636-3638 (1985).

11 Seebeck, F. P. In Vitro Reconstitution of Mycobacterial Ergothioneine Biosynthesis. *Journal of American Chemical Society* **132**, 6632 (2010).

12 Seki, M., Mori, Y., Hatsuda, M. & Yamada, S.-I. A Novel Synthesis of (+)-Biotin from L-Cysteine. *Journal of Organic Chemistry* **67**, 5527-5536 (2002).

13 Schubert, M. P. Compounds of Thiol Acids with Aldehydes. *Journal of Biological Chemistry* **114**, 341-350 (1936).

14 Goldberg, S. I. & Sahli, M. S. Asymmetric Selection via Elimination. Pyrolyses of Optically Active Sulfoxides to Optically Active Olefins. *Journal of Organic Chemistry* **32**, 2059–2062 (1967).

15 McKenzie, L. C., Huffman, L. M. & Hutchison, J. E. The Evolution of a Green Chemistry Laboratory Experiment: Greener Brominations of Stilbene. *Journal of Chemical Education*, 306-310 (2005).

16 Hensarling, R. M. *et al.* Photocaged pendent thiol polymer brush surfaces for postpolymerization modifications via thiol-click chemistry. *Journal of Polymer Science Part A: Polymer Chemistry* **51**, 1079-1090, doi:10.1002/pola.26468 (2013).

17 Fukushima, N. *et al.* Synthesis of a photocontrollable hydrogen sulfide donor using ketoprofenate photocages. *Chemical communications* **50**, 587--589 doi:10.1039/c3cc47421f (2014).

18 Song, H. *et al.* Mechanistic studies of a novel C-S lyase in ergothioneine biosynthesis: the involvement of a sulfenic acid intermediate. *Scientific reports* **5**, 11870, doi:10.1038/srep11870 (2015).

19 Pedersen, E., Loksha, Y., El-Barbary, A., El-Badawi, M. & Nielsen, C. Synthesis of 2-Hydroxymethyl-1H-imidazoles from 1,3-Dihydroimidazole-2-thiones. *Synthesis* **2004**, 116-120, doi:10.1055/s-2003-44370 (2004).

20 Wang, L. Z. *et al.* Quantification of L-ergothioneine in human plasma and erythrocytes by liquid chromatography-tandem mass spectrometry. *Journal of Mass Spectrometry* **48**, 406-412, doi:10.1002/jms.3150 (2013).

21 Heath, H., Lawson, A. & Rimington, C. 488. 2-Hercaptoglyoxalines. Part I. The Synthesis of Ergothioneine. *Journal of Chemical Society*, 2215-2217, doi:10.1039/JR9510002215 (1951).

22 Jain, R., Avramovitch, B. & Cohen, L. A. Synthesis of Ring-Halogenated Histidines and Histamines *Tetrahedron* **54**, 3235-3242 (1998).

23 Schmirt, G. L. & Cohen, L. A. Oxidative Degradation of Imidazoles by Bromine or N-Bromosuccinimide. *Biochemistry* **4**, 533-538 (1965).

24 Reginald, H., Mitchell, Y. H. L. & Richard, V. W. N-Bromosuccinimide-Dimethylformamide: A Mild, Selective Nuclear Monobromination Reagent for Reactive Aromatic Compounds. *Journal of Organic Chemistry* **44**, 4733 (1979).

25 Khonde, P. L. & Jardine, A. Improved synthesis of the super antioxidant, ergothioneine, and its biosynthetic pathway intermediates. *Organic & biomolecular chemistry* **13**, 1415-1419, doi:10.1039/c4ob02023e (2015).

26 Jardine, M. A. & Khonde, L. P. Process for synthesizing ergothioneine and related compounds WO 2016/046618 A1 (**2016**).

27 Wang, G., Li, Z., Ha, C. & Ding, K. Direct Oxidation of N-Benzylamides to Aldehydes or Ketones by N-Bromosuccinimide. *Synthetic Communications* **38**, 1629-1637, doi:10.1080/00397910801929697 (2008).

28 Baker, S. R., Parsons, A. F. & Wilson, M. A Radical Approach to Debenzylation of Amides. *Tetrahedron Letters* **39**, 331-332 (1998).

Chapter 3 Synthesis and biotransformation of 2-cysteinylhercynine by EgtE (*C-S* lyase enzyme)

EgtE, a PLP-dependent enzyme catalyzes the *C-S* cleavage of 2-cysteinylhercynine sulfoxide to yield *L*-ergothioneine, ammonia and pyruvate. The chemistry and the biotransformation of the substrates involved in this step will be discussed in depth.

In order to study this last step, the synthesis of the 2-cysteinylhercynine sulfoxide (natural EgtE substrate) was required. Consequently, the sulfide precursor, 2-cysteinylhercynine thioether and the over oxidized sulfone, 2-cysteinylhercynine sulfone would also be obtained. The stable isotopically labelled hercynine-d_3 and ergothioneine-d_3 would be accessed to shed light on the mechanism of *C-S* lyase by the EgtE enzyme as well as enzyme-substrate specificity.

3.1. Synthesis of hercynine and its stable isotope labelled versions, hercynine-d_3 as well as ESH-d_3

Genghof *et al*. have demonstrated that in mycobacteria, endogenous hercynine is in fact the biosynthetic precursor of ergothioneine.[1] Early ergothioneine biosynthetic pathway elucidation studies in various organisms (such as bacteria and fungi) utilized radiolabeled intermediates.[2] Due to the huge safety risk associated with the use of radiological techniques

and the non-availability of these techniques in our laboratory, it was decided to utilize stable isotopic, deuterated intermediates instead. It is noteworthy that these labelled intermediates are valuable internal standards for the quantitation of pathway metabolites during external stimuli, drug treatment or metabolomics studies.

3.1.1. Synthesis of hercynine and hercynine-d_3

Hercynine **3.3** and hercynine-d_3 **3.4** were synthesized following multiple strategies, starting with *L*-histidine **3.1**, dimethylation *via* reductive amination was followed by quaternarization to yield the target compounds. (Scheme 3.1)

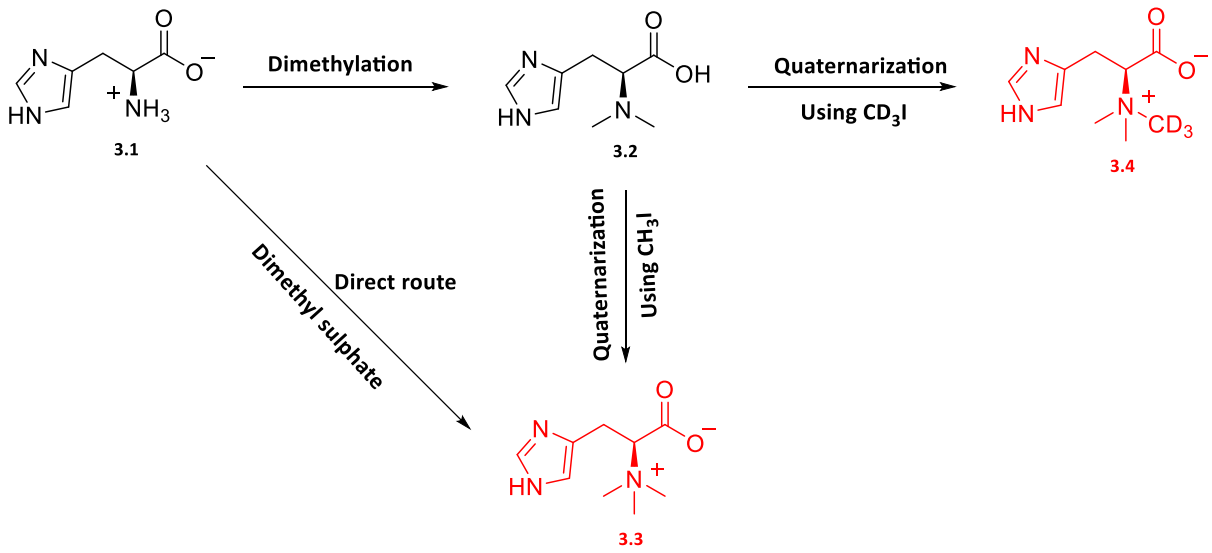

Scheme 3.1. Two steps synthesis strategy of hercynine 3.3 and hercynine-d_3 3.4. Reagents and conditions. **Dimethylation**: **First approach:** 37% solution CH_2O, $NaBH_4$, H_2O, ice water bath (0-5 °C), 3 hrs, quantitatively; **Second approach:** 37% solution of CH_2O, $NaBH(OAc)_3$ /CH_3CN, 18-24 hrs at rt; **Quaternarization:** NH_4OH, MeOH, 24 hr at rt, using CD_3I (61%) or using CH_3I 3.3, (42%); **Direct route**: Dimethyl sulphate, NaOH (10%), 0°C to rt.

3.1.1.1. One-pot synthesis of hercynine using dimethyl sulphate mediated *N*-alkylation.

Hercynine **3.3** can be synthesized in one pot by reacting histidine **3.1** under aqueous basic conditions (NaOH 10%) with dimethyl sulphate as an alkylating reagent. This one pot *N*-α trimethylation method was previously reported by Fattori *et al.*[3] (Scheme 3.2)

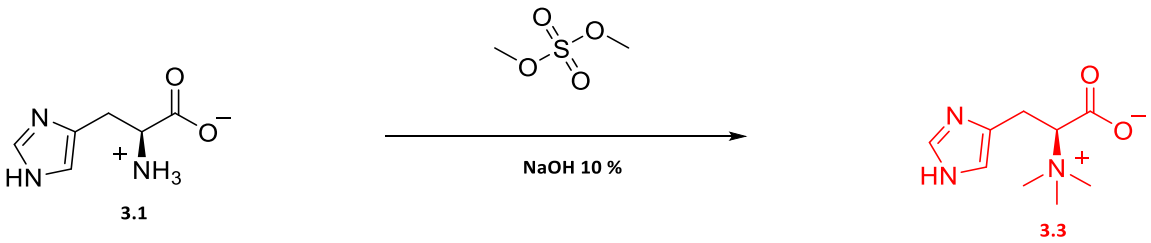

3.1 3.3

Scheme 3.2. One-pot synthesis of hercynine 3.3.

Hercynine **3.3** synthesized according to this method required C18 reverse phase chromatography to remove sulphate salts (by-products). Hercynine was synthesized in a crude yield of 92%. However, the NMR analysis of hercynine synthesized accordingly revealed small contamination with *N*-monomethyl-histidine and *N,N*-dimethyl histidine intermediate products, which can be removed with difficulty by ionic exchange chromatography. Therefore, alternative approach for the synthesis of hercynine was considered.

3.1.1.2. Dimethylation using *in situ* reduction.

Histidine **3.1** was dimethylated using 37% formaldehyde in H_2O in the presence of an excess of $NaBH_4$ (2-3 mol equivalents) under cooling in an ice water bath to yield N^{α},N^{α}-dimethyl-*L*-histidine **3.2** quantitatively. (Scheme 3.3)

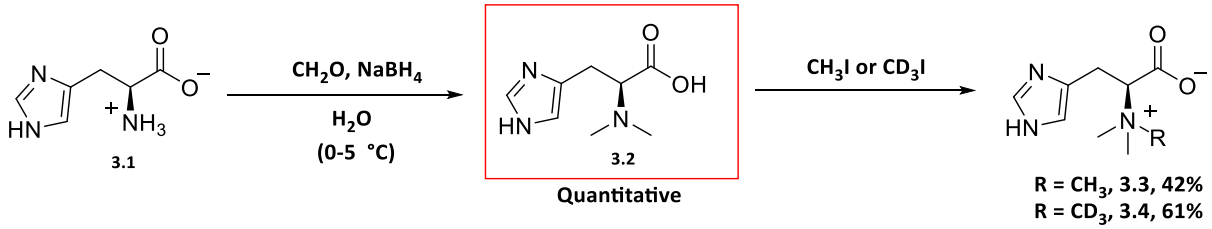

Scheme 3.3. Synthesis of hercynine 3.3 and hercynine-*d*$_3$ 3.4 via improved synthesis of N^{α},N^{α}-dimethyl histidine 3.2.

An exothermic reaction between $NaBH_4$ and water produced hydrogen gas *in situ* and $NaBO_3$.n H_2O salts as side products. This highly exothermic reaction is controlled by cooling the reaction vessel in an ice bath at 0-5 °C to slow down the side reaction. The imine intermediate resulting from the reaction between histidine **3.1** and formaldehyde is reduced by $NaBH_4$ to form N^{α},N^{α}-dimethyl-*L*-histidine **3.2** quantitatively, after C18 reverse phase flash chromatography to remove $NaBO_3$.n H_2O salts.

The ^{1}H NMR spectrum of N^{α},N^{α}-dimethyl-*L*-histidine **3.2** revealed two aromatic signals resonating both as a singlet at δ_H 7.70 and 6.95 ppm confirming the presence of the imidazole ring. A key feature was a slightly deshielded proton signal resonating as a singlet at δ_H 2.51 ppm, integrating for 6 protons. This confirmed the successful introduction of two equivalents of *N*-methyl groups to the amine. (Figure 3.1.)

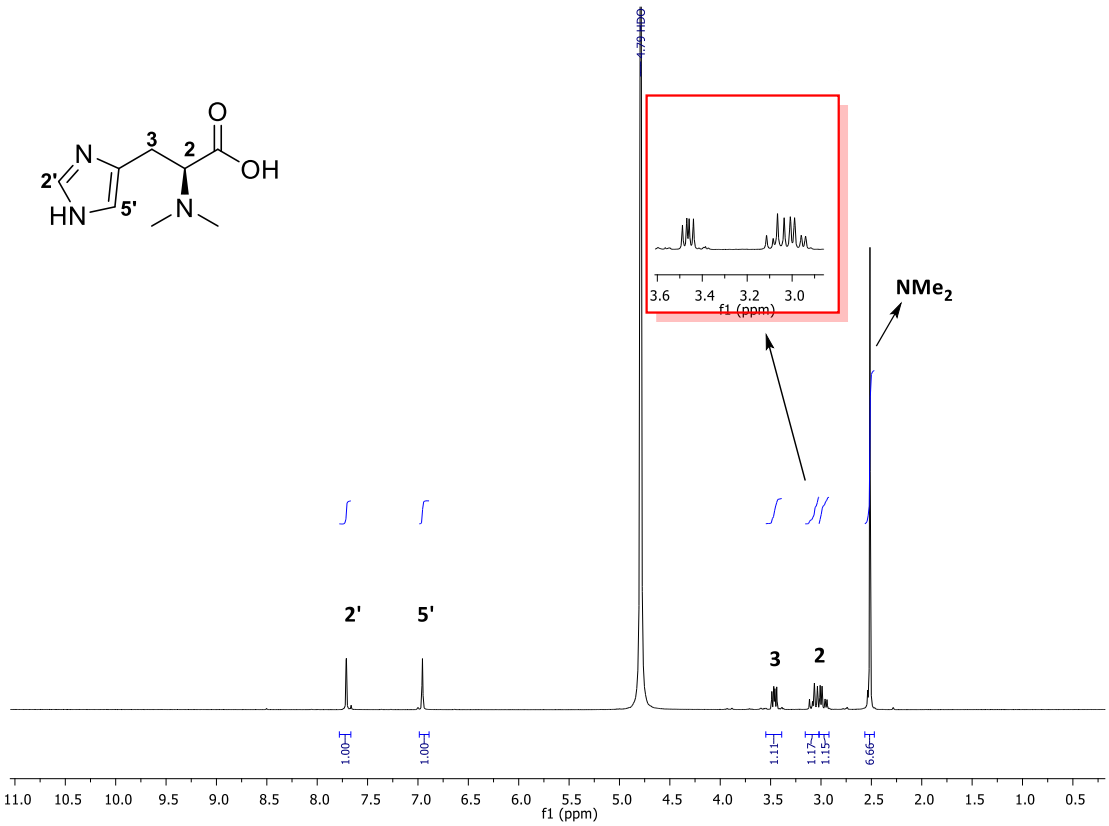

Figure 3.1. **^{1}H NMR of *N*$^{\alpha}$,*N*$^{\alpha}$-dimethyl-*L*-histidine 3.2 at 300 MHz.**

The ^{13}C NMR spectrum of *N*$^{\alpha}$,*N*$^{\alpha}$-dimethyl-*L*-histidine **3.2** revealed seven carbon signals resonating at δ_C 176.6, 135.8, 133.4, 117.4, 70.9, 41.4 and 27.1 ppm respectively, hence confirming the identity of *N*$^{\alpha}$,*N*$^{\alpha}$-dimethyl histidine **3.2.** (Figure 3.2)

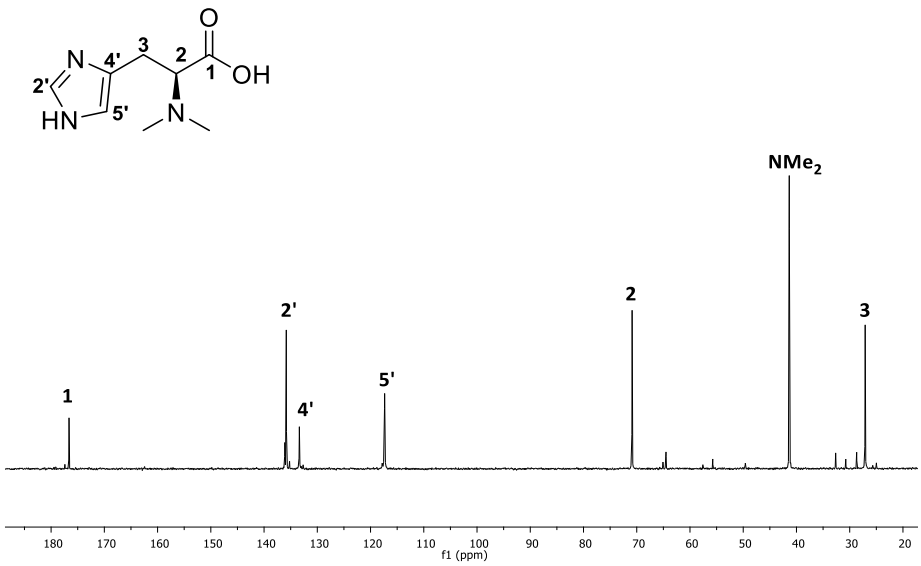

Figure 3.2. ^{13}C NMR of N^{α},N^{α}-dimethyl-*L*-histidine 3.2 at 101 MHz.

Furthermore, the EI$^+$ mass spectrum displayed a molecular ion at *m/z* 184.0 $[MH]^+$ calculated for $C_8H_{14}N_3O_2$ (184.1) $[MH]^+$ and a fragment corresponding to a loss of carbonyl at *m/z* 139.0 calculated for $C_7H_{12}N_3$ (139.0) $[M\text{-}CO_2]^+$, thus supporting the structure of N^{α},N^{α}-dimethyl-*L*-histidine **3.2.**

3.1.1.3. Dimethylation using sodium triacetoxyborohydride.

L-histidine **3.1** was dimethylated *via* reductive amination by reacting 37% formaldehyde solution with sodium triacetoxyborohydride used as a reducing reagent with acetonitrile as solvent in the presence of a catalytic amount of glacial acetic acid.

N^{α},N^{α}-dimethyl-*L*-histidine **3.2** synthesized as described above was found to be very difficult to purify. Hence, the crude product **3.2** was obtained after filtration through celite (to remove inorganic salts) and drying under high vacuum. Quaternarization was conducted using

iodomethane to afford hercynine **3.3** in a yield of 42% after two steps. Alternatively, iodomethane d_3 afforded the hercynine-d_3 **3.4** product in a moderate yield of 61% (in two steps) after C18 reverse phase chromatography and crystallization. The difference in yield between hercynine **3.3** and hercynine-d_3 **3.4** could be attributed to the quality of the starting material, as CD_3I was better quality than CH_3I which decomposed faster over time. (Scheme 3.4)

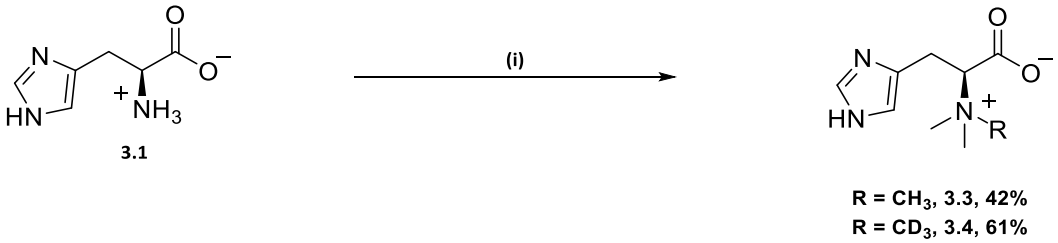

Scheme 3.4. Synthesis of hercynine 3.3 or hercynine-d_3 3.4. Reagents and conditions. (i) a) 37% solution of CH_2O, $NaBH(OAc)_3$ /CH_3CN, 18-24 hrs at rt; b) NH_4OH, MeOH, 24 hr at rt, using CD_3I **(**61% after 2 steps) or using CH_3I (42% after 2 steps).

The ^1H NMR spectrum of hercynine-d_3 **3.4** revealed two aromatic protons resonating at δ_H 7.84 and 7.12 ppm, respectively. Three aliphatic protons resonating as a doublet of doublets (J = 10.6, 4.7 Hz) at δ_H 4.01 ppm was characteristic of the α-amino acid proton and the methylene protons, which were deshielded and resonated as a multiplet from δ_H 3.39 to 3.36 ppm. A singlet signal integrating for 6 protons was attributed to the N^{α},N^{α}-dimethyl protons in deuterated (d_3) form supporting the structure of hercynine-d_3 **3.4**.

The ^{13}C NMR spectrum corroborated by ESI/QTOF analysis confirmed the structure of hercynine-d_3 **3.4**. A high-resolution mass spectrum revealed the molecular ion at *m/z* 201.1414 $[M]^+$calculated for $C_9H_{13}D_3N_3O_2^+$ (201.1431) $[M]^+$. (Figure 3.3)

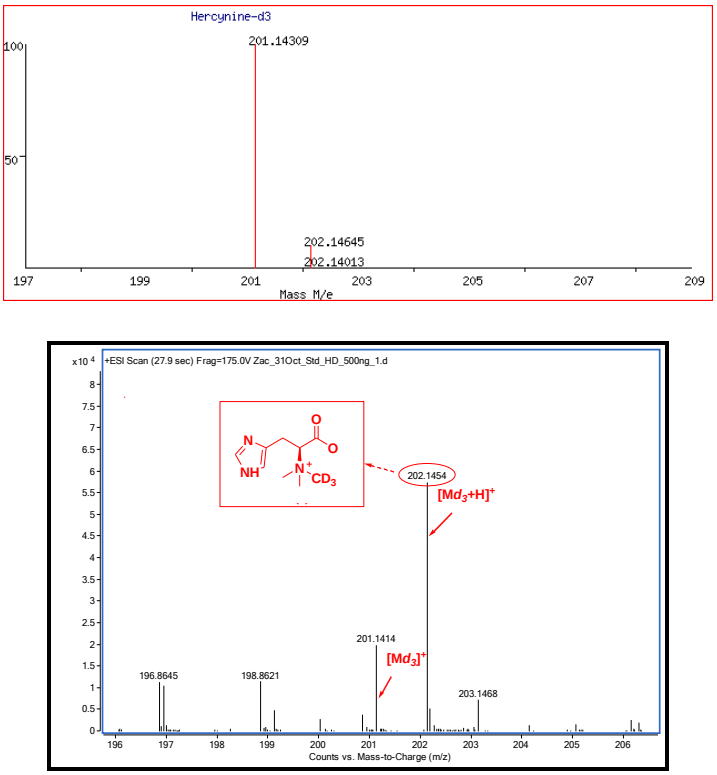

Figure 3.3. Top. Theoretical HRMS isotopic pattern calculated for $C_9H_{13}D_3N_3O_2^+$ $[M]^+$. **Bottom**. Experimental ESI/QTOF mass spectra of hercynine-*d*$_3$ **3.4** in positive ion mode.

The ^{1}H NMR spectrum of hercynine **3.3** displayed two aromatic signals resonating at δ_H 7.89 ppm and 7.11 ppm respectively, suggesting the presence of the imidazole ring. A key characteristic signal was a singlet resonance at δ_H 3.35 ppm integrating for 9 protons proving successful quaternarization.

The ^{13}C NMR spectrum of hercynine **3.3** revealed seven carbon signals resonating at δ_C 170.9, 136.1, 131.2, 116.7, 78.4, 52.2 and 25.0 ppm respectively confirming the identity of hercynine **3.3**.

Furthermore, the EI^+ mass spectrum displayed molecular ion at *m/z* 197.1 $[M]^+$ calculated for $C_9H_{15}N_3O_2^+$ (197.1) $[M]^+$ and a characteristic base peak corresponding to a loss of three

methyls at *m/z* 152.0 calculated for $C_6H_6N_3O_2$ (152.0) $[M-(CH_3)_3]^+$, thus supporting the structure of hercynine **3.3.**

It is noteworthy that Reinhold *et al.* have synthesized hercynine *via* Pd/C catalytic hydrogenation of the histidine imine produced in a presence of 37% solution of formaldehyde in water. Subsequent quaternarization with iodomethane under basic conditions gave hercynine **3.3** in an overall yield of 73%.[4] However this approach was not attempted, because it requires a tedious ionic chromatographic purification as well as the use of a huge amount of resin that makes it unattractive especially in Kg scale synthesis.

3.1.1.4. Synthesis of stable isotopically labelled ergothioneine-d_3

The synthesis of *L*-ergothioneine-d_3 **3.7** was performed in three steps starting from a commercially available mercaptohistidine **3.5** (or synthesized according to the literature[5]). The thiol group of mercaptohistidine **3.5** was protected by a *t*-butyl group in order to selectively dimethylate the α-amino group, (*S*)-3-(2-(*tert*-butylthio)-1*H*-imidazol-4-yl)-2-(dimethylamino) propanoic acid **3.6** was isolated in a low yield of 33.7%. Quaternarization using iodomethane-d_3 and the subsequent removal of the *S*-*t*-butyl protecting group afforded the target compound, ESH-d_3 **3.7** quantitatively. This method was adapted from the Trampota patent.[5] (Scheme 3.5)

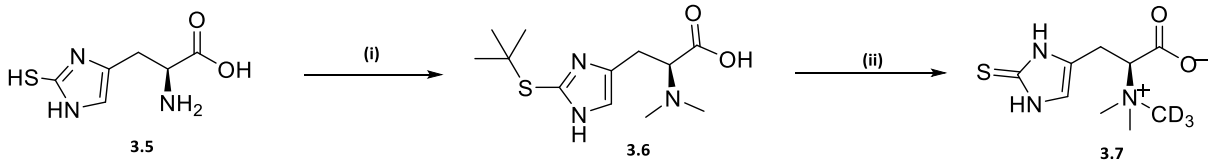

Scheme 3.5. Synthesis of ESH-d_3 (3.7). Reagents and conditions: i) a) *t*-butanol/HCl, refluxed for 3-4 hrs; b) 37% solution CH_2O, $NaBH(OAc)_3$ /THF, 6-8 hrs at 10 °C, 33.7%; ii) a) NH_4OH, CD_3I/MeOH, 24 hr, rt; b) HCl, 2-mercaptopropionic acid refluxed for 21 h (quantitative).

The ^{1}H NMR spectrum of ESH-d_3 **3.7** displayed the characteristic aromatic proton resonating as a singlet at δ_H 6.95 ppm suggesting the presence of a mercapto heterocyclic ring. A deshielded proton resonating as a multiplet from δ_H 4.34 – 4.13 ppm and two protons resonated as doublet of doublets (J = 11.3, 8.5 Hz) at δ_H 3.41 ppm suggesting the presence of an α-amino acid. Key features in the ^{1} H NMR spectrum were the down field resonance of a singlet integrating for 6 protons (deuterated protons are blank in ^{1} H NMR) from δ_H 3.01 ppm in **3.6** to δ_H 3.39 ppm indicative of the presence of a N^{α},N^{α},-dimethyl CD_3 group; and the disappearance of the singlet resonated at δ_H 1.50 ppm in **3.6** supporting the successful *t*-butyl deprotection.

The ^{13}C NMR spectrum of ESH-d_3 **3.7** revealed seven carbon resonances at δ_C 180.3, 134.9, 119.1, 115.8, 75.5, 52.5 and 22.7 ppm respectively, thus confirming the identity of ESH-d_3 **3.7**. Moreover, a high-resolution mass spectrum (ESI^+) displayed the molecular ion at *m/z* 233.1160 $[M]^+$ calculated for $C_9H_{13}D_3N_3O_2S^+$ (233.1152) $[M]^+$ and a characteristic fragmentation pattern as shown in the Figure 3.4, thus supporting the structure of ESH-d_3 **3.7**.

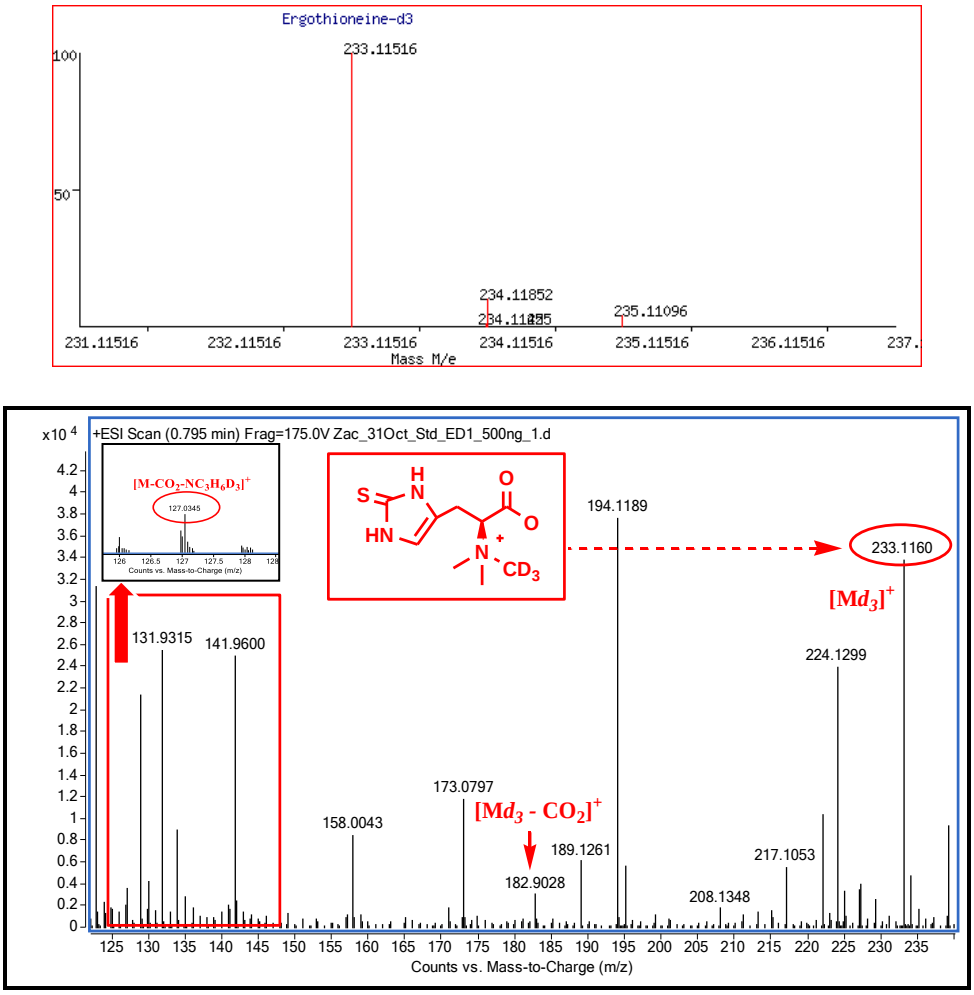

Figure 3.4. Top. Theoretical HRMS isotopic pattern calculated for $C_9H_{13}D_3N_3O_2S^+$ $[M]^+$. **Bottom**. Experimental ESI/QTOF mass spectra of ergothioneine-d_3 **(3.7)** in positive ion mode.

3.2. Total synthesis of 2-cysteinylhercynine sulfoxide and 2-cysteinylhercynine sulfone

3.2.1. Synthesis of 2-cysteinylhercynine sulfoxide (EgtE enzyme substrate)

The natural EgtE substrate, 2-cysteinylhercynine sulfoxide **3.8** was first isolated from cell-free extracts of *Neurospora crassa* by Ishikawa *et al.*[6] Later on, it was synthesized by enzymatic

action of EgtB and EgtC on hercynine and γ-glutamylcysteine.[7] Song *et al*. isolated and characterized 2-cysteinylhercynine sulfoxide (EgtE natural substrate) produced biosynthetically by the enzymatic action of OvoA enzyme on hercynine and cysteine.[8]

Synthesized 2-cysteinylhercynine thioether **2.19** was oxidized using 2.4 mol equivalents of 30% H_2O_2 in a presence of a catalytic amount of para toluene sulfonic acid (0.07 mmol) at room temperature to afford 2-cysteinylhercynine sulfoxide **3.8** as a yellow solid in good yield of 71% according to a published method by Rostami *et al.*[9] (Scheme 3.6)

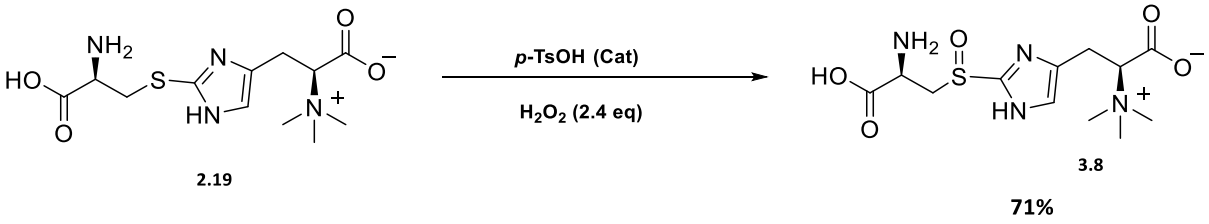

Scheme 3.6. Synthesis of 2-cysteinylhercynine sulfoxide 3.8.

A previously reported mechanism of selective oxidation of sulfides to sulfoxides in H_2O_2 using catalytic sulfuric acid was published by Shaabani *et al.*[10] and Rostami *et al.*[9] They proposed two plausible mechanisms, the first hypothesis is that the catalyst, para-toluene sulfonic acid **3.9** might act as a proton source which transfer a proton to peroxide to generate a reactive oxygen species **3.11.** The latter reacts with the sulfide **3.12** to form the target sulfoxide **3.14**, after deprotonation of the hydrosulfonium cation **3.13** by para-toluene sulfonate **3.10**, thus regenerating the catalyst. (Scheme 3.7)

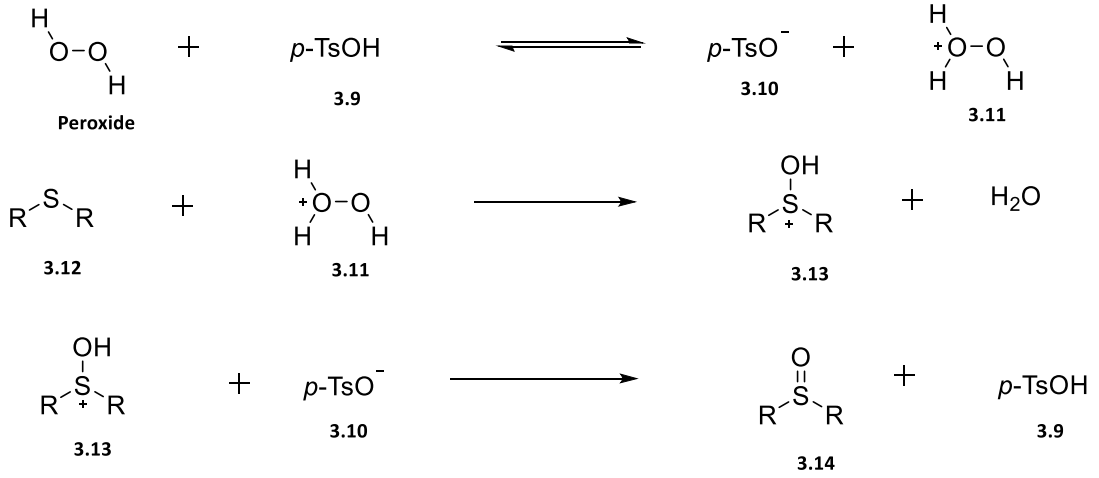

Scheme 3.7. Proposed mechanism of sulfoxidation using H_2O_2 and *p*-TsOH acting as a proton source.

An alternative hypothesis is that the selective sulfoxidation could proceed through oxygen transfer on the sulfide **3.12** by pertolylsulfonic acid **3.15** (reactive intermediate) which is formed *in situ* by the reaction between peroxide and para-toluene sulfonic acid **3.9**. (Scheme 3.8)

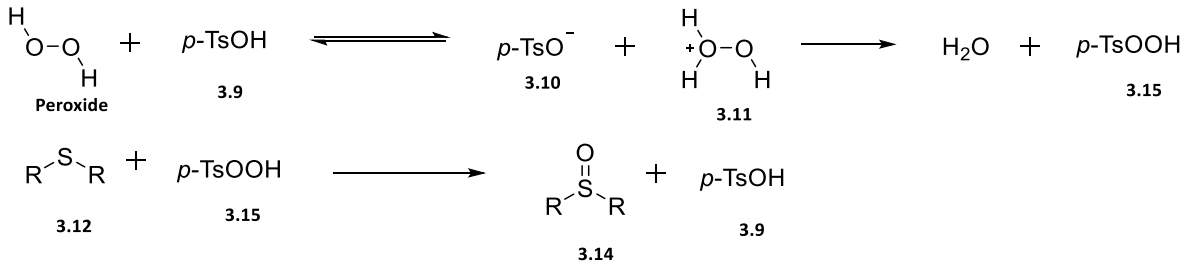

Scheme 3.8. **Proposed mechanism of sulfoxidation proceeding through *per*tolylsulfonic acid 3.9 (reactive intermediate)**

The ^{1}H NMR spectrum of 2-cysteinylhercynine sulfoxide **3.8** displayed one aromatic signal that resonated at δ_H 8.01 ppm attributed to proton H-5' of the imidazole ring. A key diagnostic

signal was the downfield shift of the methylene proton adjacent to the sulfoxide which resonated as doublet of doublets in the ^{1}H NMR spectrum of thioether **2.19** from 3.50-3.36 ppm to 3.65 ppm (J = 15.0, 3.3 Hz), thus suggesting the successful introduction of sulfoxide (electron withdrawing group).

The ^{13}C NMR spectrum of 2-cysteinylhercynine sulfoxide **3.8** revealed two carbonyl signals resonating at δ_C 171.8 and 170.1 ppm, respectively. Three aromatic signals resonating at δ_C 156.6, 129.5 and 125.5 ppm suggesting the presence of an imidazole heterocyclic. Five aliphatic carbon signals resonating at δ_C 72.5, 49.5, 49.1, 43.5 and 20.8 ppm, thus confirming the identity of 2-cysteinylhercynine sulfoxide **3.8**.

Furthermore, a high-resolution mass spectrum (ESI+) displayed the molecular ion at m/z 334.1321 [MH]+ calculated for $C_{12}H_{22}N_4O_5S^+$ (334.1311) $[MH]^+$, and a characteristic base peak corresponding to a loss of three methyls and carbonyl at *m/z* 241.0321 calculated for $C_8H_9N_4O_3S$ (241.0395) $[M-(CH_3)_3-CO_2-2H]^+$, hence supporting the structure of 2-cysteinylhercynine sulfoxide **3.8**. (Figure 3.5)

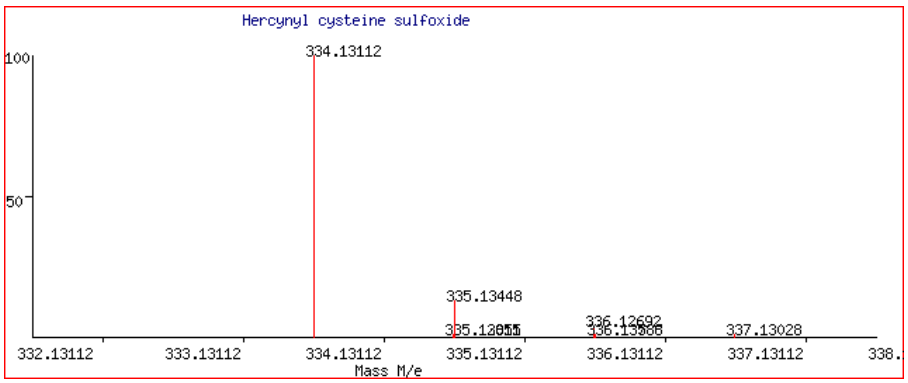

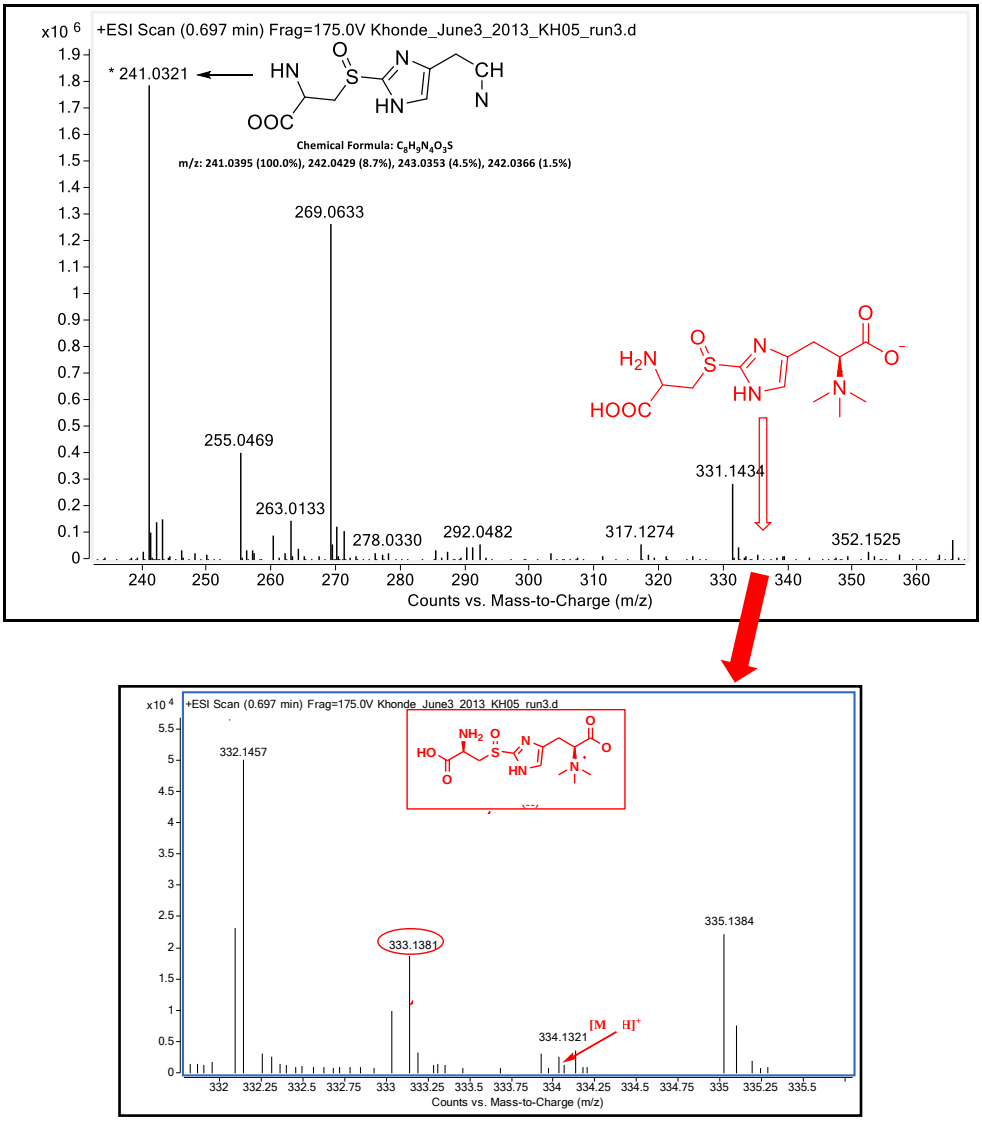

Figure 3.5. Top. Theoretical HRMS isotopic pattern calculated for $C_{12}H_{22}N_4O_5S^+$ 334.1311 $[MH]^+$. **Bottom**. Experimental ESI/QTOF mass spectra of 2-cysteinylhercynine sulfoxide **3.8** in positive ion mode.

3.2.2. Synthesis of 2-cysteinylhercynine sulfone

It is well known that 2-cysteinylhercynine sulfoxide **3.8** is the EgtE enzyme substrate.[7] However, it was proposed to synthesize the sulfone derivative, which will be assayed in order to better understand the impact of the oxidation state at the sulfur atom on the *C-S* lyase

activity of the EgtE enzyme. This will shed light on the mechanism of the *C-S* lyase of EgtE as well as enzyme-substrate specificity.

2-Cysteinylhercynine thioether **2.19** was oxidized all the way to the 2-cysteinylhercynine sulfone **3.16** at room temperature (65%) by using a large excess of 30% solution of H_2O_2, 4.8 mol equivalents, in a presence of catalytic amount of boric acid (0.08 mmol) according to a method published by Rostami *et al*.[11] (Scheme 3.9)

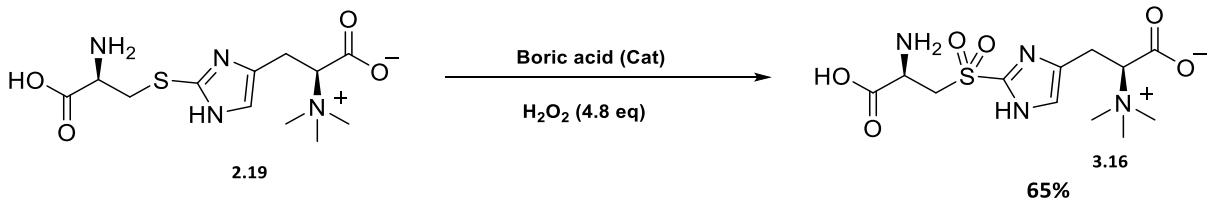

Scheme 3.9. Synthesis of 2-cysteinylhercynine sulfone 3.16.

A key characteristic signal in the ^{1}H NMR spectrum of 2-cysteinylhercynine sulfone **3.16** was one aromatic proton resonating as a singlet at δ_H 8.01 ppm. Two deshielded protons resonating both as doublet of doublets at δ_H 4.52 ppm and 3.89 ppm respectively, characteristic of α-amino protons and one singlet δ_H 2.89 ppm integrating for 9 protons, thus supporting the structure of 2-cysteinylhercynine sulfone **3.16**.

Another key diagnostic feature was the downfield shift of methylene protons resonating as doublet of doublets in the ^{1}H NMR spectrum of thioether **2.19** from 3.50-3.36 ppm to δ_H 3.67 ppm, thus supporting a successful oxidation of the sulfur atom adjacent to the methylene.

The ^{13}C NMR spectrum corroborated by mass spectrum (ESI^+) confirmed the structure of 2-cysteinylhercynine sulfone **3.16**. An high-resolution mass spectrum (ESI^+) revealed the molecular ion at *m/z* 349.1177 $[M]^+$, calculated for $C_{12}H_{21}N_4O_6S^+$ (349.1182) $[M]^+$. (Figure 3.6)

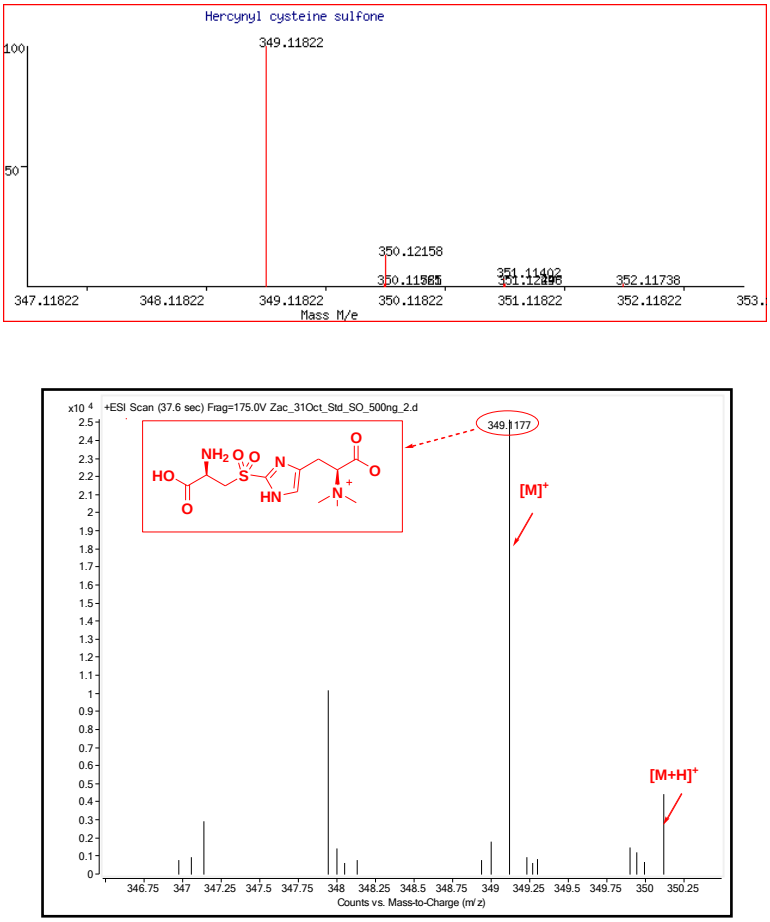

Figure 3.6. **Top.** Theoretical HRMS isotopic pattern calculated for $C_{12}H_{21}N_4O_6S^+$ $[M]^+$. **Bottom**. Experimental ESI/QTOF mass spectra of 2-cysteinylhercynine sulfone **3.16** in positive ion mode.

3.3. *In vitro* reconstitution of ergothioneine biosynthesis in *Mycobacterium smegmatis.*

Having successfully synthesized the ergothioneine biosynthetic precursors, hercynine-d_3 **3.4**, 2-cysteinylhercynine thioether **2.19** and sulfoxide **3.8**, the *in vitro* reconstituted synthesis of

ergothioneine in mycobacteria was attempted as illustrated in the simplified flow chart below. (Figure 3.7)

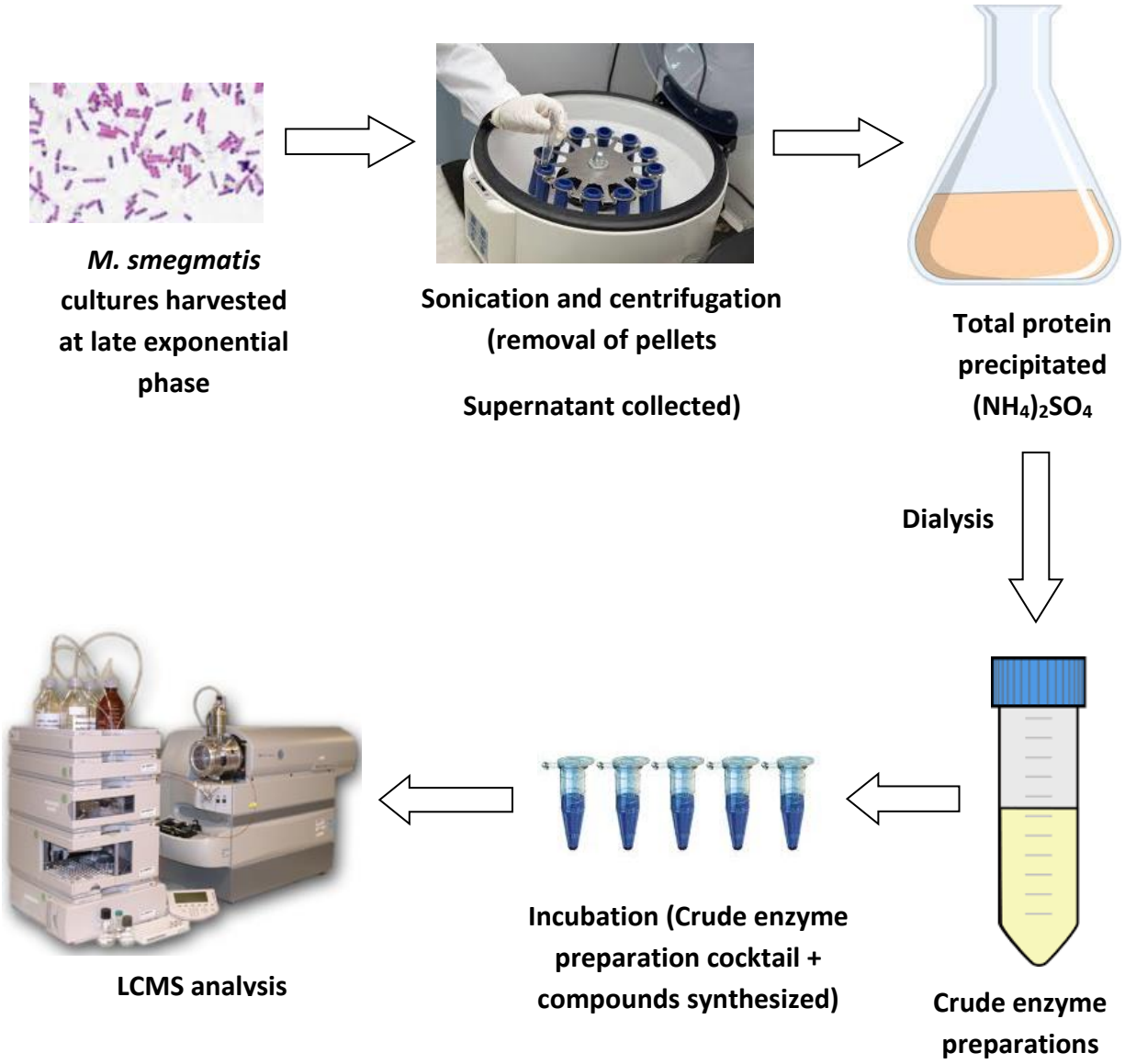

Figure 3.7. Simplified flow chart of the biotransformation mediated by EgtE crude enzyme preparations.

The last step of mycobacterial ergothioneine biosynthesis is catalyzed by EgtE (a PLP-dependent enzyme) which involves the lysis of the *C-S* bond of 2-cysteinylhercynine sulfoxide

3.8 to form ergothioneine.[7] The study of this transformation will help to understand the mechanism of the *C-S* bond lysis.

Seebeck published the reconstitution of the mycobacterial ergothioneine biosynthesis pathway. He managed to isolate all enzymes implicated in the pathway but failed to overexpress the EgtE enzyme.[7] The aim was to isolate EgtE *via* classic protein purification, but due to the lack of access to a pure *M. smegmatis* EgtE enzyme at the time of this research, *Mycobacterium smegmatis* cell-free lysate enzymatic preparations were utilized in the study. However, very recently mycobacterial EgtE enzyme was successfully isolated and characterized by Song *et al.*[12]

3.3.1. Total protein quantitation

Mycobacterium smegmatis cell-free extracts were isolated from cultures grown and harvested at the late exponential phase according to a published method by El-Sayed.[13] The total protein concentration was evaluated for reproducibility purposes and was calculated from a calibration curve established by the Bradford method. The total protein concentration was found to be 10 μg/μL.

3.3.2. Ergothioneine quantitation

A LCMS method was utilised to monitor the biotransformation of 2-cysteinylhercynine thioether **2.19**, 2-cysteinylhercynine sulfoxide **3.8**, 2-cysteinylhercynine sulfone **3.16** as well

as hercynine-d_3 **3.4** synthesized. This technique was chosen due to its sensitivity therefore requiring a very small amount of sample.

The production of ESH was monitored at retention time of 1.5 min. (Figure 3.8) The high-resolution mass spectrum (ESI^+) of the natural ESH displayed peaks at *m/z* 230.0958 $[M]^+$ and at *m/z* 231.0980 corresponding to $[M]^+$ and $[M + H]^+$ respectively. (Figure 3.9)

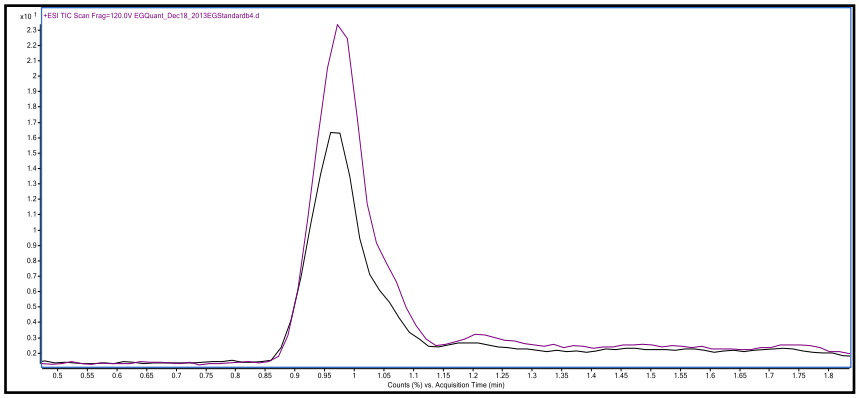

Figure 3.8. Overlaid TIC of ergothioneine (Top 25 ng mL^{-1}, bottom 12.5 ng mL^{-1} concentrations). Retention time of 1.5 min. (Positive ionization mode) (ESI^+) and column (Eclipse + C18 RRHD 1.8 µm.2.1 X 50, Agilent 1290 infinity, Germany)

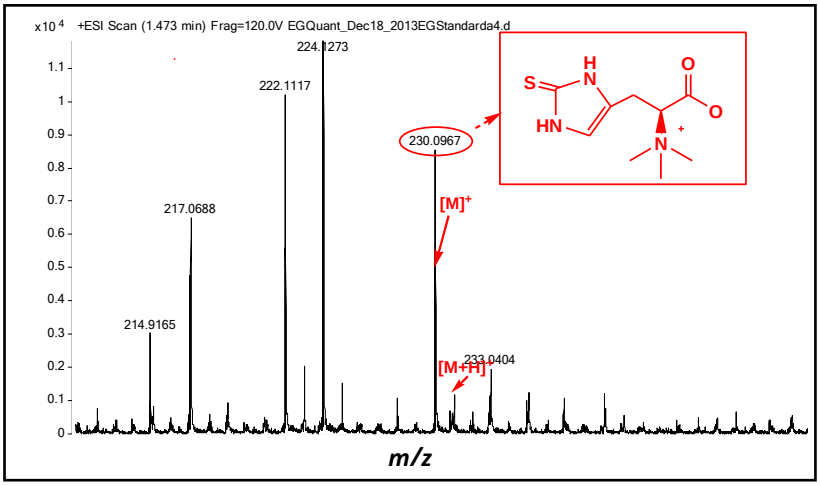

Figure 3.9. ESI/QTOF mass spectra of ESH standard in positive ion mode.

The calibration curve was established from eight different concentrations (0.78, 1.56, 3.125, 6.25, 12.5, 25, 50, 100 ng mL^{-1}) of ESH prepared in triplicate. (Figure 3.10) The limit of quantitation (LOQ) for ESH was 0.78 ng mL^{-1} (lowest concentration of ESH standard used to construct the calibration curve) similar to the one reported by Wang *et al.*[14] while the limit of detection (LOD) for ESH was 9 pg mL^{-1} (LOD is the lowest concentration of ESH standard required to display a LCMS response and determined experimentally). The expected range of quantitation was 0.78-100 ng mL^{-1}. (0.78 ng mL^{-1} (lowest concentration) and 100 ng mL^{-1} (highest concentration) used to construct the calibration curve in the experiment, therefore any value outside this range is considered not accurate for the experiments)

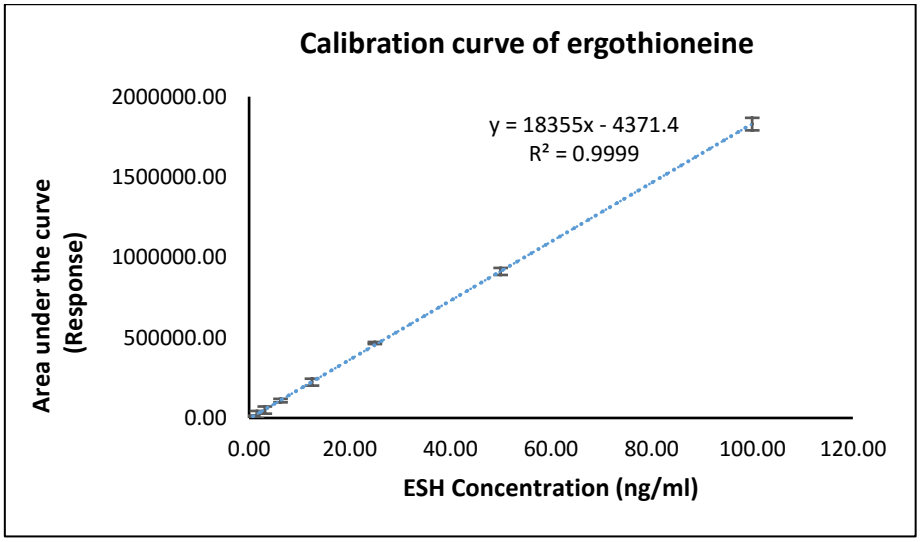

Figure 3.10. Calibration curve of ESH.

3.3.3. Biotransformation of EgtE substrates to ergothioneine using crude *M. smegmatis* enzyme preparations.

Biotransformation of synthesized substrates using cell-free *Mycobacterium smegmatis* crude enzyme preparations were assayed in triplicate, repeated several times (more than three

times) and these results were reproducible. Reactions (100 µL) were allowed to incubate at 37°C for 1 day at pH = 7.4 (20 mM Tris-HCl buffer) and the production of ergothioneine was quantified using LCMS. (experimental section).[15]

The negative control reaction containing only the crude *M. smegmatis* cell-free extract was also treated under the same conditions as the ergothioneine precursors. The concentration of ESH thus obtained was 5.70 (±0.30) ng mL^{-1}, which equate to that of endogenous ESH. This concentration was above the limit of detection (0.78 ng mL^{-1}), thus any increase in the concentration of ESH in the experiment above 1 ng mL^{-1} is considered enough to be ascribed to basal levels or biotransformation of the respective substrates by the crude endogenous enzymes of the ESH pathway.

3.3.3.1. Enzymatic synthesis of ergothioneine-d_3 (3.7) using hercynine-d_3 (3.4) as a substrate.

As anticipated, when hercynine-d_3 (**3.4**) was used as the substrate in the enzymatic reaction, the endogenous concentration (baseline) of ESH remained unchanged. However, as expected, the LCMS analysis of the enzymatic reaction mixture revealed the production of ESH-d_3 (**3.7**) at the same retention with the natural ESH (1.5 min). (Scheme 3.10)

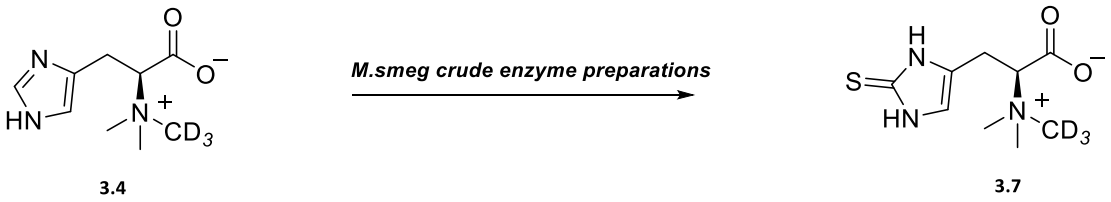

3.4 3.7

Scheme 3.10. Enzymatic biotransformation of hercynine-d_3 (3.4).

The high-resolution mass spectrum (ESI^+) displayed a peak at *m/z* 233.1161 corresponding to $[M + D_3]^+$. Peak values at *m/z* 230.0958 $[M]^+$ or at *m/z* 231.0980 $[M + H]^+$ belonging to the natural ESH were not detected in the chromatogram. This clearly shows that the crude *M. smegmatis* enzymes (dialyzed extract) transformed the hercynine-d_3 (**3.4**) into ESH-d_3 (**3.7**). This proved that the isolated crude enzyme extract was fully functional in the reconstitution of ESH synthesis. (Figure 3.11)

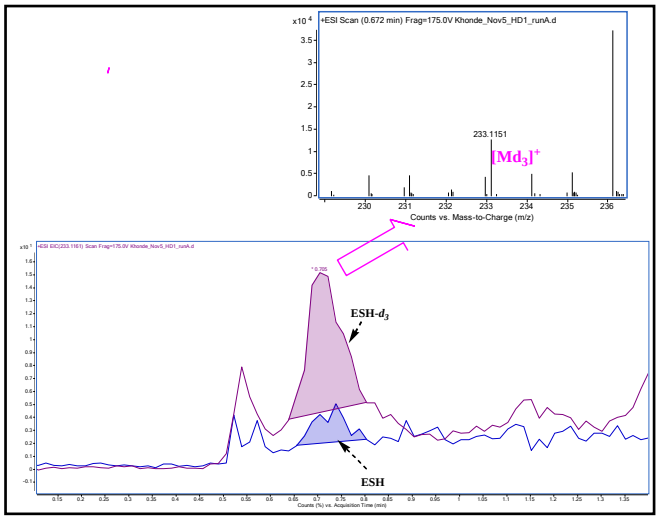

Figure 3.11. LCMS spectrum of ESH-d_3 (3.7) *in vitro* reconstititued experiment using hercynine-d_3 (3.4) as substrate.

3.3.3.2. Biotransformation of EgtE substrates to ergothioneine using crude *M. smegmatis* enzyme preparations

Three cysteinyl hercynine derivatives were assayed in the presence of the crude *M. smegmatis* enzymatic preparations. EgtE substrate, 2-cysteinylhercynine sulfoxide **3.8** biosynthetically produced the highest concentration of ESH (22.6 ±0.3 ng mL^{-1}). The 2-cysteinylhercynine thioether **2.19** appeared to be almost as good a substrate as the 2-cysteinylhercynine sulfoxide **3.8** producing 19.2 (±0.2) ng mL^{-1} ESH. However, 2-cysteinylhercynine sulfone **3.16** did not produce any noticeable amount of ESH as the 4.3 (±0.1) ng mL^{-1} detected was attributed to endogenous ESH. (Figure 3.12 & Figure 3.13)

Thus, the EgtE enzyme recognized both, 2-cysteinylhercynine thioether **2.19** and 2-cysteinylhercynine sulfoxide **3.8** as substrates, while the sulfone **3.16** could not be cleaved in the active site of the EgtE enzyme.

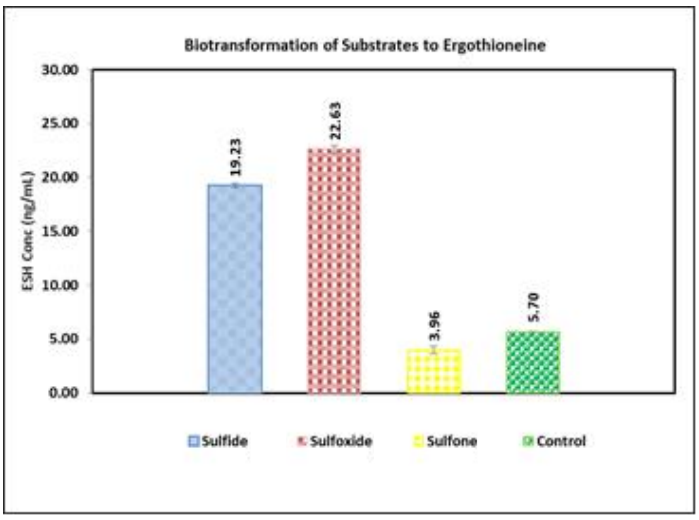

Figure 3.12. ***In vitro*** **reconstitution of ESH**; 100 µL reactions containing 20 mM Tris HCl pH= 7.4, 20 mM NaCl, 0.2 mM $FeSO_4.7\ H_2O$, 0.5 mM mercaptoethanol, 83 µL of crude *M. smegmatis* enzymes and 50 mM of either (a) 2-cysteinylhercynine thioether (**2.19**); (b) 2-cysteinylhercynine sulfoxide (**3.8**); (c) 2-cysteinylhercynine sulfone

(**3.16**) and (d) control. The crude enzyme reactions were incubated for 1 day at 37° C followed by analysis by LC/MS.

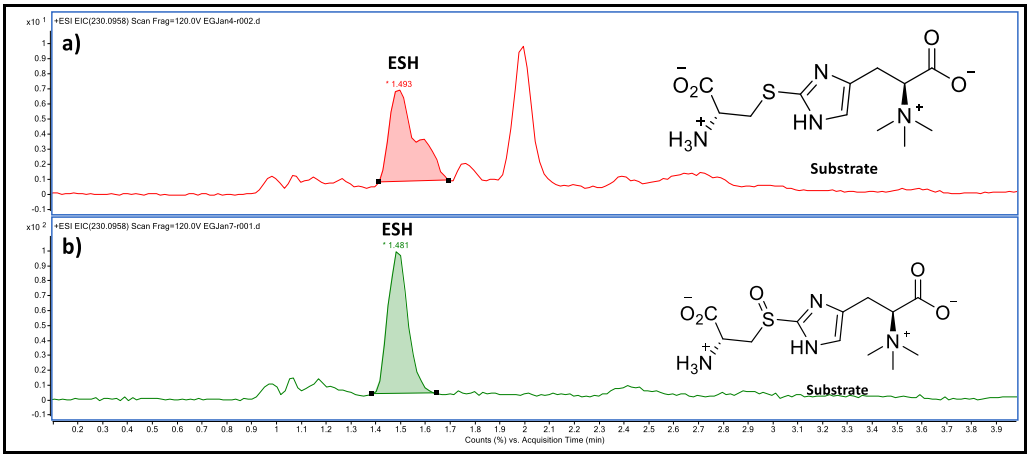

Figure 3.13. TIC extracted for ESH *in-vitro* reconstititued experiment using substrate: (a) 2-cysteinylhercynine thioether **(2.19)** as substrate, (b) 2-cysteinylhercynine sulfoxide **(3.8)** as substrate.

3.3.4. Non-enzymatic cleavage of the *C-S* bond catalyzed by PLP

It is well known that PLP-dependent transformations can also undergo enzyme-free conversion albeit with a much slower rate and specificity.[16] Thus, the non-enzymatic treatment of the sulfide (**2.19**) with 50 mM PLP at 37 °C resulted in an efficient formation of ESH (96 ±2 ng mL^{-1}) (green line). However, under the same conditions, the sulfoxide (**3.8**) (blue line) and sulfone (**3.16**) (orange line) produced no ESH at all. (Figure 3.14) Thus the oxidation state of the sulfur atom is crucial for the *C-S* bond lysis as only the sulfur **2.19** displayed an efficient cleavage.

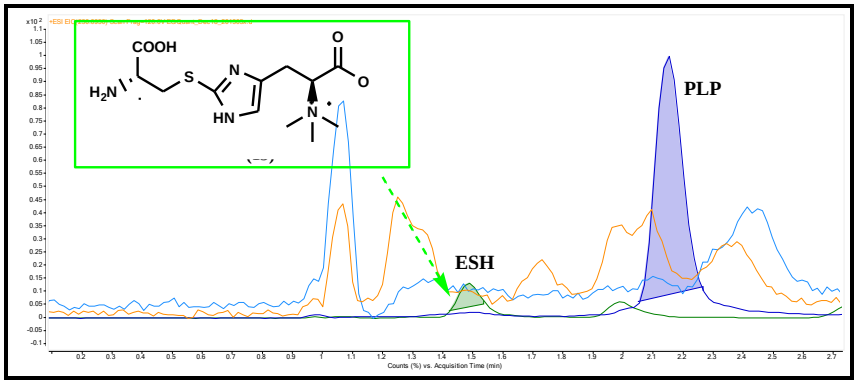

Figure 3.14. Non enzymatic production of ESH catalysed by PLP. TIC extracted for **ESH** and **PLP** using 2-cysteinylhercynine thioether (**2.19**) (green line), 2-cysteinylhercynine sulfoxide (**3.8**) (blue line) and 2-cysteinylhercynine sulfone (**3.16)** (orange line).

3.3.5. *Mycobacterium smegmatis* EgtE inhibition by 2-cysteinylhercynine sulfone

2-Cysteinylhercynine sulfone **3.16** did not produce any ESH either when assayed using cell-free crude *M. smegmatis* enzyme preparation or under enzyme-free PLP-mediated conditions.

When 100 µL reactions containing 50 mM 2-cysteinylhercynine sulfone **3.16** and either 50 mM 2-cysteinylhercynine thioether **2.19** or 50 mM 2-cysteinylhercynine sulfoxide **3.8** were incubated with cell-free *M. smegmatis* enzymatic preparation at pH = 7.4 (20 mM Tri-HCl buffer) at 37 °C for 1 day, insignificant amounts of ESH produced, 8 and 4.3 (±0.1) ng mL^{-1} of ESH were detected respectively. That were within the range of the endogenous ESH concentration (5.7 (±0.3) ng mL^{-1}). (Figure 3.15 & Figure 3.16)

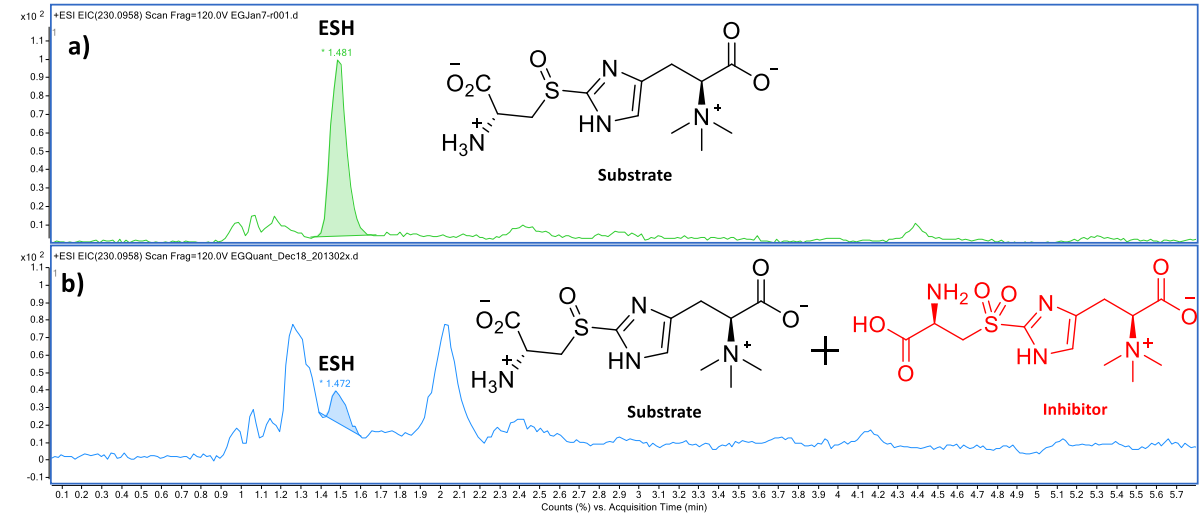

Figure 3.15. LCMS spectrum of *M. smegmatis.* ESH enzymes inhibition. (**a**) TIC extracted for ESH in enzymatic reaction using sulfoxide (**3.8**) as a substrate. (**b)** TIC extracted for ESH in the enzymatic reaction using sulfoxide (**3.8**) and sulfone (**3.16**) as an inhibitor.

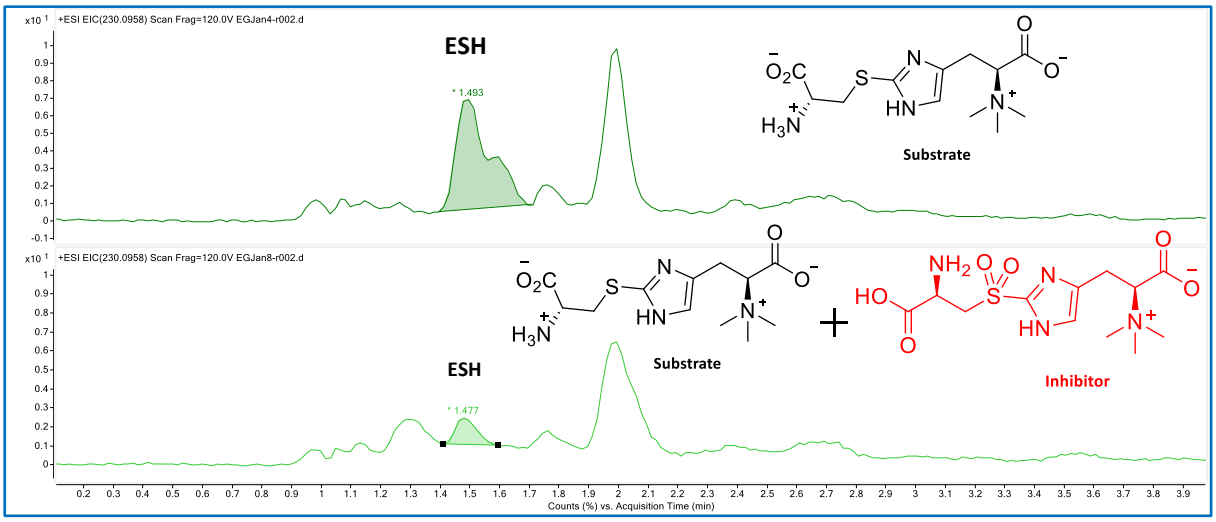

Figure 3.16. LCMS spectrum of *M. smegmatis.* ESH enzymes inhibition. (**a**) TIC extracted for ESH in enzymatic reaction using sulfide (**2.19**) as a substrate (**b)** TIC extracted for ESH in the enzymatic reaction using sulfide (**2.19**) and sulfone (**3.16**) as an inhibitor.

When sulfone **3.16** was added to the 2-cysteinylhercynine thioether **2.19** enzymatic reaction, ESH biosynthesis was inhibited by 60%. Inhibition of ESH biosynthesis was over 80% when

sulfone **3.16** was added to the 2-cysteinylhercynine sulfoxide **3.8** enzymatic reaction. (Figure 3.17).

Percentage ESH inhibition was determined using this formula: % $_{\text{ESH inhibition}}$ = (ESH$_{\text{substrate}}$-ESH $_{\text{after inhibition by sulfone}}$)/ESH $_{\text{substrate}}$; eg. % $_{\text{ESH thioether}}$ = (19.23-7.60)/19.23 = 60% and % $_{\text{ESH sulfoxide}}$ = (22.93-4.26)/22.93 = 81%.

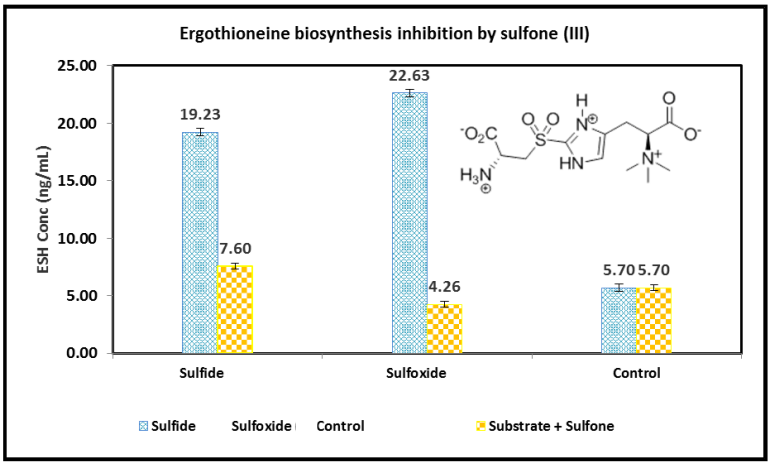

Figure 3.17. Ergothioneine biosynthesis inhibition studies contain; 100 µL reactions containing 20 mM Tris HCl pH= 7.4, 20 mM NaCl, 0.2 mM $FeSO_4.7\ H_2O$, 0.5 mM mercaptoethanol, 83 µL of crude *M. smegmatis* enzymes and 50 mM of either substrate sulfide (**2.19**), sulfoxide (**3.8**) alone or in the presence of sulfone (**3.16**) respectively (c) control no substrates.

These findings have suggested that adding 2-cysteinylhercynine sulfone **3.16** to the enzymatic reaction mixtures significantly inhibits the *in vitro* biosynthesis of ESH in *M. smegmatis,* hence 2-cysteinylhercynine sulfone **3.16** can be identified as an inhibitor of ESH biosynthesis.

3.3.6. Minimum Inhibitory Concentration (MIC) of 2-cysteinylhercynine sulfone, ESH-inhibitor.

The minimum inhibitory concentration inhibition of 2-cysteinylhercynine sulfone **3.16** was assayed against *Mycobacterium smegmatis* strain mc^2 155 using a broth dilution method with the Alamar blue stain used for visualization as shown in the Figure 3.18.[17]

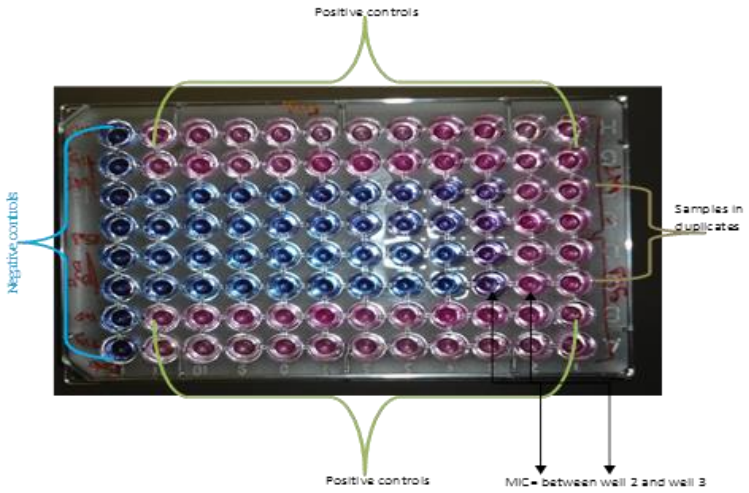

Figure 3.18. Broth dilution method.

Even though 2-cysteinylhercynine sulfone **3.16** did not exhibit better MIC's than existent TB-drugs such as Isoniazid (INH) and Rifampin (RIF) used as positive control in this study; 2-cysteinylhercynine sulfone **3.16** still inhibited *M. smegmatis* growth at concentrations of 1600–1700 μg/mL (experiment performed in triplicate). Due to the fact that sulfone **3.16** (ESH-inhibitor) inhibits *Mycobacterium smegmatis* growth, may suggest that the sulfone inhibitor could be toxic to the cell. 2-Cysteinylhercynine sulfone **3.16** in combination with

either Isoniazid (INH) or Rifampin (RIF) did not show synergy in the inhibition of *Mycobacterium smegmatis*.

3.3.7. Proposed mechanism of *C-S* lyase of sulfide (2.19), sulfoxide (3.8) and sulfone (3.16) catalysed by PLP.[15]

C-S lyases are a subclass of enzymes that catalyse the cleavage of *C-S* bond by other processes than by hydrolysis or oxidation. Most *C-S* lyase enzymes cleave sulfur substrates through elimination, hence generating either a double bond or a new ring. In the literature, only few sulfoxides have been reported as substrates of *C-S* lyase enzymes.

However, many PLP-dependent *C-S* lyases have been previously reported in primary metabolism or xenobiotic detoxification,[18] such examples include cysteine *S*-conjugate β-lyases.[19] Recently, they are reported in secondary metabolism[7,12,15], that GliI, a PLP dependent *C-S* lyase involved in the key step of the biosynthetic pathway of gliotoxin (secondary metabolite) was extensively studied by Scharf *et al.*[20]

This section will be dedicated to discussing the proposed mechanism of the PLP-dependent *C-S* lyase, EgtE.

The pKa value of the amino acid α-hydrogen usually is in the range 20–30 and many enzymes effectively increase the α-hydrogen acidity with the aid of a coenzyme, PLP. PLP-dependent enzymes exist in their native state as an internal aldimine (Schiff base) with the ε-amino group of a lysine residue present in the catalytic site. The amino acid substrate displaces the lysine

from the internal aldimine to form a new aldimine, termed external aldimine. The formation of such an external aldimine can reduce the pKa value of the α-proton of the substrate from 30 to as low as 6.[16]

PLP-dependent enzymes have been differentiated on the basis of their tertiary structures, more specifically according to fold types I–V. EgtE is classified as a fold type V which is found mainly in enzymes that catalyze β-replacement and β-elimination reactions. In the absence of a crystal structure of EgtE, structure homology analysis amongst mycobacteria is not possible. However, a putative β-lyase from *E. tasmaniensis* appeared to catalyse this step but has a sequence similarity to EgtE of *M. smegmatis* and *M.tb* of only 14%.

Thus, the proposed mechanism of this *C–S* β-lyase utilising 2-cysteinylhercynine thioether (**2.19**) as a substrate was based on that of the well characterized cystalysin from *Treponema denticola* which shares 31% sequence identity to the β-lyase from *E. tasmaniensis.*[21] It may well be that actinomycetes have similar β-lyases at work.[22] It has also been observed to be a rather facile non-enzymatic (PLP only) β-elimination with the 2-cysteinylhercynine thioether (**2.19**). (Figure 3.19)

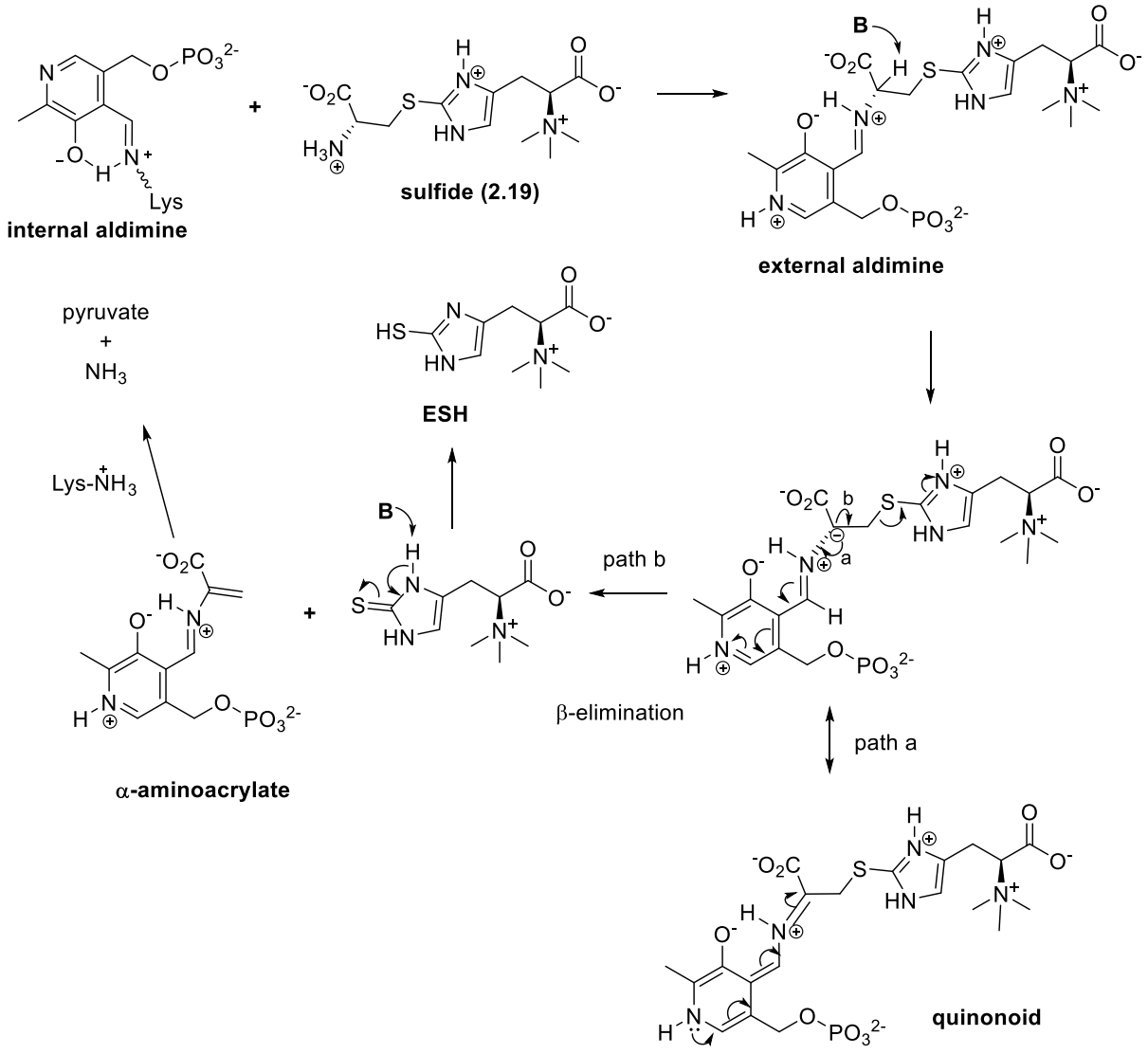

Figure 3.19. β-Elimination of the sulfide (2.19).[15]

However, the conversion of the natural substrate, 2-cysteinylhercynine sulfoxide (**3.8**), to ESH is not consistent with the literature.[7] Elimination of an unstable (β-amino-β-carboxyethyl)ergothioneine sulfinate (**3.17**) is envisaged, whereby self-condensation leads to the thiosulfinate, which in turn decomposes to ESH and an equivalent amount of relatively stable (β-amino-β-carboxyethyl)ergothioneine sulfenic acid (**3.18**). (Figure 3.20)

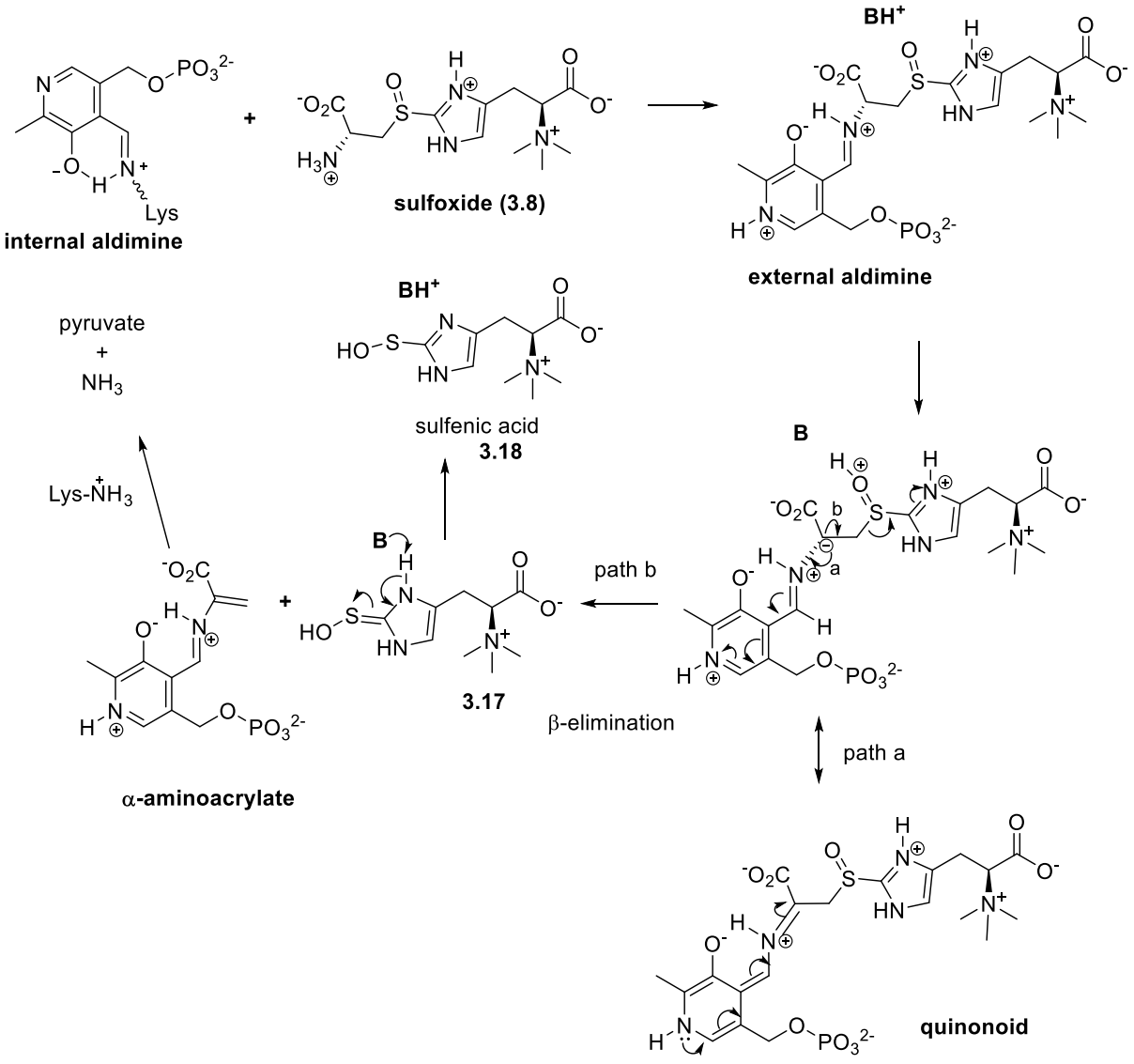

Figure 3.20. β-Elimination of the sulfoxide (3.8).[15]

Subsequently, the latter sulfenic acid **3.18** can be reduced to the thiol, ESH, with the aid of excess mercaptoethanol, but this may be difficult under the current experimental conditions.[23] The 2-cysteinylhercynine sulfoxide (**3.8**) does not lead to the production of ESH in the absence of a reductant, such as mercaptoethanol. This mechanism was further confirmed by Song *et al.*, who demonstrated that ESH could only be detected when incubating

2-cysteinylhercynine sulfoxide **3.8** with pure EgtE enzyme in a presence of DTT as reductant. However, *in vivo* it is suspected that natural thiols such as mycothiol, cysteine, glutathione might act as reductant to accomplish this role.[12] (Figure 3.21)

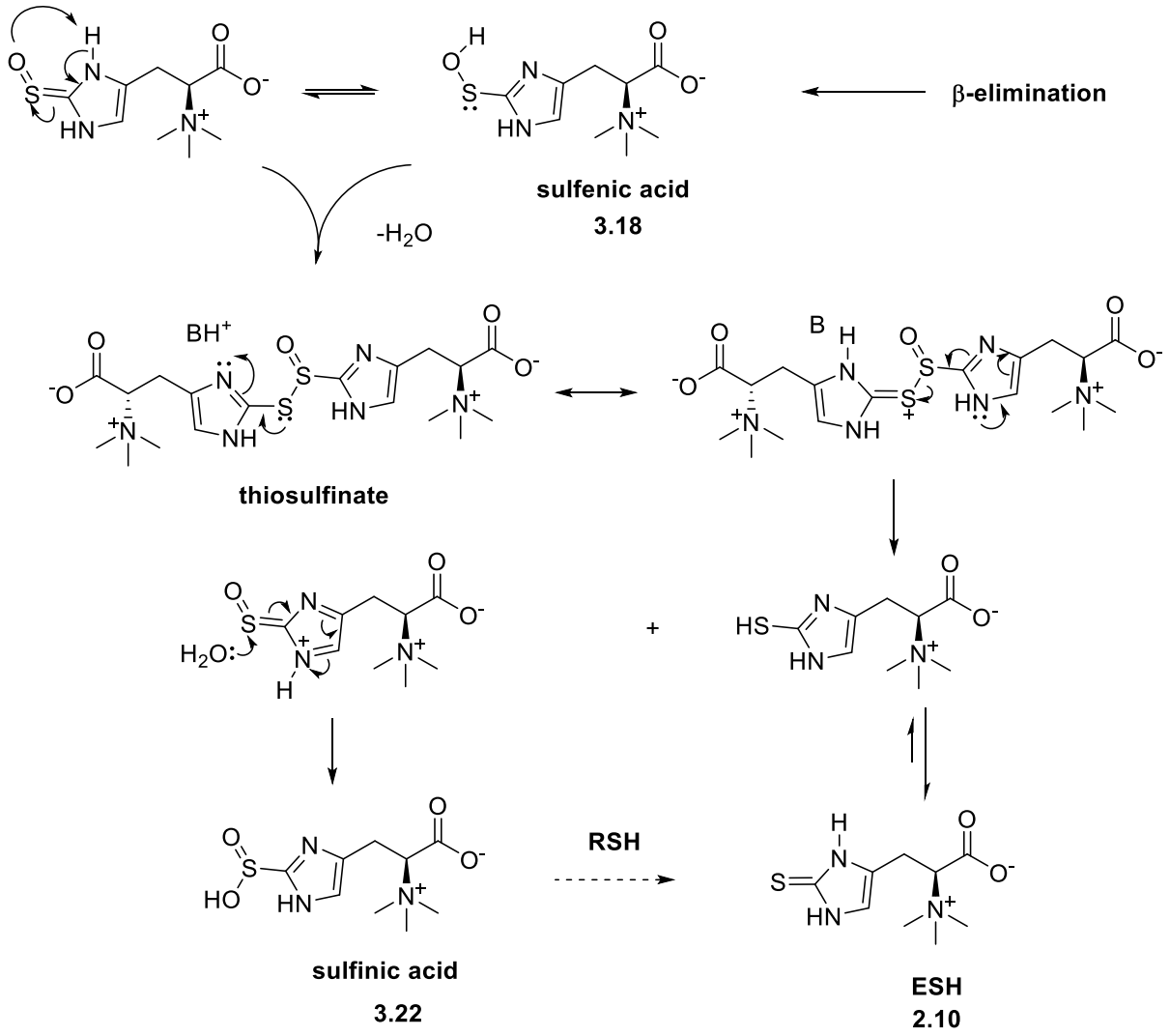

Figure 3.21. Sulfenic acid 3.18 conversion to ESH.

It is noteworthy that the involvement of sulfenic acid **3.18** as a key intermediate during the catalysis of EgtE enzyme was provided very recently by Song *et al.*[12] These authors managed to trap this unstable intermediate in a presence of cyclohexane-1,3-dione **3.19** and

characterized the sulfenic acid-cyclohexane dione adduct **3.20** isolated following cellulose chromatography. Moreover, they proposed that the highly unstable sulfenic acid **3.18** disproportionates to produce the thiol ester of thiosulfinic acid **3.21**, the latter will hydrolyse to form either ESH **2.10** or ergothioneine-2-sulfinic acid **3.22** depending on the assay conditions. However, the highly unstable sulfinic acid **3.22** degrades to hercynine **3.3** during the isolation process *via* elimination of sulfur dioxide under acidic conditions.[24] (Figure 3.22)

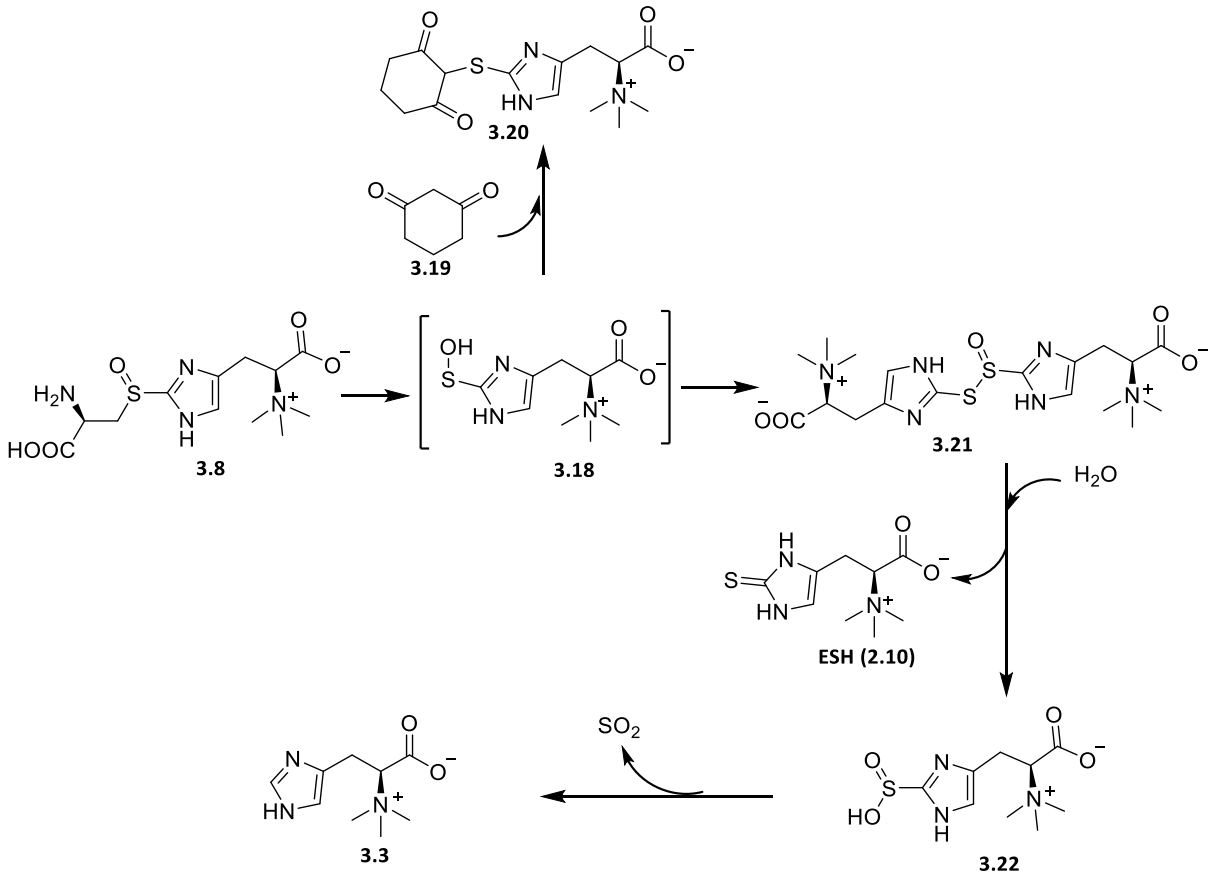

Figure 3.22. Proposed model explaining EgtE reaction using sulfoxide (3.8) as a substrate. (Adapted from song *et al.*[12])

ESH inhibition by 2-cysteinylhercynine sulfone **3.16** could proceed through system stabilisation resulting to the formation of very stable quinonoid conjugated intermediates (4

possible intermediates) which cannot be *C-S* cleaved, hence no ESH cannot be detected. (Figure 3.23)

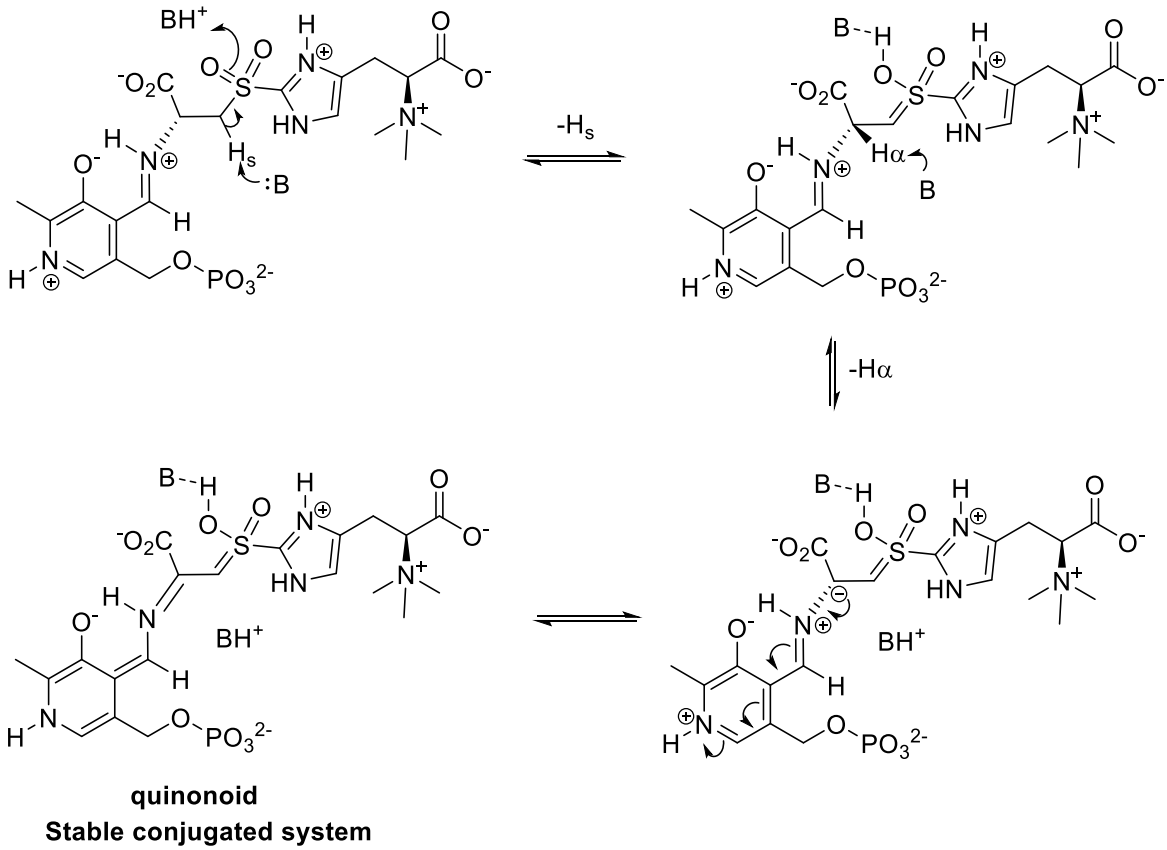

Figure 3.23. Stabilisation of the sulfone (3.16).

3.3.8. Summary of major findings

In summary, 2-cysteinylhercynine thioether **2.19** was synthesized in 5 sequential steps in a good overall yield of 64-70%. Catalytic oxidation of the thioether **2.19** yielded 2-cysteinylhercynine sulfoxide **3.8** in a good yield of 71%, or if further oxidised, 2-cysteinylhercynine sulfone **3.16** in a moderate yield of 65%. (Scheme 3.11)

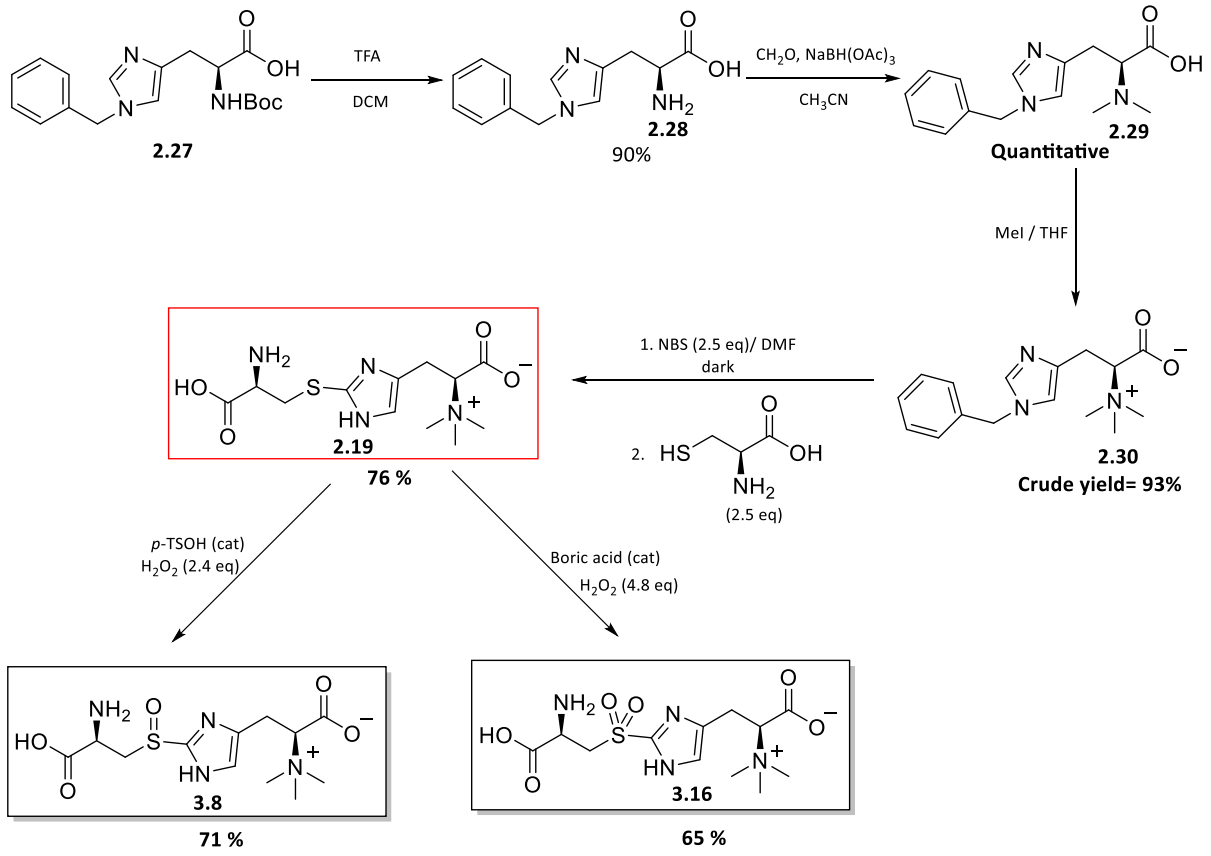

Scheme 3.11. Synthesis of cysteinylhercynine thioether 2.19, sulfoxide 3.8 and sulfone 3.16.[15]

It has been found that 2-cysteinylhercynine thioether **2.19** and 2-cysteinylhercynine sulfoxide **3.8** biosynthetically produced ESH, with 2-cysteinylhercynine sulfoxide **3.8** producing the highest amount of ESH (22.6 ng mL^{-1}) thus suggesting that the sulfoxide intermediate **3.8** is the preferred biological EgtE substrate. This finding was later on confirmed by Song *et al*. based on kinetic parameters determined using purified *M. smegmatis* EgtE enzyme.[12]

When performing the non-enzymatic PLP-mediated reactions, only 2-cysteinylhercynine thioether **2.19** produced ESH (96 ±2 ng mL^{-1}), while either 2-cysteinylhercynine sulfoxide **3.8** or 2-cysteinylhercynine sulfone **3.16** produce no ESH at all. (Scheme 3.12)

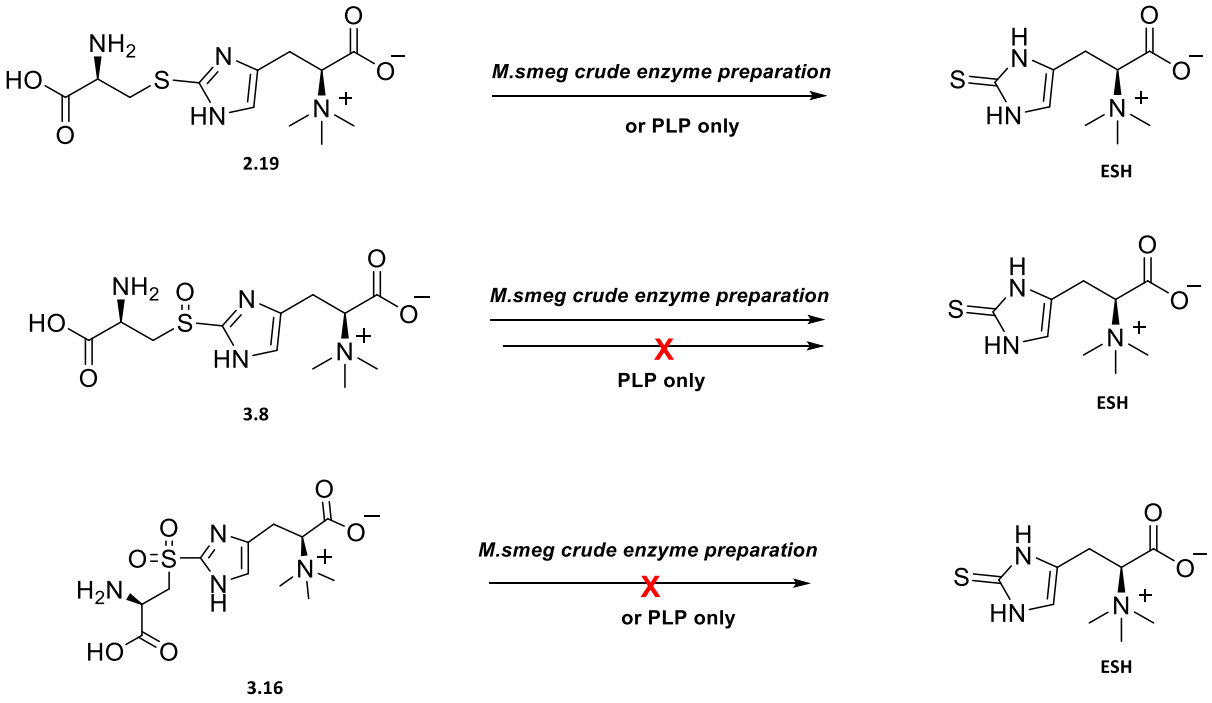

Scheme 3.12. Biotransformation and non enzymatic PLP-mediated reactions of cysteinylhercynine thioether (2.19), sulfoxide 3.8 and sulfone (3.16).

3.4. Derivatization and detection of thiols

3.4.1. Rationale

It was proposed to develop a method for detection of thiols particularly *L*-ergothioneine. This method has to be cheaper, almost instantaneous, less interference and allowing ESH detection even at very low level.

Recently, Sotgia *et al.* developed a simple, fast, accurate method for routine quantification of ESH in whole blood using ultra-performance liquid chromatography and UV-vis detection while achieving a limit of detection (LOD) and limit of quantification (LOQ) of 3.85 and 11.67 µmol/L, respectively.[25] Although, this method appeared to be attractive, it remains very expensive as it uses costly chromatographic columns and equipment, therefore it was advised to develop a different approach which would involve relatively cheaper reagents and equipment such as UV-vis spectrophotometer.

A well known UV-vis spectrophotometric method is well documented.[26,27] This method involves the monitoring of the formation of a specific adduct which exerted a strong absorbance at about λ_{max} 420 nm resulting from the reaction of Ellman's reagent (5,5'-dithio-bis(2-nitrobenzoic acid) and free thiols like coumpounds as well as enzymes having SH-groups. However, it was reported incomplete reactions of certain substrates mostly hindered protein sulfhydryls with Ellman's reagent even after a prolonged reaction time. Therefore, Riener *et al* substitute Ellman's reagent by 4,4'-dithiodipyridine (DTDP), which reacts efficiently with hindered protein sulfhydryls even without the use of cystamine as a catalyst.[27]

Furthermore the same autors optimised the sensitivity, the limit of detection and the assay time of DTDP and traditional Ellman/cystamine methods.[27]

It is well known that simple as well as complex thiols react easily, rapidly and selectively with propiolic ester (methyl and ethyl propiolic ester) to yield thioacrylates which exhibited characteristic UV-vis absortion at λ_{max} 280-290 nm. This procedure utilised inexpensive reagents and allows the detection and quantitation of thiols even at nanomolar level using NMR as well as UV-vis spectrophotometric techniques.[28]

Zacharis *et al.* systematically studied ethyl propiolate (EP) as a novel derivating reagent for thiols and this derivatization reaction was also investigated under flow conditions and UV detection at λ_{max} 285 nm.[29] Moreover the same group optimized this method to detect and quantify glutathione (GSH) in vegetables.[30]

3.4.2. Propiolic acid, a reagent for thiol detection, tagging and derivatization

During the course of this investigation, propiolic acid was utilized rather than their ester derivatives (novel approach) as a reagent for thiol detection, tagging and derivatization. Propiolic acid is very cheap, stable and less volatile than their ester derivatives.

Several thiols were assayed such as *L*-cysteine, *N*-acetyl cysteine, thiophenol, before assaying the non-enzymatic cleavage of 2-cysteinylhercynine thioether **2.19** by PLP, in order to detected the formation of *L*-ergothioneine.

3.4.2.1. *L*- cysteine

The Owen method[28] was followed using propiolic acid as thiol derivatizing instead of methyl or ethyl propiolates. (Scheme 3.13)

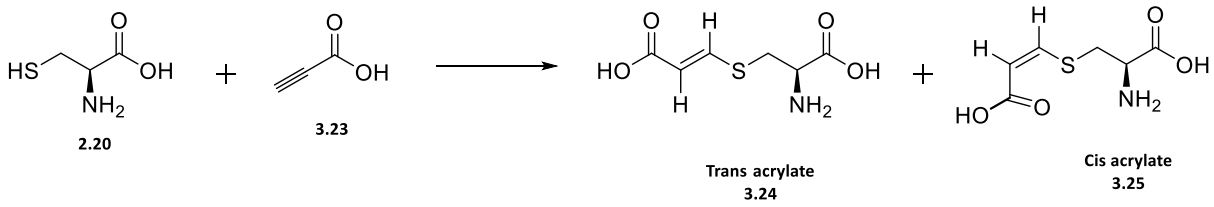

Scheme 3.13. Synthesis of thioacrylates 3.20 and 3.21 obtained from the reaction of propiolic acid 3.23 and *L*-cysteine 2.20

UV-vis spectrophotometric analysis of this reaction at µM (micromolar) level revealed a characteristic absorption at λ_{max} 275 nm suggesting successful formation of thioacrylates. (Figure 3.24)

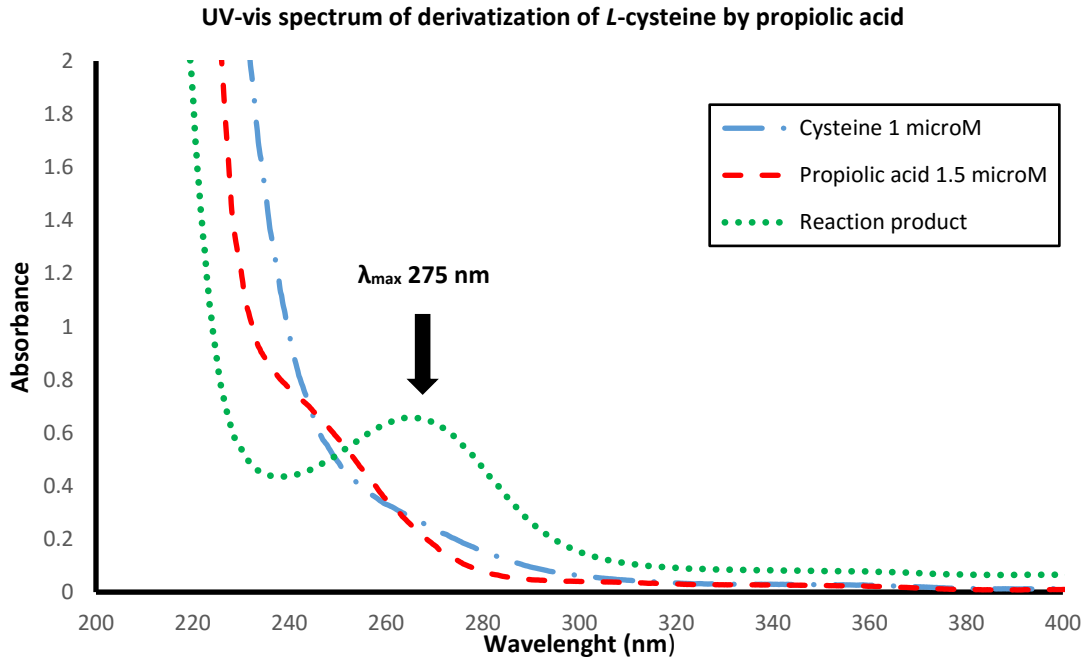

Figure 3.24. UV-vis spectrum monitoring the formation of thioacrylate formed from the reaction between *L*-cysteine 2.20 and propiolic acid 3.23 (at 25°C)

The ^{1}H NMR spectrum of *L*-cysteine is blank at region above 5.5 ppm, while thioacrylates displayed a characteristic NMR patterns at this region, hence the reaction was assayed at NMR scale.

It is noteworthy that Owen managed to isolate the *cis* isomer **3.25** at good yield of 65% after recrystallisation in water. The isolation of thioacrylates **3.24** and or **3.25** were not attempted during our investigation, however proton NMR spectrum analysis of the crude reaction mixture revealed the presence of two isomers both resonating as doublet, *cis* (*J* = 10.1 Hz) and *trans* (*J* = 15.3 Hz) at the ratio of 2.5:1 or 70:30 around 7.8 to 5.6 ppm, thus supporting Owen's finding that the *cis* isomer is predominant even when propiolic acid **3.23** is utilized as thiol derivatization reagent instead of methyl or ethyl propiolate.(Figure 3.25)

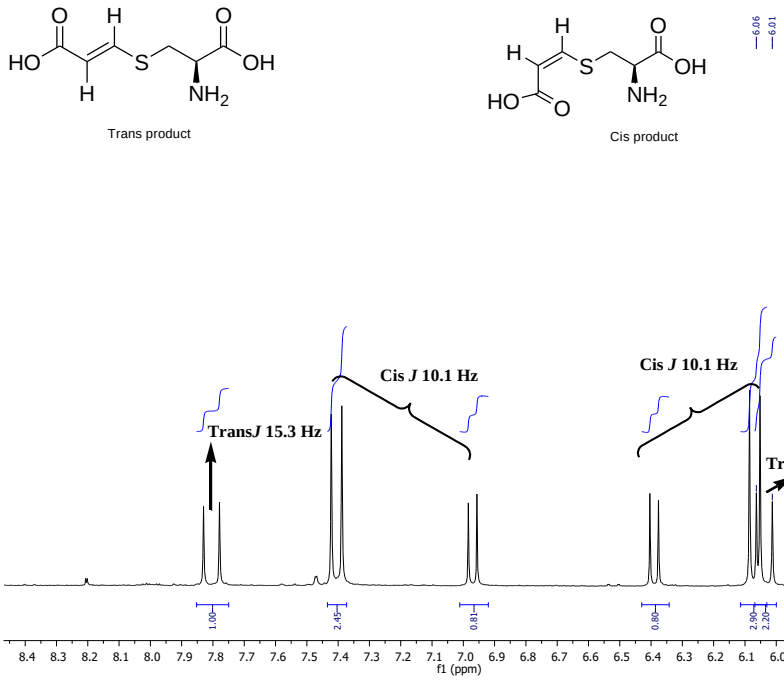

Figure 3.25. ^{1}H NMR spectrum of crude reaction of cysteine (2.20) and propiolic acid (3.23) in D_2O at 300 MHz from 8.4 to 5.6 ppm.

3.4.2.2. *N*-Acetyl cysteine and thiophenol

N-Acetyl cysteine and thiophenol were also assayed. Surprisingly the reaction of *N*-acetyl cysteine with propiolic acid did not reveal any characteristic thioacrylate absorptions.(Figure 3.26) Though, the reaction of thiophenol with propiolic acid displayed even stronger absorption around 270-280 nm, unfortunately this maxima absorption cannot entirely be attributed to thioacrylates as it coincides with the thiophenol (aromatic compound) spectrum, which itself displayed a strong absorbance at the same region. (Figure 3.27) However, these results were not investigated further to evaluate the scope and limitations of this method.

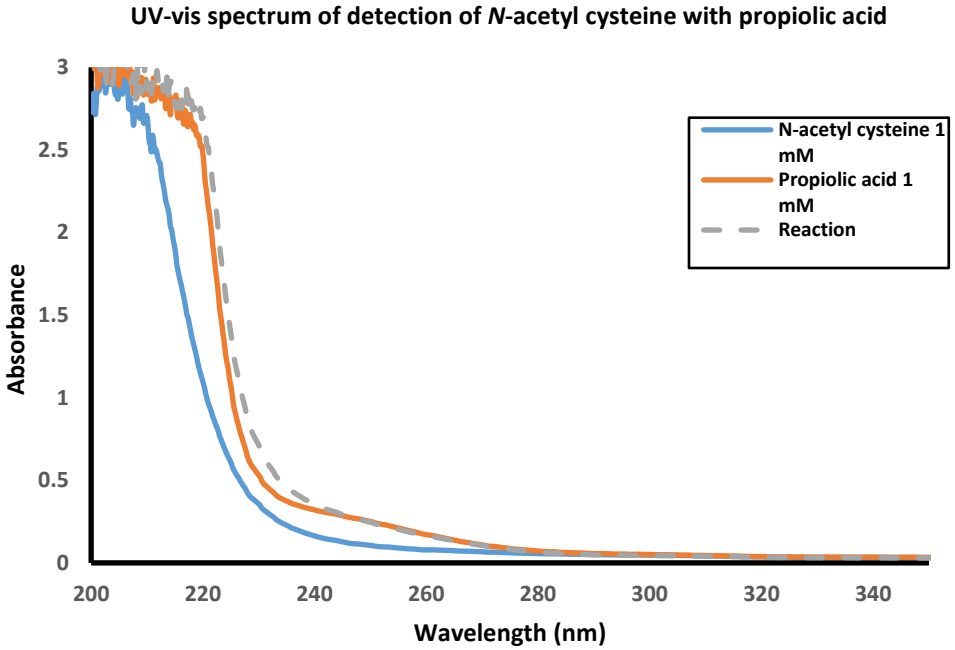

Figure 3.26. UV-vis spectrum of the reaction of propiolic acid 3.23 with *N*-acetyl cysteine (at 25°C).

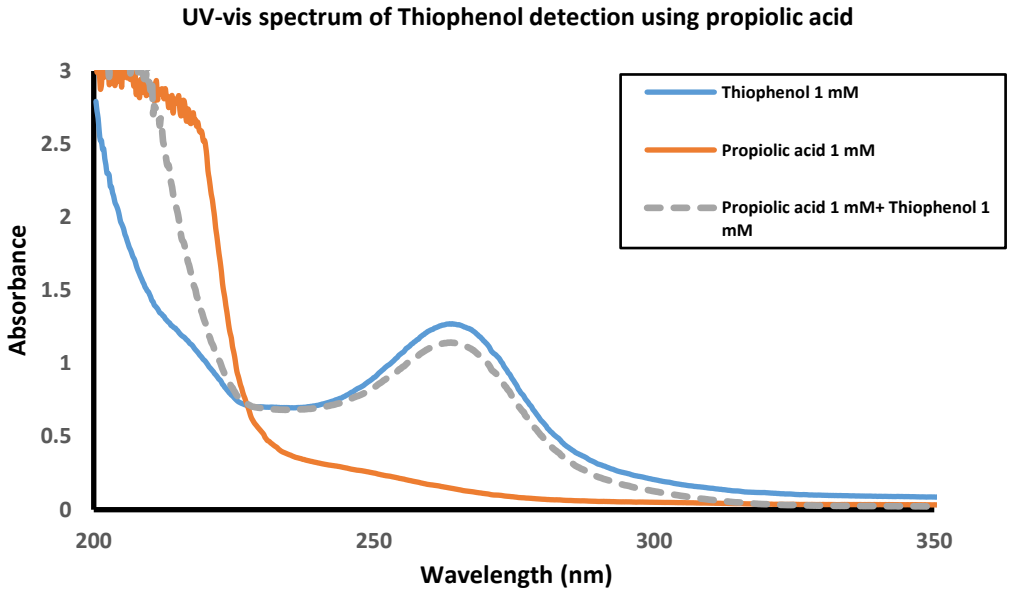

Figure 3.27. UV-vis spectrum of the reaction of propiolic acid 3.23 with thiophenol (at 25°C).

3.4.2.3. *In situ L*-ergothioneine detection and derivatization during non-enzymatic cleavage of *C-S* bond of 2-cysteinylhercynine thioether 2.19

The discovery of non-enzymatic cleavage of the *C-S* bond of 2-cysteinylhercynine thioether **2.19** catalysed by PLP was one of the breakthroughs during the course of this research. Therefore, the direct *in situ* derivatization of *L*-ergothionine **2.10**, product of this reaction was successfully attempted. (Scheme 3.14)

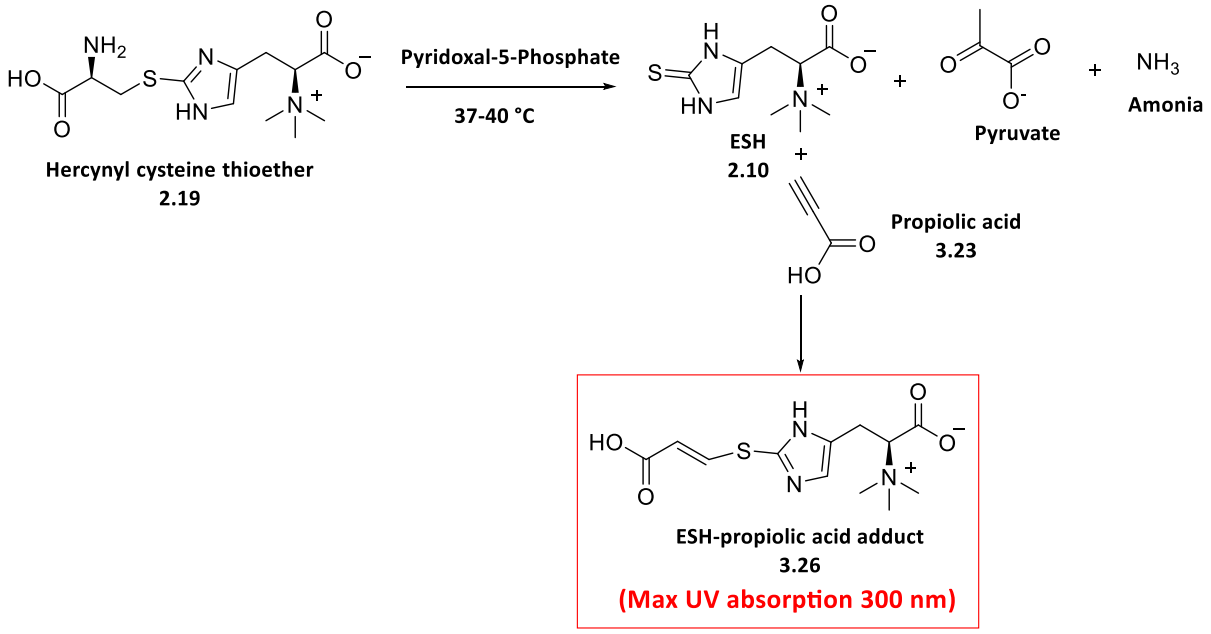

Scheme 3.14. ***In situ*** **derivatization of** ***L*****-ergothioneine (2.10) by using propiolic acid (3.23) during the enzymatic-free cleavage of 2-cysteinylhercynine thioether (2.19).**

The formation of thioacrylate derivative (ESH-propiolic acid adduct) **3.26** was monitored by UV-vis spectrophotometry. Even at the low level of 5 mM, the UV-vis spectrum revealed a strong absorption at λ_{max} 300 nm attributed to be characteristic of thioacrylate **3.26.** Thus, confirming that *L*-ergothioneine **2.10** can be detected *in situ* after successfully being derivatized by propiolic acid **3.24**, while no interferences were observed. (Figure 3.28)

The calibration curve can aid to quantify *L*-ergothioneine, nevertheless the limit of quantitation and limitation or scope of this method were not evaluated.

Is it noteworthy that this method can also be utilized to monitor the rate of the thiol oxidation in the sulfurization reaction. (Chapter 2, section 2.3.2.2)

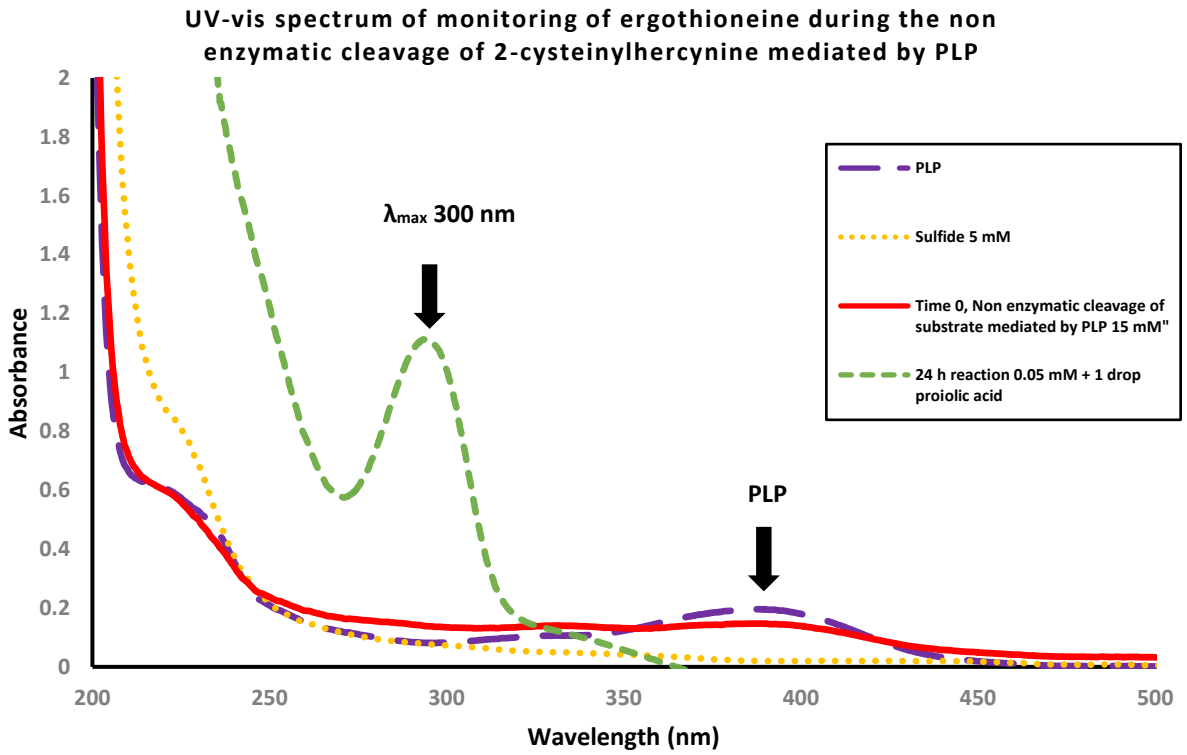

Figure 3.28. UV-vis spectrum of the reaction of propiolic acid (3.23) with *L*-ESH (2.10) produced *in situ* during the PLP-mediated *C-S* lysis of 2-cysteinylhercynine (2.19) (at 25°C).

3.5. References

1 Genghof, S. D. & Van Damme, O. Biosynthesis of Ergothioneine from Endogenous Hercynine in *Mycobacterium smegmatis*. *Journal of bacteriology* **95** (1968).

2 Melville, D. B., Genghof, D. S., Inamine, E. & Kovalenko, V. Ergothioneine in microorganisms. *Journal of Biological Chemistry* **223**, 9-17 (1956).

3 Fattori, D. *et al.* Design and Synthesis of Novel Sulfonamide-Containing Bradykinin hB2 Receptor Antagonists. 2. Synthesis and Structure-Activity Relationships of r,r-Cycloalkylglycine Sulfonamides. *Journal of medicinal chemistry* **50**, 550 (2007).

4 Reinhold, V. N., Ishikawa, Y. & Melville, D. B. Synthesis of α-N-methylated histidines. *Journal of medicinal chemistry* **11**, 258 (1968).

5 Miroslav Trampota. Process for the synthesis of L-(+)-ergothioneine US 7,767,826 B2 (**2010**).

6 Ishikawa, Y., Israel, S. E. & Melville, D. B. Participation of an Intermediate Sulfoxide in the Enzymatic Thiolation of the Imidazole Ring of Hercynine to Form Ergothioneine. *Journal of Biological Chemistry* **249, 14**, 4420 (1974).

7 Seebeck, F. P. In Vitro Reconstitution of Mycobacterial Ergothioneine Biosynthesis. *Journal of American Chemical Society* **132**, 6632 (2010).

8 Song, H. *et al.* Cysteine oxidation reactions catalyzed by a mononuclear non-heme iron enzyme (OvoA) in ovothiol biosynthesis. *Organic letters* **16**, 2122-2125, doi:10.1021/ol5005438 (2014).

9 Rostami, A., Hassanian, F., Ghorbani-Choghamarani, A. & Saadati, S. Selective Oxidation of Sulfides to Sulfoxides using H_2O_2Catalyzed by p-Toluenesulfonic Acid (p-TsOH) Under Solvent-Free Conditions. *Phosphorus, Sulfur, and Silicon and the Related Elements* **188**, 833-838, doi:10.1080/10426507.2012.710681 (2013).

10 Shaabani, A. & Rezayan, A. H. Silica sulfuric acid promoted selective oxidation of sulfides to sulfoxides or sulfones in the presence of aqueous H2O2. *Catalysis Communications* **8**, 1112-1116, doi:10.1016/j.catcom.2006.10.033 (2007).

11 Rostami, A. & Akradi, J. A highly efficient, green, rapid, and chemoselective oxidation of sulfides using hydrogen peroxide and boric acid as the catalyst under solvent-free conditions. *Tetrahedron Letters* **51**, 3501-3503, doi:10.1016/j.tetlet.2010.04.103 (2010).

12 Song, H. *et al.* Mechanistic studies of a novel C-S lyase in ergothioneine biosynthesis: the involvement of a sulfenic acid intermediate. *Scientific reports* **5**, 11870, doi:10.1038/srep11870 (2015).

13 El-Sayed, A. S. Purification and characterization of a new L-methioninase from solid cultures of Aspergillus flavipes. *Journal of microbiology* **49**, 130-140, doi:10.1007/s12275-011-0259-2 (2011).

14 Wang, L. Z. *et al.* Quantification of L-ergothioneine in human plasma and erythrocytes by liquid chromatography-tandem mass spectrometry. *Journal of Mass Spectrometry* **48**, 406-412, doi:10.1002/jms.3150 (2013).

15 Khonde, P. L. & Jardine, A. Improved synthesis of the super antioxidant, ergothioneine, and its biosynthetic pathway intermediates. *Organic & biomolecular chemistry* **13**, 1415-1419, doi:10.1039/c4ob02023e (2015).

16 Toth, K. & Richard, J. P. Covalent Catalysis by Pyridoxal: Evaluation of the Effect of the Cofactor on the Carbon Acidity of Glycine. *Journal of American Chemical Society* **129**, 3013-3021 (2007).

17 Wallace, J. R., Nash, R. D., Steele, C. L. & Steingrube, V. Susceptibility Testing of Slowly Growing Mycobacteria by a Microdilution MIC Method with 7H9 Broth. *Journal of Clinical Microbiology* **24**, 976-981 (1986).

18 Mikkelsen, M. D., Naur, P. & Halkier, B. A. Arabidopsis mutants in the C-S lyase of glucosinolate biosynthesis establish a critical role for indole-3 acetaldoxime in auxin homeostasis. *The Plant Journal* **37**, 770-777, doi:10.1111/j. 1365-313X.2003.02002.x (2004).

19 Cooper, A. J. L. *et al.* Cysteine S-conjugate β-lyases: important roles in the metabolism of naturally occurring sulfur and selenium-containing compounds, xenobiotics and anticancer agents. *Amino acids* **41**, 7–27, doi:10.1007/s00726-010-0552-0 (2011).

20 Scharf, D. H. *et al.* Epidithiol Formation by an Unprecedented Twin Carbon–Sulfur Lyase in the Gliotoxin Pathway. *Angewandte Chemie* **124**, 10211 –10215, doi:10.1002/ange.201205041 (2012).

21 Krupka, H. I., Huber, R., Holt, S. C. & Clausen, T. Crystal structure of cystalysin from *Treponema denticola*: a pyridoxal-5' phosphate-dependent protein acting as a haemolytic enzyme. *The EMBO Journal* **19** 3168-3178 (2000).

22 Flavin, M. & Segal, A. Purification and Properties of the Cystathionine γ-Cleavage Enzyme of Neurospora. *Journal of Biological Chemistry* **239**, 2220-2227. (1964).

23 Sivaramakrishnan, S., Cummings, A. H. & Gates, K. S. Protection of a single-cysteine redox switch from oxidative destruction: On the functional role of sulfenyl amide formation in the redox-regulated enzyme PTP1B. *Bioorganic & medicinal chemistry letters* **20**, 444-447, doi:10.1016/j.bmcl.2009.12.001 (2010).

24 Pedersen, E., Loksha, Y., El-Barbary, A., El-Badawi, M. & Nielsen, C. Synthesis of 2-Hydroxymethyl-1H-imidazoles from 1,3-Dihydroimidazole-2-thiones. *Synthesis* **2004**, 116-120, doi:10.1055/s-2003-44370 (2004).

25 Sotgia, S. *et al.* Quantification of L-ergothioneine in whole blood by hydrophilic interaction ultra-performance liquid chromatography and UV-detection. *Journal of separation science* **36**, 1002-1006, doi:10.1002/jssc.201201016 (2013).

26 Zhang, X.-Y., Piao, Y.-L., Cui, S.-Y. & Lee, Y.-I. Determination of reduced glutathione, cystein and total thiols in pine pollen powder by in situ derivatization. *Microchemical Journal* **112**, 1-6, doi:10.1016/j.microc.2013.09.011 (2014).

27 Riener, C. K., Kada, G. & Gruber, H. J. Quick measurement of protein sulfhydryls with Ellman's reagent and with 4,4'-dithiodipyridine. *Analytical Bioanalytical Chemistry* **373**, 266–276, doi:10.1007/s00216-002-1347-2 (2002).

28 Owen, T. C. Thiol detection, derivatization and tagging at micromole to nanomole levels using propiolates. *Bioorganic chemistry* **36** 156–160, doi:10.1016/j.bioorg.2008.02.003 (2008).

29 Zacharis, C. K., Tzanavaras, P. D. & Themelis, D. G. Ethyl-propiolate as a novel and promising analytical reagent for the derivatization of thiols: study of the reaction

under flow conditions. *Journal of pharmaceutical and biomedical analysis* **50**, 384-391, doi:10.1016/j.jpba.2009.05.020 (2009).

30 Zacharis, C. K., Tzanavaras, P. D. & Zotou, A. Ethyl propiolate as a post-column derivatization reagent for thiols: development of a green liquid chromatographic method for the determination of glutathione in vegetables. *Analytica chimica acta* **690**, 122-128, doi:10.1016/j.aca.2011.02.003 (2011).

Chapter 4 Synthesis of γ-glutamylcysteinylhercynine sulfoxide, the glutamine amidohydrolase enzyme (EgtC) substrate

4.1 Introduction

*Mycobacterium tuberculosi*s and the saprophyte *Mycobacterium smegmatis* contain a five-gene cluster (*egtABCDE*) that enables the cells to produce ESH from the primary metabolites cysteine, glutamate, histidine, and *S*-adenosylmethionine.[1]

Actinobacteria including mycobacteria prefer γ-glutamylcysteine over cysteine as sulfur source to produce ESH.[2] Although the reason remains unclear, a plausible explanation could be that these microorganisms avoid the "cysteine problem". Accordingly, cysteine is readily auto-oxidized and the terminal 1,2-aminothiol group of cysteine complexes with redox active transition metals such as iron and copper. Consequently reducing the availability of cysteine intracellularly.[2]

Mycobacteria which grows under a high O_2 partial pressure environment, would have less available intracellular cysteine, therefore γ-glutamylcysteine is utilised as a safer sulfur source. In γ-glutamylcysteine, the α-amino group of the cysteine moiety is coupled to the γ-CO_2H of glutamic acid, hence it cannot bind to transition metals. Moreover, γ-glutamylcysteine biosynthesis being ATP driven is not affected by a very low cysteine concentration, thus actinobacteria having *egtA* and *egtC* genes would still produce ergothioneine even under cysteine poor and /or O_2-rich environments.[3]

Amongst all enzymes implicated in mycobacterial ergothioneine biosynthesis, only EgtB, a formylglycine-generating like enzyme (FGE), uses γ-glutamylcysteine. EgtB catalyzes the oxidative coupling between hercynine and γ-glutamylcysteine to produce γ-glutamyl cysteinyl hercynine sulfoxide (EgtC enzyme substrate). The knock out/ knock down studies of this particular EgtC enzyme substrate is important from a drug discovery point of view. EgtC catalyses the removal of γ-glutamyl from γ-glutamyl cysteinyl hercynine sulfoxide (EgtC enzyme substrate), therefore knocking down of this enzyme would help understanding the mechanism of γ-glutamyl cysteinyl dependence by mycobacteria. Knowledge that could allow the design of potential EgtC inhibitors. The EgtC substrate can aid in the screening of potential prodrugs targeting mycobacterial EgtC enzyme.

Intensive efforts have been conducted in our laboratory to synthesize all the ergothioneine's biosynthetic pathway metabolites. The latter would be considered as valuable tools for studies to better characterise the enzymes of the ergothioneine pathway in *Mycobacterium tuberculosis*.[4,5] At the time of this research, the EgtC substrate was the only ergothioneine biosynthetic pathway intermediate that was not yet chemically synthesized. However, it was enzymatically produced by Seebeck in a very small quantity (250 ug).[6]

In this chapter the design and the total synthesis of γ-glutamylcysteinylhercynine sulfoxide or (2*S*)-3-(2-(((*R*)-2-((*S*)-4-amino-4-carboxybutanamido)-2-carboxyethyl)sulfinyl)-1*H*-imidazol-4-yl)-2-(trimethylammonio)propanoate (the EgtC enzyme substrate) is described.

4.2. Retrosynthetic strategies of EgtC enzyme substrate

Strategies toward the total synthesis of the EgtC enzyme substrate, (2*S*)-3-(2-(((*R*)-2-((*S*)-4-amino-4-carboxybutanamido)-2-carboxyethyl)sulfinyl)-1*H*-imidazol-4-yl)-2-(trimethylammonio) propanoate (**4.1**) was explored in depth. Three methods were investigated following the retrosynthesis strategy utilized as shown in the Figure 4.1

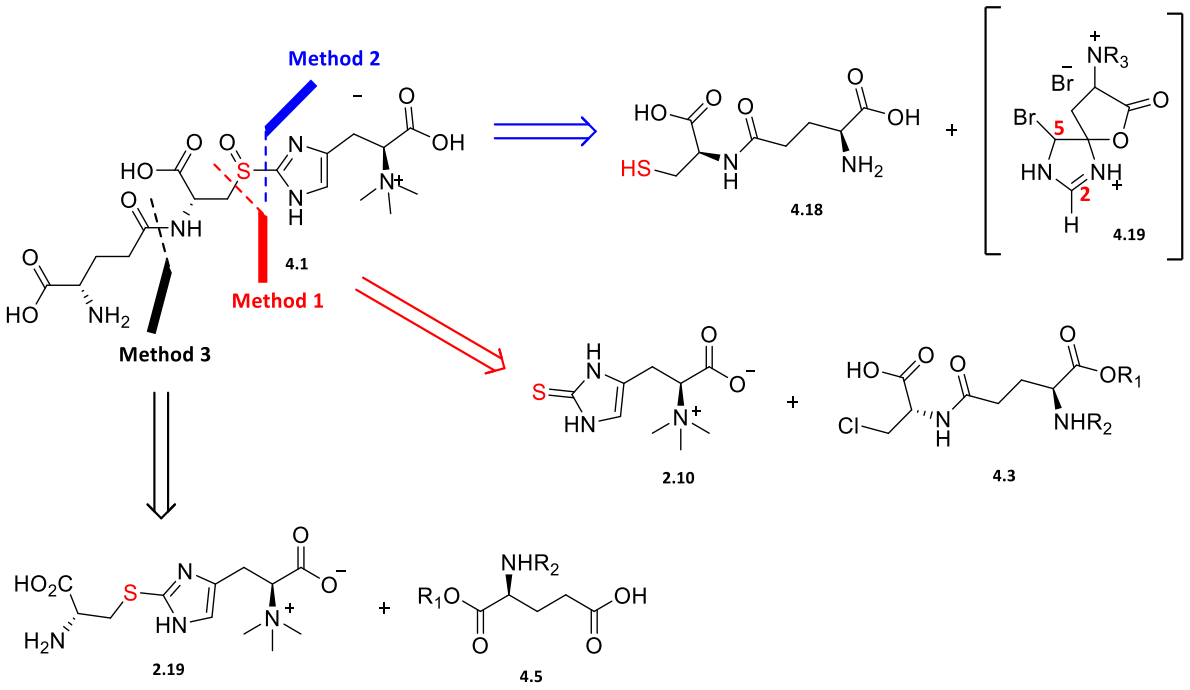

Figure 4.1. EgtC substrate retrosynthetic strategies.

The proposed retrosynthetic strategies consider cleavage on the distal side of the hercynine moiety, cleavage on the left side of the sulfur atom (method 1) or on the right side of the sulfur atom (method 2). In method 3 there is a disconnection between the carbonyl carbon of the γ-glutamic acid moiety and the *N*-amino moiety of 2-cysteinylhercynine thioether **2.19**.

The major difference amongst these strategies are based on the choice of the thiol fragment used as a synthon. Ergothioneine **2.10** (discussed in chapter 2) was the synthon used in method 1, while γ-glutamylcysteine **4.18** and 2-cysteinylhercynine thioether **2.19** (discussed in chapter 2) were the synthons for the method 2 and 3, respectively.

4.3. Synthesis of EgtC enzyme substrate through *S*-alkylation of ergothioneine. (Method 1)

4.3.1. Retrosynthetic analysis

The envisioned strategy was based on using a starting material that already include a mercapto histidine moiety. *S*-alkylation of *L*-ergothioneine **2.10** by the protected N^5-((*S*)-1-carboxy-2-chloroethyl)-*L*-glutamine intermediate **4.3** to form γ-glutamylcysteinylhercynine thioether **4.2**, subsequently the sulfide can be oxidized to its sulfoxide derivative **4.1**, the target compound. The N^5-((*R*)-1-carboxy-2-chloroethyl)-*L*-glutamine intermediate **4.3** can be derived from the protected γ-glutamylserine **4.4**, a dipeptide formed by amide coupling between the protected glutamic acid **4.6** and the protected serine **4.5**. (Scheme 4.1)

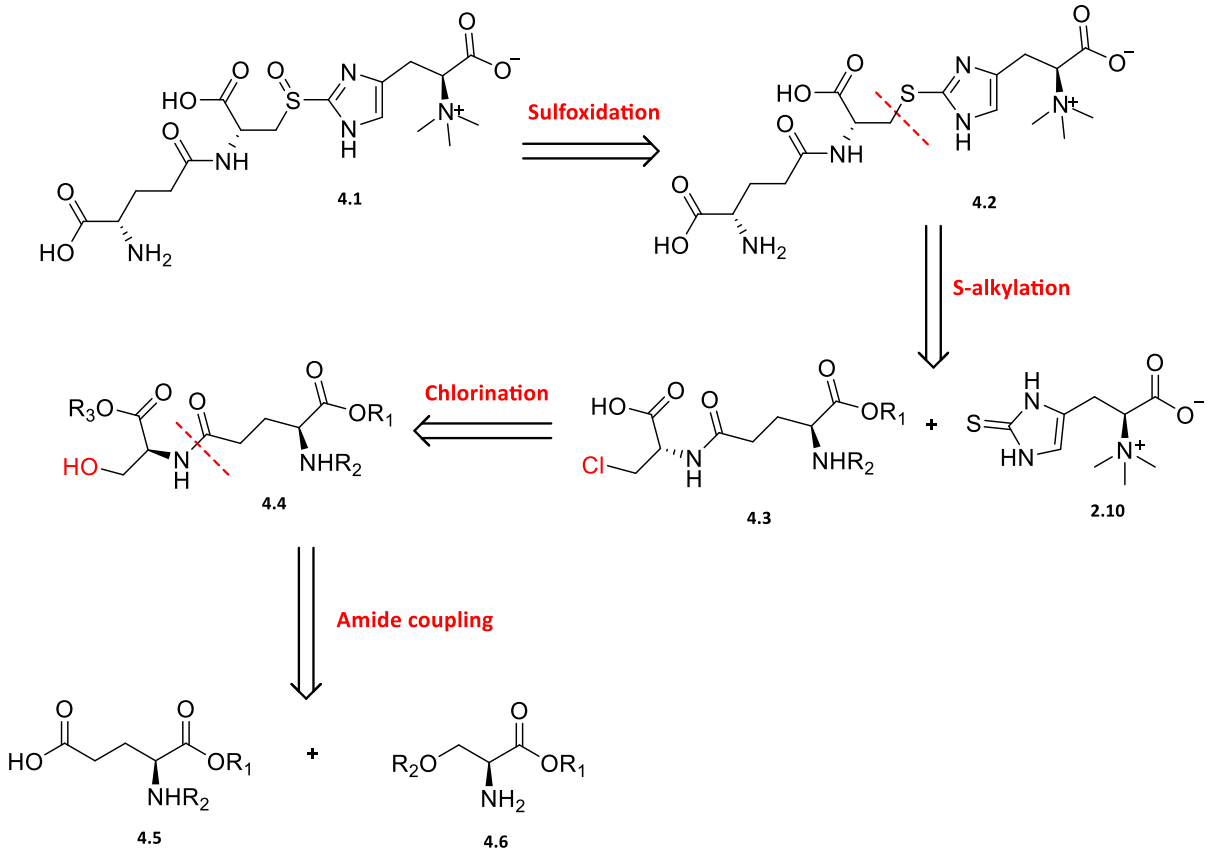

Scheme 4.1. Retrosynthetic strategy of EgtC substrate 4.1 involving *S*-alkykation of ergothioneine 2.10

4.3.2. Synthesis of benzyl N^5-((*S*)-1-(benzyloxy)-3-chloro-1-oxopropan-2-yl)-N^2-(*tert*-butoxycarbonyl)-*L*-glutaminate

The synthesis of the key intermediate, benzyl N^5-((*S*)-1-(benzyloxy)-3-chloro-1-oxopropan-2-yl)-N^2-(*tert*-butoxycarbonyl)-*L*-glutaminate **4.13** involved four sequential steps, protection of simple amino acids, amide coupling, selective deprotection and substitution of the hydroxyl group by a chloro group. (Scheme 4.2)

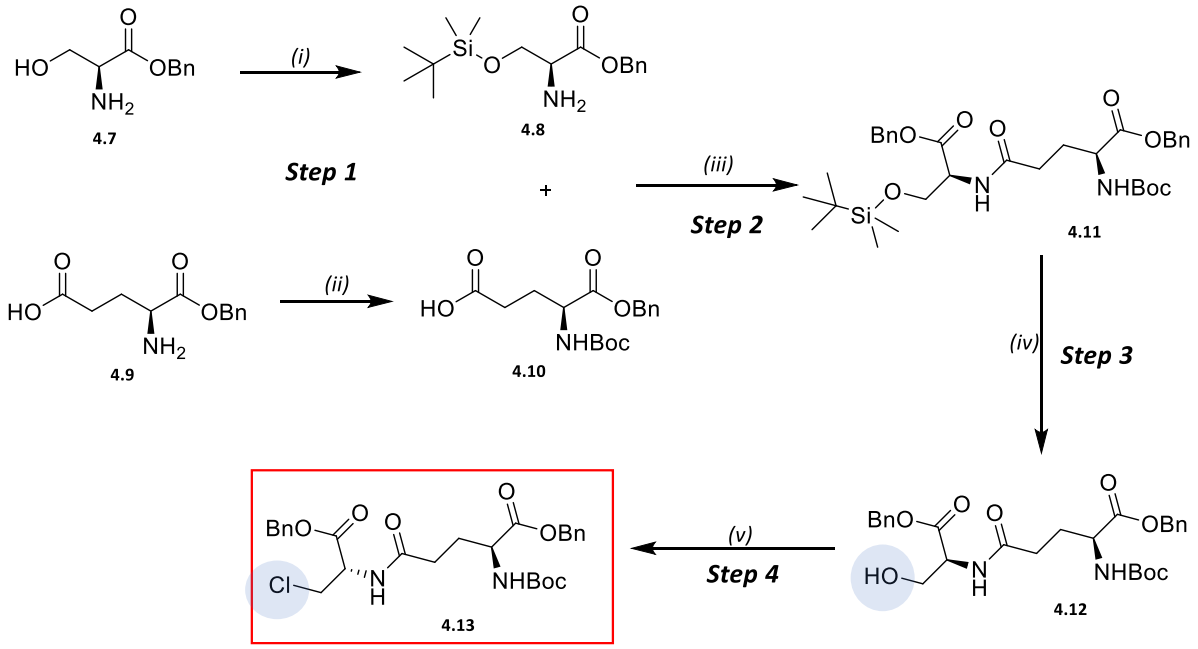

Scheme 4.2. Synthesis of benzyl N^5-((*S*)-1-(benzyloxy)-3-chloro-1-oxopropan-2-yl)-N^2-(*tert*-butoxycarbonyl)-*L*-glutaminate 4.13. Reagents and conditions. (i) TBDMSCl, DBU/CH_3CN, 0 °C to rt, overnight, quantitative; (ii) $(Boc)_2O$, Et_3N/H_2O/dioxane, overnight at rt (quantitative); (iii) EDC. HCl, DIPEA, HOBt, DCM, 24 hr at rt, 86%; (iv) TBAF (1M in THF)/ dry THF, 5-10 h at rt, 59%; (v) 2,4,6-trichloro[1,3,5]triazine/DMF, DCM, 21 h at rt, 83%.

The hydroxyl group of a commercially available benzyl *L*-serinate **4.7** was protected as the TBDMS according to literature procedures.[7] Benzyl O-(*tert*-butyldimethylsilyl)-*L*-serinate **4.8** was isolated quantitatively after aqueous work up and organic extraction. The NMR data were fully in accordance fully with the one reported by Gagnepain *et al.*[7]

Commercially available (*S*)-4-amino-5-(benzyloxy)-5-oxopentanoic acid **4.9,** was quantitatively converted into the Boc protected product. The presence of an up-field singlet at δ_H 1.49 ppm in the ^1H NMR spectrum of **4.10** was consistent with the successful Boc introduction.

The next step involved the amide coupling of benzyl O-(*tert*-butyldimethylsilyl)-*L*-serinate **4.8** with (*S*)-5-(benzyloxy)-4-((*tert*-butoxycarbonyl)amino)-5-oxopentanoic acid **4.10** in the presence of *N*-(3-dimethylaminopropyl)-*N*'-ethylcarbodiimide (EDC) hydrochloride, *N*,*N*-diisopropylethylamine (DIPEA) and hydroxy-benzotriazole (HOBt) to give the dipeptide **4.11**, in an excellent yield of 86%. Key signals in the ^{1}H NMR spectrum of **4.11** were three up-field signals resonating as a singlet at δ_H 0.85 ppm (for *t*-butyl), a multiplet from δ_H 0.09 to -0.04 ppm (for 2 X CH_3) and a singlet at δ_H 1.43 ppm (for *Boc*). A downfield signal resonating as a multiplet from δ_H 7.31 to 7.27 ppm integrating for 10 protons and two methylene proton signals resonating as a multiplet from δ_H 5.27 to 5.06 ppm intergrating for 4 protons, thus confirming the presence of two benzyl groups. Additionaly, ^{13}C NMR and EI$^+$ mass spectrum revealed the sodium adduct assigned to *m/z* 651.2 and calculated for $C_{33}H_{48}N_2NaO_8Si$ (651.3) with a mass fragmentation corresponding to a loss of a Boc group $[MH–Boc]^+$ to give *m/z* 529.2, thus confirming the structure of **4.11**.

Step 3 entailed selective silyl (TBDMS) deprotection which was achieved by reaction compound **4.11** with tetra *n*-butylammonium fluoride (TBAF) in anhydrous THF. The desilylated product **4.12** was isolated in a moderate yield of 59%. A key diagnostic in the ^{1}H NMR spectrum of **4.12** was the disappearance of *tert*-butyl dimethyl silyl signals (δ_H 0.85 ppm (9 protons) and multiplet from δ_H 0.09 to -0.04 ppm (6 protons)) providing evidence for the complete desilylation of compound **4.11.** The proton NMR of the desilylated product **4.12** α aromatic protons resonating as a multiplet from δ_H 7.39 to 7.30 ppm integrating for 10 protons, and methylene protons resonating as a multiplet from δ_H 5.24 to 5.04 ppm integrating for 4 protons, thus supporting the presence of two benzyl groups. Two α carbon

protons were also shown in the proton NMR of **4.12**, both signals resonating as triplets at δ_H 3.44 and 3.61 ppm, hence confirming the presence of two amino acid moieties. The ^{13}C NMR spectra corroborated by mass spectra confirmed the structure of benzyl N^5-((*S*)-1-(benzyloxy)-3-hydroxy-1-oxopropan-2-yl)-N^2-(*tert*-butoxycarbonyl)-*L*-glutaminate **4.12**.

The final step (step 4) entailed the substitution of the hydroxyl group of **4.12** by a chloro group. This was achieved according to the methodology described by Lidia *et al*.[8] by reacting the alcohol compound **4.12** with the 2,4,6-trichloro[1,3,5]triazine (TCT)/DMF complex known as Vilsmeier-Haack type complex to yield the crude target compound, benzyl N^5-((*S*)-1-(benzyloxy)-3-chloro-1-oxopropan-2-yl)-N^2-(*tert*-butoxycarbonyl)-*L*-glutaminate **4.13** in a 83% yield (crude yield). Attempts to purify the synthesized product **4.13** by SiO_2 gel chromatography resulted in its degradation as revealed by NMR, therefore the product was used in the next step without any further purification. The lability of compound **4.13** is not unexpected due to the reactive nature of the methylene chloride side chain.

As expected the ^1H NMR spectrum of benzyl N^5-((*S*)-1-(benzyloxy)-3-chloro-1-oxopropan-2-yl)-N^2-(*tert*-butoxycarbonyl)-*L*-glutaminate **4.13** was similar to the ^1H NMR spectrum of starting material **4.12**. Strong evidence was provided by the EI^+ mass spectrum which displayed a molecular ion at *m/z* 532.1 for $[^{35}M, 14.5\%]^+$ and 534.0 for $[^{37}M, 4.8\%]^+$ calculated for $C_{27}H_{33}{}^{35}ClN_2O_7$ (*m/z*) 532.2 $[^{35}M]^+$ and $C_{27}H_{33}{}^{37}ClN_2O_7$ (*m/z*) 534.2 $[^{37}M]^+$, with an intensity ratio of peaks of 3:1 characteristic isotopic patterns of chlorinated molecule; moreover, fragments corresponding to a loss of Boc group were observed at *m/z* 431.1 ($[^{35}M\text{-Boc}]^+$,

61.9%) and 433.1 ([^{37}M-Boc]$^+$, 20.2%]$^+$ calculated for $C_{22}H_{24}{}^{35}ClN_2O_5$ (431.1) and for $C_{22}H_{24}{}^{37}ClN_2O_5$ (433.1), thus supporting the structure of **4.13**.

With both retrosynthons, the benzyl N^5-((*S*)-1-(benzyloxy)-3-chloro-1-oxopropan-2-yl)-N^2-(*tert*-butoxycarbonyl)-*L*-glutaminate **4.14** and ergothioneine **2.10** (synthesized and discussed in the chapter 2) in our possession, the next challenge was to attempt an S-alkylation reaction, similar to that which was described by Ishikawa *et al.*[9] This method involves treatment of a protected chloro methyl peptide **4.13** with ergothioneine **2.10** in a presence of Et_3N. (Scheme 4.3)

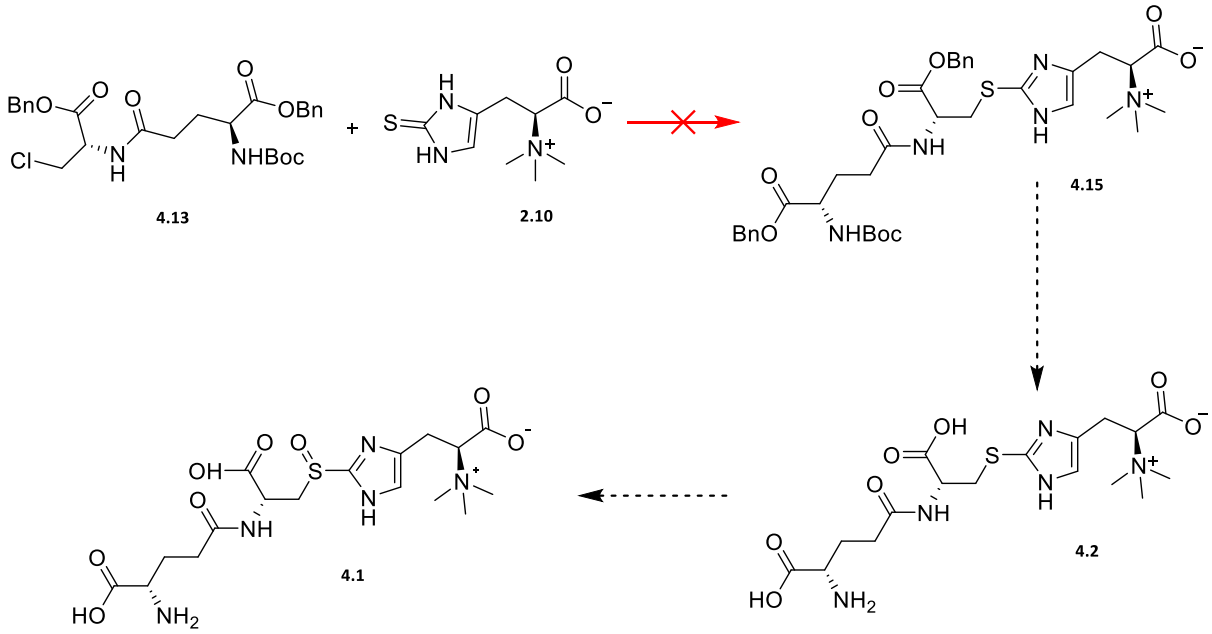

Scheme 4.3. Attempted *S*-alkylation of ergothioneine 2.10 by benzyl N^5-((*S*)-1-(benzyloxy)-3-chloro-1-oxopropan-2-yl)-N^2-(*tert*-butoxycarbonyl)-*L*-glutaminate 4.13. Reagents and conditions. Et_3N, CH_3CN, rt to 60°C.

The mechanistic detail of this reaction was suggested by Ishikawa *et al.*[9] it was proposed that the reaction could possibly proceed through a cyclo ethylenimine-2 carboxylic acid derivative **4.16** (reactive intermediate) formed *via* the intramolecular substitution of the chloro intermediate **4.13.** Subsequent nucleophilic attack of the sulfur atom of ergothioneine **2.10** *via* S_N2 on the reactive cyclo ethylenimine intermediate results in the formation of two possible thioether products. (Scheme 4.4)

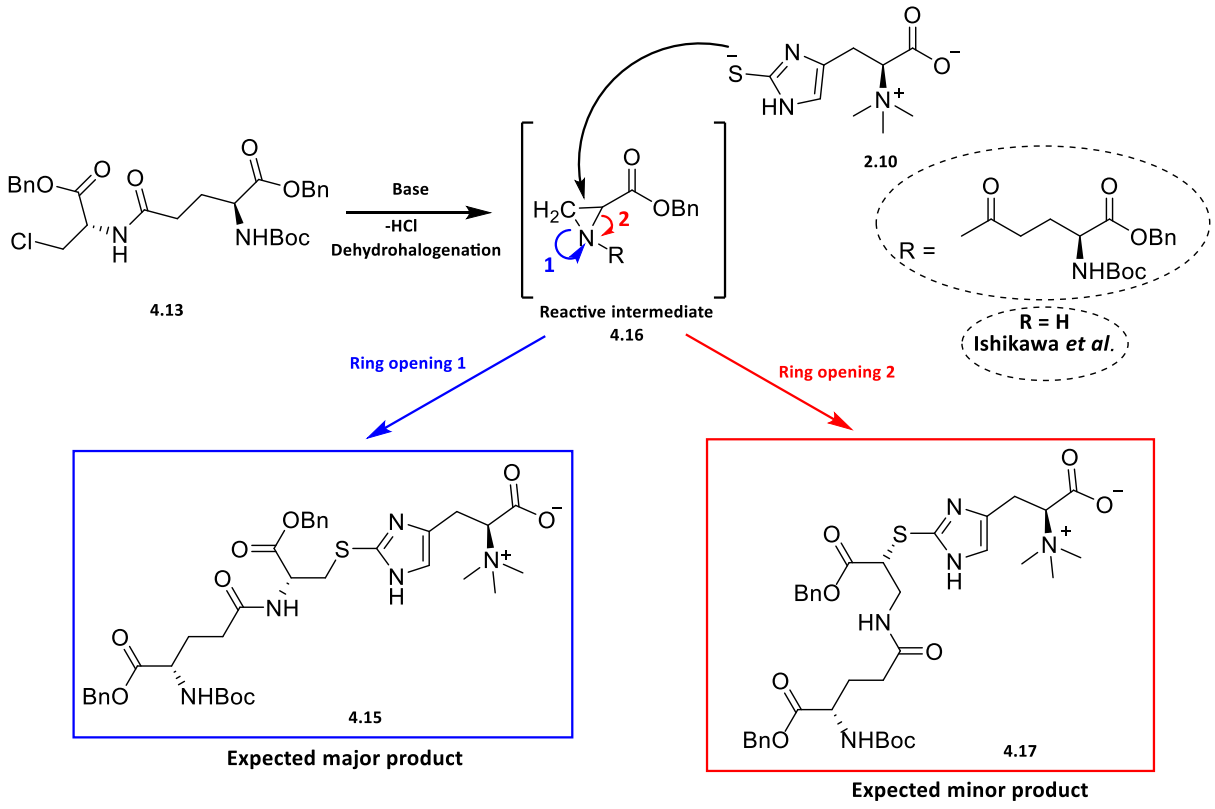

Scheme 4.4. Proposed mechanism of formation of thioether 4.15 similarly to the one suggested by Ishikawa et *al.*[9]

Many conditions were investigated for the *S*-alkylation of ergothioneine **2.10** by benzyl N^5-((*S*)-1-(benzyloxy)-3-chloro-1-oxopropan-2-yl)-N^2-(*tert*-butoxycarbonyl)-*L*-glutaminate **4.13**, such as reaction time, temperature and concentration, but none has proven successful. When

the reaction was performed at room temperature, no product was formed as we believed that the formation of the reactive intermediate, the cyclo enimine **4.16**, is highly hindered and is not straightforward. However, when the reaction was allowed to reflux at 60 °C for a prolonged time (up to 1 day), TLC analysis of the reaction mixture revealed multiple overlapping spots, inseparable by silica gel chromatography, hence no purification was attempted. NMR analysis of the crude reaction mixture, did not reveal any characteristic signal of the desired product **4.15** and was inconclusive.

One plausible explanation could be the instability of the alkyl chloride substrate of this reaction, the benzyl N^5-((*S*)-1-(benzyloxy)-3-chloro-1-oxopropan-2-yl)-N^2-(*tert*-butoxycarbonyl)-*L*-glutaminate **4.13**, as established earlier. Due to the failure of this *S*-alkylation reaction, this synthetic approach was abandoned and an alternative route was then investigated.

4.3.2. Synthesis of γ-glutamylserine (N^5-((*S*)-1-carboxy-2-hydroxyethyl)-*L*-glutamine)

With the protected γ-glutamylserine **4.12** in our hand, global deprotection gave γ-glutamylserine **4.14**. The latter peptide was not commercially available and thought to be useful as a γ-glutamylcysteine isostere. This alcohol is a valuable intermediate towards the synthesis of activated (halogenated) derivatives γ-glutamylserine which could be

investigated as alternative to the instable alkyl chlorinatined version **4.13.** Especially when the need of alternative esters is required.

The deprotection of γ-glutamylserine **4.12** was accomplished in a one pot synthesis by catalytic hydrogenation on Pd/C under acidic conditions (TFA) in a protic solvent (methanol) to afford γ-glutamylserine **4.14** in excellent yield of 95%. (Scheme 4.5)

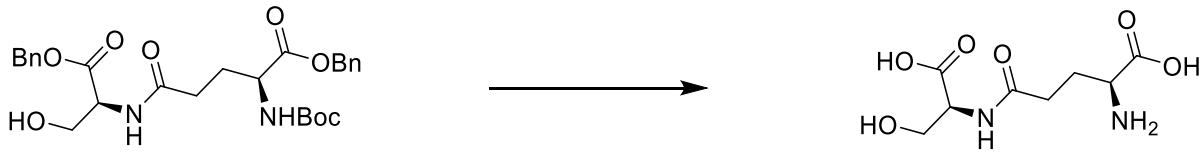

4.12 **4.14**

Scheme 4.5. Synthesis of N^5-((*S*)-1-carboxy-2-hydroxyethyl)-*L*-glutamine 4.14. Reagents and conditions. H_2/Pd/C (10%), TFA, MeOH, 24 hr at rt, 95%.

The disappearance of aromatic proton signals resonating at δ_H 7.3 ppm, methylene proton signals around δ_H 5.2 ppm and Boc signal resonating at 1.44 ppm present in the ^{1}H NMR spectrum of **4.12**, was a confirmation of successful deprotection of **4.12**. The proton NMR of γ-glutamyl serine **4.14** revealed two α carbon protons resonating at δ_H 4.27 ppm and 4.03 ppm suggesting the presence of two amino acids. The proton NMR spectrum of **4.14** also revealed three methylene protons resonating as multiplets from δ_H 3.94 to 3.62 ppm, 2.81 to 2.56 ppm and 2.47 to 2.16 ppm; hence supporting the structure of **4.14**.

4.4. Biomimetic synthesis of (2*S*)-3-(2-(((*R*)-2-((*S*)-4-amino-4-carboxybutanamido)-2-carboxyethyl)sulfinyl)-1*H*-imidazol-4-yl)-2-(trimethylammonio) propanoate. (Method 2)

In this approach, the action of EgtB is mimicked. The non-heme iron sulfoxide synthetase enzyme (EgtB) of the mycobacterial ergothioneine biosynthetic pathway, catalyzes the O_2-dependent *C-S* bond formation between γ-glutamylcysteine and hercynine.[6,10]

The retrosynthetic strategy entailed the construction of sulfur-carbon (*S-C)* bond by coupling a dipeptide, γ-glutamylcysteine **4.18** as a sulfur source with an activated hercynine **4.19**. The resulting thioether can be oxidized by either *m*CPBA in the presence of protecting groups or H_2O_2 after deprotection. It is noteworthy that this strategy was successfully utilized in the literature in the synthesis of the 2-cysteinylhercynine thioether, the only difference being the use of cysteine as a sulfur source rather than γ-glutamylcysteine **4.18**.[5,11,12] Bromolactone hercynine **4.19** is generated *in situ* via the bromination of the protected hercynine **4.22**, whereas the dipeptide γ-glutamylcysteine **4.18** was derived from an amide coupling between protected glutamic acid **4.21** and protected cysteine **4.20**. (Figure 4.2)

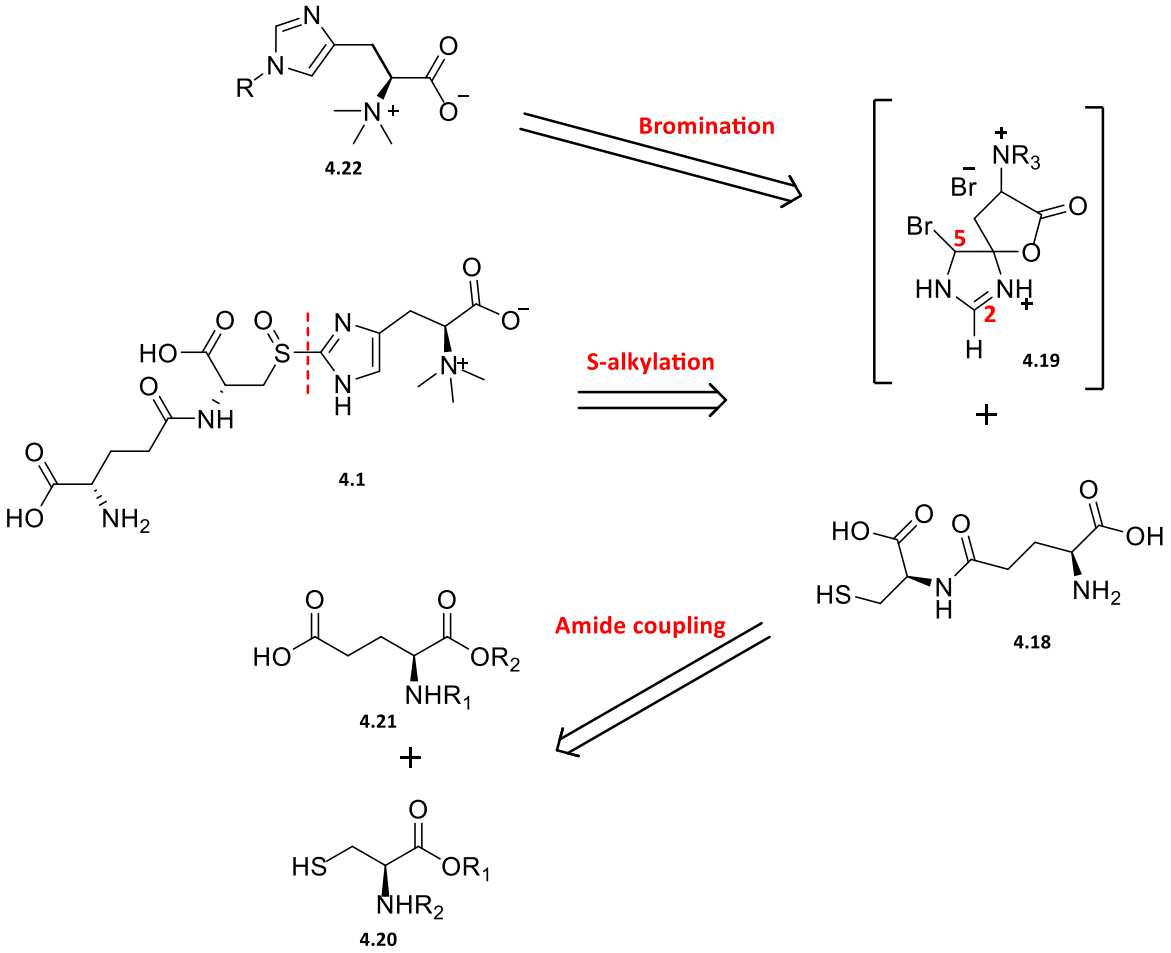

Figure 4.2. Biomimetic retrosynthetic strategy of EgtC enzyme substrate

4.4.1. Synthesis of *O, S*-dibenzyl-*L*-cysteinate

The benzyl protecting group was preferred for the protection of the sulfur and carboxylic acid groups of cysteine **2.20**, leaving the Boc group available for selective deprotection and subsequent amide coupling. The benzyl protecting group introduces some hydrophobicity to the molecule which proved to be useful for SiO_2 gel chromatographic purification, especially when working with a polar amino acid, even more the benzyl protecting group can easily be removed under neutral conditions such as Pd/C catalytic hydrogenation.

Firstly, the synthesis of *O,S*-dibenzyl-*L*-cysteinate **4.23** was attempted in two steps, starting with a selective *S*-benzylation performed as described in the literature,[13,14] using benzyl bromide in ethanol under basic conditions (NaOH) to yield *S*-benzyl-*L*-cysteine **4.26** in good yield of 86%. *Boc* protection of the amino group of *S*-benzyl-*L*-cysteine **4.26** prior to the benzylation yield *O,S*-dibenzyl-*N*-(*tert*-butoxycarbonyl)-*L*-cysteinate **4.28** in an excellent yield of 95% after two steps. Finally, standard Boc deprotection (TFA) yield the desired protected cysteine, *O,S*-dibenzyl-*L*-cysteinate **4.23,** in an excellent overall yield of 86%. (Scheme 4.6)

Noteworthy is that *O,S*-dibenzyl-*L*-cysteinate **4.23** was synthesized according to this approach in multi-gram scale quantities (10.8 g) from cysteine (7.5 g) in a good overall yield of 84%, after four sequential steps without the need of any SiO_2 column purifications.

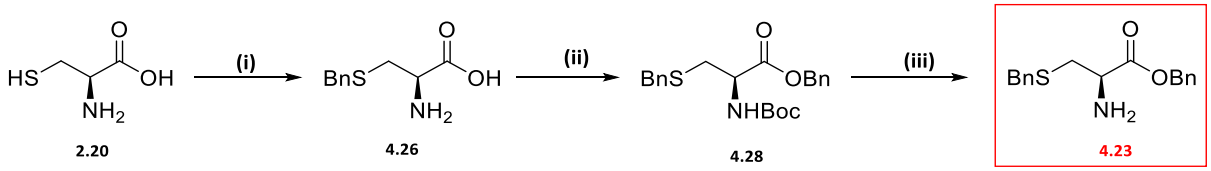

Scheme 4.6. Synthesis of *O,S*-dibenzyl-*L*-cysteinate 4.23. Reagents and conditions. (i) NaOH/EtOH, BnBr (1 eq), rt 1-2 hrs, 80%; (ii) a) $(Boc)_2O$, NaOH, THF/H_2O, 24 hr at rt; b) BnBr/DMF, 24 hr at rt, 95% after two steps (iii) TFA, 16 hr at rt, 91%. Overall yield of 86%.

The ^1H NMR spectrum of *O,S*-dibenzyl-*L*-cysteinate **4.23** displayed two downfield signals both resonating as a multiplet from δ_H 7.39 – 7.30 integrating for 5 protons (assigned for *O*-CH_2-**Ph**) and from δ_H 7.28 – 7.21 (assigned to *S*-CH_2-**Ph**), thus supporting the structure of **4.23**. (Figure 4.3)

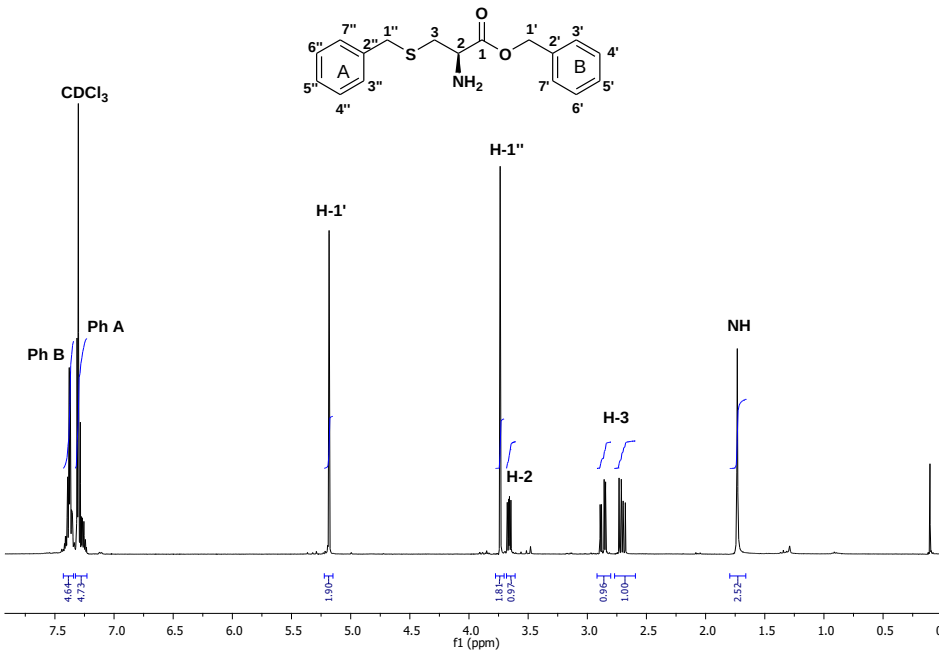

Figure 4.3. ^{1}H NMR spectrum of *O,S*-dibenzyl-*L*-cysteinate 4.23 in $CDCl_3$ at 300 MHz.

Furthermore, the ^{13}C NMR spectrum (Figure 4.4) corroborated by EI^+ MS analysis confirmed the structure of **4.23**.

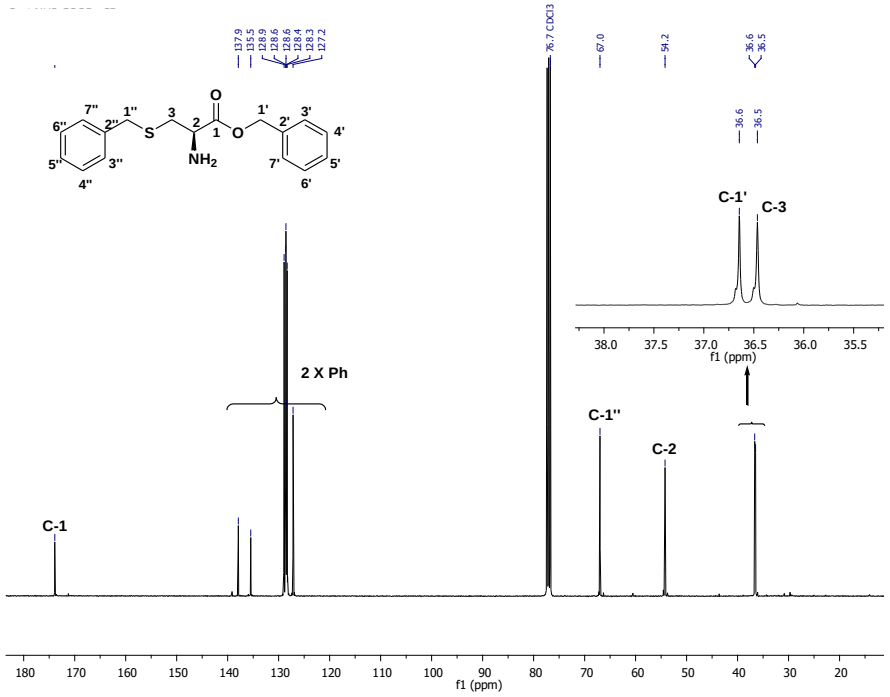

Figure 4.4. ^{13}C NMR spectrum of *O,S*-dibenzyl-*L*-cysteinate 4.23 in $CDCl_3$ at 101 MHz.

4.4.2. Synthesis of γ-glutamylcysteine (N^5-((*R*)-1-carboxy-2-mercaptoethyl)-*L*-glutamine)

γ-Glutamylcysteine **4.18** is usually synthesized enzymatically by action of an immobilized γ-glutamyltranspeptidase which catalyzed the α,γ amide bond linkage between cysteine and glutamic acid.[15] γ-Glutamylcysteine **4.18** can also be isolated from a culture medium fermented by a specific over expressing γ-glutamylcysteine yeast strain (*saccharomyces cerevisiae* strain).[16,17] The need for gram quantities of the commercially available γ-glutamylcysteine **4.18** has motivated us to undertake a multigram-scale synthesis of this key intermediate.

The synthesis of γ-glutamylcysteine **4.18** involved DIC amide coupling between two suitably protected amino acids, **4.10** and **4.23** synthesized earlier. Followed by the one-pot removal of the benzyl and Boc protecting group as outlined in the Scheme 4.7 below. The target product, γ-glutamylcysteine **4.18** was isolated in mg quantities an excellent yield of 85% upon filtration and followed by C18 reverse phase chromatography.

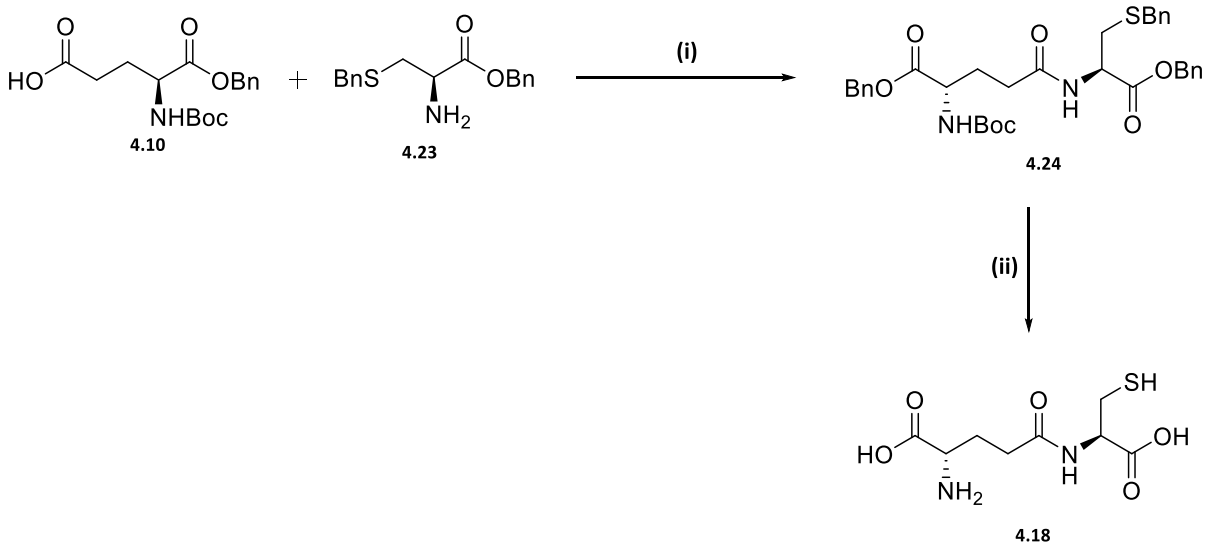

Scheme 4.7. Synthesis of γ-glutamylcysteine 4.18. Reagents and conditions. (i) DIC, HOBt, DIPEA, DCM, 24 hr at rt, 92%; (ii) H_2, Pd/C (10%), TFA, MeOH, 24 hr at rt, 85%.

The proton NMR spectrum of γ-glutamylcysteine **4.18** revealed three sets of methylene protons, one resonating as doublet at δ_H 3.87 ppm assigned to the cysteine β-carbon protons, multiplets from δ_H 2.82 to 2.47 ppm and from δ_H 2.38 to 2.20 ppm belonging to glutamic acid β and γ protons, respectively. ^{1}H NMR data was consistent with those reported in the literature.[18]

The ^{13}C NMR spectrum of γ-glutamylcysteine **4.18** displayed three carbonyl signals resonating at δ_C 173.2, 170.5 and 156.9 ppm as well as five aliphatic carbon signals resonating at δ_C 51.2,

47.8, 29.3, 25.3 and 23.3 ppm, respectively, thus confirming the carbon skeleton identity of the synthesized γ-glutamylcysteine **4.18**. (Figure 4.5)

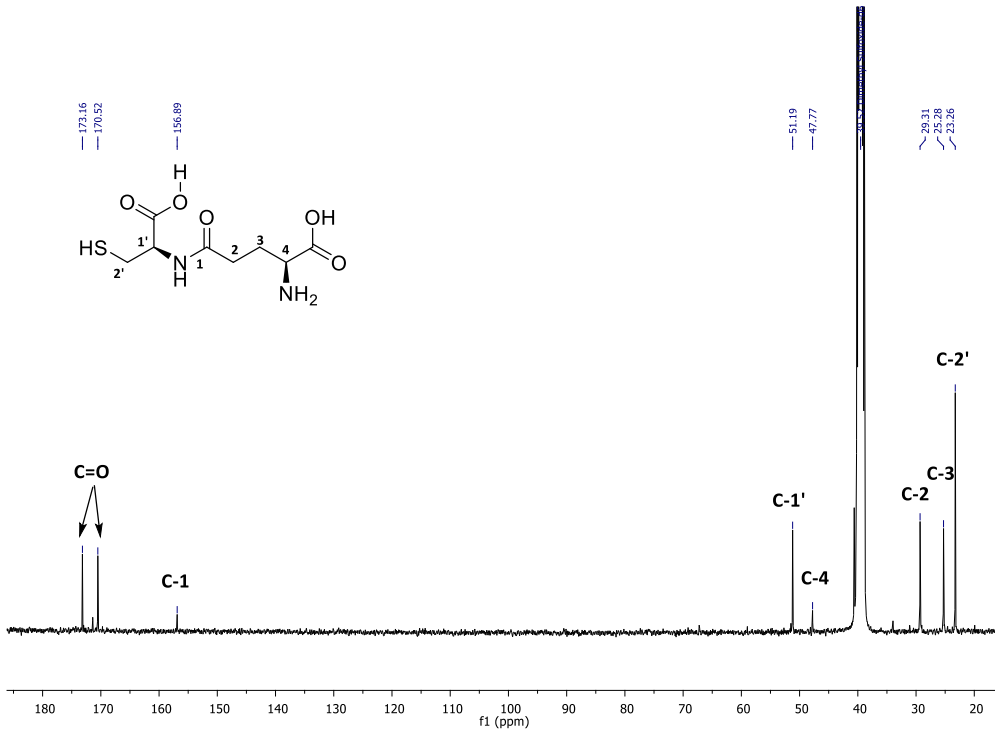

Figure 4.5. ^{13}C NMR spectrum of γ-glutamylcysteine (4.18) in DMSO-*d*$_6$ at 101 MHz.

Futhermore, the ESI$^+$ mass spectrum displayed the molecular ion $[MH]^+$ at *m/z* 251.2 calculated for $C_8H_{15}N_2O_5S$ (251.1), thus supporting the structure of γ-glutamylcysteine **4.18.**

4.4.3. Synthesis and characterization of (*S*)-3-(2-(((*R*)-2-((*S*)-4-amino-4-carboxybutanamido)-2-carboxyethyl)thio)-1*H*-imidazol-4-yl)-2-(trimethylammonio) propanoate

With γ-glutamylcysteine **4.18** in our possession, the next target was to synthesize the γ-glutamylcysteinylhercynine thioether **4.2**. The sulfurization reaction was carried out according to our improved procedure[5] (discussed in the chapter 2). *N*-benzyl hercynine **2.30** was brominated with an excess of *N*-bromosuccinimide (NBS) (2.0 mol equivalents) in DMF solvent. Subsequently the sulfur source, γ-glutamylcysteine **4.18** was added in one portion. Reverse phase C18 column chromatography yielded the desired product **4.2** in a very low yield of 7% as outlined in the Scheme 4.8.

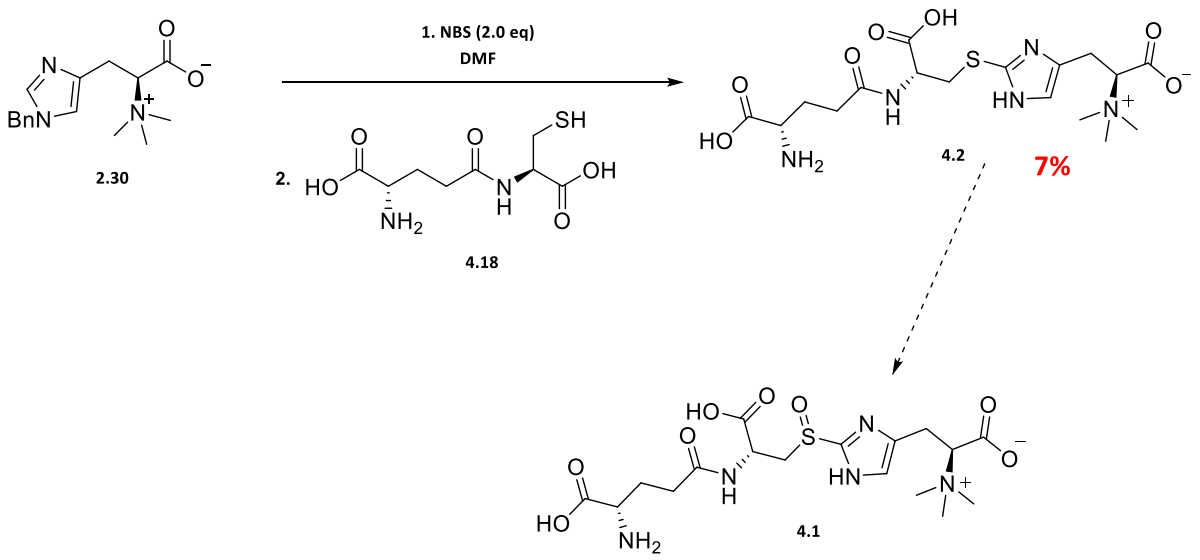

Scheme 4.8. Synthesis of (*S*)-3-(2-(((*R*)-2-((*S*)-4-amino-4-carboxybutanamido)-2-carboxyethyl)thio)-1*H*-imidazol-4-yl)-2-(trimethylammonio) propanoate 4.2. Reagents and conditions. NBS (2.0 eq), *N*-Bn hercynine **2.30**, DMF, 1-3 hrs at rt, 7%. (method adapted from Khonde et *al*.[5])

The ^{1}H NMR spectrum of (*S*)-3-(2-(((*R*)-2-((*S*)-4-amino-4-carboxybutanamido)-2-carboxyethyl)thio)-1*H*-imidazol-4-yl)-2-(trimethylammonio)propanoate **4.2** displayed one aromatic deshielded signal resonating as a singlet at δ_H 8.52 ppm, and three α amino acid signals resonating as a multiplet in the region from δ_H 4.31 to 4.17 integrating for two protons assigned to the amino acid protons (γ-glutamylcysteine moiety), and from δ_H 3.97 to 3.83 ppm integrating for one proton assigned to α amino acid proton (hercynine moiety). It also displayed one singlet signal resonating at δ_H 3.78 ppm integrating for 9 protons assigned to the *N,N,N*-trimethyl group, and three sets of methylene signals resonated as two doublet of doublets at δ_H 3.61, 3.50 ppm (J = 12.2, 6.5 Hz) and two multiplet signals from δ_H 2.70 to 2.56 ppm and δ_H 2.27 to 2.08 ppm was also observed in the proton NMR of **4.2**, thus supporting the structure of (*S*)-3-(2-(((*R*)-2-((*S*)-4-amino-4-carboxybutanamido)-2-carboxyethyl)thio)-1*H*-imidazol-4-yl)-2-(trimethylammonio)propanoate **4.2.**

Only 2 mg of the extremely hygroscopic thioether **4.2** was recovered after C18 reverse column chromatography.

Mechanistically, it has been proposed that the reaction could proceed through the formation of the 5-bromohercynine lactone derivative **4.29** (reactive intermediate).[11,12] The latter reacts with γ-glutamylcysteine **4.18**, the sulfur source, to yield the target thioether **4.1** after rearomatization as outlined in the Scheme 4.9. (Mechanism discussed in depth in the chapter 2).

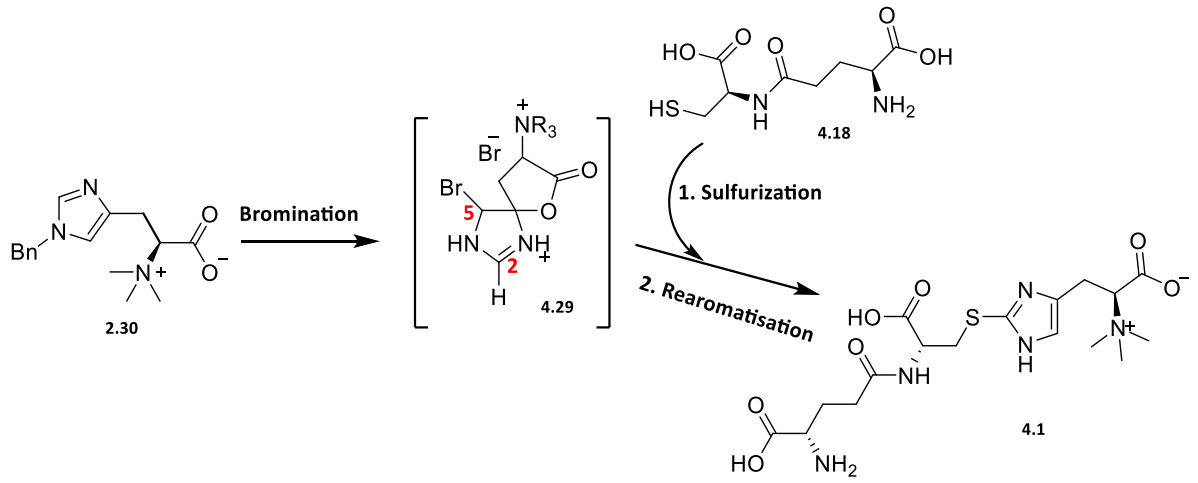

Scheme 4.9. Putative mechanism of the sulfurization of the protected hercynine derivative 2.30 by γ-glutamylcysteine 4.18.

Before investigating an alternative strategy, a study was conducted to shed light on the potential reason for the low yielding synthesis (7%) of the thioether **4.2** *via* the sulfurization reaction as descrived above. NBS/DMF is a strong oxidative medium, therefore it was suspected that the oxidation of the γ-glutamylcysteine **4.18**, a side reaction competing with the sulfurization could be the reason for the low yielding observed.

4.4.4. UV-vis spectroscopic study of the oxidation of γ-GluCys as a competing side reaction during sulfurization.

The proposed mechanism as illustrated in the scheme 4.10 above suggests that the reactive intermediate is the highly unstable 5-bromolactone **4.29**.[11,12] During the course of the investigation, the bromination step was improved, thus minimising the formation of a

multitude of decomposition by-products as a result of the degradation of the lactone **4.29**. (Improved method described in the chapter 2 and published earlier)[5].

The NBS-mediated bromination was followed by the sulfurization reaction using γ-glutamylcysteine **4.18** as a sulfur source. It is well known that free thiols can readily oxidize to their disulfides. NBS/DMF is an oxidative medium, a possible side reaction is the oxidation of γ-glutamylcysteine **4.18** to form its disulfide derivative **4.30**. (Scheme 4.10)

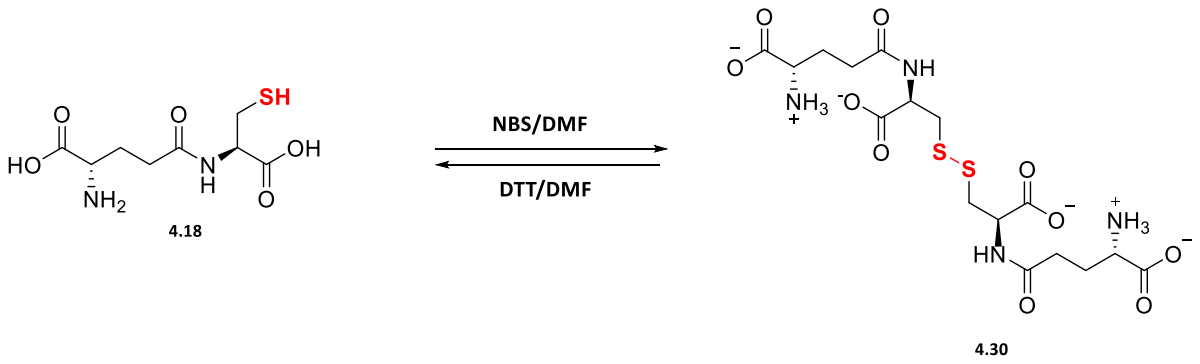

Scheme 4.10. Oxidation of γ-GluCys 4.18 in NBS/DMF to form its disulfide derivative 4.30 which can be reduced by DTT.

UV-vis spectroscopy was used to monitor the oxidation of the sulfur in the reaction mixture. Disulfides do not react with the thiol derivatizing reagent, DTNB (5,5'-Dithio-bis-(2-nitrobenzoic acid)) while the free thiol **4.35** reacts rapidly with DTNB **4.32** to form the thiol-TNBA (thio-2-nitrobenzoic acid) adduct **4.38** and TNBA **4.37** by-product which absorbs in the characteristic UV-vis region between 412-420 nm.[19] Disulfide **4.31** does not react with DTNB but it can be reduced to its free thiol derivative **4.35** by DTT.[20] (Scheme 4.11 & Scheme 4.12)

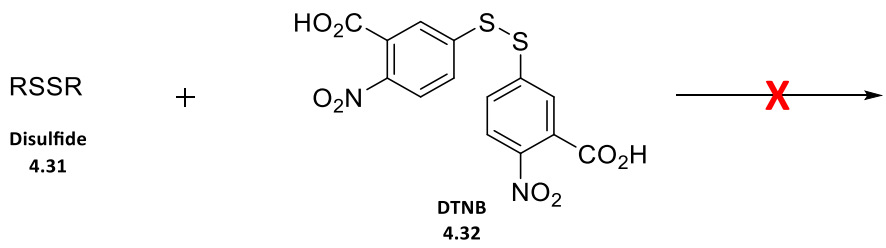

Scheme 4.11. Disulfide does not react with 5,5'-Dithio-bis-(2-nitrobenzoic acid) (DTNB) [Ellman's reagent]

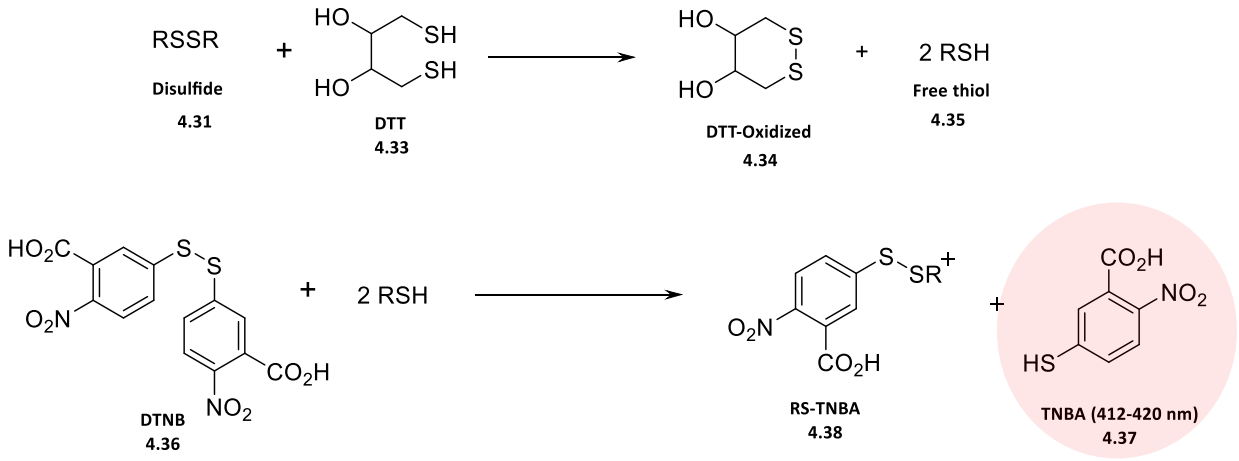

Scheme 4.12. Reduction of disulfide to free thiol by DTT (1,4-Dithiothreitol, Cleland's reagent) and derivatization of free thiol compounds (RSH) by 5,5'-Dithio-bis-(2-nitrobenzoic acid) (DTNB) generating TNBA adduct detected at λ_{max} 412 – 420 nm.

The oxidation of the sulfur source, γ-GluCys **4.18**, led to the formation of γ-GluCys disulphide **4.30** in NBS/DMF very rapidly, hence less γ-GluCys **4.18** (free thiol) was available for the sulfurization, which explains the low yield observed using this approach.

DTNB was added to a mixture of γ-glutamylcysteine 1 mM/NBS/DMF which were allowed to react for 5 min. UV-vis analysis revealed no absorption above 400 nm (yellow line), supporting the absence of a detectable free thiol (γ-GluCys **4.18**), this suggests that γ-GluCys **4.18** (free thiol) is rapidly oxidized to γ-GluCys disulfide **4.30** under these conditions. The characteristic

UV-vis band absorption (λ_{max} 412- 420 nm) was revealed only after the reaction mixture was reduced by DTT prior to DNTB reaction (blue line), thus further suggested the presence of γ-GluCys disufide **4.30**. (Figure 4.6)

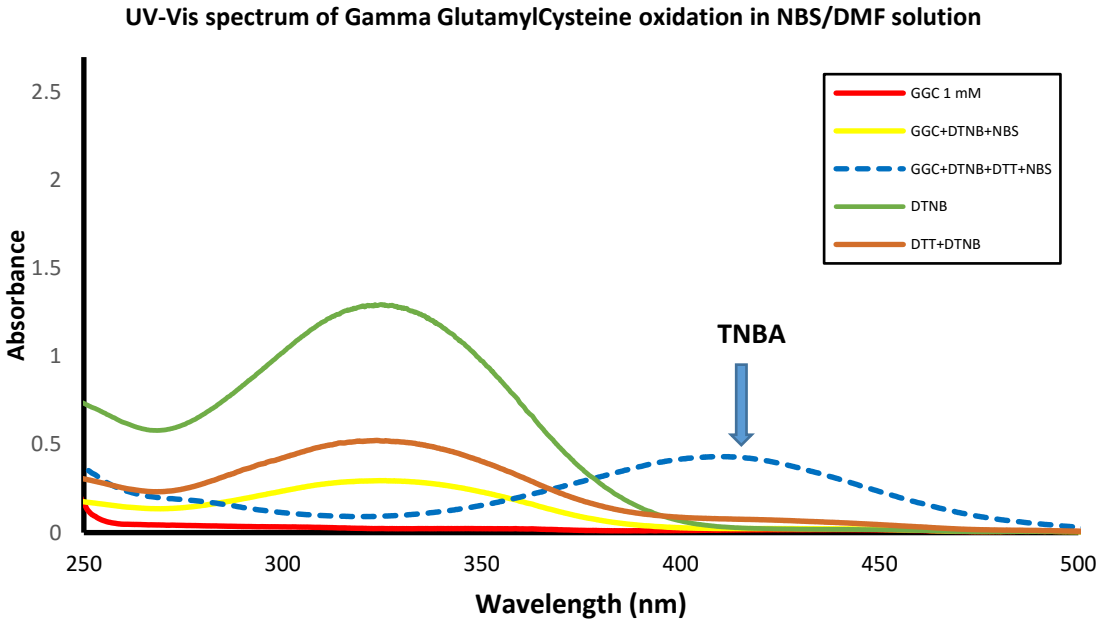

Figure 4.6. UV-vis spectroscopy monitoring of the oxidation of γ-GluCys 4.18 (1 mM) in presence of NBS/DMF (at 25°C).

A comparative study was undertaken using cysteine under the same conditions. The study showed that γ-GluCys **4.18** oxidized very rapidly within the first minute while the formation of cystine (cysteine disulphide) was complete after 1 h of the reaction (dash blue line). (Figure 4.7)

The very rapid oxidation of γ-GluCys **4.18** in NBS/DMF could explain the low yield of **7%** of the sulfurization as there was almost no free thiol available to react. Noteworthy, Birtic *et al.* determined the standard reduction potential of bis γ-GluCys/ 2 γ-GluCys experimentally to be

-238 mV.[21] This supports the facile oxidation of γ-GluCys **4.30** under reaction conditions thus supporting our findings.

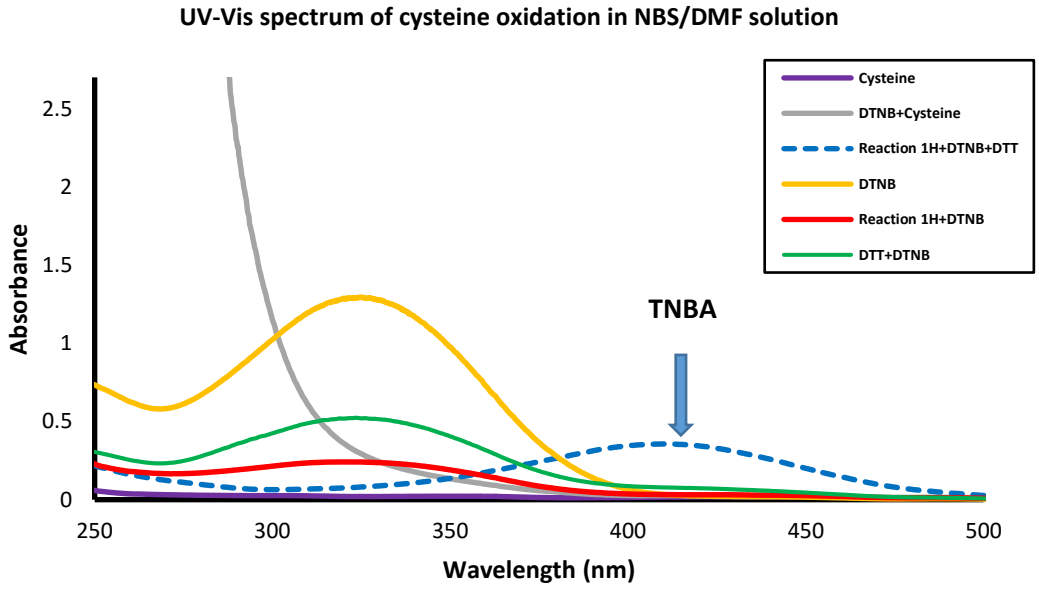

Figure 4.7. UV-vis spectroscopy monitoring of the oxidation of cysteine (1 mM) in a presence of NBS/DMF (at 25°C).

In the other hand, the sulfurization using cysteine as a sulfur source affords a better yield (76%) as published earlier,[5] (detailed in the chapter 2). This experiment illustrates the fact that the formation of cystine (cysteine disulphide) in a presence of NBS/DMF proceeds somewhat slower within 1 hr.

This route yield the thioether **4.2** in a very low yield, hence this synthetic strategy is not easily scalable. Due to the oxidation side reaction, the optimization of the yield was not attempted further and another synthesis strategy was therefore investigated.

4.5. Synthesis of (2*S*)-3-(2-(((*R*)-2-((*S*)-4-amino-4-carboxybutanamido)-2-carboxyethyl)sulfinyl)-1*H*-imidazol-4-yl)-2-(trimethylammonio) propanoate. (Method 3)

Due to successful optimisation of the 2-cysteinylhercynine thioether synthesis,[5] the envisioned strategy to synthesize γ-glutamylcysteinylhercynine sulfoxide **4.1** (EgtC enzyme substrate) was based on using a synthon that already has the required thioether moiety. The target compound **4.1** can thus be formed by sulfoxidation of the thioether precursor **4.2**, which in turn is constructed *via* the amide coupling between the protected γ-glutamate **4.5** and the protected hercynylcysteine thioether **4.39.** (Figure 4.8)

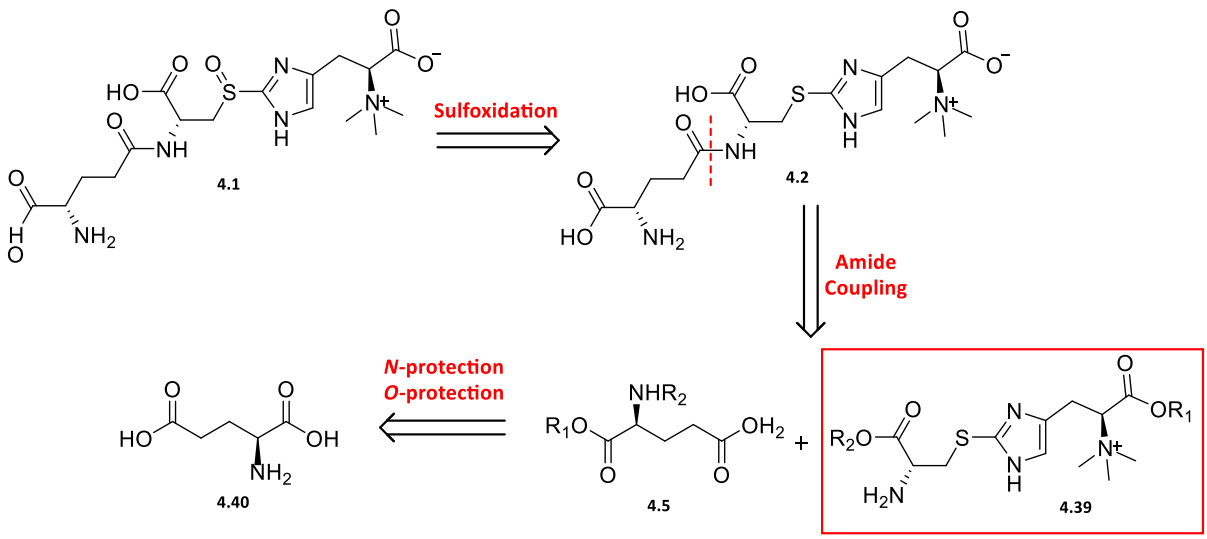

Figure 4.8. Retrosynthetic analysis of (2*S*)-3-(2-(((*R*)-2-((*S*)-4-amino-4-carboxybutanamido)-2-carboxyethyl)sulfinyl)-1*H*-imidazol-4-yl)-2-(trimethylammonio) propanoate proceeding through amide coupling of the protected hercynylcysteine thioether 4.39 (EgtE enzyme substrate).

4.5.1. Synthesis of (2*S*)-3-(2-(((*R*)-2-((*S*)-4-amino-4-carboxybutanamido)-2-carboxyethyl)sulfinyl)-1*H*-imidazol-4-yl)-2-(trimethylammonio)propanoate

The synthesis of (2*S*)-3-(2-(((*R*)-2-((*S*)-4-amino-4-carboxybutanamido)-2-carboxyethyl) sulfinyl)-1*H*-imidazol-4-yl)-2-(trimethylammonio) propanoate **4.1** using the described retrosynthesis strategy above consisted of four consecutive steps, including protection of the staring material, 2-cysteinylhercynine thioether **2.19** (described in the chapter 2), followed by amide coupling as well as a sulfoxidation. (Scheme 4.13)

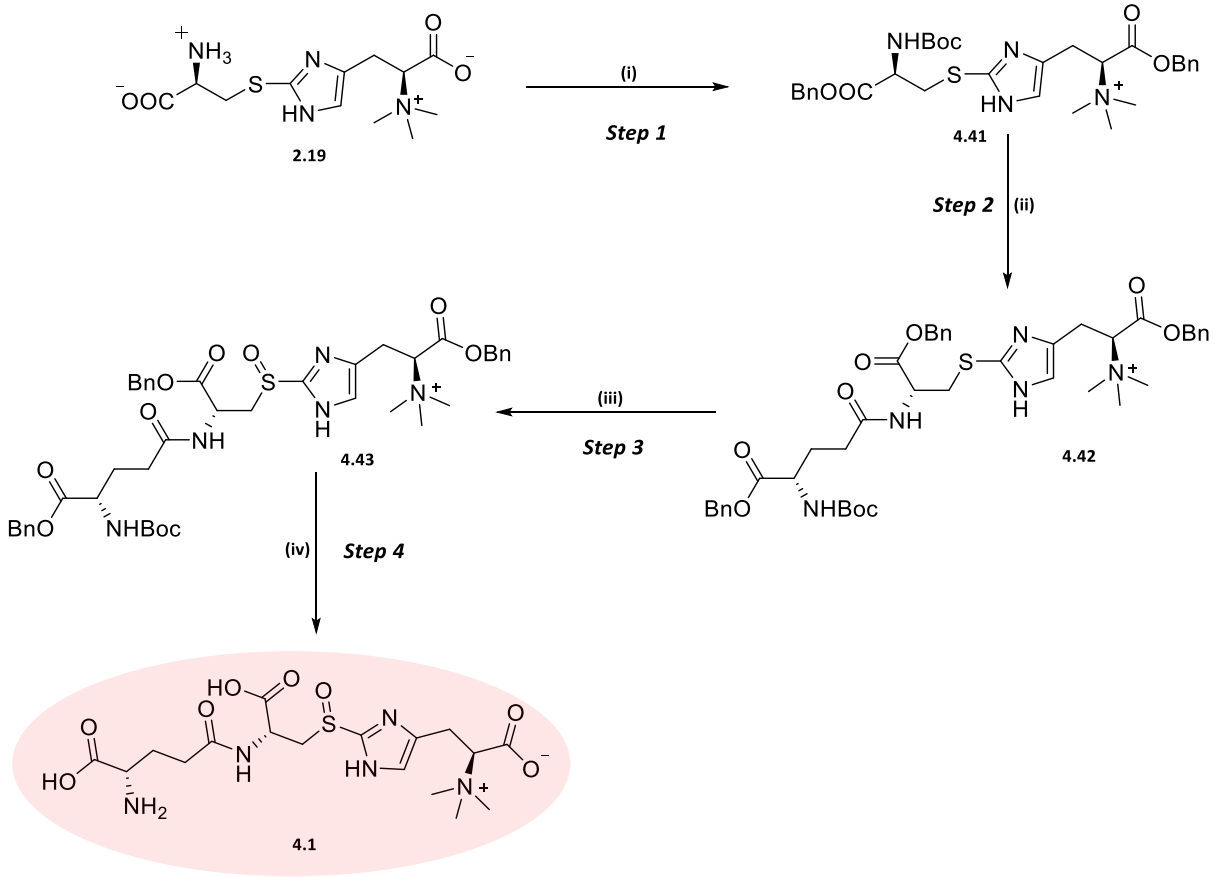

Scheme 4.13.Total synthesis of (2*S*)-3-(2-(((*R*)-2-((*S*)-4-amino-4-carboxybutanamido)-2 carboxyethyl)sulfinyl)-1*H*-imidazol-4-yl)-2-(trimethylammonio) propanoate 4.1. Reagents and conditions. (i) a. $(Boc)_2O$, CH_3CN/H_2O, overnight at rt; b. BnBr, DMF, 24 hr at rt, 33%; (ii) a. TFA, DCM, overnight at rt; b. DIC, DIPEA, HOBt, N-Boc α-

glutamate benzyl ester **4.10**, DCM, 24 hr at rt, 88%; (iii) *m*CPBA, DCM, 6 hr at rt, 72%; (iv) TFA, Pd/C, H_2, MeOH, 2 days at rt, 65%. Overal yield of 14%.

4.5.1.1. Protection of 2-cysteinylhercynine thioether 2.19. (Step 1)

2-Cysteinylhercynine thioether **2.19** was double protected in an one-pot synthesis by Boc and benzyl groups under basic conditions (NaOH) according to a method published by Arnaud *et al.*[22]

The compound, (*S*)-1-(benzyloxy)-3-(2-(((*R*)-3-(benzyloxy)-2-((*tert*-butoxycarbonyl)amino)-3-oxopropyl)thio)-1*H*-imidazol-4-yl)-*N,N,N*-trimethyl-1-oxopropan-2-aminium **4.41** was isolated in a low yield of 33% after SiO_2 column chromatography without any prior aqueous work up. Attempted aqueous work up to remove salts prior to SiO_2 gel column chromatography purification led to an even lower yield of 18%, suggesting that a considerable amount of material was lost during the purification process, as the protected product **4.41** is amphiphilic thus making it extremely difficult to efficiently perform organic solvent extraction from the aqueous medium.

The proton NMR spectrum of **4.41** displayed an up-field signal resonating as a singlet at δ_H 1.41 ppm integrated for 9 protons suggesting the presence of Boc protecting group. A downfield signal resonating as a multiplet from δ_H 5.36 to 5.03 ppm integrated for 4 protons and a further downfield signal resonating as a multiplet from δ_H 7.27 to 7.42 ppm integrating for 10 protons suggesting the presence of two benzyl ester groups, thus confirming the successful double protection of 2-cysteinylhercynine thioether **2.19** to form (*S*)-1-(benzyloxy)-3-(2-(((*R*)-3-(benzyloxy)-2-((*tert*-butoxycarbonyl)amino)-3-oxopropyl)thio)-1*H*-imidazol-4-yl)-

N,N,N-trimethyl-1-oxopropan-2-aminium **4.41.** The ^{13}C NMR spectrum of **4.41** provided further evidence of the successful protection as it displayed the correct amount of carbon signals supporting the carbon skeleton of **4.41**.

4.5.1.2. Synthesis of (*S*)-1-(benzyloxy)-3-(2-(((*R*)-3-(benzyloxy)-2-((*S*)-5-(benzyloxy)-4-((*tert*-butoxycarbonyl)amino)-5-oxopentanamido)-3-oxopropyl)thio)-1*H*-imidazol-4-yl)-*N,N,N*-trimethyl-1-oxopropan-2-aminium. (Step 2)

Step 2 entailed the Boc removal followed by the amide coupling in a presence of DIC,[23] HOBt and DIPEA to yield the amide **4.42** in a yield of 88%.

Key diagnostic signals in the proton NMR spectrum of **4.42** was the appearance of a characteristic *Boc* signal resonating at δ_H 1.42 ppm; two methylene signals resonating at δ_H 2.19 ppm as a doublet of doublets and as a multiplet from δ_H 2.08 ppm to 1.89 ppm respectively. One α-amino acid proton resonating at δ_H 3.99 ppm as doublet of doublets of doublets belonging to the γ-glutamate moiety. In addition, the proton NMR spectrum displayed a multiplet and an overlapped singlet signal resonating from δ_H 7.46 ppm to 7.25 ppm integrating for 16 protons assigned for three phenyls and one aromatic imidazole proton confirming the structure of **4.42**. ^{13}C NMR spectrum provided further evidence as it revealed five carbonyl signals resonating at δ_C 173.1 (2C), 172.0, 171.2, 155.3 and 149.3 ppm, consistent with the structure of **4.42**.

4.5.1.3. Sulfoxidation of the protected γ-glutamyl cysteinyl hercynine thioether. (Step 3)

Catalytic methods to efficiently oxidize sulfur to the sulfoxide using H_2O_2 is well documented.[24,25]

It was practical to utilize the relatively non-polar protected **4.42** as a substrate for the sulfoxidation, thus allowing the sulfoxidation with a milder oxidant (1.1 mol equivalent of *m*CPBA) in DCM solvent. This approach provides better control thus preventing any over oxidation. Subsequent removal of benzyl and Boc protecting groups would provide the target compound, (2*S*)-1-(benzyloxy)-3-(2-(((*R*)-3-(benzyloxy)-2-((*S*)-5-(benzyloxy)-4-((*tert*-butoxycarbonyl)amino)-5-oxopentanamido)-3-oxopropyl)sulfinyl)-1*H*-imidazol-4-yl)-*N,N,N*-trimethyl-1-oxopropan-2-aminium **4.43**.

Step 3 involved the sulfoxidation of the thioether **4.42** by *m*CPBA in DCM to yield the sulfoxide **4.43** in a good yield of 72%. (Scheme 4.14)

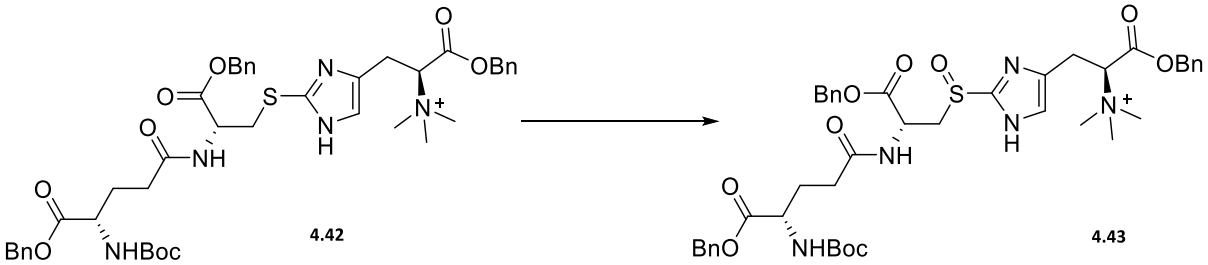

Scheme 4.14. Synthesis of (2*S*)-1-(benzyloxy)-3-(2-(((*R*)-3-(benzyloxy)-2-((*S*)-5-(benzyloxy)-4-((*tert*-butoxycarbonyl)amino)-5-oxopentanamido)-3-oxopropyl)sulfinyl)-1*H*-imidazol-4-yl)-*N,N,N*-trimethyl-1-oxopropan-2-aminium 4.43. Reagents and conditions. *m*CPBA, DCM, 6 hr at rt, 72%.

A key diagnostic signal in the proton NMR spectrum of **4.43** was the methylene proton directly bonded to the sulfur atom resonating as a multiplet shifted further downfield from the region

of δ_H 2.67 – 2.44 ppm in **4.42** to the region of δ_H 4.45 – 4.20 ppm as observed in the NMR spectrum of **4.43**. The strong downfield shift suggests the successful oxidation of sulfur to the sulfoxide, which exerts an electron withdrawing strong deshielding effect to its adjacent methylene proton. The diastereotopicity introduced by the sulfoxidation was clearly revealed as a ratio of 3.5:1 whereby methylene proton adjacent to sulfoxide group resonated as multiplets from δ_H 4.31 to 4.25 ppm for the major diastereoisomer and from δ_H 4.24 to 4.20 ppm for the minor diastereoisomer. (Figure 4.9)

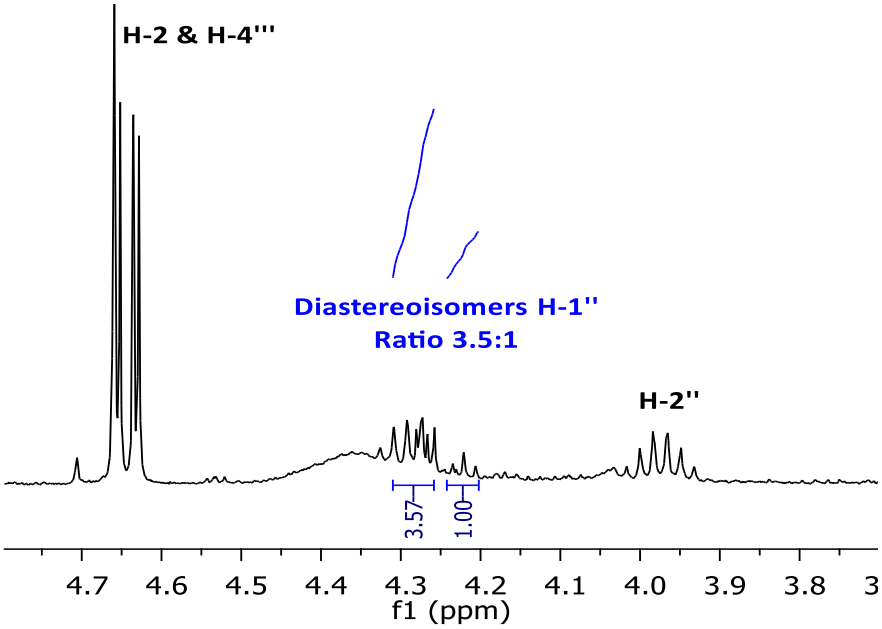

Figure 4.9. Portion of ^{1}H NMR spectrum of the sulfoxide 4.43 (between δ_H 4.7-3.8 ppm) illustrating the diastereotopicity.

Furthermore, the FTIR spectrum revealed a characteristic strong absorption band at 1048 cm^{-1} and 1026 cm^{-1} corresponding to the sulfoxide functional group, thus supporting the successful oxidation of the thioether **4.42** to the sulfoxide **4.43.**

The last step (step 4) entailed the complete removal of protecting groups in a one-pot synthesis. The latter was achieved by Pd/C hydrogenation of the protected sulfoxide **4.43** in 20% TFA/MeOH. The target compound, (2*S*)-3-(2-(((*R*)-2-((*S*)-4-amino-4-carboxybutanamido)-2-carboxyethyl)sulfinyl)-1*H*-imidazol-4-yl)-2-(trimethylammonio)propanoate **4.1** was obtained in a moderate yield of 65%. The target compound **4.1** was synthesized in an overall yield of 14%.

The evidence of structure of (2*S*)-3-(2-(((*R*)-2-((*S*)-4-amino-4-carboxybutanamido)-2-carboxyethyl)sulfinyl)-1*H*-imidazol-4-yl)-2-(trimethylammonio)propanoate **4.1** was furnished by spectroscopic techniques. Two dimensional NMR; HSQC and COSY (Figure 4.10) were utilized to support a full structural assignment.

The proton NMR spectrum of **4.1** revealed the disappearance of all three phenyl protons in the region of δ_H 7.40 – 7.25 ppm and Boc signal at δ_H 1.42 ppm thus confirming the successful deprotection of **4.43** to yield the target compound **4.1**. The NMR data of **4.1** were consistent with those reported by Seebeck.[6] However, amino acid residues of a peptide are ionisable and the net charge of a peptide is therefore dependent on the pH of the medium. Studies revealed that the chemical shifts of a peptide observed in the NMR is strongly pH-dependent, which could explain the slightly downfield shift in some chemical shifts of the synthesized substrate compared to the natural one.[26]

4.5.1.4. Table 4.1. NMR comparison of synthetic and biosynthetic γ-glutamylcysteinylhercynine sulfoxide (EgtC enzyme substrate) 4.1.

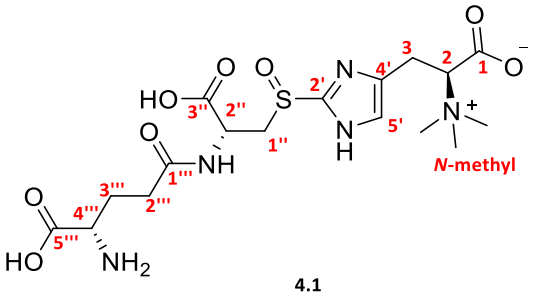

4.1

Positions	Synthetic[a] ^{1}H NMR 400 MHz	Biosynthetic[b] ^{1}H NMR 600 MHz	Synthetic[b] ^{13}C NMR 101 MHz	Biosynthetic[a] ^{13}C NMR
1			174.9	
2	4.01 (m, 1H)	3.97 (1H, m)	85.6	79
3	3.63 (dd, *J* = 11.6, 4.1 Hz, 1H, H-3a) 3.53 (dd, *J* = 11.6, 8.6 Hz, 1H, H-3b)	3.18-3.38 (m, 2H, pro-R and pro-S)	27.7	27
2'			133.9	
4'			129.7	
5'	7.65 (s, 1H)	7.29 (s, 1H)	128.8	124
1''	4.28 (dt, *J* = 13.2, 6.7 Hz, 2H, major diastereoisomer), 4.24	3.65 (m, 2H, pro-R and pro-S)	44.0 (major diastereoisomer)	

	– 4.20 (m, 2H, H-1" minor diastereoisomer)		43.9 (minor diastereoisomer)	
2''	4.48 (m, 1H)	3.97 (1H, m)	56.1	56
3''			182.0	
1'''			177.1	
2'''	2.83 – 2.58 (m, 2H)	2.48 (t, *J* = 7.6 Hz, 2 H)	36.7	33
3'''	2.41 – 2.21 (m, 2H)	2.16 (m, 2 H)	29.4	28
4'''	Overlapped 4.48 (m, 1H)	3.92 (t, *J* = 6.33 Hz, 2 H)	53.7	55
5'''			182.0	
N-methyl	3.94 (s, 9H)	3.15 (s, 9 H)	52.1	54

[a] Recorded in D_2O (pD non determined) [b] Taken from Seebeck[6] (recorded in D_2O, 20°C, pD = 5.0)

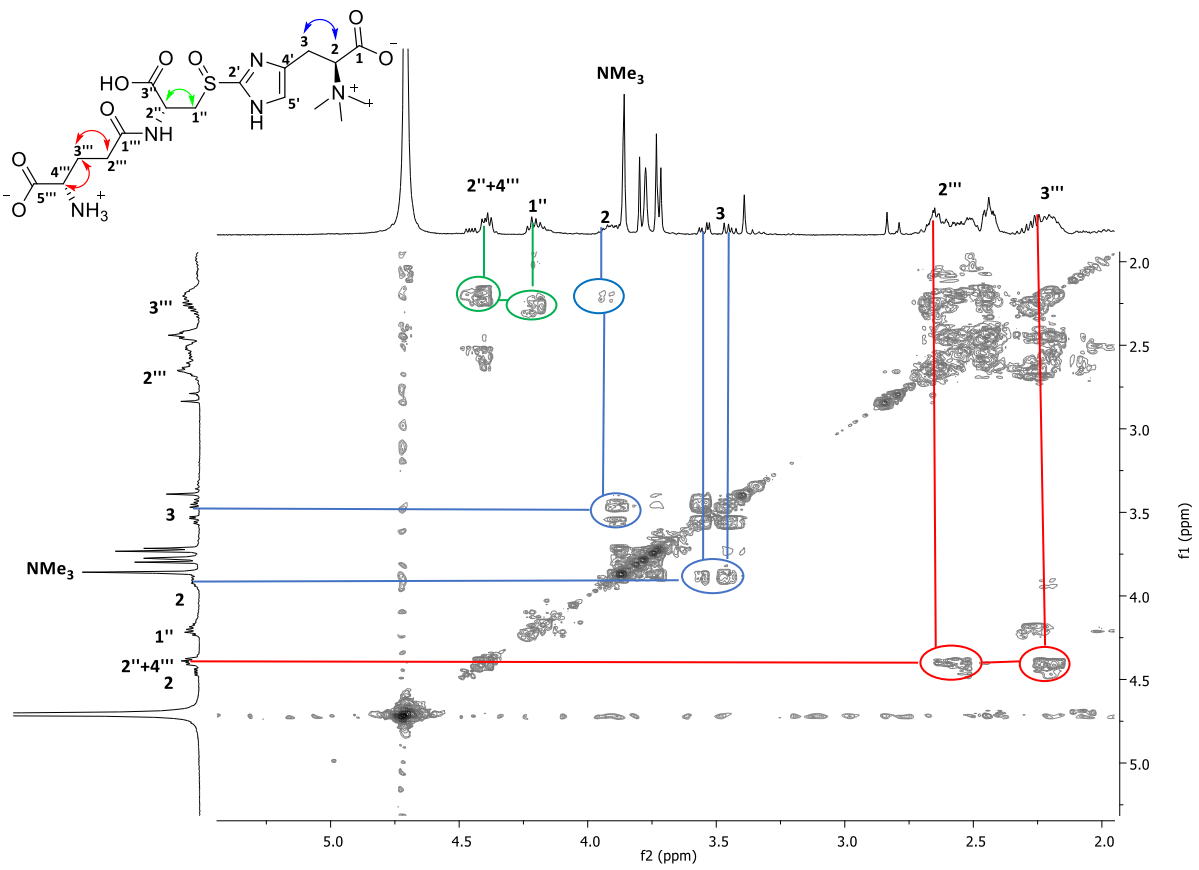

Figure 4.10. COSY ^{1}H - ^{1}H NMR spectrum of (2*S*)-3-(2-(((*R*)-2-((*S*)-4-amino-4-carboxybutanamido)-2-carboxyethyl)sulfinyl)-1*H*-imidazol-4-yl)-2-(trimethylammonio)propanoate or γ-glutamylcysteinylhercynine sulfoxide (4.1) in D_2O.

4.6. Conclusion

Three possible synthetic routes were explored and discussed in depth in this chapter, resulting in the successful first synthesis of the target compound, (2*S*)-3-(2-(((*R*)-2-((*S*)-4-amino-4-carboxybutanamido)-2-carboxyethyl)sulfinyl)-1*H*-imidazol-4-yl)-2-(trimethylammonio)propanoate **4.1**.

Despite the fact that the method 2 utilizing γ-glutamylcysteine **4.18** as a sulfur source for the sulfurization, led to the synthesis of the thioether intermediate **4.1** in a low yield of 7%, this

approach can still be improved. Several improvements can be conducted such as the optimization of the reaction conditions, including slow addition of γ-glutamylcysteine (sulfur source), lower temperature to reduce the rate of the oxidation side reaction or the addition of a easy removable or recyclable reducing reagent *in situ* thus allowing the availability of the free sulfur **4.18** required for the sulfurization reaction.

The availability of this metabolite (EgtC enzyme substrate) will provide a tool for future *tuberculosis* drugs discovery research, thus paving the way for further research to shed light on the role played by ergothioneine in the survival of *Mycobacterium tuberculosis.*

Very recently, Seebeck *et al.* solved the co-crystal complex of $EgtC_{C2A}$ (1.8 A°) complexed with the natural sulfoxide **4.1,** thus establishing the chirality of the natural sulfoxide **4.1** (EgtC enzyme substrate) to be of *S*-configuration for the sulfur atom.[3] Even though asymmetric sulfoxidation of thioether is well documented, it was not attempted in this synthetic route.[27,28] It is noteworthy that further studies can be conducted including the asymmetric sulfoxidation of the protected thioether intermediate **4.42** in order to yield an enriched diastereoisomer of the EgtC enzyme substrate **4.1**, which will shed more light on the sulfoxide substrate-EgtC enzyme interactions and specificity.

Amongst all the three synthetic routes, it appeared that the total synthesis of the mycobacterial EgtC enzyme substrate (glutamine amidohydrolase enzyme substrate) proceeding through amide coupling of EgtE enzyme substrate (method 3), is the best as it is scalable while utilizing overall less expensive materials, one drawback would be that this

route involves multiple steps (including the synthesis of the key intermediate, 2-cysteinylhercynine thioether, the EgtE enzyme substrate.

4.7. References

1 Allegra Vit, Gabriel T. Mashabela, Wulf Blankenfeldt & Seebeck, F. P. Structure of the Ergothioneine-Biosynthesis Amidohydrolase EgtC. *ChemBioChem* **16**, 1490 (2015).

2 Fahey, R. C. Glutathione analogs in prokaryotes. *Biochimica et biophysica acta* **1830**, 3182-3198, doi:10.1016/j.bbagen.2012.10.006 (2013).

3 Vit, A., Mashabela, G. T., Blankenfeldt, W. & Seebeck, F. P. Structure of the Ergothioneine-Biosynthesis Amidohydrolase EgtC. *Chembiochem* **16**, 1490-1496, doi:10.1002/cbic.201500168 (2015).

4 Khonde, L. P. Synthesis of Mycobacterial Ergothioneine biosynthetic pathway. *MSc Thesis, University of Cape Town* (2013).

5 Khonde, P. L. & Jardine, A. Improved synthesis of the super antioxidant, ergothioneine, and its biosynthetic pathway intermediates. *Organic & biomolecular chemistry* **13**, 1415-1419, doi:10.1039/c4ob02023e (2015).

6 Seebeck, F. P. In Vitro Reconstitution of Mycobacterial Ergothioneine Biosynthesis. *Journal of American Chemical Society* **132**, 6632 (2010).

7 Gagnepain, J., Moulin, E. & Furstner, A. Gram-scale synthesis of iejimalide B. *Chemistry* **17**, 6964-6972, doi:10.1002/chem.201100178 (2011).

8 Lidia, L. D., Giacomelli, G. & Porcheddu, A. An Efficient Route to Alkyl Chlorides from Alcohols Using the Complex TCT/DMF. *Organic letters* **4**, 553-555 (2002).

9 Ishikawa, Y., Israel, S. E. & Melville, D. B. Participation of an Intermediate Sulfoxide in the Enzymatic Thiolation of the Imidazole Ring of Hercynine to Form Ergothioneine. *Journal of Biological Chemistry* **249, 14**, 4420 (1974).

10 Goncharenko, K. V., Vit, A., Blankenfeldt, W. & Seebeck, F. P. Structure of the sulfoxide synthase EgtB from the ergothioneine biosynthetic pathway. *Angewandte Chemie* **54**, 2821-2824, doi:10.1002/anie.201410045 (2015).

11 Erdelmeier, I., Daunay, S., Lebel, R., Farescour, L. & Yadan, J.-C. Cysteine as a sustainable sulfur reagent for the protecting-group-free synthesis of sulfur-containing

amino acids: biomimetic synthesis of l-ergothioneine in water. *Green Chemistry* **14**, 2256, doi:10.1039/c2gc35367a (2012).

12 Ito, S. Synthesis of 2-S-cysteinylhistidine and 2-mercaptohistidine via bromolactone derivative of histidine. *The Journal of organic chemistry* **50**, 3636-3638, doi:10.1021/jo00219a044 (1985).

13 Maldonado, P. D. *et al.* Role of allyl group in the hydroxyl and peroxyl radical scavenging activity of S-allylcysteine. *The journal of physical chemistry. B* **115**, 13408-13417, doi:10.1021/jp208233f (2011).

14 Jia, Y. *et al.* The synthesis and biological evaluation of novel Danshensu-cysteine analog conjugates as cardiovascular-protective agents. *European journal of medicinal chemistry* **55**, 176-187, doi:10.1016/j.ejmech.2012.07.016 (2012).

15 Bridge, W. J. & Zarka, M. H. Process for the synthesis of γ-glutamylcysteine WO2006/102722A1 (**2006**).

16 Suehiro, M., Kawasaki, K., Nishiuchi, H. & Nishimura, Y. Method for producing γ-glutamylcysteine. EP 1 428 873 A2 (**2004**).

17 Jinn, T. L. *et al.* Saccharomyces Cerevisiae Strains For Hyper-producing Glutathione and Gamma-Glutamylcysteine and Processes of Use US 2007/0196382 Al (**2007**).

18 Hopkinson, R. J., Barlow, P. S., Schofield, C. J. & Claridge, T. D. Studies on the reaction of glutathione and formaldehyde using NMR. *Organic & biomolecular chemistry* **8**, 4915-4920, doi:10.1039/c0ob00208a (2010).

19 Zhang, X.-Y., Piao, Y.-L., Cui, S.-Y. & Lee, Y.-I. Determination of reduced glutathione, cystein and total thiols in pine pollen powder by in situ derivatization. *Microchemical Journal* **112**, 1-6, doi:10.1016/j.microc.2013.09.011 (2014).

20 Hualei, L. Dithiothreitol (Cleland's Reagent). *Free radical biology & medicine* **77:222**, 1 (2003).

21 Birtic, S., Colville, L., Pritchard, H. W., Pearce, S. R. & Kranner, I. Mathematically combined half-cell reduction potentials of low-molecular-weight thiols as markers of seed ageing. *Free radical research* **45**, 1093-1102, doi:10.3109/10715762.2011.595409 (2011).

22 Arnaud, O. *et al.* Potent and fully noncompetitive peptidomimetic inhibitor of multidrug resistance P-glycoprotein. *Journal of medicinal chemistry* **53**, 6720-6729, doi:10.1021/jm100839w (2010).

23 Han, S.-Y. & Kim, Y.-A. Recent development of peptide coupling reagents in organic synthesis. *Tetrahedron* **60**, 2447-2467, doi:10.1016/j.tet.2004.01.020 (2004).

24 Rostami, A. & Akradi, J. A highly efficient, green, rapid, and chemoselective oxidation of sulfides using hydrogen peroxide and boric acid as the catalyst under solvent-free conditions. *Tetrahedron Letters* **51**, 3501-3503, doi:10.1016/j.tetlet.2010.04.103 (2010).

25 Rostami, A., Hassanian, F., Ghorbani-Choghamarani, A. & Saadati, S. Selective Oxidation of Sulfides to Sulfoxides using H_2O_2Catalyzed by p-Toluenesulfonic Acid (p-TsOH) Under Solvent-Free Conditions. *Phosphorus, Sulfur, and Silicon and the Related Elements* **188**, 833-838, doi:10.1080/10426507.2012.710681 (2013).

26 Platzer, G., Okon, M. & McIntosh, L. P. pH-dependent random coil (1)H, (13)C, and (15)N chemical shifts of the ionizable amino acids: a guide for protein pK a measurements. *J Biomol NMR* **60**, 109-129, doi:10.1007/s10858-014-9862-y (2014).

27 Cotton, H. *et al.* Asymmetric synthesis of esomeprazole. *Tetrahedron: Asymmetry* **11**, 3819–3825 (2000).

28 Wojaczynska, E. & Wojaczynski, J. Enantioselective Synthesis of Sulfoxides: 2000-2009. *Chemical reviews* **110**, 4303–4356 (2010).

Chapter 5 Advances toward the synthesis of ovothiols

In this chapter, the main focus will be to address interesting advances conducted in the field of histidine like compounds. After successfully developed interesting synthetic strategies for the synthesis of ergothioneine and its biosynthetic pathway metabolites as discussed in previous chapters. It was therefore decided to apply that knowledge gained in the synthesis of ovothiols, structurally similar to ergothioneine, with a *N*-methyl at the more hindered position of the imidazole ring (*N*-3 position) and a thiol group at the 5-position.

5.1. Introduction

Ovothiols are 3-methyl-5-mercaptohistidines derivatives first isolated from marine invertebrates. It exists as three types of ovothiols, denoted A, B and C, they differ amongst them by their degree of methylation at the α-amino group. Ovothiol A has a free α-amino group, while ovothiol B and C are α-mono and α,α-dimethylated, respectively. (Figure 5.1)

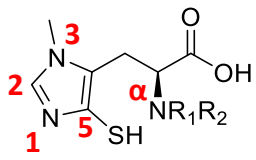

	R_1	R_2
Ovothiol A	**H**	**H**
Ovothiol B	**H**	**CH_3**
Ovothiol C	**CH_3**	**CH_3**

Figure 5.1. Structure of ovothiols (A, B & C).

The thiolate group of ovothiol exhibits the lowest basicity amongst all natural thiols, with a pK_{SH} of 1.42 that makes it readily oxidizable, hence ovothiol is a potent natural antioxidant.[1]

Ovothiols were first isolated from eggs and ovarian tissues of marine invertebrates by Turner *et al.*[2] Ovothiol A isolated from starfish *Evasterias troschelii*, whereas ovothiol B and C were isolated from the scallop *Chlamys hastate* and sea urchin *Strongylocentrotus purpuratus*, respectively.[2]

It has been suggested that ovothiols protect *trypanosomatid* parasites, such as *Leishmania donovani* and *Crithidia fasciculata* from oxidative stress produced by their macrophages during infection.[3] It is reported that ovothiol C is present in millimolar concentration in sea urchin eggs and are responsible for the protection of eggs during oxidative envelope maturation.[2] Ovothiols display interesting physical properties that have encouraged the scientific community to study its nutritional benefits for humans.

Ovothiol analogues were synthesized and their *in vitro* antioxidant properties evaluated, interestingly, 1-methyl-2-(3-trifluoromethylphenyl)-4-mercaptoimidazole has been shown to be a potent agent in mammalian cerebral protection.[4]

Moreover, recent research demonstrated that ovothiol A could be active against the proliferation of Hep-G2, human liver cancer cells.[5]

5. 2. Biosynthesis of Ovothiols

The biosynthesis of ovothiol involves three sequential steps. The enzyme OvoA, a sulfoxide synthase (characterized from the bacterium *Erwinia tasmaniensis* and the pathogenic protist *Trypanosoma cruzi*) catalyzes the first step of the biosynthesis. That initial step involves the oxidative coupling between cysteine and histidine to generate *S*-(5'-*L*-histidyl)-*L*-cysteine

sulfoxide.[1] It is argued that OvoA is similar to EgtB; the latter is a mononuclear non-heme iron enzyme which catalyzes the oxidative sulfurization of hercynine by γ-glutamylcysteine in the biosynthesis of ergothioneine.[6,7] OvoA and EgtB are both iron-dependent enzymes and they share a homologue domain with formylglycine-generating enzymes.[8]

OvoB catalyzes the second step, the *C*-*S* bond lysis of *S*-(5'-*L*-histidyl)-*L*-cysteine sulfoxide to produce 5-mercaptohistidine. The latter is believed to be methylated by a C-terminal methyltransferase domain. (Scheme 5.1)

However, the first enzyme implicated in the biosynthesis of ovothiols, OvoA, has been proposed to be a potential drug target for anti-infective therapy.[8]

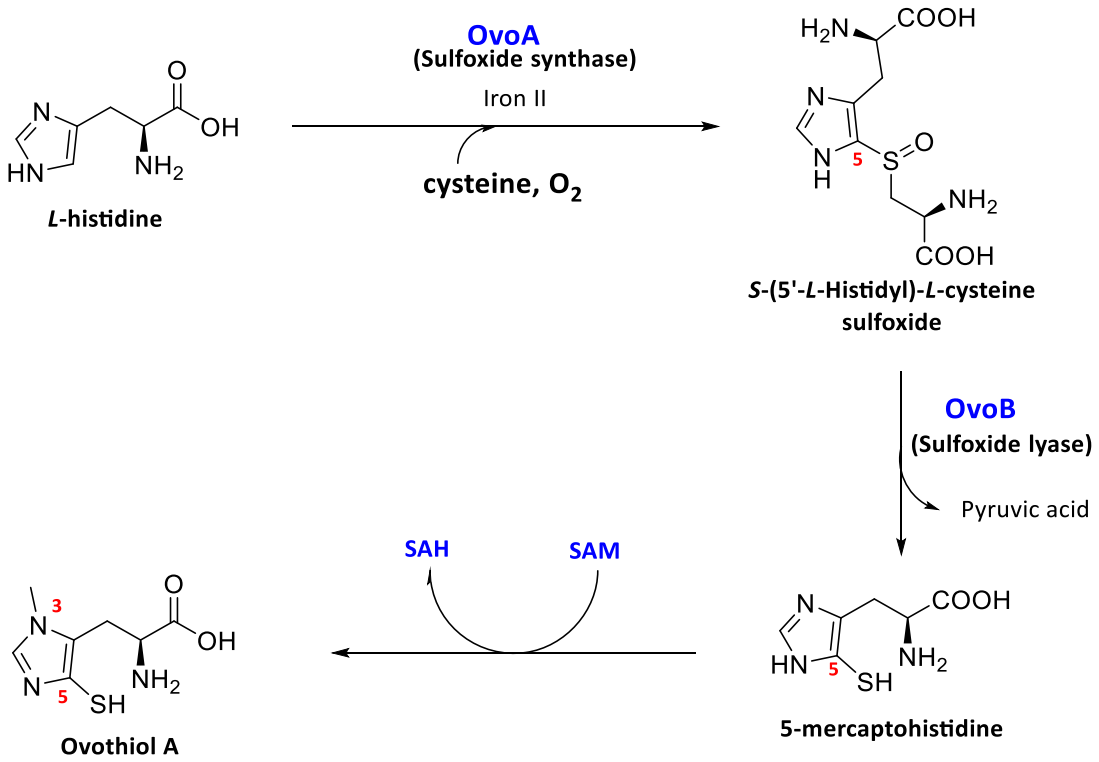

Scheme 5.1. Ovothiols biosynthesis pathway.

5.3. Ovothiol synthesis

Unfortunately, the availability of ovothiol A is limited, its isolation from natural marine sources such as sea urchin and algae is labour intensive and not cost effective.[2,9]

However, ovothiol A total synthesis methods are well documented, but these procedures are not simple and require multiple steps.[10,11] This is mainly due to the fact that the 4-mercaptohistidine core is constructed from simple starting materials such as *N*-methyl-prop-2-yn-1-amine or 1*H*-imidazole rather than *L*-histidine, which is more closely related. (Figure 5.2)

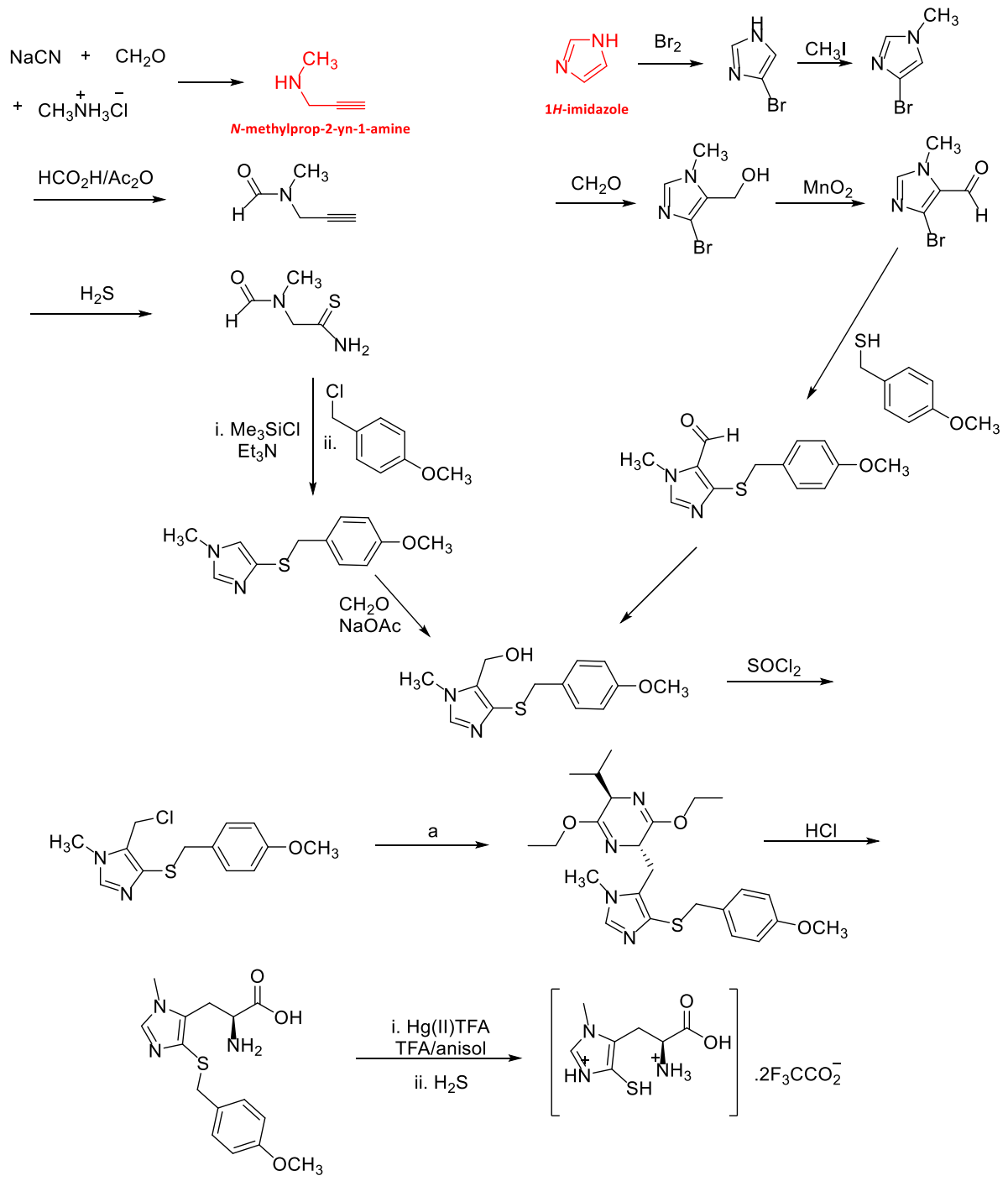

Figure 5.2. Previous ovothiols total synthesis routes proposed by Ohba et *al.*[11] (right) and Holler et *al.*[10] (left)

Reactant a is (*R*)-2,5-dihydro-3,6-diethoxy-2-isopropylpyrazine, *n*-butyllithium. (Scheme adapted from Mirzahosseini *et al.*[12])

However, recently Mirzahosseini *et al.* claimed to have developed a cost effective synthesis of ovothiol A starting with *L*-histidine as a starting material. That strategy is attractive as it reduces drastically the number of steps, including many synthetic challenges.[12]

5.4. Design and synthesis of ovothiol A using *L*-histidine as a starting material

Due to the synthesis interest in ergothioneine, knowledge and skills gained is applicable to the synthesis of ovothiols. To this end, two main reactions, regioselective *N*-methylation and bromination, were investigated and will be thoroughly discussed.

5.4.1. Retrosynthetic analysis

The ovothiol A retrosynthetic strategy involves the regioselective thionation at the 5-position of the imidazole heterocyclic ring using two synthons, (*S*)-2-amino-3-(4-bromo-1-methyl-1*H*-imidazol-5-yl) propanoic acid **5.2** and a sulfur source **5.3**. The Intermediate **5.2** is constructed by regioselective bromination at 5-position of the imidazole heterocyclic ring of N^{Π}-methyl-*L*-histidine **5.4** which is derived from *L*-histidine **5.5** a simple starting material and biosynthetic precursor of the target compound, ovothiol **5.1** (Figure 5.3).

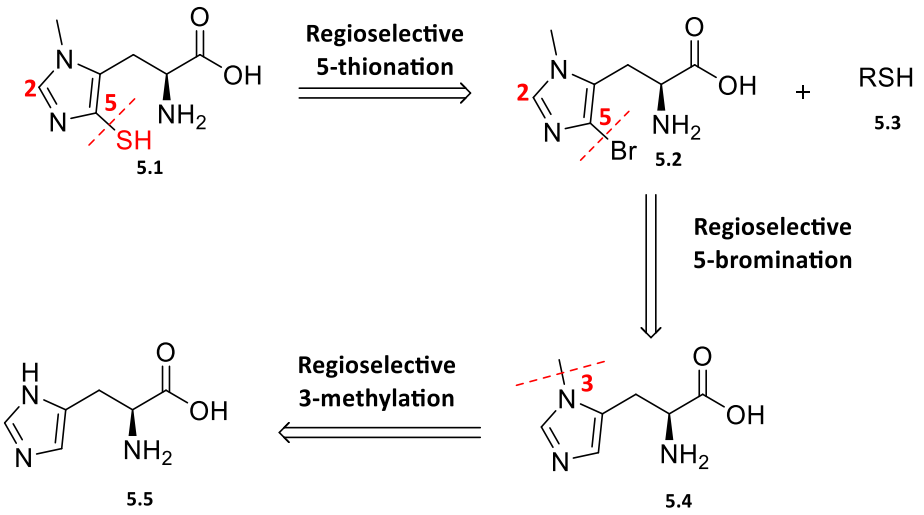

Figure 5.3. Ovothiol A retrosynthetic analysis.

5.4.2. Regioselective methylation at *N*-3 position of the imidazole heterocyclic ring

Histidine possesses three ionizable functions, acidic carboxylic group (pK_{a1} 1.82), basic amino acid group (pK_{a2} 9.17) and imidazole side chain (pK_{a3} 6.00), with an isoelectronic point pI of 7.59 whereby histidine exists predominantly as a zwitterion.

The imidazole heterocyclic ring exists in three exchangeable tautomeric conformations in aqueous buffer solutions. Two tautomers (denoted ε and δ) are neutral predominantly at high pH and act as hydrogen bond acceptors or donors, whereas the cationic tautomer is dominant at low pH.[13] (Figure 5.4)

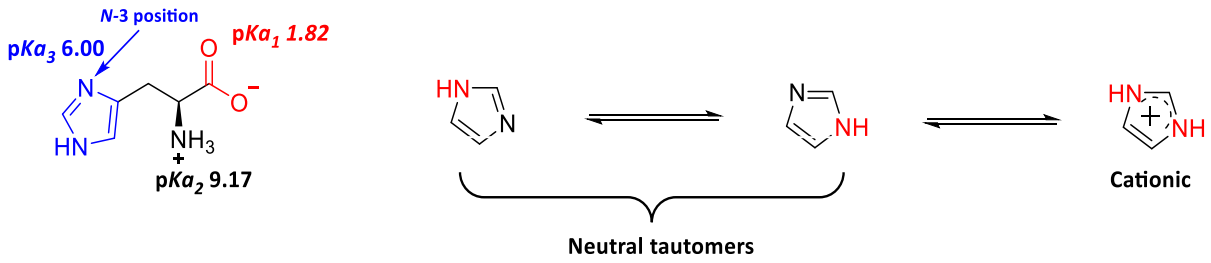

Figure 5.4. pK_a of histidine ionisable functions (left), imidazole tautomeric conformations (right).

The first challenge was to achieve a selective methylation at the hindered *N*-3 position of the imidazole ring. In order to achieve that task, it was imperative to first and foremost protect any competing functional groups, the amino and carboxylic acid, respectively groups, thus directing the methylation at the desired position.

Van Den Berge *et al*. developed an attractive method for the regioselective *N*-methylation of substituted imidazole derivatives to furnish the less stable, most sterically hindered isomer.[14] These authors developed a mild sequence strategy which involved a protection, methylation and deprotection to yield the more hindered *N*-methylated imidazole isomer, the 1,5 isomer as the major product. (Scheme 5.2)

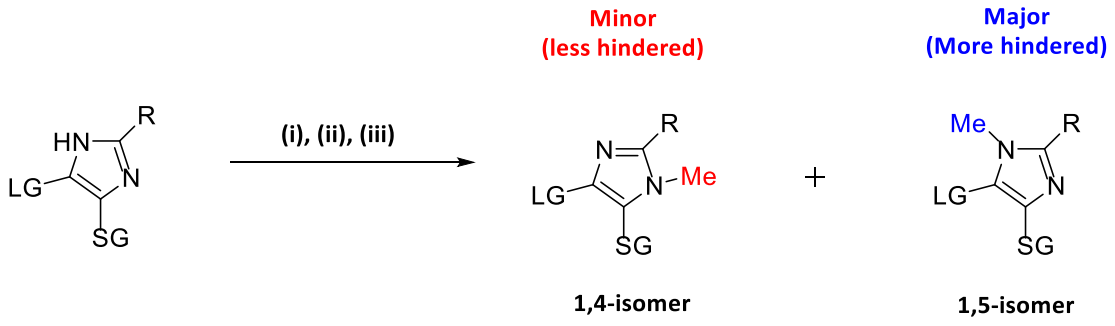

Scheme 5.2. Van Den Berge *et al*.[14] *N*-methylation strategy. Reagents and conditions. (i) $PhSO_2Cl$, Et_3N, CH_3CN, 8h; (ii) MeOTf, 24 hr; (ii) MeBuNH, heated at 80 °C.

The protecting group strategy is crucial for the success of this methodology. The proton in the imidazole heterocyclic ring is delocalised and a rapid tautomerism equilibrium of (*NH*)-derivatives is established between the two nitrogen atoms.[14] Due to the fact that the *N*-alkylation of the less hindered nitrogen is relatively faster, the *N*-alkylation by a relatively smaller group leads to a mixture of the *N*-1 methylated (major) and the *N*-3 methylated (minor) product. But using a bulky *N*-alkylating group leads to almost exclusively one isomer at less hindered *N*-1 position, thus will direct the next alkylation to the more hindered *N*-3 position of the imidazole ring.[14] It is noteworthy that the regioselective *N*-alkylation is only governed by steric factors as electronic properties of substituents have no significant effect (Scheme 5.3. [14]

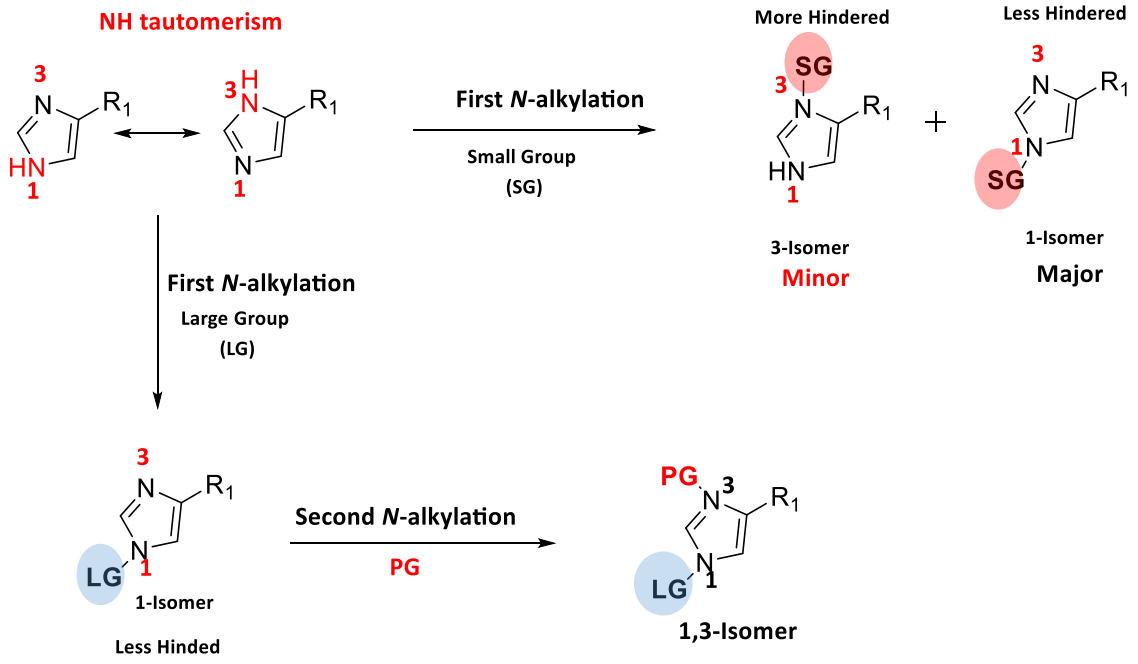

Scheme 5.3. Steric hindrance directs *N*-alkylation on the imidazole ring.

The first step entailed the complete protection of *L*-histidine (starting material) by a bulky protecting group. Subsequently *N*-3 regioselective methylation of the protected histidine.

However, several protecting groups as well as methylating reagents were investigated and will be discussed thoroughly.

5.4.2.1. Synthesis of *tert*-butyl (*S*)-4-(3-(benzyloxy)-2-((*tert*-butoxycarbonyl)amino)-3-oxopropyl)-1*H*-imidazole-1-carboxylate

Bulky *tert*-butyl carbonate (Boc) and benzyl groups were chosen to protect the amino and carboxylic acid groups respectively prior to attempted regioselective *N*-methylation, due to their relatively well documented easy introduction and removal.

The synthesis of *tert*-butyl (*S*)-4-(3-(benzyloxy)-2-((*tert*-butoxycarbonyl)amino)-3-oxopropyl)-1*H*-imidazole-1-carboxylate was conducted in two consecutive steps, double Boc protection of *L*-histidine **5.5** to yield N^{α},N^{τ}-bis(*tert*-butoxycarbonyl)-*L*-histidine **5.6** in a yield of 63%. Subsequent benzyl esterification of N^{α},N^{τ}-bis(*tert*-butoxycarbonyl)-*L*-histidine **5.6** in DMF in the presence of Cs_2CO_3 afforded the target compound, *tert*-butyl (*S*)-4-(3-(benzyloxy)-2-((*tert*-butoxycarbonyl)amino)-3-oxopropyl)-1*H*-imidazole-1-carboxylate **5.7** in an excellent yield of 91%. (Scheme 5.4)

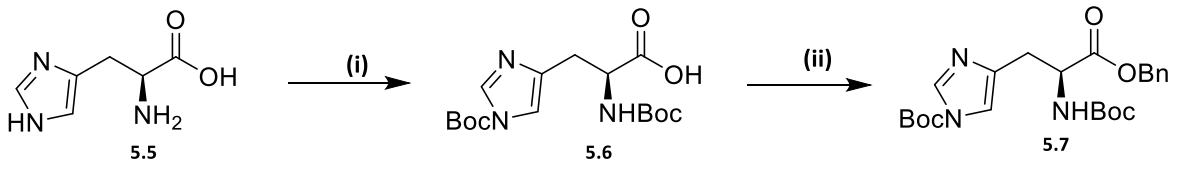

Scheme 5.4. Synthesis of *tert*-butyl *(S)*-4-(3-(benzyloxy)-2-((*tert*-butoxycarbonyl)amino)-3-oxopropyl)-1*H*-imidazole-1-carboxylate. Reagents and conditions. (i) $(Boc)_2O$ (2 eq), $NaHCO_3$, H_2O/THF (2:1), 24 hr at rt, 63%;[15] (ii) Cs_2CO_3 (1.5 eq), BnBr (1.02 eq)/DMF, 22 hr at rt, 91%.

Evidence of successful double Boc protection was provided by a proton NMR spectrum of **5.6** which revealed the presence of two singlets, one resonated at δ_H 1.61 ppm integrating for 9 protons slightly deshielded and attributed to the Boc group of the imidazole ring, while the second resonated at δ_H 1.46 ppm integrating for 9 protons assigned to the Boc on the α-amino group. The ^{13}C NMR spectrum of **5.6** revealed twelve carbon signals resonating at δ_C 173.1, 155.2, 146.2, 137.0, 136.5, 115.6, 86.4, 79.7, 52.8, 29.7, 28.4 and 27.8 ppm respectively, thus supporting the carbon skeleton of N^{α},N^{C}-bis(*tert*-butoxycarbonyl)-*L*-histidine **5.6**.

A key diagnostic signal in the ^{1}H NMR spectrum of *tert*-butyl (*S*)-4-(3-(benzyloxy)-2-((*tert*-butoxycarbonyl)amino)-3-oxopropyl)-1*H*-imidazole-1-carboxylate **5.7** was the appearance of a multiplet that resonated from δ_H 7.38 ppm to 7.27 ppm integrating for 5 protons and a methylene proton that resonated as a quartet (J = 12.3 Hz) at δ_H 5.14 ppm, thus supporting successful benzyl esterification. The ^{13}C NMR spectrum of *tert*-butyl (*S*)-4-(3-(benzyloxy)-2-((*tert*-butoxycarbonyl)amino)-3-oxopropyl)-1*H*-imidazole-1-carboxylate **5.7** recorded the correct numbers of carbon signals thus supporting the carbon skeleton identity of the target compound **5.7**. Furthermore, the EI$^+$ mass spectrum displayed the molecular ion peak at *m/z* 445.1 $[M]^+$ calculated for $C_{23}H_{31}N_3O_6$ 445.2 $[M]^+$. The fragments corresponding to the loss of one Boc and two Boc groups were also present in the spectrum at *m/z* 345.1 and 244.0 respectively, thus providing further evidence of the structure of *tert*-butyl (*S*)-4-(3-(benzyloxy)-2-((*tert*-butoxycarbonyl)amino)-3-oxopropyl)-1*H*-imidazole-1-carboxylate **5.7**.

5.4.2.2. Regioselective methylation at the *N*-3 position to yield (*S*)-4-(3-(benzyloxy)-2-((*tert*-butoxycarbonyl)amino)-3-oxopropyl)-1-(*tert*-butoxycarbonyl)-3-methyl-1*H*-imidazol-3-ium

With *tert*-butyl (*S*)-4-(3-(benzyloxy)-2-((*tert*-butoxycarbonyl)amino)-3-oxopropyl)-1*H*-imidazole-1-carboxylate **5.7** in hand, the next challenge was to attempt a regioselective methylation at the hindered *N*-3 position of the imidazole heterocyclic ring. Several conditions were investigated, initially the reaction was carried out similarly to the conditions published by Mirzahosseini *et al.*[12] Accordingly, 2.5 mol equivalents of iodomethane in methanol (at 0 °C) was utilized, but did not reveal any new product, only the starting material was recovered. Therefore alternative conditions were explored as summarized in the Table 5.1.

Parameters such as temperature, solvents, reaction time and mol equivalents of iodomethane were thoroughly investigated, unfortunately none proved to be successful.

Solvent	MeI (eq)	Temp (°C)	Time	Yield (%)[a]	Product(s) isolated
THF	1.2-3	rt	Up to 2 days	-	No reaction
THF	**3**	**60**	**2 days**	**85**	**5.9:5.10 (1:1 ratio[b])**
DMF	1.2-3	rt	Up to 2 days	-	No reaction
DMF	1.2	70	2 days	69	**5.9**:**5.10** (1.5:1 ratio[b])

[a] Isolated yield after SiO_2 gel column purification. [b] ratio determined by NMR.

Table 5.1. Methylation of *tert*-butyl (*S*)-4-(3-(benzyloxy)-2-((*tert*-butoxycarbonyl)amino)-3-oxopropyl)-1*H*-imidazole-1-carboxylate **5.7** under various reaction conditions.

The best conditions were found to be the use of 3 mol equivalents of iodomethane in THF solvent, refluxing at 60 °C for longer time up to 2 days thus affording a mixture of two isomers (**5.9** & **5.10**) inseparable by SiO_2 gel chromatography, in a good yield of 85%. (Scheme 5.5)

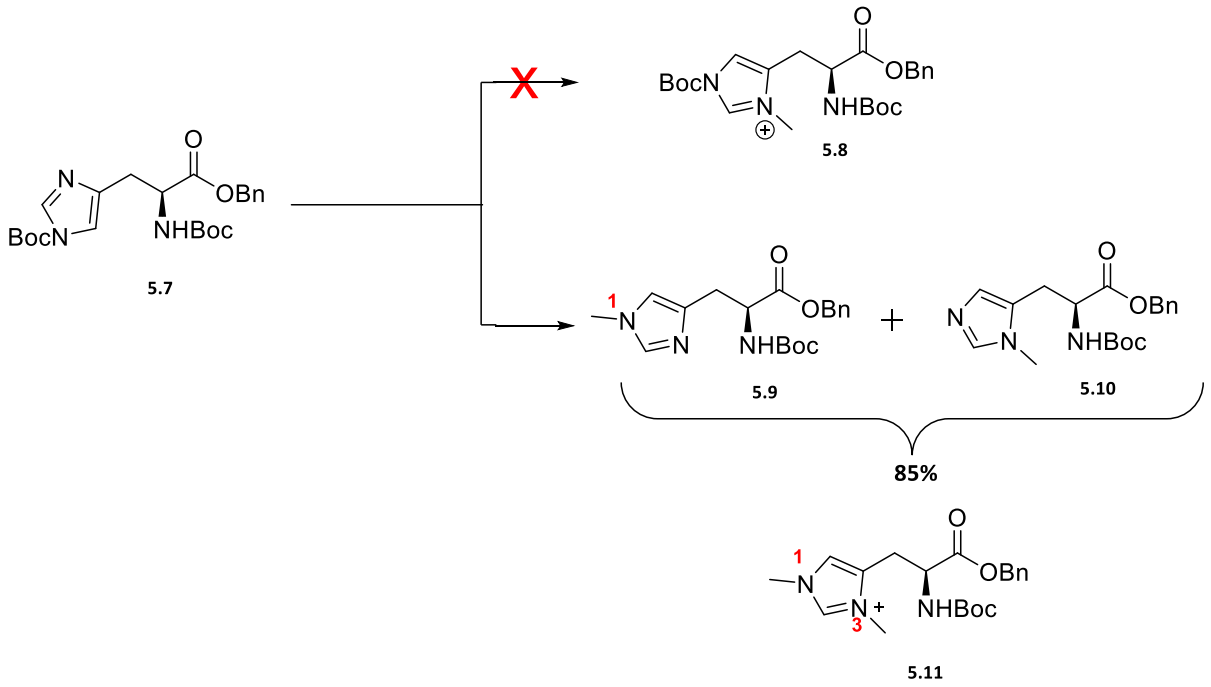

Scheme 5.5. Methylation of *tert*-butyl (*S*)-4-(3-(benzyloxy)-2-((*tert*-butoxycarbonyl)amino)-3-oxopropyl)-1*H*-imidazole-1-carboxylate 5.7. Reagents and conditions. CH_3I, THF, reflux at 60 °C, up to 2 days, 85%.

The major challenge for this reaction is the parallel Boc deprotection on the imidazole heterocyclic ring. Mirzahosseini *et al.* also reported a similar parallel Boc deprotection to the methylation when treating N^{α},N^{ζ}-bis(*tert*-butoxycarbonyl)-*L*-histidine with MeI in methanol even under milder conditions.[12]

It was therefore suspected that the labile Boc group on the imidazole ring migrated before the methylation occurred, this probably explains the fact that this reaction yields a mixture of these two isomers. It is noteworthy that TLC analysis showed an additional very polar spot

which was isolated and the NMR analysis revealed the product to be the dimethyl imidazolium salt, (*S*)-4-(3-(benzyloxy)-2-((*tert*-butoxycarbonyl)amino)-3-oxopropyl)-1,3-dimethyl-1*H*-imidazol-3-ium **5.11**, an unavoidable contamination as a large excess of iodomethane were utilized, the latter by-product was successfully removed during the purification process.

Key diagnostic signals in the ^{1}H NMR spectrum of the isolated products (**5.9** & **5.10**) were the appearance of two methyl signals resonating at δ_H 3.88 ppm and 3.85 ppm respectively, thus confirming the presence of the two regioisomers, benzyl N^{α}-(*tert*-butoxycarbonyl)-N^{τ}-methyl-*L*-histidinate **5.9** and benzyl N^{α}-(*tert*-butoxycarbonyl)-N^{π}-methyl-*L*-histidinate **5.10**, in the ratio of 1:1 based upon integration of their respective methyl peaks. The ^{1}H NMR spectrum also displayed two methylene proton signals, both resonating as doublet of doublets at δ_H 3.43 ppm and 3.29 ppm respectively. A disappearance of the *t*-Boc signal resonating at δ_H 1.61 ppm in ^{1}H NMR spectrum of *tert*-butyl (*S*)-4-(3-(benzyloxy)-2-((*tert*-butoxycarbonyl)amino)-3-oxopropyl)-1*H*-imidazole-1-carboxylate **5.7** confirmed the parallel Boc removal.

5.4.2.3. Methylation of *tert*-butyl (*S*)-4-(2-((*tert*-butoxycarbonyl)amino)-3-methoxy-3-oxopropyl)-1*H*-imidazole-1-carboxylate

Similar methylation conditions were performed on a different substrate, *tert*-butyl (*S*)-4-(2-((*tert*-butoxycarbonyl)amino)-3-methoxy-3-oxopropyl)-1*H*-imidazole-1-carboxylate **5.12** to determine the scope of this reaction.

Tert-butyl (*S*)-4-(2-((*tert*-butoxycarbonyl)amino)-3-methoxy-3-oxopropyl)-1*H*-imidazole-1-carboxylate **5.12** was treated with excess of iodomethane (2 mol equivalents) in THF solvent. TLC showed that the reaction proceeded very slowly at room temperature, even when the reaction was allowed to react for up to 2 days, only 21% of the product was recovered after silica gel chromatography since there were a lot unreacted starting material. However, the temperature was not raised hoping to avoid the formation of two regioisomers. Again, even at milder conditions, NMR analysis revealed the presence of the two regioisomers. These results suggest that the removal of the Boc group on the imidazole ring prevented the regioselective *N*-methylation of the imidazole heterocyclic ring under these reaction conditions. (Scheme 5.6)

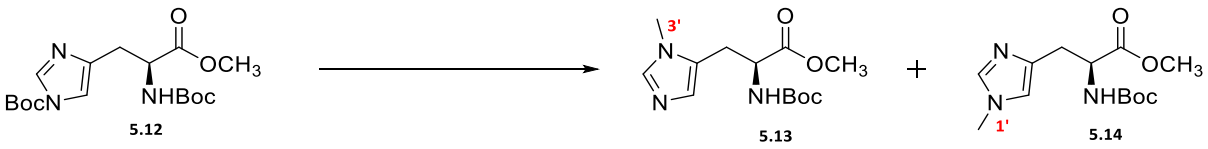

Scheme 5.6. Methylation of *tert*-butyl (S)-4-(2-((*tert*-butoxycarbonyl)amino)-3-methoxy-3-oxopropyl)-1*H*-imidazole-1-carboxylate 5.12. Reagents and conditions. MeI (2 eq), THF, rt for 2 days, 21%.

The ^{1}H NMR spectrum of the isolated product provided strong evidence of the presence of two isomers (**5.13** & **5.14**). Key diagnostic signals were the methyl protons, of which two methyl group protons resonated at δ_H 4.00 ppm and 3.96 ppm, attributed to the *N*-methyl imidazole. The other methyl proton resonating at δ_H 3.80 ppm assigned to the methyl ester group. In addition, the disappearance of singlet around δ_H 1.61 ppm confirmed the removal of Boc on the imidazole ring.

Based upon the results, it has been concluded that the Boc group was not the best protecting group to achieve selective regioselective *N*-methylation of the imidazole as it leads to a mixture of regioisomers probably due to its labile nature under the reaction conditions especially using iodomethane as the alkylating reagent.

Therefore an alternative methylating reagent as well as other bulky protecting group that are more stable under the reaction conditions were investigated.

5.4.2.4. Methylation of N^{α},N^{C}-dibenzyl-*L*-histidinate

Due to the failure of regioselective methylation at the first attempt on histidines derivatives **5.7** and **5.12,** an alternative bulky protecting group were utilised. Thus, a benzyl group which is more stable under acidic and basic conditions was utilized as a substitute for the Boc protecting group.

Histidine methyl ester hydrochloride **5.15** was benzylated at the *N*-α and *N*-1 imidazole positions in a good yield of 81%, by treatment of α-amino ester **5.15** with 2.2 molar equivalents of benzyl bromide under basic conditions (NaOH) in a mixture of H_2O:THF (1:2). (Scheme 5.7)

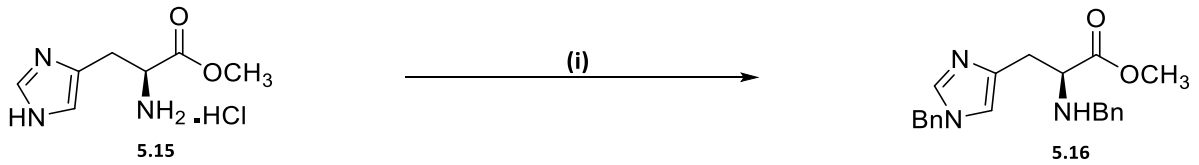

5.15 5.16

Scheme 5.7. Synthesis of methyl N^{α},N^{C}-dibenzyl-*L*-histidinate 5.16. Reagents and conditions. (i) Benzyl bromide (2.2 eq), NaOH (2.2 eq)/H_2O:THF (1:2), 24 hr at rt, 81%.

The proton NMR specctrum of methyl N^{α},N^{ζ}-dibenzyl-*L*-histidinate **5.16** revealed two signals resonating both as a multiplet, integrating for 5 protons each, from δ_H 7.30 ppm to 7.27 ppm and from δ_H 7.15 ppm to 7.08 ppm, consistent with the presence of two phenyl groups. The proton NMR spectrum of **5.16** also displayed two methylene protons, one more deshielded, resonating as a quartet (J = 14.5 Hz) at δ_H 5.43 ppm assigned to the methylene attached to the N-1' of the imidazole, and the other methylene resonating as two sets of doublets at δ_H 3.72 ppm (J = 13.7 Hz) and at δ_H 3.51 ppm (J = 13.7 Hz) assigned to the methylene on the *N*-α amino group. Thus supporting the successful double benzylation of histidine methyl ester hydrochloride **5.15**. (Figure 5.5)

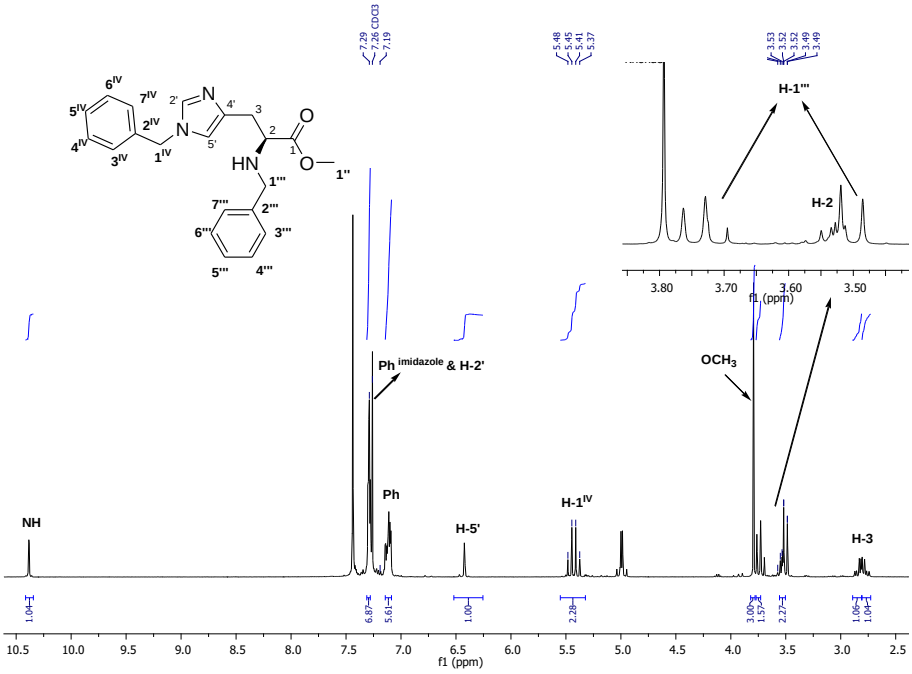

Figure 5.5. ^{1}H NMR spectrum of methyl N^{α},N^{ζ}-dibenzyl-*L*-histidinate 5.16 in $CDCl_3$ at 400 MHz.

The ^{13}C NMR spectrum of methyl N^{α},N^{ζ}-dibenzyl-*L*-histidinate **5.16** recorded the right amount of carbon signals, thirteen carbon signals resonating at δ_C 170.9, 137.7, 133.1, 132.0, 129.4,

128.7, 127.8, 119.8, 58.6, 54.9, 53.4, 51.1 and 33.5 ppm, thus confirming the carbon skeleton of N^{α},N^{ζ}-dibenzyl-*L*-histidinate **5.16**.

Finally with methyl N^{α},N^{ζ}-dibenzyl-*L*-histidinate **5.16** in hand, the regioselective methylation was attempted. Many conditions were investigated, using THF as solvent and iodomethane as alkylating reagent at 60 °C. After 2 days neither TLC nor NMR analysis did not reveal any new product and only starting material was recovered. This suggested that methyl N^{α},N^{ζ}-dibenzyl-*L*-histidinate **5.16** is highly hindered therefore the methylation at *N*-3 position of the imidazole is a difficult task. (Scheme 5.8)

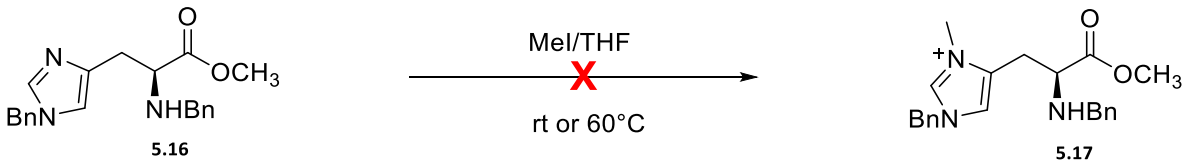

5.16 5.17

Scheme 5.8. Attempted *N*-3 regioselective methylation of methyl N^{α},N^{ζ}-dibenzyl-*L*-histidinate 5.16.

Van Den Berge *et al*. used methyl triflate, a more powerful methylating reagent than iodomethane to successfully alkylate at the hindered nitrogen of the imidazole heterocyclic ring.[14] However, the authors were unsuccessful in the attempted *N*-methylation of the very hindered *N*-sulfonyl phenyl protected imidazole. Alternative alkylating reagents such as ethyl triflate, ethyl bromoacetate, or benzyl bromide were also unsuccessful.[14] Thus suggesting that the more hindered the imidazole ring is the more challenging the *N*-methylation.

A more powerful methylating reagent, dimethyl sulfate, was subsequently considered. Finally, the regioselective *N*-methylation at the *N*-3 position of the imidazole was successfully achieved in a good yield of 72%. (*S*)-1-benzyl-4-(2-(benzylamino)-3-methoxy-3-oxopropyl)-3-

methyl-1*H*-imidazol-3-ium **5.17** was obtained by milder reacting methyl N^{α},N^{τ}-dibenzyl-*L*-histidinate **5.16** with dimethyl sulfate as alkylating reagent in anhydrous DMF. (Scheme 5.9)

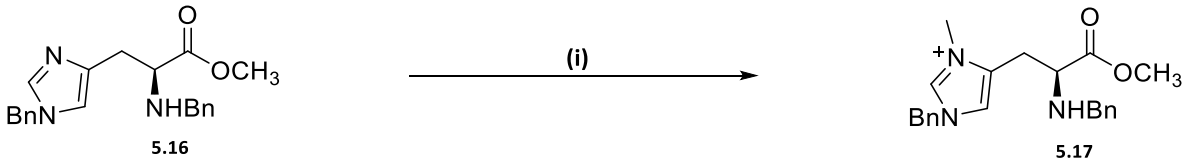

5.16 5.17

Scheme 5.9. Synthesis of (*S*)-1-benzyl-4-(2-(benzylamino)-3-methoxy-3-oxopropyl)-3-methyl-1*H*-imidazol-3-ium 5.17. Reagents and conditions. (i) Me_2SO_4, DMF, 24-48 hr at rt, 72%.

The evidence of successful regioselective methylation at *N*-3 position on the imidazole was provided by the proton NMR spectrum of (*S*)-1-benzyl-4-(2-(benzylamino)-3-methoxy-3-oxopropyl)-3-methyl-1*H*-imidazol-3-ium **5.17** which revealed the appearance of a methyl proton resonating as a singlet at δ_H 3.54 ppm deshielded due to its presence on the imidazole ring (Figure 5.6).

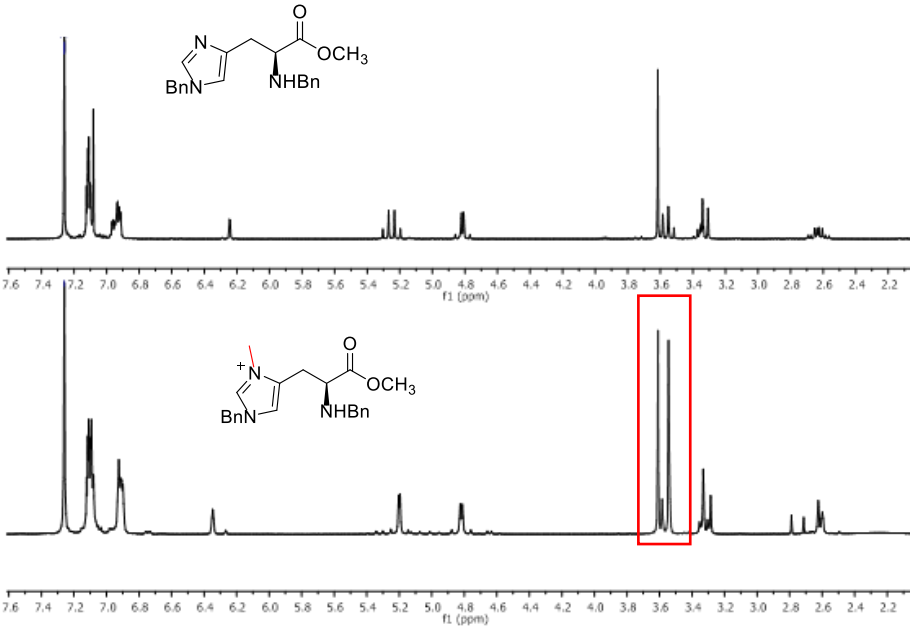

Figure 5.6. Expanded ^{1}H NMR spectrum showing successful regioselective methylation of 5.16 to yield 5.17 in $CDCl_3$ at 400 MHz.

The ^{13}C NMR spectrum of (*S*)-1-benzyl-4-(2-(benzylamino)-3-methoxy-3-oxopropyl)-3-methyl-1*H*-imidazol-3-ium **5.17** recorded the correct amount of carbon signals, resonating at δ_C 171.1, 138.3, 133.4, 132.2, 129.5, 129.0, 127.8, 120.0, 58.8, 54.9, 53.4, 51.9, 51.1 and 24.6 ppm, thus supporting the carbon skeleton of **5.17** as shown in the Figure 5.7.

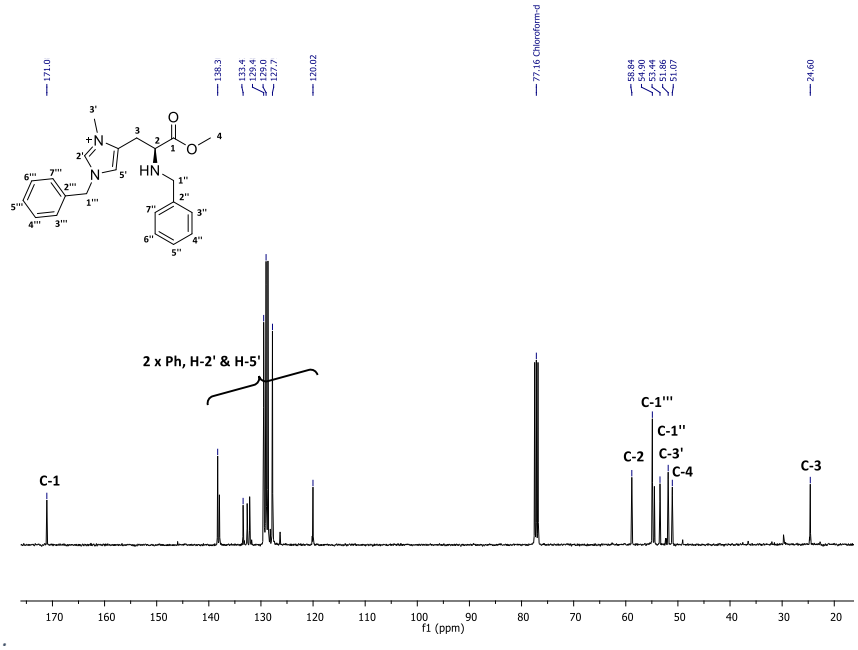

Figure 5.7. ^{13}C NMR spectrum of (*S*)-1-benzyl-4-(2-(benzylamino)-3-methoxy-3-oxopropyl)-3-methyl-1*H*-imidazol-3-ium 5.17 in $CDCl_3$ at 101 MHz.

Furthermore, two dimensional NMR, HSQC, COSY (Figure 5.8) and HMBC (Figure 5.9) were utilized for a full structural assignment.

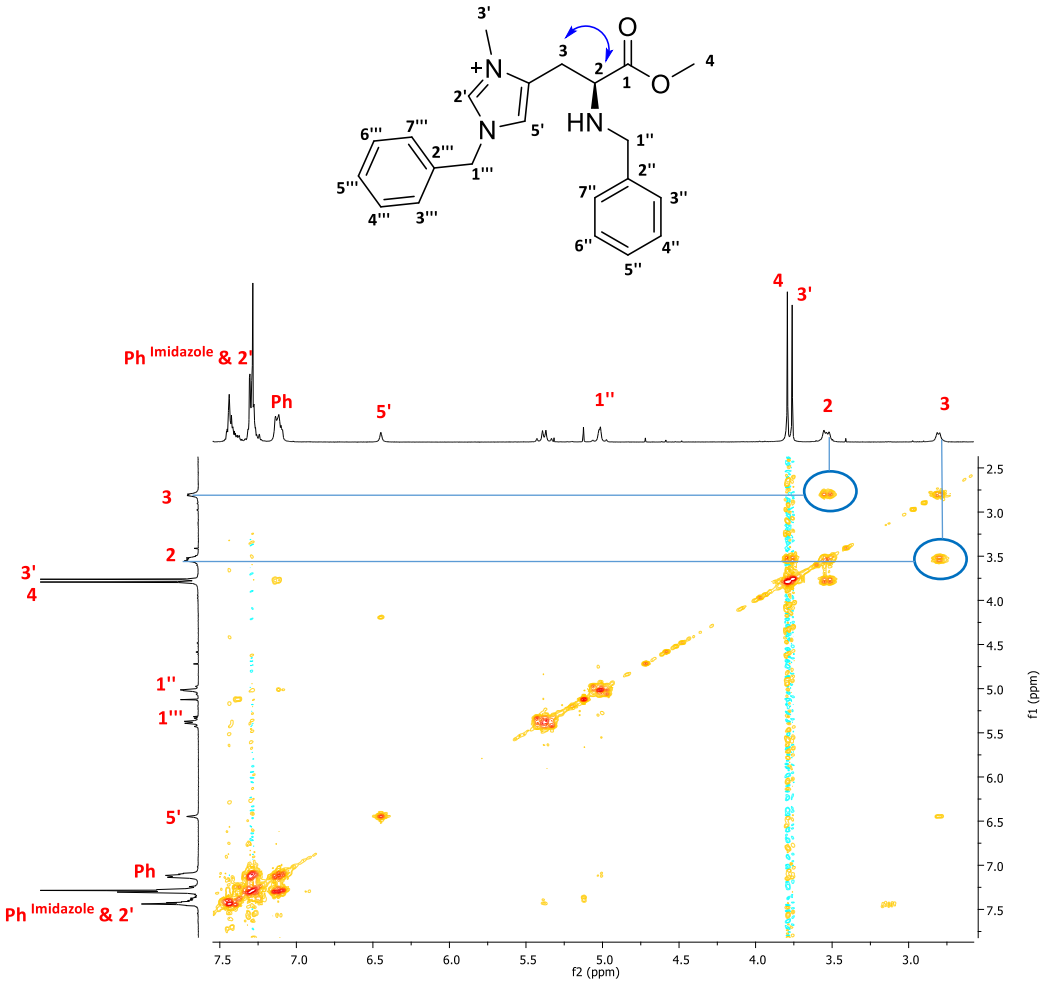

Figure 5.8. COSY-NMR spectrum of (*S*)-1-benzyl-4-(2-(benzylamino)-3-methoxy-3-oxopropyl)-3-methyl-1*H*-imidazol-3-ium 5.17 in $CDCl_3$.

2D-HMBC NMR spectrum in particular, clearly shows diagnostic ^{1}H-^{13}C correlations on the imidazole heterocyclic ring; a ^{3}J through bond coupling between the methyl protons on the nitrogen at the *N*-3' position and the C4' carbon (blue) as well as another ^{3}J through-bond coupling with the C2' carbon (red), hence unambiguously confirmed the position of the methyl at the hindered *N*-3 position of the heterocyclic imidazole ring. (Figure 5.9)

All the remaining ^{1}H-^{13}C correlations were consistent with the structure of (*S*)-1-benzyl-4-(2-(benzylamino)-3-methoxy-3-oxopropyl)-3-methyl-1*H*-imidazol-3-ium **5.17.**

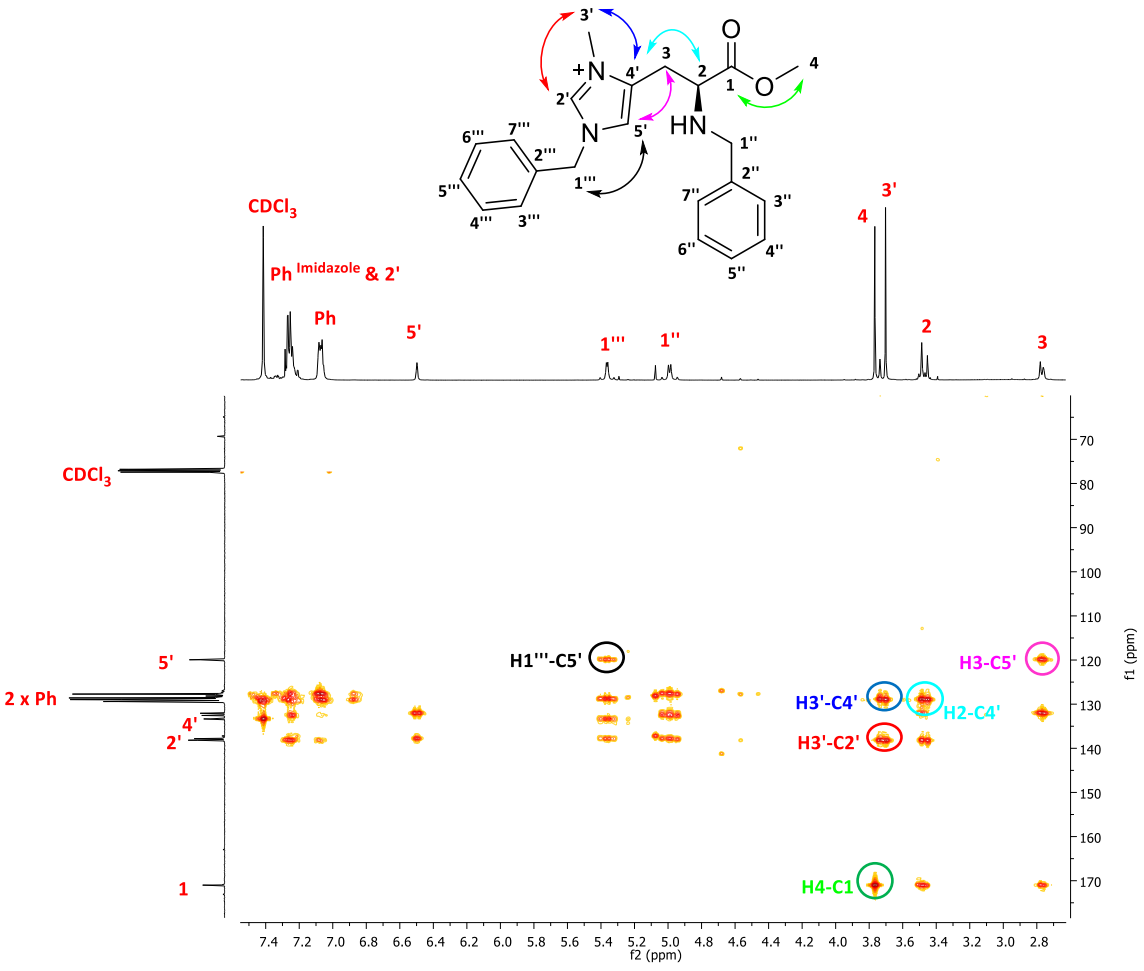

Figure 5.9. A portion expanded HMBC-NMR spectrum of (*S*)-1-benzyl-4-(2-(benzylamino)-3-methoxy-3-oxopropyl)-3-methyl-1*H*-imidazol-3-ium 5.17 in $CDCl_3$.

Finally, the EI^+ mass spectrum displayed the molecular ion peak at *m/z* 364.2 $[M]^+$ calculated for $C_{22}H_{26}N_3O_2$ 364.2 $[M]^+$ and the base peak at *m/z* 348.2 calculated for $C_{21}H_{22}N_3O_2$ 348.2 $[M\text{-}CH_3\text{-}H]^+$ corresponding to the loss one methyl and proton, thus providing further evidence of the structure of (*S*)-1-benzyl-4-(2-(benzylamino)-3-methoxy-3-oxopropyl)-3-methyl-1*H*-imidazol-3-ium **5.17**.

Having successfully synthesized (*S*)-1-benzyl-4-(2-(benzylamino)-3-methoxy-3-oxopropyl)-3-methyl-1*H*-imidazol-3-ium **5.17**, the next challenge was to attempt the regioselective bromination at the 5-position of the imidazole.

5.4.3. Bromination at the 5-position of the imidazole ring

Bromination at the 5-position of the imidazole ring of (*S*)-1-benzyl-4-(2-(benzylamino)-3-methoxy-3-oxopropyl)-3-methyl-1*H*-imidazol-3-ium **5.17**, was envisaged as achievable by treatment with mild brominating reagent, NBS in acetonitrile solvent. A slight excess of NBS (1.1 mol equivalent) was added portion wise over 5-10 min period at 5°C to minimise any possible di-brominated and poly brominated side products. After 5 hr, TLC analysis of the reaction mixture revealed the formation of a product migrating as a single new spot. The NMR analysis of the reaction mixture revealed clearly the disappearance of the proton H-5' at δ_H 6.42 ppm, thus providing further evidence of the successful bromination. Unfortunately, several attempts to isolate the brominated product **5.18** failed, as it decomposed upon either aqueous work up or SiO_2 gel chromatography.

Therefore, the crude brominated product **5.18** could be used as substrate for thionation reaction without further purification.

It is noteworthy that mechanistically the bromination does not proceed through a lactone intermediate as the carboxylic acid is not free, hence the carbonyl group could not cyclise with the imidazole ring.[16]

It is well known that halo aromatic compounds, in particular (5 or 2-bromo) imidazole derivatives do not smoothly undergo *S*-alkylation. The substitution of the bromo atom by sulfur derivative requires harsh conditions as highlighted by the work of Iddon and co-workers.[17] These authors successfully *S*-alkylated 2,4,5-tribromo-1-ethoxymethylimidazole with sodium methanethiolate in HMPA solvent at a temperature of 82 °C. However, this reaction seemed to be solvent-dependent, when HMPA was substituted by DMF the yield dropped drastically from 44% to 3%.[17]

Noteworthy, Mirzahosseini *et al*. utilized a stable surfur source, (4-tolyl) methanethiol to substitute the bromine atom of an activated imidazole ring by sulfur *via* modified Ullman reaction.[12] The authors claimed that the addition of CuI as a catalyst resulted in no reaction. Noticeably the reaction mixture turned deep purple, thus speculating the formation of a stable complex resulting from the chelation between the imidazole ring of histidine and transition metal (Cu).

Whereas Ohba *et al*. treated the activated imidazole intermediate, 4-bromo-1-methyl-1*H*-imidazole-5-carbaldehyde with either thiophenol, (4-methoxyphenyl) methanethiol or 1-naphthalenethiol under basic conditions (NaH) in DMF solvent to successfully *S*-alkylate at the 5-position of the imidazole heterocyclic ring.[11] (Figure 5.2).

Unfortunately, the removal of the *para*-methyl benzyl protecting group required the use of mercury (II) trifluoroacetate in TFA and toxic H_2S gas.[10-12] This led to unavoidable mercury contamination of the target compound, hence ovothiol is isolated as a trifluoroacetate salt. Moreover, these harsh conditions could probably lead to a racemization of the final product.

Very recently, Daunay *et al* reported an oxidative introduction of sulfur regioselectively at the 5-position of the imidazole heterocyclic ring using thioacetic acid as a sulfur source.[18] The method involved bromination of the histidine derivative bearing a free carboxylic acid group using either bromine or NBS, prior to sulfurization. The deacetylation, step of the sequence was conducted by refluxing at 90°C in water in a presence of a large excess of 3-mercaptopropionic acid (10 mol equivalents).[18] This method appeared very attractive for the completion of the total synthesis of ovothiols.

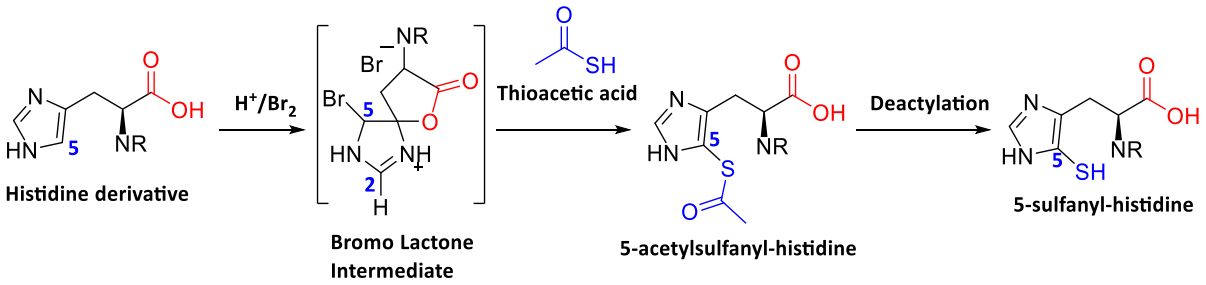

Scheme 5.10. Regioselective sulfurization at the 5-position of imidazole ring using thioacetic acid according to Daunay *et al.*[18]

However, the *S*-alkylation of the synthesized brominated product, (*S*)-1-benzyl-4-(2-(benzylamino)-3-methoxy-3-oxopropyl)-5-bromo-3-methyl-1*H*-imidazol-3-ium **5.18** using sulfur sources such as thioacetic acid, (4-methoxyphenyl) methanethiol or (4-tolyl) methanethiol was not attempted, bearing in mind that our goal was only to synthesize intermediates toward the synthesis of ovothiols while applying skills and knowledge gained during the synthesis of ergothioneine.

5.4.4. Summary

Advances toward the synthesis of ovothiol A was successfully conducted and several chemical synthetic challenges were thoroughly discussed. Successful regioselective methylation at the *N*-3 position of the imidazole heterocyclic ring was achieved using dimethyl sulfate as an alkylating reagent. The benzyl group was found to be the best protecting group for the *N*-1 atom of the imidazole ring. Bromination at the 5-position of the imidazole ring was successfully achieved, even though the brominated product **5.18** was found to be unstable upon work up or SiO_2 gel purification.

It is believed that the thionation reaction requires a stable sulfur to be achieved successfully since the *S*-alkylation of the imidazole ring is not straightforward. However, the newly published work by Daunay *et al* could be used to investigate regioselective *S*-alkylation at the 5-position of the imidazole ring. Hence, the regioselective *S*-alkylation subsequent to regioselective *N*-methylation and bromination strategy developed in this work could lead to the synthesis of ovothiols, in fewer steps, without the need of tedious purification process, more intriguingly utilizing *L*-histidine, the ovothiol's biosynthetic precursor as a simple starting material (Scheme 5.11).

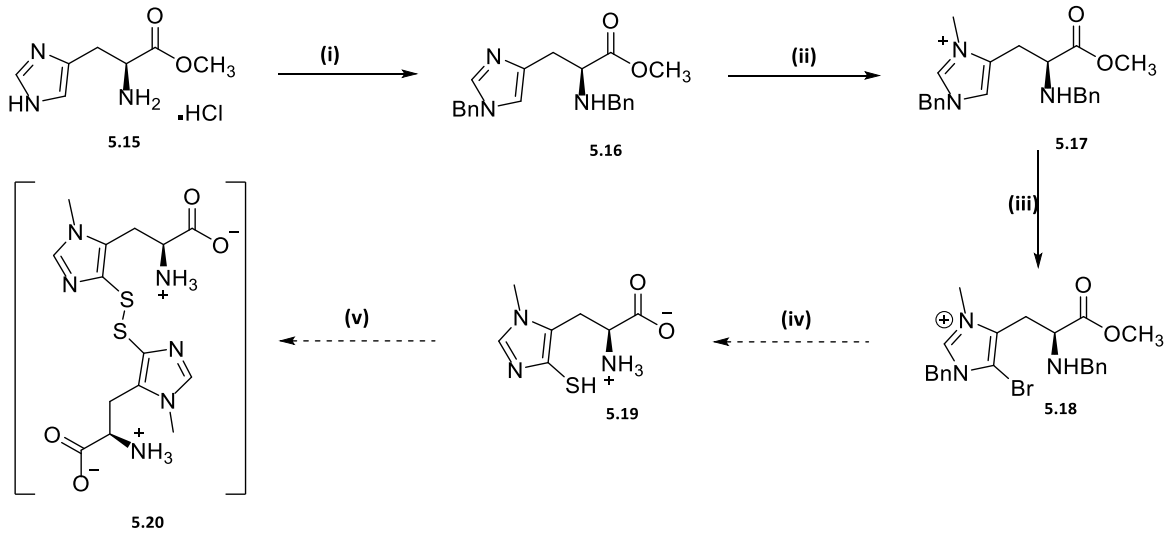

Scheme 5.11. Proposed ovothiol A synthesis route. Reagents and conditions. (i) Benzyl bromide (2.2 eq), NaOH (2.2 eq)/H_2O:THF (1:2), 24 hr at rt, 81%; (ii) Me_2SO_4, DMF, 24-48 hrs at rt, 72%; (iii) NBS, CH_3CN, 0 °C to rt (iv) thionation and benzyl deprotection (v) air (O_2), For analytical purpose ovothiol A has to be intentionally oxidized to its stable disulfide **5.20** for characterization and direct comparison with the literature.[10]

5.5. References

1 Vogt, R. N., S. C. Spies, H. S. C. & Steenkamp, D. J. The biosynthesis of ovothiol A (N^1-methyl-4-mercaptohistidine) Identification of S-(4'-L-histidyl)-L-cysteine sulfoxide as an intermediate and the products of the sulfoxide lyase reaction. *European Journal of Biochemistry* **268**, 5229–5241 (2001).

2 Eric Turner, Rachel Klevit, Lisa J. Hager & Shapiro, B. M. Ovothiols, a Family of Redox-Active Mercaptohistidine Compounds from Marine Invertebrate Eggs. *Biochemistry* **26**, 4028-4036 (1987).

3 Castellano, I. *et al.* Shedding light on ovothiol biosynthesis in marine metazoans. *Scientific reports* **6** 21506, doi:10.1038/srep21506 (2016).

4 Vamecq, J. *et al.* Potent mammalian cerebroprotection and neuronal cell death inhibition are afforded by a synthetic antioxidant analogue of marine invertebrate cell protectant ovothiols. *European Journal of Neuroscience* **17**, 1110-1120 (2003).

5 Russo, G. L., Russo, M., Castellano, I., Napolitano, A. & Palumbo, A. Ovothiol isolated from sea urchin oocytes induces autophagy in the Hep-G2 cell line. *Marine drugs* **12**, 4069-4085, doi:10.3390/md12074069 (2014).

6 Song, H. *et al.* Cysteine oxidation reactions catalyzed by a mononuclear non-heme iron enzyme (OvoA) in ovothiol biosynthesis. *Organic letters* **16**, 2122-2125, doi:10.1021/ol5005438 (2014).

7 Mashabela, G. T. & Seebeck, F. P. Substrate specificity of an oxygen dependent sulfoxide synthase in ovothiol biosynthesis. *Chemical communications* **49**, 7714-7716, doi:10.1039/c3cc42594k (2013).

8 Braunshausen, A. & Seebeck, F. P. Identification and characterization of the first ovothiol biosynthetic enzyme. *Journal of the American Chemical Society* **133**, 1757-1759, doi:10.1021/ja109378e (2011).

9 Holler, T. P. & Hopkins, P. B. Ovothiols as Free-Radical Scavengers and the Mechanism of Ovothiol-Promoted NAD(P)H-0_2 Oxidoreductase Activity. *Biochemistry* **29, No. 7**, 1953-1961 (1990).

10 Holler, T. P., Ruan, F., Spaltenstein, A. & Hopkins, P. B. Total Synthesis of Marine Mercaptohistidines: Ovothiols A, B, and C. *Journal of Organic Chemistry* **54**, 4570-4575 (1989).

11 Ohba, M., Mukaihira, T. & Fujii, T. Preparatory Study for the synthesis of the Starfish Alkaloid Imbricatine. Syntheses of 5-Arylthio-3-methyl-L-histidines. *Chemical and Pharmaceutical Bulletin* **42** 1784-1790 (1994).

12 Mirzahosseini, A., Sándor Hosztafi, S., Tóth, G. & Noszála, B. A cost-effective synthesis of enantiopure ovothiol A from L-histidine, its natural precursor. *ARKIVOC* **vii**, 1 (2014).

13 Hansena, A. L. & Kay, L. E. Measurement of histidine pKa values and tautomer populations in invisible protein states. *PNAS*, E1705–E1712, doi:10.1073/pnas.1400577111 (2014).

14 Van Den Berge, E. & Robiette, R. Development of a regioselective N-methylation of (benz)imidazoles providing the more sterically hindered isomer. *The Journal of organic chemistry* **78**, 12220-12223, doi:10.1021/jo401978b (2013).

15 Abdo, M. R. *et al.* Brucella suis histidinol dehydrogenase: synthesis and inhibition studies of a series of substituted benzylic ketones derived from histidine. *Bioorganic & medicinal chemistry* **15**, 4427-4433, doi:10.1016/j.bmc.2007.04.027 (2007).

16 Ito, S. Synthesis of 2-S-Cysteinylhistidine and 2-Mercaptohistidine via Bromo Lactone Derivative of Histidine. *Journal of Organic Chemistry* **50**, 3636-3638 (1985).

17 Iddon, B., Khan, N. & Lim, B. L. Azoles. Part 4. Nucleophilic Substitution Reactions of Halogenoimidazoles. *Journal of Chemical Society Perkin Trans. 1*, 1431-1443 (1987).

18 Daunay, S., Lebel, R., Farescour, L., Yadan, J. C. & Erdelmeier, I. Short protecting-group-free synthesis of 5-acetylsulfanyl-histidines in water: novel precursors of 5-sulfanyl-histidine and its analogues. *Organic & biomolecular chemistry* **14**, 10473-10480, doi:10.1039/c6ob01870j (2016).

Chapter 6 Conclusion

The natural thiohistidines ergothioneine and ovothiols are powerful antioxidants and the interest in them have been increasing over the last few decades. Studies conducted independently by two research groups, Steyn lab[1,2] and Sao emani and co-workers,[3] suggested that enzymes implicated in the biosynthesis of ergothioneine could act as potential anti-tuberculosis drugs target.

The increasing benefit of ergothioneine in human as well as its possible link to bacteriological disease such as tuberculosis is of interest. However, its availability is somewhat limited, isolation from natural sources is a troublesome task and the available total synthesis was hampered by many drawbacks.[4,5] This thesis described an improved synthesis of ergothioneine addressing many drawbacks of previous methods, hence achieving a good overall yield of 54-70%, while proceeding at milder conditions 25-40 °C (energy saving).[6,7]

Early ergothioneine biosynthetic pathway elucidation studies utilized radiolabelled intermediates. However, due to the safety risk associated with these radiological techniques, the stable deuterated labelled intermediates were synthetized as alternative. These stable deuterated isotopic labelled intermediates are valuable internal standards in the quantitation of pathway metabolites during external stimuli, drug treatment or metabolomics studies.

EgtE (PLP-dependent enzyme) catalysed the last step of the ergothioneine biosynthesis pathway that involves *C-S* lyase of 2-cysteinylhercynine sulfoxide to form ergothioneine.[8] The inhibition of PLP-dependent enzymes has led to discovery of many drugs in the market, one successful example is difluoromethylornithine (DFMO), an efficient drug against Human African trypanosomiasis (HAT).[9,10] This thesis describes the synthesis of the natural EgtE enzyme pathway substrate, 2-cysteinylhercynine sulfoxide and its related compounds were successfully synthesized, hence many experiments were conducted in a presence or absence of cell-free *Mycobacterium smegmatis* enzymatic preparations to better understand the *C-S* lyase mechanism. During the course of this study, an important observation was established that 2-cysteinylhercynine thioether and 2-cysteinylhercynine sulfoxide could undergo efficient *C-S* cleavage to produce ergothioneine. However, the thioether proved to be a better substrate for enzyme-free PLP mediated cleavage. Interestingly, 2-cysteinylhercynine sulfone did not produce any ergothioneine at all and was found to be inhibitor of ESH biosynthesis. 2-Cysteinylhercynine sulfoxide *in vitro* inhibits the growth of *Mycobacterium smegmatis*, hence highlighting the importance of the sulfur oxidation state and the essentiality of ergothioneine for the survival of mycobacteria. With the availability of the crystal structure of almost all ergothioneine enzymes, *in silico* design and synthesis of ergothioneine inhibitors could provide a novel class of anti-tuberculosis drugs.[11-14]

Mycobacterium tuberculosis prefers γ-glutamylcysteine over cysteine as their sulfur source to produce ergothioneine, due to the “cysteine problem”. Therefore, the first total synthesis of EgtC enzyme pathway substrate, γ-glutamylhercynylcysteine sulfoxide was successfully

conducted. Three synthetic routes were thoroughly investigated and the EgtC enzyme substrate was successfully synthesised and characterised.

Ovothiols also received a huge interest for the design of potential trypanosomal drugs. In particular, the 5-histidyl-cysteine sulfoxide synthetase (OvoA), the enzyme which catalyzes the initial step of ovothiols biosynthesis have been proposed to be a potential drug target for infective disease. Moreover, several synthesized ovothiol analogues have shown therapeutic properties in human, such as 1-methyl-2-(3-trifluoromethylphenyl)-4 mercaptoimidazole which is demonstrated to be a potent agent in mammalian cerebral protection. [15]

Lastly, this thesis describes many challenges toward the synthesis of ovothiols starting with the commercially available *L*-histidine. Regioselective *N*-methylation as well as the selective bromination on the imidazole ring were successfully achieved thus paving the way for the improved total synthesis of ovothiols. Future studies could focus on developing a strategy for the sulfurization at 5-position required to obtain ovothiols using stable sulfur sources.

The abundant stream of biology publications is indicative of the growing importance of ergothioneine worldwide. Overall, this thesis provides very important tools as well as valuable knowledge concerning natural thiohistidines synthesis. Hence, providing a platform for the future development of novel therapeutics useful as anti-tuberculosis, antitrypanosomal and anticancer drugs.

6.1. References

1 Saini, V. *et al.* Ergothioneine Maintains Redox and Bioenergetic Homeostasis Essential for Drug Susceptibility and Virulence of *Mycobacterium tuberculosis*. *Cell Reports* **14**, 572–585, doi:10.1016/j.celrep.2015.12.056 (2016).

2 Richard-Greenblatt, M. *et al.* Regulation of Ergothioneine Biosynthesis and Its Effect on *Mycobacterium tuberculosis* Growth and Infectivity. *The Journal of biological chemistry* **290**, 23064-23076, doi:10.1074/jbc.M115.648642 (2015).

3 Emani, C. S. *et al.* Ergothioneine Is a Secreted Antioxidant in *mycobacterium smegmatis*. *Antimicrobial agents and chemotherapy* **57**, 3202 (2013).

4 Miroslav Trampota. Process for the synthesis of L-(+)-ergothioneine US 7,767,826 B2 (**2010**).

5 Erdelmeier, I., Daunay, S., Lebel, R., Farescour, L. & Yadan, J.-C. Cysteine as a sustainable sulfur reagent for the protecting-group-free synthesis of sulfur-containing amino acids: biomimetic synthesis of l-ergothioneine in water. *Green Chemistry* **14**, 2256, doi:10.1039/c2gc35367a (2012).

6 Khonde, P. L. & Jardine, A. Improved synthesis of the super antioxidant, ergothioneine, and its biosynthetic pathway intermediates. *Organic & biomolecular chemistry* **13**, 1415-1419, doi:10.1039/c4ob02023e (2015).

7 Jardine, M. A. & Khonde, L. P. Process for synthesizing ergothioneine and related compounds WO 2016/046618 A1 (**2016**).

8 Seebeck, F. P. In Vitro Reconstitution of Mycobacterial Ergothioneine Biosynthesis. *Journal of American Chemical Society* **132**, 6632 (2010).

9 Meyskens, J. F. L. & Gerner, E. W. Development of Difluoromethylornithine (DFMO) as a Chemoprevention Agent. *Clinical Research Cancer* **5**, 945–951 (1999).

10 Fairlamb, A. H. Chemotherapy of human African trypanosomiasis: current and future prospects. *TRENDS in Parasitology* **19, No. 11**, 488-494, doi:10.1016/j.pt.2003.09.002 (2003).

11 Goncharenko, K. V., Vit, A., Blankenfeldt, W. & Seebeck, F. P. Structure of the sulfoxide synthase EgtB from the ergothioneine biosynthetic pathway. *Angewandte Chemie* **54**, 2821-2824, doi:10.1002/anie.201410045 (2015).

12 Vit, A., Mashabela, G. T., Blankenfeldt, W. & Seebeck, F. P. Structure of the Ergothioneine-Biosynthesis Amidohydrolase EgtC. *Chembiochem* **16**, 1490-1496, doi:10.1002/cbic.201500168 (2015).

13 Vit, A., Misson, L., Blankenfeldt, W. & Seebeck, F. P. Crystallization and preliminary X-ray analysis of the ergothioneine-biosynthetic methyltransferase EgtD. *Acta crystallographica. Section F, Structural biology communications* **70**, 676-680, doi:10.1107/S2053230X1400805X (2014).

14 Jeong, J. H., Cha, H. J., Ha, S. C., Rojviriya, C. & Kim, Y. G. Structural insights into the histidine trimethylation activity of EgtD from *Mycobacterium smegmatis*. *Biochemical and biophysical research communications* **452**, 1098-1103, doi:10.1016/j.bbrc.2014.09.058 (2014).

15 Castellano, I. *et al.* Shedding light on ovothiol biosynthesis in marine metazoans. *Scientific reports* **6** 21506, doi:10.1038/srep21506 (2016).

Chapter 7 Experimental section

7.1. Synthesis and Characterisation of Compounds

7.1.1. General Procedures

All solvents were dried by appropriate techniques and freshly distilled before use. All commercially available reagents were purchased from Sigma-Aldrich, Merck or AK Scientific and were used without further purification.

Unless otherwise stated, reactions were performed under an inert atmosphere of nitrogen in oven dried glassware and monitored by thin-layer chromatography (TLC) carried out on Merck silica gel 60-F_{254} sheets (0.2 mm layer) pre-coated plates and products visualized under UV light at 254 nm or by spraying the plate with an ethanolic solution of ninhydrin (2% v/v) followed by heating.

Normal phase column chromatography was effected by using Merck Kieselgel silica gel 60 (0.040-0.063 mm) and compounds eluted with the appropriate solvent mixtures. Reverse phase chromatography was effected by using Biotage KP-C-18-HS and compounds eluted with millipore water and AR methanol (gradient from water 100% to a mixture of water/MeOH 85:15) unless otherwise stated. All compounds were dried under vacuum before yields were determined and spectroscopy analysis performed.

Nuclear magnetic resonance spectra (^{1}H and ^{13}C) were recorded on a Varian Mercury 300 MHz (75 MHz for ^{13}C), Varian Unity 400 MHz (101 MHz for ^{13}C), a Bruker unity 400 MHz (101 MHz for ^{13}C), or a Bruker unity 600 MHz (151 MHz for ^{13}C) and were carried out in $CDCl_3$,

DMSO-d_6 and D_2O as the solvents unless otherwise stated. Chemical shifts are given in ppm relative to tetramethylsilane (TMS, δ = 0.00 ppm), which is used as internal standard. Assignments were confirmed by COSY, APT and HSQC analysis, when required. Coupling constants (*J*) are reported in Hertz (Hz). The spin multiplicities are indicated by the symbol s (singlet), d (doublet), dd (doublet of doublets), ddd (doublet of doublets of doublets), t (triplet), m (multiplet), q (quartet) and br (broad).

Optical rotations were obtained using a Perkin Elmer 141 polarimeter at 20 °C. The concentration *c* refers to g/100mL. Melting points were determined using a Reichert-Jung Thermovar hot-plate microscope and are uncorrected. Infra-Red spectra were recorded on a Perkin-Elmer FT-IR spectrometer (in cm^{-1}) from 4000 cm^{-1} to 450 cm^{-1}. The numbering scheme given for each compound is for assignment purposes only and not necessarily consistent with the IUPAC naming convention. UV-Vis studies were conducted on UV-Vis spectrophotometer Agilent technology Cary 60 and the spectrums were processed using Scan Application version 5.0.0.99 software and graphs plot using Excel 2013.

Mass spectra were recorded on a JEOL GC MATE II magnetic sector mass spectrometer (direct insertion probe-MS) and the base peaks are given, University of Cape Town.
LCMS analyses were carried out with a UHPLC Agilent 1290 Infinity Series (Germany), accurate mass spectrometer Agilent 6530 Quadrupole Time Of Flight (QTOF) equipped with an Agilent jet stream ionization source (positive ionization mode) (ESI^+) and column (Eclipse + C_{18} RRHD 1.8 µm.2.1 X 50, Agilent, Germany).

Enzymatic reactions were allowed to incubate in Nuaire incubator (DH Autoflow CO_2 Air – jarcketed Incubator), and centrifuged in Eppendorf© centrifuge (Model 5810R, Germany), Tygerberg Stellenbosch University, Cape Town, South Africa.

7.1.2. Synthesis and characterization of Compounds

_N_-benzyl _L_-histidine (2.28)

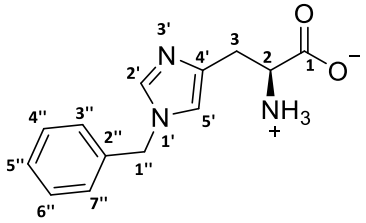

In dichloromethane (10 mL) was suspended N^{ε}-benzyl-N^{α}-(*tert*-butoxycarbonyl)-*L*-histidine **(2.27)** (750 mg, 2.17 mmol) followed by the addition of trifluoroacetic acid (1 mL) with cooling in an ice bath. The resulting homogenous solution was allowed to stir at room temperature until complete deprotection as showed by thin layer chromatography. Solvent was removed and triturated with Et2O (15 mL) and dried to afford *N*-benzyl *L*-histidine TFA salt **(2.28)** as white crystals (700 mg, 90%). Mp: 230-233 °C, (Lit. 240 °C)[10]; ^{1}H NMR (400 MHz, DMSO) δ 9.01 (s, 1H, H-2'), 7.50 (s, 1H, H-5'), 7.39 (m, 5H, Phenyl), 5.37 (s, 2H, H-1''), 4.22 (t, *J* = 7.0 Hz, 1H, H-2), 3.22 (dd, *J* = 15.6, 7.0 Hz, 1H, H-3a), 3.14 (dd, *J* = 15.6, 7.0 Hz, 1H, H-3b); ^{13}C NMR (101 MHz, DMSO) δ 170.1 (C-1), 136.3 (C-2''), 135.8 (C-2'), 130.0 (C-4'), 129.4 (C-5'' C-6''), 129.0 (C-7''), 128.6 (C-3''C-4''), 120.6 (C-5'), 51.7 (C-1''), 51.6 (C-2), 26.3 (C-3).

N^{ε}-benzyl-N^{α},N^{α}-dimethyl-*L*-histidine (2.29)[1]

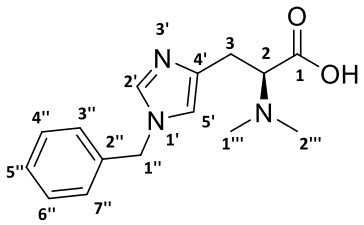

In CH_3CN (20 mL) was suspended *N*-benzyl *L*-histidine **(2.28)** (1.30 g, 5.30 mmol) followed by the addition of formaldehyde (1.2 mL, 15.5 mmol, 37%). To the resulting homogenous solution was added $NaBH(OAc)_3$ (3.20 g, 15.5 mmol) and the solution was allowed to stir at room temperature for 24 hr. Undesirable salts were filtered thought celite and the solvent evaporated to dryness, reverse phase C18 column chromatography afforded N^{ε}-benzyl-N^{α},N^{α}-dimethyl-*L*-histidine **(2.29)** as a colourless solid (1.4 g, quantitative). Mp: 70-73 °C (dec); ^{1}H NMR (300 MHz, D_2O) δ 8.73 (s, 1H, H-2'), 7.51 – 7.37 (m, 5H, Ph), 7.34 (m, 1H, H-5'), 5.35 (s, 2H, H-1''), 4.31 (dd, *J* = 9.5, 4.7 Hz, 1H, H-2), 3.48 (dd, *J* = 15.4, 4.7 Hz, 1H, H-3a), 3.39 (dd, *J* = 15.4, 9.5 Hz, 1H, H-3b), 2.96 (s, 6H, H-1''' H-2'''); ^{13}C NMR (101 MHz, D_2O) δ 168.7 (C-1), 135.2 (C-2'), 135.1 (C-2''), 133.6 (C-4'), 129.4 (C-3'' C-4''), 128.5 (C-5'' C-6''), 127.6 (C-7''), 121.0 (C-5'), 66.0 (C-2), 65.9 (C-1''), 52.9 (C-1''' C-2'''), 21.9 (C-3); LRMS (EI^+) *m/z* calculated for $C_{15}H_{19}N_3O_2$ 273.1 $[M]^+$ found 273.1 ($[M]^+$, 7%), calculated for $C_{14}H_{19}N_3$ 229.2 $[M\text{-}CO_2]^+$ found 229.1 ($[M\text{-}CO_2]^+$, 58%), calculated for $C_{12}H_{13}N_2$ $[M\text{-}H\text{-}CO_2\text{ -}N(CH_3)_2]^+$ 185.1 found 185.1 ($[M\text{-}H\text{-}CO_2\text{ –}N(CH_3)_2]^+$, 69%).

(*S*)-3-(1-benzyl-1*H*-imidazol-4-yl)-2-(trimethylammonio) propanoate (2.30)[1]

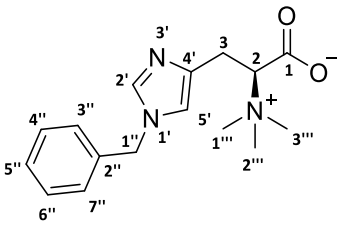

In dry tetrahydrofuran (10 mL) was added N^{ε}-benzyl-N^{α},N^{α}-dimethyl-*L*-histidine **(2.29)** (200 mg, 0.732 mmol) and MeI (50 µL, 125 mg, 0.878 mmol). The resulting solution was allowed to stir at room temperature in the dark for 1-2 days. The solvent was removed and crystallization in the absolute ethanol afforded (*S*)-3-(1-benzyl-1*H*-imidazol-4-yl)-2-(trimethylammonio) propanoate **(2.30)** as yellow solid (197 mg, 93%). Mp: 90-93 °C; ^{1}H NMR (300 MHz, D_2O) δ 8.32 (s, 1H, H-2'), 7.63 – 7.34 (m, 5H, Ph), 7.25 (s, 1H, H-5'), 5.34 (s, 2H, H-1''), 3.99 – 3.87 (m, 1H, H-2), 3.50 – 3.20 (m, 2H, H-3), 3.33 (s, 9H, H-1'''H-2'''H-3'''); ^{13}C NMR (101 MHz, D_2O) δ 170.4 (C-1), 137.1 (C-2'), 135.7 (C-2''), 132.0 (C-4'), 129.2 (C-3''C-4''), 128.7 (C-5''C-6''), 128.0 (C-7''), 119.4 (C-5'), 78.0 (C-2), 52.3 (C-1''' C-2''' C-3'''), 51.4 (C-1''), 24.8 (C-3); LRMS (ESI^+) *m/z* calculated for $C_{16}H_{22}N_3O_2^+$ 288.2 $[MH]^+$ found 288.2 ($[MH]^+$, 65%), calculated for $C_{15}H_{22}N_3^+$ 244.2 $[M\text{-}CO_2]^+$ found 244.2 ($[M\text{-}CO_2]^+$, 15%), calculated for $C_{12}H_{13}N_3$ 199.1 $[M\text{-}CO_2 –(CH_3)_3]^+$ found 199.2 ($[[M\text{-}CO_2 –(CH_3)_3]^+$; 12%).

Hercynylcysteine thioether (or 2-cysteinylhercynine thioether) (One pot synthesis) (2.19)[1]

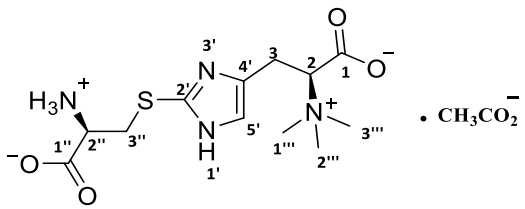

In dimethylformamide (8 mL) was dissolved (*S*)-3-(1-benzyl-1*H*-imidazol-4-yl)-2-(trimethylammonio) propanoate **(2.30)** (595 mg, 2.43 mmol) followed by the addition of *N*-bromosuccinimide (1.80 g, 6.08 mmol). The resulting solution was allowed to stir at room temperature until complete disappearance of the starting material (thin layer chromatography monitoring), the solution became red-orange indicating the successful bromination.

After successful bromination, *L*-cysteine HCl. H_2O (1.07 g, 6.08 mmol) was added in one portion and the resulting solution was allowed to stir at room temperature for 24 hr. Reverse phase chromatography C18 afforded the product, 2-cysteinylhercynine thioether **(2.19)** was isolated in the form of a yellow hygroscopic solid as acetate salt (695 mg, 76%). $[\alpha]^{20}_{D}$ = -17° (*c* = 0.5, H_2O); ^{1}H NMR (400 MHz, D_2O) δ 7.41 (m, 1H), 4.54 (dd, *J* = 7.7, 4.4 Hz, 1H, H-2''), 4.42 (t, *J* = 5.0 Hz, 1H, H-2), 3.50 (dd, *J* = 15.2, 4.4 Hz, 1H, H-3a''), 3.36 (dd, *J* = 15.2, 7.7 Hz, 1H, H-3b''), 3.19 (m, 2H, H-3), 2.80 (s, 9H, NMe_3), 2.75 (s, 3H, acetate); ^{13}C NMR (101 MHz, D_2O) δ 170.3 (C-1''), 170.0 (C-1), 129.4 (C-2'), 128.9 (C-4'), 120.9 (C-5'), 61.0 (C-2), 54.4 (C-2''), 51.7 (C-1'''C-2'''C-3'''), 36.3 (C-3''), 23.9 (C-3); HRMS (ESI^+): *m/z* 317.1284 $[M]^+$. Calculated for $C_{12}H_{21}N_4O_4S^+$ found 317.1277 $[M]^+$.

_S_-(β-amino-β-carboxyethyl)ergothioneine sulfoxide or (2_R_)-2-ammonio-3-((4-((_S_)-2-carboxylato-2-(trimethylammonio)ethyl)-1_H_-imidazol-2-yl)sulfinyl) propanoate or 2-cysteinylhercynine sulfoxide (3.8) [2]

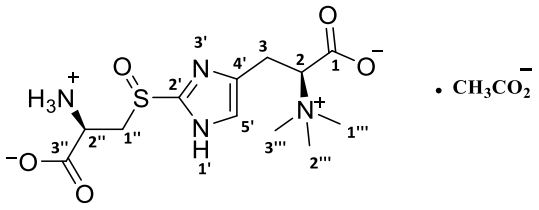

To a solution of H_2O_2 (30%, 224 mg, 6.58 mmol, 2.4 eq) were added hercynylcysteine thioether **(2.19)** (870 mg, 2.32 mmol) and para-toluene sulfonic acid (15 mg, 0.08 mmol). The resulting reaction mixture was allowed to stir at room temperature for 24 hr. At the end, the reaction mixture was lyophilised to dryness. C18 reverse phase chromatography afforded *S*-(β-amino-β-carboxyethyl) ergothioneine sulfoxide acetate salt **(3.8)** as a yellow solid (640 mg, 71%). $[\alpha]^{20}_D$ = -4° (*c* = 0.5, H_2O); ^{1}H NMR (300 MHz, D_2O) δ 8.01 (s, 1H, H-5'), 4.49 (dd, *J* = 8.6, 3.3 Hz, 1H, H-2''), 3.90 (dd, *J* = 16.1, 9.3 Hz, 1H, H-2), 3.65 (dd, *J* = 15.0, 3.3 Hz, 2H, H-1''), 3.52 (dd, *J* = 9.3, 4.9 Hz, 1H, H-3a), 3.44 (dd, *J* = 9.3, 4.9 Hz, 1H, H-3b), 2.86 (s, 9H, NMe_3), 2.79 (s, 3H, acetate); ^{13}C NMR (101 MHz, D_2O) δ 171.8 (C-3''), 170.1 (C-1), 156.6 (C-2'), 129.5 (C-4'), 125.5 (C-5'), 72.5 (C-2), 49.5 (NMe_3), 49.1 (C-1''), 43.5 (C-2''), 20.8 (C-3); HRMS (ESI^+): *m/z* 334.1311 $[MH]^+$. Calculated for $C_{12}H_{22}N_4O_5S^+$, found 334.1321 $[MH]^+$.

_S_-(β-amino-β-carboxyethyl)ergothioneine sulfone or (_R_)-2-ammonio-3-((4-((_S_)-2-carboxylato-2-(trimethylammonio)ethyl)-1_H_-imidazol-2-yl)sulfonyl) propanoate or 2-cysteinylhercynine sulfone (3.16)[1,3]

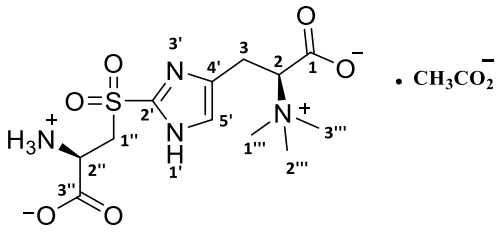

Hercynylcysteine thioether **(2.19)** (810 mg, 2.07 mmol) was added to a solution of H_2O_2 (30%, 416 mg, 12.2 mmol, 4.8 eq) and boric acid (5 mg, 0.08 mmol). The reaction mixture was allowed to stir at room temperature for 24 hr. At the end of the reaction, the solvent was evaporated under high vacuum to afford the crude product, which was purified by C18 reverse phase chromatography to afford *S*-(β-amino-β-carboxyethyl)ergothioneine sulfone acetate salt **(3.16)** as a yellow solid (545 mg, 65%). $[\alpha]^{20}_D$ = +4° (*c* = 0.5, H_2O); ^{1}H NMR (300 MHz, D_2O) δ 8.01 (s, 1H, H-5'), 4.52 (dd, *J* = 8.3, 3.1 Hz, 1H, H-2''), 3.89 (dd, *J* = 16.1, 9.3 Hz, 1H, H-2), 3.68 (dd, *J* = 15.0, 2.8 Hz, 2H, H-1''), 3.59 – 3.43 (m, 2H. H-3), 2.85 (s, 9H, NMe_3), 2.79 (s, 3H, acetate); ^{13}C NMR (101 MHz, D_2O) δ 171.7 (C-3''), 170.0 (C-1), 159.8 (C-2'), 156.6 (C-4'), 132.9 (C-5'), 64.3 (C-2), 56.7 (C-1''), 49.4 (NMe_3), 49.1 (C-2''), 34.7 (C-3); HRMS (ESI$^+$): *m/z* 349.1177 $[M]^+$. Calculated for $C_{12}H_{21}N_4O_6S^+$, found 349.1182 $[M]^+$.

_S_-(2-nitrobenzyl) ethanethioate (2.38)[4]

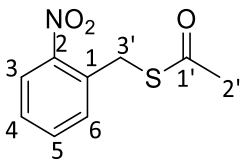

To THF (10 mL) were added potassium thioacetate (1.20 g, 9.81 mmol) and 2-nitrobenzylbromide (400 mg, 1.85 mmol) at room temperature. The resulting reaction mixture was allowed to stir overnight at room temperature. The solvent was removed under vacuum and the residue was suspended in H_2O (20 mL) and extracted with EtOAc (3 x 25 mL). Combined organic layers were dried over $MgSO_4$ and the solvent evaporated under reduced pressure to afford *S*-(2-nitrobenzyl) ethanethioate **(2.38)** as a yellow liquid (378 mg, 97%). ^{1}H NMR (300 MHz, $CDCl_3$) δ 8.02 (d, *J* = 9.4 Hz, 1H, H-3), 7.62 (d, *J* = 7.7 Hz, 1H, H-6), 7.55 (t, *J* = 6.8 Hz, 1H, H-4), 7.41 (t, *J* = 8.5 Hz, 1H, H-5), 4.41 (s, 2H, H-3'), 2.31 (s, 3H, H-2'). Proton NMR was in accordance with the one reported by Fukushima *et al*.[4]

(2-nitrophenyl)methanethiol (2.39)[4]

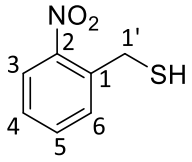

S-(2-nitrobenzyl) ethanethioate **(2.38)** (379 mg, 1.79 mmol) was dissolved in methanol (10 mL) followed by the addition of concentrated HCl (32%) (1 mL) drop wise. The resulting reaction mixture was allowed to stir overnight at 60 °C. The solvent was removed and residue suspended in 2 N HCl (10 mL). The aqueous layer was extracted with EtOAc (3 x 25 mL) and dried over Na_2SO_4 to afford (2-nitrophenyl)methanethiol **(2.39)** as a yellow solid (220 mg, 73%). Proton NMR revealed a sufficiently pure product which was used without any further purification. ^{1}H NMR (300 MHz, $CDCl_3$) δ 8.02 (d, *J* = 8.2 Hz, 1H, H-3), 7.58 (t, *J* = 7.5 Hz, 1H, H-4), 7.48 (d, *J* = 5.8 Hz, 1H, H-6), 7.36 (t, *J* = 7.7 Hz, 1H, H-5), 4.02 (d, *J* = 8.4 Hz, 2H, H-1'), 2.13

(t, J = 8.4 Hz, 1H, SH). ^{13}C NMR (101 MHz, CDCl3) δ 133.7 (C-2), 133.4 (C-3), 133.1 (C-1), 132.8 (C-5), 128.7 (C-4), 125.5 (C-6), 26.4 (C-1'). NMR data were in accordance with the literature.[4]

Ergothioneine or (*S*)-3-(2-thioxo-2,3-dihydro-1*H*-imidazol-4-yl)-2-(trimethylammonio) propanoate (2.10).

Method 1.

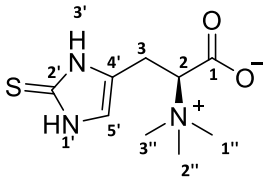

The synthesis of ergothioneine was carried out as reported by Trampota *et al.*[5] 107 mg of *L*-(+)-ergothioneine **(2.10)** was synthesized. Mp:276-279 °C literature 275-277 °C[5]; $[\alpha]^{20}_{D}$ = +138.21° (c = 1; H_2O)[5]; R_f silica gel: 0.3 (methanol/water 9:1); ^{1}H NMR (400 MHz, D_2O) δ 7.05 (s, 1H, H-5'), 3.76 (dd, *J* = 11.7, 4.0 Hz, 1H, H-2), 2.88 (m, 2H, H-3), 2.75 (s, 9H, NMe_3); ^{13}C NMR (101 MHz, D_2O) δ 177.0 (C-1), 161.2 (C-2'), 128.9 (C-4'), 103.4 (C-5'), 60.6 (C-2), 55.6 (NMe_3), 24.9 (C-3); ν_{max} (KBr)/cm^{-1} 3138s (NH) 1746s (RCOOH), 1995m (N=C-S), 1403s (C=C aromatic ring); HRMS (ESI$^+$): *m/z* 230.0963 $[M]^+$ calculated for $C_9H_{16}N_3O_2S^+$, found 230.0958 $[M]^+$.

Method 2. C-S bond cleavage of 2-cysteinylhercynine thioether (or hercynylcysteine thioether) (2.19) afforded ergothioneine

In H_2O (3 mL) were dissolved 2-cysteinylhercynine thioether **(2.19)** (48 mg, 0.15 mmol) and pyridoxal-5 phosphate (31 mg, 0.15 mmol). The reaction mixture was allowed to stir overnight at 40 °C (pH 4-5). The solvent was removed by lyophilisation; reverse phase C18 and Dowex-(H^+ form) column chromatography afforded **(2.10)** as a yellowish solid (26 mg, 76%) which

was analysed by NMR. Data demonstrated the presence of ergothioneine and was consistent with that reported in the literature.[5-7]

Method 3. Using thioacetic acid as a sulfur source [8]

In dimethylformamide (2 mL) was dissolved (*S*)-3-(1-benzyl-1*H*-imidazol-4-yl)-2-(trimethylammonio) propanoate **(2.30)** (150 mg, 0.36 mmol) followed by the addition of *N*-bromosuccinimide (141 mg, 0.792 mmol). The resulting solution was allowed to stir at room temperature until complete disappearance of the starting material (thin layer chromatography monitoring), the solution became red-orange indicating the successful bromination. After successful bromination, thioacetic acid (4-5 mol eq) was added in one portion and the resulting solution was allowed to stir at room temperature for 24 hr in the dark. DMF was removed under high vacuum and the crude residue was dissolved in MeOH (3 mL) followed by the addition of NaOMe (0.2 M), the yellow orange solution immediately discoloured to become pale yellow. The reaction mixture was allowed to stir at room temperature for 2-3 hr, the pH was adjusted to 7-8 by Amberlyte-15 (H^+ form) and the solvent removed to dryness. C18 reverse phase column chromatography was attempted to afford a product which had a small amount of desulfurized and acetylated products. The yield was calculated by integration of NMR signals (total yield of 64%).

N^{α},N^{α}-dimethyl-*L*-histidinate (3.2)

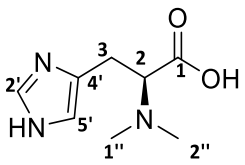

To a solution of *L*-histidine (250 mg, 1.61 mmol) and formaldehyde (37%, 0,4 mL) in H_2O (5 mL) was added $NaBH_4$ (128 mg, 3.38 mmol) portion wise with cooling in an ice water bath (0-5 °C). The reaction mixture was allowed to stir in the ice water bath for 3 hr until reaction reached completion as revealed by thin layer chromatography. Solvent was removed to dryness and the residue was purified by C18 reverse phase chromatography to yield N^{α},N^{α}-dimethyl-*L*-histidinate **(3.2)** as a white solid (293 mg, quantitative). ^{1}H NMR (300 MHz, D_2O) δ 7.70 (s, 1H, H-2'), 6.95 (s, 1H, H-5'), 3.46 (dd, *J* = 9.0, 5.8 Hz, 1H, H-2), 3.07 (dd, *J* = 14.7, 9.0 Hz, 1H, H-3a), 2.97 (dd, *J* = 14.7, 5.8 Hz, 1H, H-3b), 2.51 (s, 6H, H-1'' H-2'');^{13}C NMR (101 MHz, D_2O) δ 176.6 (C-1), 135.8 (C-2'), 133.4 (C-4'), 117.4 (C-5'), 70.9 (C-2), 41.4 (C-1'' C-2''), 27.1 (C-3); LRMS (EI$^+$) *m/z* calculated for $C_8H_{14}N_3O_2$ 184.1 found 184.0 ([MH]$^+$, 7.3%), calculated for $C_7H_{12}N_3$ 139.0 found 139.0 ([M-CO_2]$^+$, 34. 8%).

_L_-hercynine or (_S_)-1-carboxy-2-(1_H_-imidazol-4-yl)-_N,N,N_-trimethylethan-1-aminium (3.3)[9,10]

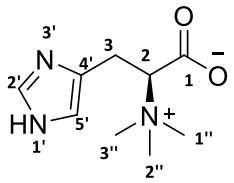

N^{α},N^{α}-dimethyl-*L*-histidinate **(3.2)** (649 mg, 3.56 mmol) was dissolved in methanol (20 mL), and the pH of the solution was adjusted to 8-9 with a concentrated solution of NH_4OH (25%, 80 µL), followed by the addition of iodomethane (700 mg, 4.93 mmol). The resultant solution was allowed to stir at room temperature for 24 hr. The solvent was evaporated to dryness to afford a crude product which was recrystallized in a mixture of warm methanol and diethyl ether to yield the iodide salt form of *L*-hercynine **(3.2)** as a white solid (489 mg, 42%). Mp:

240-242°C (with decomposition); ν_{max} KBr/cm^{-1} 3435s (N-H) 1632m (RCOOH) 1496 w (C=C Aromatic) 1335w (C-N); $[\alpha]^{20}_{D}$ = +48.7° (*c* = 0.9, 5 N HCl); ^{1}H NMR (400 MHz, D_2O) δ 7.89 (s, 1H, H-2'), 7.11 (s, 1H, H-5'), 3.98 (dd, *J* = 10.6, 4.8 Hz, 1H, H-2), 3.35 (s, 9H, H-1''H-2''H-3''), 3.40 – 3.29 (m, 2H, H-3); ^{13}C NMR (101 MHz, D_2O) δ 170.9 (C-1), 136.1 (C-2'), 131.2 (C-5'), 116.7 (C-4'), 78.4 (C-2), 52.2 (C-1''C-2''C-3''), 25.0 (C-3); LRMS (EI$^+$) *m/z* calculated for $C_9H_{16}N_3O_2^+$ 198.1 found 198.1 ([M+H]$^+$; 31.4%); calculated for $C_9H_{15}N_3O_2^+$ 197.1 found 197.1 ([M]$^+$; 53.4%); calculated for $C_6H_6N_3O_2$ 152.0 found 152.0 ([M-$(CH_3)_3$]$^+$; 100%).

_L_-Hercynine synthesis (3.3) (one pot)[11]

L-histidine (250 mg, 1.60 mmol) was dissolved in NaOH (10%, 4 mL) followed by the addition of Me_2SO_4 (0.5 mL, 626 mg, 4.96 mmol). The reaction was allowed to stir for 30 min at 0 °C and for further 30 min at room temperature. The solution was neutralized with 0.5 N HCl, and lyophilised to dryness. The residue was triturated with Et_2O and the residue purified by reverse phase C18 column chromatography to remove salts (by products) to yield *L*-hercynine **(3.3)** as white hygroscopic solid (290 mg).

Deuterated hercynine or (*S*)-3-(1*H*-imidazol-4-yl)-2-(dimethyl(methyl-*d*$_3$)ammonio) propanoate (3.4)

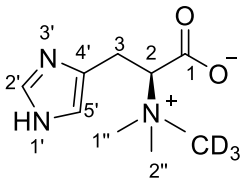

To a solution of *L*-histidine (200 mg, 1.29 mmol) in CH_3CN (10 mL) was added formaldehyde (37%, 157 mg, 145 µL, 1.93 mmol) in one portion. The solution was allowed to equilibrate to

room temperature, thereafter sodium triacetoxyborohydride (615 mg, 2.90 mmol) and acetic acid glacial (73 µL) were added while the internal temperature was maintained at 0-5°C. The resulting solution was allowed to stir at room temperature for a 18-24 hr period. The reaction was quenched by the addition of HCl (5%, 5 mL) to pH ≤ 1 and then extracted with EtOAc (5 x 20 mL). The organic layer was separated, washed with brine, dried (anhydrous $MgSO_4$) and filtered. The filtrate was evaporated under vacuum to obtain crude N^{α},N^{α}-dimethyl-*L*-histidinate **(3.2)** which was used without further purification.

Crude N^{α},N^{α}-dimethyl-*L*-histidinate **(3.2)** (374 mg, 2.02 mmol) was dissolved in MeOH (5 mL), the solution adjusted to pH 9-10 with concentrated ammonia (25%), followed by the addition of iodomethane-d_3 (489 mg, 3.03 mmol). The solution was allowed to stir at room temperature for 24 hr. The solvent was evaporated under high vacuum to dryness. Reverse phase chromatography (C18) and recrystallization in a mixture of warm EtOH/H_2O afforded deuterated hercynine **(3.4)** as a yellow solid (249 mg, 61%). Mp: 142-145 °C (dec); ^{1}H NMR (300 MHz, D_2O) δ 7.84 (s, 1H, H-2'), 7.12 (s, 4H, H- H-5'), 4.01 (dd, *J* = 10.6, 4.7 Hz, 1H, H-2), 3.38 (s, 6H, H-1'' H-2''), 3.39 – 3.36 (m, 2H, H-3); HRMS (ESI$^+$): *m/z* 201.1431 $[M]^+$. Calculated for $C_9H_{13}D_3N_3O_2^+$ found 201.1414 $[M]^+$.

Mecaptohistidine or (*S*)-2-amino-3-(2-mercapto-1*H*-imidazol-4-yl) propanoic acid (3.5)

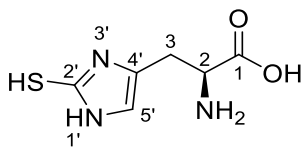

The synthesis of mercaptohistidine **(3.5)** was carried out as reported by Trampota *et al.*[5] Mercaptohistidine **(3.5)** was isolated as a white powder (2.01 g, 88%). Mp: 206-208°C (with

decomposition) literature 204-206°C (with decomposition)[5]; ν_{max} (KBr)/cm^{-1} 3465s + 1634s + 1129w (RNH_2 Free) 2073s (N=C-S) 1383m ($RCOO^-$); ^{1}H NMR (400 MHz, D_2O+DCl) δ 6.87 (s, 1H, H-5'), 4.31 (t, *J* = 6.6 Hz, 1H, H-2), 3.28 (dd, *J* = 16.1, 6.6 Hz, 1H, H-3a), 3.17 (dd, *J* = 16.1, 6.6 Hz, 1H, H-3b), Carboxylic acid and amine protons signals were exchanged with D_2O; ^{13}C NMR (101 MHz, D_2O) δ 170.5 (C-1), 156.6 (C-2'), 123.3 (C-4'), 116.1 (C-5'), 51.9 (C-2), 25.4 (C-3); LRMS (EI^+) *m/z* calculated for $C_6H_9N_3O_2S$ $[M]^+$ 187.0 found 187.0 ($[M]^+$; 92.7%).

(*S*)-3-(2-(*tert*-butylthio)-1*H*-imidazol-4-yl)-2-(dimethylamino) propanoic acid (3.6)[5]

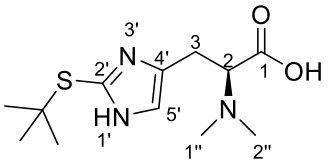

Step 1.

To a solution of mercaptohistidine **(3.5)** (2.27 g, 12.1 mmol) and *t*-butanol (2.34 g, 31.5 mmol) in distilled H_2O (18 mL) was added concentrated hydrochloric acid (4 mL, 37%) at room temperature. The resulting reaction mixture was heated to 85-90 °C and kept at this temperature for a 3-4 hr period. Subsequently, the reaction mixture was concentrated by lyophilisation. The free amino acid was liberated by adjusting the pH of the solution to 5.0 with aqueous sodium acetate, followed by lyophilisation to dryness, whereafter the amino acid was extracted with warm 2-propanol. After evaporation of the solvent, the product (*S*)-2-amino-3-(2-(*tert*-butylthio)-1*H*-imidazol-4-yl) propanoic acid was obtained as yellow crystals (1.85 g, 62.7%). $[\alpha]^{20}_D$ = +14.1° (*c* = 0.7, H_2O) lit.$[\alpha]^{25}_D$ = +13° (*c* = 1, H_2O)[5]; ν_{max} (KBr)/cm^{-1} 3448s + 1561s + 1051w (RNH_2 Free) 2237w (N=C-S) 1703m (RCOOH) 1337m (CH_3) 643 (S-R); ^{1}H NMR (400 MHz, D_2O) δ 7.60 (brs, 1H, H-5'), 4.18 (t, *J* = 3.0 Hz, 1H, H-2), 3.39 (dd,

J = 11.0, 3.0 Hz, 1H, H-3a), 3.30 (dd, *J* = 11.0, 3.0 Hz, 1H, H-3b), 1.44 (s, 9H, *t*-butyl); LRMS (EI^+) *m/z* calculated for $C_{10}H_{17}N_3O_2S$ 243.1 $[M]^+$ found 243.1 ($[M]^+$; 4.2%), 199.1 ($[M–CO_2]^+$; 7.1 %), 142.0 ($[M–CO_2–C(CH_3)_3]^+$; 4.2%).

Step 2

In a solution of THF (19 mL) was dissolved (*S*)-2-amino-3-(2-(*tert*-butylthio)-1*H*-imidazol-4-yl) propanoic acid (1.57 g, 6.45 mmol) followed by the addition of formalin (37%, 2.04 g, 25.1 mmol) portion wise. The resulting mixture was allowed to equilibrate to room temperature and then sodium triacetoxyborohydride (3.76 g, 17.7 mmol) was added while the reaction temperature was maintained at 0-5°C. The resulting suspension was allowed to stir at 10 °C for 6-8 hr. The reaction mixture was cooled to -10 °C, and acidified with 2 N HCl (pH ≤1). The resulting solution was lyophilised and the residue was mixed with 13 mL methanol followed by filtration of the undesired inorganic salts. The filtrate was lyophilised to yield the dihydrochloride salt. The free amine was liberated by triturating with aqueous sodium acetate to pH 5.0, and extraction into 2-propanol, from where it was crystallized. The product (*S*)-3-(2-(*tert*-butylthio)-1*H*-imidazol-4-yl)-2-(dimethylamino) propanoic acid **(3.6)** was obtained as colourless crystals (590 mg, 34%). ^{1}H NMR (300 MHz, D_2O) δ 6.30 (s, 1H, H-5'), 3.45 (d, *J* = 10.7 Hz, 1H, H-2), 3.08 (m, 2H, H-3), 3.01 (s, 6H, H-1'' H-2''), 1.50 (s, 9H, *t*-butyl).

Deuterated ergothioneine or (*S*)-2-(dimethyl(methyl-d_3)ammonio)-3-(2-thioxo-2,3-dihydro-1*H*-imidazol-4-yl) propanoate (3.7)

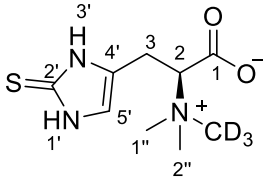

(*S*)-3-(2-(*tert*-butylthio)-1*H*-imidazol-4-yl)-2-(dimethylamino) propanoic acid **(3.6)** (110 mg, 0.405 mmol) was dissolved in MeOH (3 mL) and the pH was adjusted to 8.8-9.0 with ammonium hydroxide, followed by the addition of iodomethane-d_3 (70 mg, 0.61 mmol) and the solution was allowed to stir at room temperature for 24 h. The mixture was concentrated under vacuum and the resulting white solid (ammonium chloride) was filtered and the cake was washed with methanol. The combined filtrates were evaporated to dryness to afford a crude, *S*-(*tert*-butyl) ergothioneine-d_3. In the presence of 2-mercaptopropionic acid (1.70 g; 16.1 mmol), crude *S*-(*tert*-butyl) ergothioneine-d_3 was dissolved in 2 mL H_2O followed by the addition of HCl (1 mL, 32%). The resulting mixture was refluxed for 21 hr. After cooling the reaction mixture was extracted with EtOAc (3 x 15 mL) and then the aqueous layer was adjusted to pH 7 with a solution of ammonia (25% v/v) followed by lyophilisation. The residue was again extracted with EtOAc (3 x 20 mL) followed by partitioning in a mixture of distilled water: EtOAc 50:50 (v/v). The aqueous layer was retained and the organic phase discarded. The aqueous phase was lyophilised to dryness. Purification by reverse phase chromatography (C18) and recrystallization afforded (*S*)-2-(dimethyl(methyl-d_3)ammonio)-3-(2-thioxo-2,3-dihydro-1*H*-imidazol-4-yl) propanoate **(3.7)** as a yellow solid (93 mg, quantitative). Mp:158-160 °C (dec); ^{1}H NMR (400 MHz, D_2O) δ 6.95 (s, 1H, H-5'), 4.34 – 4.13 (m, 1H, H-2), 3.41 (dd, *J*

= 11.3, 8.5 Hz, 2H, H-3), 3.39 (s, 6H, H-1'' H-2''); ^{13}C NMR (101 MHz, D_2O) δ 180.3 (C-1), 134.9 (C-2'), 119.1 (C-4'), 115.8 (C-5'), 75.5 (C-2), 52.5 (C-1'' C-2'' C-3''), 22.7 (C-3); HRMS (ESI$^+$): *m/z* 233.1152 [M]$^+$. Calculated for $C_9H_{13}D_3N_3O_2S^+$, found 233.1160 [M]$^+$.

Benzyl *O*-(*tert*-butyldimethylsilyl)-*L*-serinate (4.8)

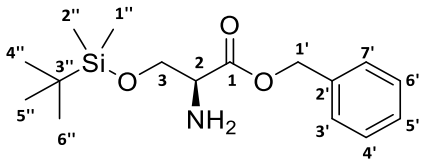

To a suspension of *L*-serine benzyl ester hydrochloride **(4.7)** (1.00 g, 4.31 mmol) and TBDMSCl (0.68 g, 4.53 mmol) in CH_3CN (130 mL), was added DBU (1.31 g, 1.30 mL, 8.63 mmol) with cooling at 0 °C. The resulting homogenous solution was allowed to stir overnight at room temperature. The solvent was evaporated in under vacuum, the residue was suspended in H_2O (15 mL) and the aqueous phase extracted with EtOAc (3 × 20 mL). The combined organic layers were dried over $MgSO_4$ and evaporated to dryness to afford benzyl O-(*tert*-butyldimethylsilyl)-*L*-serinate **(4.8)** as a yellowish oil (1.34 g, 99.9%). The NMR analysis showed a pure compound which was used in the next step without any further purification. For analytical purposes, a sample was purified by flash chromatography (hexane/EtOAc 5:1 to 1:5); ^{1}H NMR (400 MHz, $CDCl_3$) δ 7.43-7.26 (m, 5H, Ph), 5.19 (d, *J* = 1.7 Hz, 2H, H-1'), 3.98 (dd, *J* = 9.7, 4.2 Hz, 1H, H-3a), 3.84 (dd, *J* = 9.7, 3.8 Hz, 1H, H-3b), 3.57 (t, *J* = 3.8 Hz, 1H, H-2), 1.76 (br.s, 2H, NH), 0.88 (s, 9H, H-4''H-5''H-6''), 0.06 (s, 3H, H-2''), 0.03 (s, 3H, H-1''); ^{13}C NMR (101 MHz, $CDCl_3$) δ 174.0 (C-1), 135.8 (C-2'), 128.6 (C-3'C-7'), 128.3 (C-4'C-5'C-6'), 66.7 (C-1'), 65.4 (C-2), 56.7 (C-3), 25.8 (C-4''C-5''C-6''), 18.2 (C-3''), -5.6 (C-1''), -5.5 (C-2''); LRMS (EI$^+$) didn't

display the molecular ion but fragment at *m/z* calculated for $C_8H_{20}NOSi$ [M–COOBn] (174.1) found 174.0 ([M–COOBn]$^+$; 37.5%).

(*S*)-5-(benzyloxy)-4-((*tert*-butoxycarbonyl)amino)-5-oxopentanoic acid (4.10)

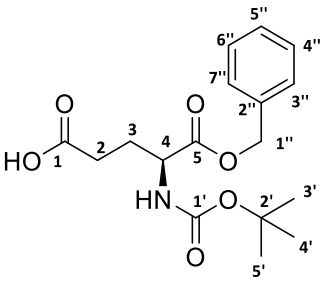

L-Glutamic benzyl ester **(4.9)** (150 mg, 0.632 mmol) was dissolved in a mixture of H_2O:dioxane (2:1, 12 mL) followed by the addition of Et_3N (88 µL, 64 mg, 0.63 mmol). The resulting homogeneous solution was cooled to 0 °C and $(Boc)_2O$ (152 mg, 0.696 mmol) was added portion wise. The reaction mixture was allowed to stir overnight at room temperature. The solvent was removed under vacuum, and the residue partitioned between EtOAc:H_2O (1:1, 50 mL). The aqueous phase was extracted with EtOAc (4 x 15 mL), the combined organic layers washed with brine (20 mL), dried over Na_2SO_4 and the solvent was evaporated to afford crude (*S*)-5-(benzyloxy)-4-(*tert*-butoxycarbonylamino)-5-oxopentanoic **(4.10)** as a yellowish oil (213 mg, quantitative). For analytical purposes, a small amount was purified by flash SiO_2 column chromatography (CH_2Cl_2 100; CH_2Cl_2:MeOH 80:20). ^{1}H NMR (300 MHz, $CDCl_3$) δ 7.44 – 7.31 (m, 5H, Ph), 5.20 (d, *J* = 2.1 Hz, 2H, H-1''), 4.64 (dd, *J* = 9.4, 2.9 Hz, 1H, H-4), 2.72 – 2.42 (m, 2H, H-2), 2.30 (ddd, *J* = 19.6, 13.2, 9.4 Hz, 1H, H-3a), 2.01 (ddt, *J* = 13.2, 9.4, 3.3 Hz, 1H, H-3b), 1.42 (s, 9H, Boc); ^{13}C NMR (75 MHz, $CDCl_3$) δ 173.2 (C-1), 171.2 (C-5), 149.3 (C-1'), 135.1 (C-2''), 128.7 (C-3'' C-7''), 128.6 (C-5''), 128.5 (C-4'' C-6''), 83.6 (C-2'), 67.1 (C-1''), 59.0 (C-4), 31.1 (C-

2), 27.8 (C-3'C-4'C-5'), 21.3 (C-3); LRMS (EI$^+$) *m/z* calculated for $C_{17}H_{23}NNaO_6$ 360.1 found 360.0 ([M+Na]$^+$; 20.0%), 238.1 ([MH–Boc]$^+$; 100.0%).

Benzyl *N*^{5}-((*S*)-1-(benzyloxy)-3-((*tert*-butyldimethylsilyl)oxy)-1-oxopropan-2-yl)-*N*^{2}-(*tert*-butoxycarbonyl)-*L*-glutaminate (4.11)

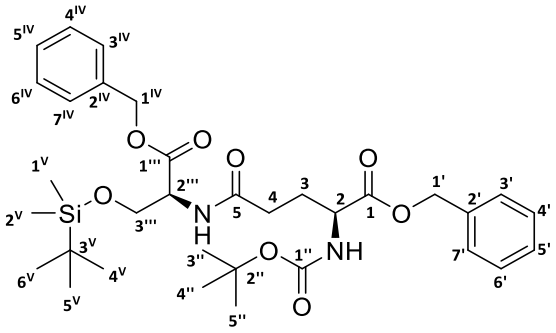

(*S*)-5-(Benzyloxy)-4-(*tert*-butoxycarbonylamino)-5-oxopentanoic acid **(4.10)** (169 mg, 0.500 mmol) was dissolved in a dry DCM (6 mL) followed by the addition of EDCI.HCl (105 mg, 0.55 mmol), HOBt (74 mg, 0.55 mmol) and DIPEA (65 mg, 88 µL, 0.55 mmol) while the internal temperature was maintained to 0 °C using an ice water bath. After 10 min, benzyl O-(*tert*-butyldimethylsilyl)-*L*-serinate **(4.8)** (186 mg, 0.60 mmol) was added with cooling at 0 °C. The resulting reaction mixture was allowed to stir at room temperature for 24 hr and monitored by TLC. The solvent was removed to dryness and the residue was partitioned into H_2O:EtOAc (1:2, 50 mL). The aqueous layer was extracted with EtOAc (4 x 15 mL), the combined organic layers were washed with brine (20 mL), dried over Na_2SO_4 and evaporated to dryness to afford a crude product as a yellow oil. Flash SiO_2 column chromatography (CH_2Cl_2 100, CH_2Cl_2:MeOH, 80:20) afforded benzyl *N*^{5}-((*S*)-1-(benzyloxy)-3-((*tert*-butyldimethylsilyl)oxy)-1-oxopropan-2-yl)-*N*^{2}-(*tert*-butoxycarbonyl)-*L*-glutaminate as a yellowish oil (270 mg; 86%). ^{1}H NMR (400 MHz, $CDCl_3$) δ 7.31 – 7.27 (m, 10H), 5.27 – 5.06 (m, 4H), 4.34 – 4.21 (m, 1H), 4.11 (dd, *J* = 10.1,

2.6 Hz, 1H), 3.96 (dd, *J* = 10.1, 2.6 Hz, 1H), 3.87 – 3.79 (m, 1H), 2.61 – 2.37 (m, 1H), 2.16 (ddd, *J* = 19.8, 12.8, 7.3 Hz, 1H), 2.03 – 1.81 (m, 2H), 1.43 (s, 9H), 0.85 (s, 9H), 0.09 – -0.04 (m, 6H). ^{13}C NMR (101 MHz, $CDCl_3$) δ 173.1 (C-5), 171.4 (C-1), 171.1 (C-1'''), 156.5 (C-1''), 135.6 (C-2'), 135.3 (C-2^{IV}), 128.6 (4C, meta), 128.4 (4C, ortho), 128.3 (C-5'), 128.2 (C-5^{IV}), 67.3 (C-1'), 67.2 (C-1^{IV}), 64.2 (C-2''), 63.3 (C-2'''), 56.2 (C-2), 54.42 (C-4), 30.4 (C-3), 28.3 (3C-Boc), 25.6 (3C, C-4^{V}, 5^{V} & 6^{V}), 18.2 (C-3^{V}), -5.7 (C-1^{V}), -5.5 (C-2^{V}); LRMS (EI$^+$) *m/z* calculated for $C_{33}H_{48}N_2NaO_8Si$ 651.3 found 651.2 ([M+Na]$^+$; 30.0%), 529.2 ([MH–Boc]$^+$; 100.0%).

Benzyl N^5-((*S*)-1-(benzyloxy)-3-hydroxy-1-oxopropan-2-yl)-N^2-(*tert*-butoxycarbonyl)-*L*-glutaminate (4.12)

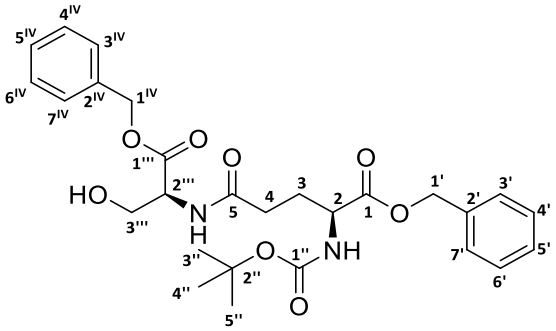

In dry THF (5 mL) was dissolved benzyl N^5-((*S*)-1-(benzyloxy)-3-((*tert*-butyldimethylsilyl)oxy)-1-oxopropan-2-yl)-N^2-(*tert*-butoxycarbonyl)-*L*-glutaminate **(4.11)** (200 mg, 0.320 mmol) followed by the addition TBAF (1 M in THF, 0.35 mmol) drop wise. The resulting reaction mixture was allowed to stir at room temperature for 5 - 10 hr (TLC monitoring). Solvent was removed to dryness, the residue was dissolved in EtOAc (25 mL) and washed with water (10 mL), brine (10 mL) and dried over Na_2SO_4 to afford crude product which was purified successively by SiO_2 (gradient CH_2Cl_2 100% to CH_2Cl_2/MeOH 80:20) and Amberlyte 15 ion exchange (H^+-form) (to trap unreacted TBAF) chromatography to yield pure product **(4.11)** as

a yellow oil (98 mg, 59%); ^{1}H NMR (400 MHz, $CDCl_3$) δ 7.39 – 7.30 (m, 10H), 5.24 – 5.04 (m, 4H, H-1' H-1^{IV}), 4.43 – 4.18 (m, 2H, H-3'''), 3.61 (t, *J* = 4.9 Hz, 1H, H-2), 3.44 (t, *J* = 6.6 Hz, 1H, H-2'''), 2.58 – 2.36 (m, 2H, H-3), 2.30 – 2.14 (m, 1H, H-4a), 2.07 – 1.87 (m, 1H, H-4b), 1.44 (s, 9H, Boc); ^{13}C NMR (101 MHz, $CDCl_3$) δ 169.8 (C-5), 153.6 (C-1), 153.5 (C-1'''), 153.0 (C-1''), 135.7 (2C, C-2' C-2^{IV}), 128.6 (2C, C-4' C-6'), 128.5 (2C, C-4^{IV} C-6^{IV}), 128.3 (2C, C-3' C-7'), 128.2 (2C, C-3^{IV} C-7^{IV}), 125.5 (2C, C-5' C-5^{IV}), 82.2 (C-2''), 71.2 (C-1'), 68.7 (C-1^{IV}), 66.4 (C-3'''), 59.4 (C-2'''), 53.2 (C-2), 31.7 (C-4), 27.8 (3C, C-3'' C-4'' C-5''), 19.2 (C-3); LRMS (EI^{+}) didn't display the molecular ion but fragment at *m/z* calculated for $C_{15}H_{16}N_2O_6$ [M – Bn – Boc –2H]$^{+}$ (320.1) found 320.1 ([M – Bn – Boc –2H]$^{+}$; 8.1%).

Benzyl *N*^{5}-((*S*)-1-(benzyloxy)-3-chloro-1-oxopropan-2-yl)-*N*^{2}-(*tert*-butoxycarbonyl)-*L*-glutaminate (4.13)

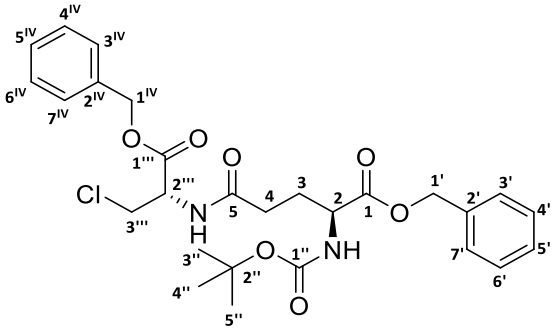

2, 4, 6-Trichloro-[1, 3, 5] triazine (56 mg, 0.11 mmol) was added portion wise in DMF (1 mL) while the internal temperature was maintained at 25 °C. After the formation of a white solid, the reaction was monitored (TLC) until complete disappearance of 2, 4, 6-trichloro-[1, 3, 5] triazine. Two hours later, benzyl *N*^{5}-((*S*)-1-(benzyloxy)-3-hydroxy-1-oxopropan-2-yl)-*N*^{2}-(*tert*-butoxycarbonyl)-*L*-glutaminate **(4.12)** (56 mg, 0.11 mmol) in CH_2Cl_2 (5 mL) was added in one portion. The resulting mixture was allowed to stir at room temperature for 21 hr. The reaction

mixture was quenched by the addition of water (10 mL). The aqueous layer was extracted with EtOAc (3 x 15 mL) and the combined organic layers were washed successively with saturated aqueous sodium carbonate (10 mL) and brine (10 mL), dried over Na_2SO_4, filtered and concentrated under vacuum to yield benzyl N^5-((*S*)-1-(benzyloxy)-3-chloro-1-oxopropan-2-yl)-N^2-(*tert*-butoxycarbonyl)-*L*-glutaminate **(4.13)** as a yellow oil (49 mg, 83%). ^{1}H NMR (400 MHz, $CDCl_3$) δ 7.26 (s, 10H, **Ph**), 5.21 – 5.09 (m, 4H, H-1' H-1^{IV}), 4.31 (dd, *J* = 7.4, 3.6 Hz, 1H, H-3a"'), 4.29 – 4.26 (m, 1H, H-3b"'), 3.67 – 3.59 (m, 1H, H-2), 3.46 (ddd, *J* = 6.6, 5.7, 2.4 Hz, 1H, H-2"'), 2.58 – 2.24 (m, 2H, H-3), 2.21 – 1.87 (m, 2H, H-4), 1.46 (s, 9H, Boc). LRMS (EI$^+$) *m/z* calculated for $C_{27}H_{33}{}^{35}ClN_2O_7$ 532.2 found 532.1 ([^{35}M]$^+$, 14.5%), calculated for $C_{27}H_{33}{}^{37}ClN_2O_7$ 534.2 found 534.0 ([^{37}M]$^+$, 4.8%); calculated for $C_{22}H_{24}{}^{35}ClN_2O_5$ 431.1 found 431.1 ([^{35}M-Boc]$^+$, 61.9%), calculated for $C_{22}H_{24}{}^{37}ClN_2O_5$ 433.1 found 433.1 ([^{37}M-Boc]$^+$, 20.2%).

***N*^{5}-*((S)*-1-carboxy-2-hydroxyethyl)-*L*-glutamine (4.14)**

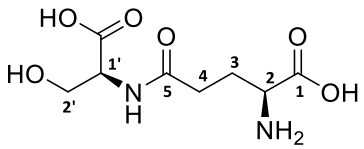

In MeOH (3 mL) were added benzyl N^5-((*S*)-1-(benzyloxy)-3-hydroxy-1-oxopropan-2-yl)-N^2-(*tert*-butoxycarbonyl)-*L*-glutaminate **(4.12)** (47 mg, 0.09 mmol) and Pd/C 10% (240 mg), followed by the addition of TFA (1 mL) with cooling in ice bath. The resulting reaction mixture was hydrogenated at room temperature for 24 hr. The catalyst was removed by filtration through celite and C18 reverse phase chromatography afforded *N*^{5}-*((S)*-1-carboxy-2-hydroxyethyl)-*L*-glutamine **(4.14)** as a yellow oil (20 mg, 95%). ^{1}H NMR (400 MHz, D_2O) δ 4.27

(ddd, *J* = 26.8, 15.2, 8.3 Hz, 1H, H-2), 4.03 (dd, *J* = 23.4, 8.7 Hz, 1H, H-1'), 3.94 – 3.62 (m, 2H, H-2'), 2.81 – 2.56 (m, 2H, H-3), 2.47 – 2.16 (m, 2H, H-4).

Benzyl (*tert*-butoxycarbonyl)-*L*-serinate[12]

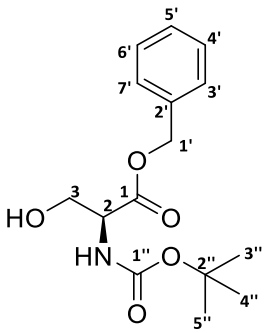

To a suspension of serine benzyl ester hydrochloride (200 mg, 0.863 mmol) and Et_3N (126 mg, 1.25 mmol) in THF (5 mL) cooled at 0°C, was added a solution of $(Boc)_2O$ (151 mg, 0.691 mmol) in THF (5 mL) drop wise over a period of 30 min. The mixture was allowed to warm to room temperature while stirring for 5 h, thereafter, the reaction temperature was raised to 50°C for further 2 h. The solvent was removed under vacuum, and the residue partitioned between Et_2O:H_2O (1:1, 50 mL). The aqueous layer was extracted with Et_2O (4 x 20 mL), the combined organic layers were successively washed with 5% $NaHCO_3$ (20 mL) and brine (20 mL). Dried over $MgSO_4$ and the solvent was evaporated to afford benzyl (*tert*-butoxycarbonyl)-*L*-serinate as a hygroscopic yellowish oil (260 mg, quantitative). The NMR showed pure product which was used in the next step without further purification. ^{1}H NMR (400 MHz, $CDCl_3$) δ 7.38-7.31 (m, 5H, Ph), 5,50 (br.s, 1H, NH), 5.21 (d, *J* = 2.3 Hz, 2H, H-1'), 4.41 (br.s, 1H, H-2), 3.97 (dd, *J* = 11.1, 3.9 Hz, 2H, H-3a), 3.89 (dd, *J* = 11.1, 3.9 Hz, 2H, H-3b), 2.44 (br.s, 1H, OH), 1.44 (s, 9H, *t*-butyl); ^{13}C NMR (101 MHz, $CDCl_3$) δ 170.7 (C-1), 155.8 (C-1''), 135.3 (C-2'), 128.6 (C-3'C-7'), 128.2 (C-4'C-6'), 126.3 (C-5'), 67.5 (C-1'), 63.5 (C-2), 55.9 (C-2''), 28.3 (C-3''4''5''), 27.4 (C-3).

The OH proton was assigned based on the D_2O wash ^1H NMR experiment. Data consistent with the literature.[12]

Benzyl (*S*)-2-((*tert*-butoxycarbonyl)amino)-3-chloropropanoate[13]

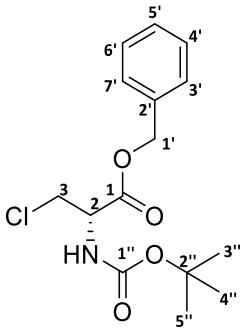

2, 4, 6-Trichloro-[1, 3, 5] triazine (179 mg; 0.971 mmol) was added portion wise in DMF (1 mL) while the internal temperature was maintained at 25 °C. After the formation of a white solid, the reaction was monitored (TLC) until complete disappearance of the starting material, thereafter CH_2Cl_2 (15 mL) was added, followed by the addition of benzyl (*tert*-butoxycarbonyl)-*L*-serinate. The resultant mixture was allowed to stir overnight at room temperature. The reaction mixture was diluted with water (15 mL), the organic layer was retained and the aqueous layer was extracted with EtOAc (3 x 20 mL). The combined organic layers were successively washed with saturated aqueous sodium carbonate (2 x 10 mL) and brine, dried (Na_2SO_4), filtered and concentrated under vacuum to yield benzyl (*S*)-2-((*tert*-butoxycarbonyl)amino)-3-chloropropanoate as a yellow solid (211 mg, 76%). Due to the instability of the product upon silica, the obtained product was used without further purification. Mp: 52-55 °C; ^1H NMR (400 MHz, $CDCl_3$) δ 7.41 – 7.29 (m, 5H), 5.40 (br.s, 1H, NH), 5.21 (d, *J* = 2.7 Hz, 2H), 4.41 (br.s, 1H), 3.94 (m, 2H), 1.44 (s, 9H); LRMS (EI^+) didn't display the

molecular ion but fragments at *m/z* calculated for $C_7H_{13}ClNO_2$ 178.1 found 178.0 ([^{35}Cl–COOBn]$^+$; 11.2%), 180.0 ([^{37}Cl–COOBn]$^+$; 2.0%).

_S_-benzyl-_L_-cysteine (4.26)[14]

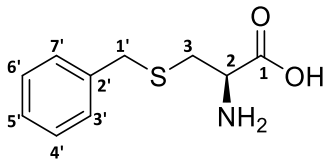

To a mixture of ethanol (70 mL) and 2N NaOH (30 mL, 2.40 g) were added *L*-cysteine hydrochloride (2.50 g, 14.2 mmol), and benzyl bromide (2.44 g, 1.7 mL, 14.2 mmol). The homogenous solution was allowed to stir at room temperature for 1-2 hr (TLC monitoring). The reaction was neutralised to pH 6-7 with careful addition of concentrated HCl. The precipitate was filtered and successively washed with water, ethanol, and Et_2O to afford *S*-benzyl-*L*-cysteine **(4.26)** as a white powder (2.4 g, 80%). Mp: 210-212 °C (Lit 215-216 °C)[15] (Lit 214 °C)[16]; ^{1}H NMR (300 MHz, D_2O) δ 7.24 – 7.06 (m, 5H, Ph), 3.94 (dd, *J* = 7.6, 4.6 Hz, 1H, H-2), 3.59 (s, 2H, H-1'), 2.85 (dd, *J* = 15.0, 4.6 Hz, 1H, H-3a'), 2.74 (dd, *J* = 15.0, 7.6 Hz, 1H, H-3b').[15] ^{13}C NMR (101 MHz, D_2O) δ 170.0 (C-1), 137.4 (C-2'), 128.9 (C-3'C-7'), 128.8 (C- 4'C-6'), 127.5 (C-5'), 52.0 (C-2), 35.4 (C-1'), 30.4 (C-3); LRMS (EI$^+$) *m/z* calculated for $C_{10}H_{13}NO_2S$ 211.1 found 211.0 ([M]$^+$; 57%); calculated for $C_9H_{12}NS$ 166.1 [M-CO_2 H]$^+$ found 166.0 ([M-CO_2 H]$^+$, 35%).

***O, S*- dibenzyl -*N*-(*tert*-butoxycarbonyl)-*L*-cysteinate (4.28)**

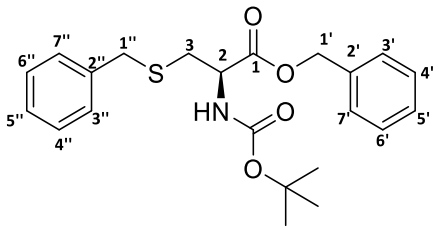

In a suspension of *S*-benzyl-*L*-cysteine **(4.26)** (315 mg, 1.50 mmol) in a mixture of H_2O:THF (2:1, 15 mL) were added NaOH (60 mg, 1.50 mmol) and $(Boc)_2O$ (393 mg, 1.80 mmol) portion wise. The resulting homogenous solution was allowed to stir at room temperature overnight. Solvents were removed to dryness and the residue was triturated with Et_2O. The residue was dissolved in DMF (6 mL), BnBr (257 mg, 180 µL, 1.50 mmol) was added in one portion and the resulting reaction mixture was allowed to stir at room temperature overnight. The reaction was quenched by the addition of H_2O (50 mL) and the aqueous layer was extracted with EtOAc (4 x 25 mL), organic layers were retained, washed with brine (15 mL) and dried over $MgSO_4$. SiO_2 gel column chromatography afforded the product as colourless solid **(4.28)** (573 mg, 95% over 2 steps). Mp: 78-79 °C; ^{1}H NMR (300 MHz, $CDCl_3$) δ 7.46 – 7.33 (m, 5H, O-CH_2-**Ph**), 7.33 – 7.21 (m, 5H, S-CH_2-**Ph**), 5.34 (br.s, 1H, NH), 5.19 (s, 2H, H-1'), 4.60 (dd, *J* = 13.9, 5.8 Hz, 1H, H-2), 3.70 (s, 2H, H-1''), 2.91 (dd, *J* = 13.9, 5.8 Hz, 1H, H-3a), 2.84 (dd, *J* = 13.9, 5.8 Hz, 1H, H-3b), 1.48 (s, 9H, Boc); ^{13}C NMR (75 MHz, $CDCl_3$) δ 171.0 (C-1), 129.0 (C=O), 137.7 (C-2'), 135.1 (C-2''), 129.0 (C-4'C-6'), 128.7 (C-3''C-7''), 128.6 (C-4''C-6''), 128.5 (C-5'), 128.3 (C-3'C-7'), 127.2 (C-5''), 80.2 (C-(Boc)), 67.4 (C-1'), 53.2 (C-2), 36.6 (C-1''), 33.6 (C-2), 28.3 (3C (Boc)); LRMS (EI$^+$) *m/z* calculated for $C_{22}H_{27}NO_4S$ $[M]^+$ 401.2 found 401.1 ($[M]^+$; 26 %); calculated for $C_{17}H_{18}NO_2S$

300.1 [M-Boc]$^+$ found 300.1 ([M-Boc]$^+$, 45%), calculated for $C_{10}H_{12}NO_2S$ 210.1 [M-Boc-Bn]$^+$ found 210.0 ([M-Boc-Bn]$^+$, 73%).

Benzyl *N,S*-dibenzyl-*L*-cysteinate (4.27)

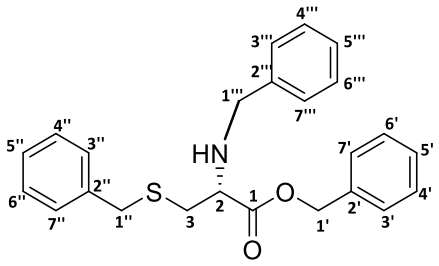

In a solution of *S*-benzyl-*L*-cysteine **(4.26)** (250 mg, 1.18 mmol) in dimethylformamide (5 mL), was added Cs_2CO_3 (384 mg, 1.18 mmol) at room temperature. After 30 min, benzyl bromide (202 mg, 1.18 mmol) was added and the resultant solution was allowed to stir at room temperature for 24 hr. A mixture of (H_2O:EtOAc, 1:1, 20 mL) was added and the organic layer retained. The aqueous layer was extracted with EtOAc (4 x 15 mL), the combined organic layers were dried over Na_2SO_4. Silica gel flash column chromatography (gradient petroleum ether 100% to petroleum ether/EtOAc 50:50) afforded benzyl *N,S*-dibenzyl-*L*-cysteinate **(4.27)** as a yellow oil (320 mg, 69%). ^{1}H NMR (300 MHz, $CDCl_3$) δ 7.54 – 7.16 (m, 15H, 3 x Ph), 5.20 (s, 2H, H-1'), 3.86 (d, *J* = 13.1 Hz, 1H, H-1a'''), 3.69 (d, *J* = 13.1 Hz, 1H, H-1b'''), 3.69 (overlapped s, 2H, H-1''), 3.51 (t, *J* = 6.5 Hz, 1H, H-2), 2.79 (dd, *J* = 11.5, 6.5 Hz, 1H, H-3a), 2.73 (dd, *J* = 11.5, 6.5 Hz, 1H, H-3b), 1.98 (br.s, 1H, NH); ^{13}C NMR (75 MHz, $CDCl_3$) δ 173.5 (C-1), 139.5 (C-2'), 137.9 (C-2''), 135.7 (C-2'''), 129.0 (C-4' C-6'), 128.8 (C-3''C-7''), 128.7 (C-4''' C-6'''), 128.6 (C-3' C-7'), 128.5 (C-4''C-6''), 128.3 (C-3'''C-7'''), 128.1 (C-5'), 127.2 (C-5''), 127.1 (C-5'''), 66.8 (C-1'), 60.1 (C-2), 51.9 (C-1'''), 36.6 (C-1''), 34.2 (C-3); LRMS (EI$^+$) *m/z* calculated for $C_{24}H_{25}NO_2S$ [M]$^+$

391.2 found 391.1 ([M]$^+$; 75%); calculated for $C_{17}H_{18}NO_2S$ 300.1 [M-Bn]$^+$ found 300.0 ([M-Bn]$^+$, 40%), calculated for $C_{16}H_{18}NS$ 256.1 [M-CO_2Bn]$^+$ found 256.1 ([M-CO_2Bn]$^+$; 94%).

***O, S*- dibenzyl *L*-cysteinate (4.23)**

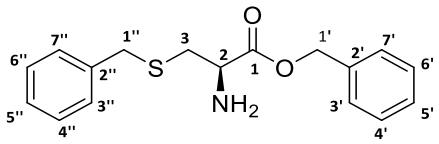

In dichloromethane (5 mL) was dissolved *O, S*-dibenzyl-*N*-(*tert*-butoxycarbonyl)-*L*-cysteinate **(4.28)** (160 mg, 0.40 mmol) followed by the addition of trifluoroacetic acid (1 mL) with cooling in an ice water bath. The resulting solution was allowed to stir at room temperature until complete disappearance of starting material as indicated by TLC. The solvent was removed, H_2O was added, the pH was adjusted to 8 with $NaHCO_3$ and the aqueous layer was extracted with EtOAc (3 x 10 mL). Organic layers were retained, washed with brine (15 mL), dried over $MgSO_4$ and filtered through a small layer of SiO_2 gel (5 g, 1 cm x 2.5 cm), solvent evaporated under vacuum to afford *O, S*-dibenzyl-*L*-cysteinate **(4.23)** as a yellow orange solid (110 mg, 91%). Mp:65-67 °C; ^{1}H NMR (400 MHz, $CDCl_3$) δ 7.39 – 7.30 (m, 5H, O-CH_2-**Ph**), 7.28 – 7.21 (m, 5H, S-CH_2-**Ph**), 5.14 (s, 2H, H-1'), 3.70 (s, 2H, H-1''), 3.62 (dd, *J* = 7.5, 4.7 Hz, 1H, H-2), 2.83 (dd, *J* = 13.5, 4.7 Hz, 1H, H-3a), 2.66 (dd, *J* = 13.5, 7.5 Hz, 1H, H-3b), 1.69 (br.s, 2H, NH); ^{13}C NMR (101 MHz, $CDCl_3$) δ 173.9 (C-1), 137.9 (C-2'), 135.5 (C-2''), 128.9 (C-4' C-6'), 128.6 (C-3'' C-7''), 128.5 (C-4'' C-6''), 128.4 (C-5'), 128.3 (C-3' C-7'), 127.2 (C-5''), 67.0 (C-1'), 54.2 (C-2), 36.5 (C-1''), 36.4 (C-3); LRMS (EI$^+$) *m/z* calculated for $C_{17}H_{19}NO_2S$ [M]$^+$ 301.1 found 301.1 ([M]$^+$; 72%); calculated for $C_{10}H_{12}NO_2S$ 210.1 [M-Bn]$^+$ found 210.0 ([M-Bn]$^+$, 79%), calculated for $C_{10}H_{13}NS$ 179.1 [M-CO_2Bn]$^+$ found 179.1 ([M-CO_2Bn]$^+$, 39%).

Benzyl N^5-((*R*)-1-(benzyloxy)-3-(benzylthio)-1-oxopropan-2-yl)-N^2-(*tert*-butoxycarbonyl)-*L*-glutaminate (4.24)

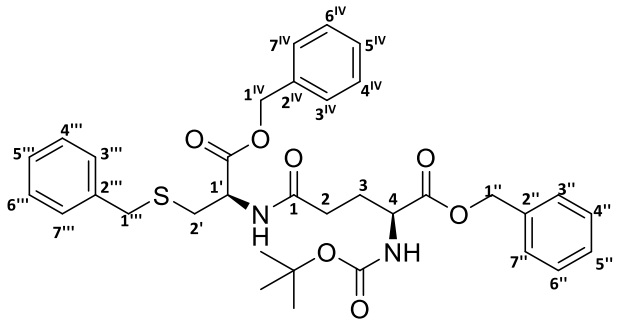

In dry dichloromethane (5 mL) were added (*S*)-5-(benzyloxy)-4-((*tert*-butoxycarbonyl)amino)-5-oxopentanoic acid **(4.10)** (101 mg, 0.30 mmol), DIC (38 mg, 50 µL, 0.30 mmol), HOBt (41 mg, 0.30 mmol) and DIPEA (39 mg, 0.30 mmol) at room temperature. Ten min later, *O,S*-dibenzyl-*L*-cysteinate **(4.23)** (75 mg, 0.25 mmol) was added and the resulting reaction mixture was allowed to stir at room temperature for 24 hr. The solvent was evaporated to dryness, residue purified by SiO_2 column chromatography (hexane/EtOAc 80:20) to give the coupling product **(4.24)** as colourless solid (144 mg, 92%). Mp: 92-95 °C; $[\alpha]^{20}_D$ = + 40.0° (*c* = 10, $CHCl_3$), ^{1}H NMR (300 MHz, $CDCl_3$) δ 7.50 – 7.32 (m, 10H, 2 X O-CH_2-**Ph**), 7.32 – 7.20 (m, 5H, S-CH_2-**Ph**), 6.47 (br.s, 1H, NH), 5.29 (br.s, 1H, NH), 5.19 (s, 4H, H-1'' H-1^{iv}), 4.90 – 4.75 (m, 1H, H-1'), 4.52 – 4.29 (m, 1H, H-4), 3.69 (d, *J* = 13.5 Hz, 1H, H-1a'''), 3.63 (d, *J* = 13.5 Hz, 1H, H-1b'''), 2.92 (dd, *J* = 13.9, 6.2 Hz, 1H, H-2'a), 2.84 (dd, *J* = 13.9, 6.2 Hz, 1H, H-2'b), 2.34 – 2.11 (m, 3H, H-3 H-2a), 2.11 – 1.82 (m, 1H, H-2b), 1.45 (s, 9H, Boc); ^{13}C NMR (101 MHz, $CDCl_3$) δ 172.1 (C-1), 171.6 (C=O), 170.6 (C=O), 155.7 (C=O (Boc)), 137.7 (C-2^{iv}), 135.3 (C-2''), 135.1 (C-2'''), 128.9 (C-4^{iv} C-6^{iv}), 128.6 (C-4''C-6''), 128.5 (C-3''' C-6'''), 128.4 (C-5''' C-7'''), 128.3 (C-5^{iv}), 128.2 (C-5''), 128.1 (C-3^{iv} C-7^{iv}), 128.1 (C-3'' C-7''), 127.2 (C-5'''), 80.1 (C(Boc)), 67.5 (C-1^{iv}), 67.2 (C-1''), 53.0 (C-1'), 51.5 (C-4), 36.4 (C-1'''), 33.5 (C-2'), 32.2 (C-2), 28.3 (3C (Boc)), 27.8 (C-3); LRMS (EI$^+$) didn't

display the molecular ion but the fragmentations at *m/z* calculated for $C_{22}H_{25}N_2O_5S$ 429.1 found 429.1 ([M-Boc-Bn]$^+$; 15%); calculated for $C_{14}H_{19}N_2O_3S$ 295.1 [M-Boc-CO_2Bn]$^+$ found 295.1 ([M-Boc-CO_2Bn]$^+$; 7%).

N^5-((*R*)-1-carboxy-2-mercaptoethyl)-*L*-glutamine (γ-glutamylcysteine) (4.18)

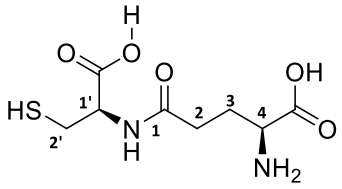

To methanol (5 mL) were added benzyl N^5-((*R*)-1-(benzyloxy)-3-(benzylthio)-1-oxopropan-2-yl)-N^2-(*tert*-butoxycarbonyl)-*L*-glutaminate **(4.24)** (115 mg, 0.19 mmol), Pd/C (10%, 600 mg) and TFA (1 mL). The resulting reaction mixture was allowed to hydrogenate at room temperature for 24 hr. The catalyst was removed by filtration through celite and washed with water. The combined filtrates were evaporated to dryness. Reverse phase C18 column chromatography afforded γ-glutamylcysteine **(4.18)** as a white solid (41 mg, 85%). ^{1}H NMR (300 MHz, D_2O) δ 4.58 – 4.36 (m, 1H, H-1'), 4.29 – 4.08 (m, 1H, H-4), 3.87 (d, *J* = 19.0 Hz, 2H, H-2'), 2.82 – 2.47 (m, 2H, H-2), 2.38- 2.20 (m, 2H, H-3), proton NMR spectrum similar with the one reported in the literature [23]; ^{13}C NMR (101 MHz, DMSO) δ 173.2 (C=O), 170.5 (C=O), 156.9 (C-1), 51.2 (C-1'), 47.8 (C-4), 29.3 (C-2), 25.3 (C-3), 23.3 (C-2'). LRMS (ESI$^+$) *m/z* calculated for $C_8H_{15}N_2O_5S$ 251.1 found 251.2 ([MH]$^+$; 10%); calculated for $C_7H_{17}N_2O^+$ 145.1 [M-CO_2-SH-H_2O]$^+$ found 145.2 ([M-CO2]+; 100%).

(*S*)-2-ammonio-5-(((*R*)-1-carboxy-2-((4-((*S*)-2-carboxylato-2-(trimethylammonio)ethyl)-1*H*-imidazol-2-yl)thio)ethyl)amino)-5-oxopentanoate (4.2)

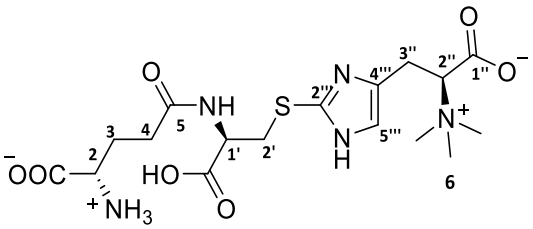

In DMF (1 mL) were added (*S*)-3-(1-benzyl-1*H*-imidazol-4-yl)-2-(trimethylammonio) propanoate **(2.30)** (21 mg, 0.05 mmol) and *N*-bromosuccinimide (18 mg, 0.10 mmol) at room temperature. The resultant reaction mixture was allowed to stir at room temperature until complete disappearance of the starting material (TLC monitoring). γ-glutamylcysteine (20 mg, 0.08 mmol, 1.6 eq) was added in one portion and the resulting reaction mixture was allowed to stir at room temperature for 1-3 hr. Solvent was removed to dryness. Reverse phase C18 column chromatography afforded the product **(4.2)** as a colourless solid (2 mg, 7%). ^{1}H NMR (300 MHz, D_2O) δ 8.52 (s, 1H, H-5'''), 4.58 – 4.40 (m, 2H, H-2 H-1'), 4.31 – 4.17 (m, 1H, H-2''), 3.97 – 3.83 (m, 2H, H-2'), 3.78 (s, 9H, NMe_3), 3.61 (dd, *J* = 12.2, 6.5 Hz, 1H, H-3a''), 3.50 (dd, *J* = 12.2, 6.5 Hz, 1H, H-3b''), 2.70 – 2.56 (m, 2H, H-4), 2.27 – 2.08 (m, 2H, H-3).

(*S*)-1-(benzyloxy)-3-(2-(((*R*)-3-(benzyloxy)-2-((*tert*-butoxycarbonyl)amino)-3 oxopropyl)thio)-1*H*-imidazol-4-yl)-*N,N,N*-trimethyl-1-oxopropan-2-aminium (4.41)

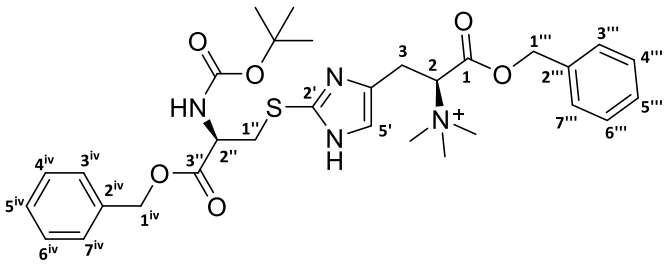

To a mixture of CH_3CN:H_2O (1:1, 4 mL) were added hercynylcysteine thioether **(2.19)** (254 mg, 0.80 mmol) and NaOH (35 mg, 0.88 mmol). The resulting reaction mixture was allowed to stir at room temperature overnight. The solvent was removed to dryness, the residue was dissolved in DMF followed by the addition of benzyl bromide (287 mg, 200 µL, 1.68 mmol) and the resulting solution was allowed to stir at room temperature for 24 hr. The solvent was removed to dryness and SiO_2 gel column chromatography afforded the product **(4.41)** as a yellow solid (155 mg, 33%). ^{1}H NMR (300 MHz, $CDCl_3$) δ 8.89 (br.s, 1H, NH), 7.49 (s, 1H, H-5'), 7.42 – 7.27 (m, 10H, 2 x **Ph**), 5.36 – 5.03 (m, 4H, **CH_2**–Ph), 4.69 – 4.51 (m, 1H, H-2"), 4.01 – 3.84 (m, 1H, H-2), 3.61 (dd, *J* = 11.2, 3.0 Hz, 1H, H-1a"), 3.39 (dd, *J* = 11.2, 7.7 Hz, 1H, H-1b"), 3.12 (dd, *J* = 11.7, 6.7 Hz, 2H, H-3), 2.73 (s, 9H, NMe_3), 1.41 (s, 9H, Boc); ^{13}C NMR (101 MHz, $CDCsl_3$) δ 177.9 (2C, C-1 C-3"), 170.6 (C=O), 135.1 (C-2'), 133.3 (C-4'), 129.4 (C-5'), 128.9 (2C, C-2"' C-2^{iv}), 128.6 (4C, C-4"' C-6"' C-4^{iv} C-6^{iv}), 128.5 (2C, C-5"' C-5^{iv}), 128.4 (4C, C-3"' C-7"' C-3^{iv} C-7^{iv}), 68.3 (C-2), 67.9 (C, Boc), 67.5 (2C, C-1"' C-1^{iv}), 53.1 (C-2"), 41.2 (C-3), 34.8 (C-1"), 29.6 (3C, NMe_3), 28.3 (3C, Boc).

(*S*)-1-(benzyloxy)-3-(2-(((*R*)-3-(benzyloxy)-2-((*S*)-5-(benzyloxy)-4-((*tert*-butoxycarbonyl)amino)-5-oxopentanamido)-3-oxopropyl)thio)-1*H*-imidazol-4-yl)-*N,N,N*-trimethyl-1-oxopropan-2-aminium (4.42)

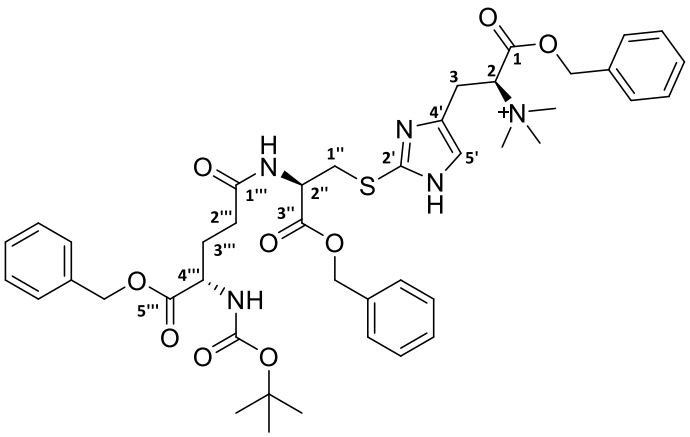

To a solution of (*S*)-1-(benzyloxy)-3-(2-(((*R*)-3-(benzyloxy)-2-((*tert*-butoxycarbonyl)amino)-3 oxopropyl)thio)-1*H*-imidazol-4-yl)-*N,N,N*-trimethyl-1-oxopropan-2-aminium **(4.41)** (37 mg, 0.06 mmol) in dichloromethane (2 mL), was added TFA (0.5 mL) with cooling in an ice bath and the resulting reaction mixture was allowed to stir at room temperature overnight until TLC confirmed complete Boc removal.

The solvent was removed to dryness and the residue was redissolved in DCM (3 mL), DIPEA (9 mg, 10 µL, 0.07 mmol), HOBt (10 mg, 0.07 mmol), (*S*)-5-(benzyloxy)-4-((*tert*-butoxycarbonyl)amino)-5-oxopentanoic acid **(4.10)** (24 mg, 0.07 mmol) and DIC (9 mg, 0.01 mmol) were added with cooling in ice bath. The resulting solution was allowed to stir at room temperature for 24 hr. The solvent was removed to dryness, water (10 mL) was added, extracted with EtOAc (4 x 10 mL), organic layers were retained and dried over $MgSO_4$. SiO_2 gel column chromatography (gradient hexane/EtOAc) afforded the desired product **(4.42)** as

a yellow oil (46 mg, 88%). ^{1}H NMR (400 MHz, $CDCl_3$) δ 7.46 – 7.25 (m, 16H, 3 x **Ph**, Overlapped s, H-5'), 5.26 – 5.08 (m, 6H, 3 x **CH_2**-Ph), 4.73 – 4.56 (m, 1H, H-2), 3.99 (ddd, *J* = 19.7, 13.3, 6.6 Hz, 1H, H-4'''), 3.91 – 3.76 (m, 1H, H-2''), 3.66 (s, 9H, NMe_3), 2.67 – 2.44 (m, 2H, H-1''), 2.43 – 2.27 (m, 2H, H-3), 2.19 (dd, *J* = 13.9, 6.8 Hz, 2H, H-2'''), 2.08 – 1.89 (m, 2H, H-3'''), 1.42 (s, 9H, Boc); ^{13}C NMR (101 MHz, $CDCl_3$) δ 173.1 (2C, C-3'' C-5'''), 172.0 (C-1'''), 171.2 (C-1), 155.3 (C=O), 149.3 (C-2'), 135.3 (3C-***ipso*** Ph), 135.1 (C-4'), 128.7 (6C-***meta*** Ph), 128.6 (3C-***para*** Ph), 128.3 (6C-***ortho*** Ph), 114.7 (C-5'), 83.6 (C-Boc), 67.2 (3C, **CH_2**-Ph), 59.0 (C-2), 51.7 (3C, NMe_3), 51.7 (C-2''), 42.3 (C-4'''), 31.1 (C-1''), 30.0 (C-2'''), 28.3 (3C, Boc), 23.5 (C-3'''), 20.5 (C-3).

(2*S*)-1-(benzyloxy)-3-(2-(((*R*)-3-(benzyloxy)-2-((*S*)-5-(benzyloxy)-4-((*tert*-butoxycarbonyl) amino)-5-oxopentanamido)-3-oxopropyl) sulfinyl)-1*H*-imidazol-4-yl)-*N,N,N*-trimethyl-1-oxopropan-2-aminium (4.43)

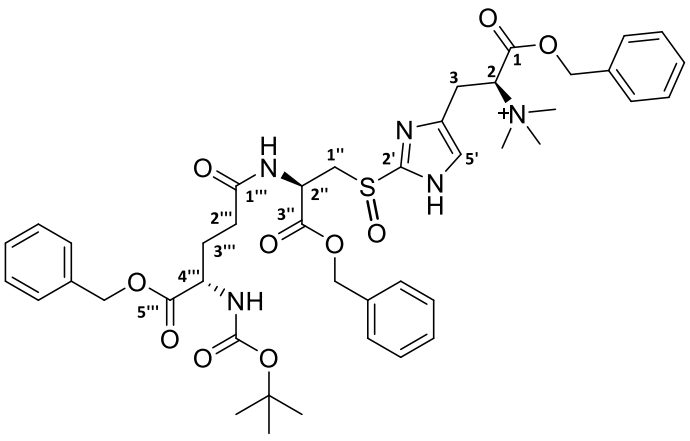

To a solution of (*S*)-1-(benzyloxy)-3-(2-(((*R*)-3-(benzyloxy)-2-((*S*)-5-(benzyloxy)-4-((*tert*-butoxycarbonyl)amino)-5-oxopentanamido)-3-oxopropyl)thio)-1*H*-imidazol-4-yl)-*N,N,N*-trimethyl-1-oxopropan-2-aminium **(4.42)** (74 mg, 0.091 mmol) in DCM (1 mL) was added

*m*CPBA (70%, 24 mg, 0.10 mmol) in ice bath (0 °C). The resulting solution was allowed to stir at room temperature for 6 hr (TLC monitoring). Solvent was removed and SiO_2 column chromatography afforded the desired sulfoxide **(4.42)** as a yellow solid (55 mg, 72%); ^{1}H NMR (400 MHz, $CDCl_3$) δ 7.41 (s, 1H, H-5'), 7.40 – 7.25 (m, 15H, 3 x **Ph**), 5.31 – 5.07 (m, 6H, 3 x **CH_2**-Ph), 4.67 – 4.57 (m, 2H, H-2 H-4'''), 4.31 – 4.25 (m, 2H, H-1" major diastereoisomer), 4.24 – 4.20 (m, 2H, H-1" minor diastereoisomer), 4.08 – 3.89 (m, 1H, H-2"), 3.66 (s, 9H, NMe_3), 2.61 – 2.47 (m, 2H, H-3), 2.41 – 2.24 (m, 2H, H-2'''), 2.07 – 1.91 (m, 2H, H-3'''), 1.42 (s, 9H, Boc); ^{13}C NMR (101 MHz, $CDCl_3$) δ 173.3 (C-1'''), 171.2 (C-1), 169.0 (2C, C-3'' C-5'''), 149.3 (C=O), 135.1 (C-2'), 134.7 (3C-***ipso*** Ph), 131.3 (C-4'), 129.8 (6C-***meta*** Ph), 128.6 (3C-***para*** Ph), 128.5 (6C-***ortho*** Ph), 128.3 (C-5'), 83.7 (C-Boc), 67.4 (3C, **CH_2**-Ph), 59.0 (3C, NMe_3), 51.8 (C-2), 47.9 (C-1'' major diastereoisomer), 45.8 (C-1'' minor diastereoisomer), (42.9 (C-4'''), 42.4 (C-2''), 31.1 (C-3), 28.3 (C-2'''), 27.8 (3C, Boc), 21.5 (C-3''').

(2*S*)-3-(2-(((*R*)-2-((*S*)-4-amino-4-carboxybutanamido)-2-carboxyethyl)sulfinyl)-2,3-dihydro-1*H*-imidazol-4-yl)-2-(trimethylammonio) propanoate (4.1)

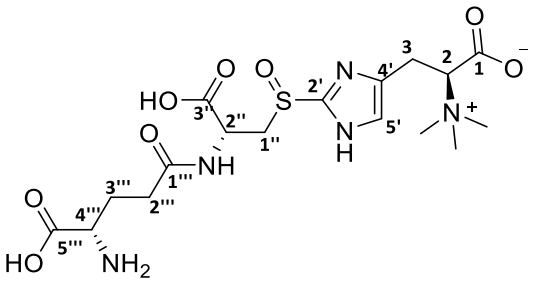

To a solution of (2*S*)-1-(benzyloxy)-3-(2-(((*R*)-3-(benzyloxy)-2-((*S*)-5-(benzyloxy)-4-((*tert*-butoxycarbonyl) amino)-5-oxopentanamido)-3-oxopropyl) sulfinyl)-1*H*-imidazol-4-yl)-*N,N,N*-

trimethyl-1-oxopropan-2-aminium **(4.42)** (30 mg, 0.036 mmol) in methanol (1 mL), were added Pd/C (10%, 100 mg) and TFA (0.2 mL) with cooling in an ice bath (0 °C). The resulting reaction mixture was allowed to hydrogenate at room temperature for 2 days until complete deprotection as monitored by paper chromatography. Pd/C was removed by filtration through celite, solvent evaporated under vacuum and reverse phase C18 column chromatography afforded the desired product **(4.1)** as white solid (11 mg, 65%). ^{1}H NMR (400 MHz, D_2O) δ 7.65 (s, 1H, H-5'), 4.48 (m, 2H, H-2" H-4'''), 4.28 (dt, *J* = 13.2, 6.7 Hz, 2H, H-1" major diastereoisomer), 4.24 – 4.18 (m, 2H, H-1'' minor diastereoisomer), 4.01 (m, 1H, H-2), 3.94 (s, 9H, NMe_3), 3.63 (dd, *J* = 11.6, 4.1 Hz, 1H, H-3a), 3.53 (dd, *J* = 11.6, 8.6 Hz, 1H, H-3b), 2.83 – 2.58 (m, 2H, H-2'''), 2.41 – 2.21 (m, 2H, H-3'''); ^{13}C NMR (101 MHz, D_2O) δ 182.0 (2C, C-5''' C-3"), 177.1 (C-1'''), 174.9 (C-1), 133.9 (C-2'), 129.7 (C-4'), 128.8 (C-5'), 85.6 (C-2), 56.1 (C-2''), 53.7 (C-4'''), 52.1 (NMe_3), 44.0 (C-1" major diastereoisomer), 43.9 (C-1" minor diastereoisomer), 36.7 (C-2'''), 29.4 (C-3'''), 27.7 (C-3); LRMS (EI^+) didn't display the molecular ion but characteristic fragmentations at *m/z* calculated for $C_{15}H_{23}N_5O_4S^+$ 369.1 $[M\text{-}2\ CO_2\text{-}3H]^+$ found 369.3 $[M\text{-}2\ CO_2\text{-}3H]^+$, calculated for $C_{12}H_{17}N_4O_4S$ 313.1 $[M\text{-}2\ CO_2\text{-}N(CH_3)_3]^+$ found 313.2 $[M\text{-}2\ CO_2\text{-}N(CH_3)_3]^+$, calculated for $C_{11}H_{18}N_4O_2S$ 269.1 $[M\text{-}3\ CO_2\text{-}N(CH_3)_3]^+$ found 269.1 $[M\text{-}3\ CO_2\text{-}N(CH_3)_3]^+$

***N*$^{\alpha}$,*N*^{c}-bis(*tert*-butoxycarbonyl)-*L*-histidine (5.6)[17]**

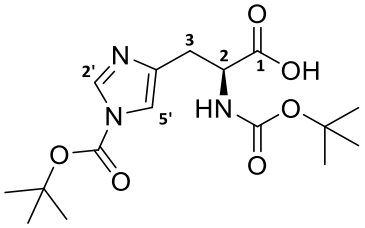

To a suspension of *L*-histidine (1.50 g, 9.70 mmol) in a mixture of H_2O:THF (2:1, 15 mL) were added $NaHCO_3$ (1.79 g, 21.3 mmol) and di-*tert*-butyl dicarbonate (4.23 g, 19.4 mmol). The resulting solution was allowed to stir at room temperature for 24 hr. At the end of the reaction (TLC monitoring), THF was removed in the rotary evaporator and the remaining water layer was extracted with EtOAc (2 x 15 mL). The pH of the water layer was adjusted to 5-6 with citric acid and extracted again with EtOAc (3 x 20 mL). The combined organic layers were washed with brine, dried over $MgSO_4$ and filtered over a small layer of SiO_2 gel to afford N^{α},N^{c}-bis(*tert*-butoxycarbonyl)-*L*-histidine **(5.6)** as a colourless solid (2.14 g, 63%). Mp: 76-79 °C (Lit 73-75 °C) [17]; $[\alpha]^{20}_{D}$ = +94° (*c* = 1, CH_2Cl_2); ^{1}H NMR (300 MHz, $CDCl_3$) δ 8.12 (s, 1H, H-2'), 7.17 (s, 1H, H-5'), 5.46 (br.s, 1H, NH), 4.48 (m, 1H, H-2), 3.27 (dd, *J* = 14.6, 3.3 Hz, 1H, H-3a), 3.19 (dd, *J* = 14.6, 5.0 Hz, 1H, H-3b), 1.61 (s, 9H, ^{Im}Boc), 1.46 (s, 9H, Boc); ^{13}C NMR (101 MHz, $CDCl_3$) δ 173.1 (C-1), 155.2 (C=O (^{Im}Boc)), 146.2 (C=O (Boc)), 137.0 (C-2'), 136.5 (C-4'), 115.6 (C-5'), 86.4 (C-(^{Im}Boc)), 79.7 (C-(Boc)), 52.8 (C-2), 29.7 (C-3), 28.4 (3C-(^{Im}Boc)), 27.8 (3C-(Boc)).

Tert-butyl (_S_)-4-(3-(benzyloxy)-2-((_tert_-butoxycarbonyl)amino)-3-oxopropyl)-1_H_-imidazole-1-carboxylate (5.7)

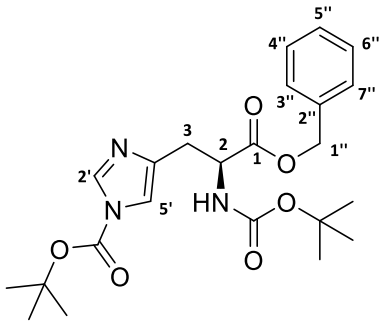

In dimethylformamide (5 mL) were added N^{α},N^{c}-bis(*tert*-butoxycarbonyl)-*L*-histidine **(5.6)** (750 mg, 2.11 mmol) and Cs_2CO_3 (1.03 g, 3.17 mmol) and the resulting solution was allowed

to stir at room temperature. After 30 min, BnBr (552 mg, 0.4 mL, 3.23 mmol) was added in one portion and the reaction mixture was allowed to stir at room temperature for 22 hr (TLC monitoring). Water (50 mL) was added and the aqueous solution was extracted by EtOAc (4 x 25 mL). Combined organic layers were washed with brine (20 mL) and dried over $MgSO_4$. Flash SiO_2 column chromatography (hexane: EtOAc, 25:75) afforded *tert*-butyl (*S*)-4-(3-(benzyloxy)-2-((*tert*-butoxycarbonyl)amino)-3-oxopropyl)-1*H*-imidazole-1-carboxylate **(5.7)** as a white solid (850 mg, 91%). Mp: 90-93 °C; $[\alpha]^{20}_D$ = -5.3° (*c* = 1, CH_2Cl_2); ^{1}H NMR (300 MHz, $CDCl_3$) δ 7.94 (s, 1H, H-2'), 7.38 – 7.27 (m, 5H, Ph), 7.01 (s, 1H, H-5'), 5.81 (br.s, 1H, NH), 5.14 (q, *J* = 12.3 Hz, 2H, H-1''), 4.69 – 4.55 (m, 1H, H-2), 3.11 – 2.92 (m, 2H, H-3), 1.60 (s, 9H, ^{Im}Boc), 1.43 (s, 9H, Boc); ^{13}C NMR (101 MHz, $CDCl_3$) δ 171.7 (C-1), 155.5 (C=O (^{Im}Boc)), 146.8 (C=O (Boc)), 138.5 (C-2''), 136.7 (C-2'), 135.6 (C-4'), 128.5 (C-4''C-6''), 128.3 (C-3''C-7''C-5''), 114.6 (C-5'), 85.5 (C (^{Im}Boc)), 79.7 (C (Boc)), 66.6 (C-1''), 53.3 (C-2), 30.2 (C-3), 28.3 (3C-(Boc)), 27.9 (3C-(^{Im}Boc)); LRMS (EI$^+$) *m/z* calculated for $C_{23}H_{31}N_3O_6$ 445.2 $[M]^+$ found 445.1 ($[M]^+$, 40%), calculated for $C_{19}H_{23}N_3O_6$ 389.2 [M-*t*-butyl]$^+$ found 389.0 ([M-*t*-butyl]$^+$, 100%), calculated for $C_{18}H_{23}N_3O_4$ 345.2 [M-Boc]$^+$ found 345.1 ([M-Boc]$^+$, 34%), calculated for $C_{13}H_{14}N_3O_2$ 244.1 [M-2 Boc]$^+$ found 244.0 ([M-2 Boc]$^+$, 17%).

Benzyl N^{α}-(*tert*-butoxycarbonyl)-N^{π}-methyl-*L*-histidinate (5.9) and benzyl N^{α}-(*tert*-butoxycarbonyl)-N^{τ}-methyl-*L*-histidinate (5.10)

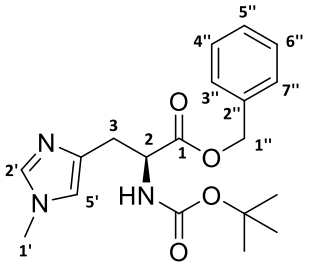

5.9

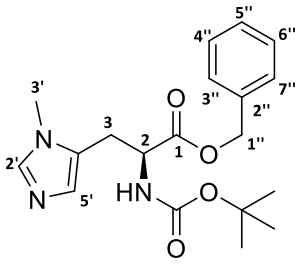

5.10

To a solution of *tert*-butyl (*S*)-4-(3-(benzyloxy)-2-((*tert*-butoxycarbonyl)amino)-3-oxopropyl)-1*H*-imidazole-1-carboxylate **(5.7)** (135 mg, 0.30 mmol) in THF (5 mL) was added iodomethane (128 mg, 60 µL, 0.90 mmol) and the resulting reaction mixture was allowed to reflux for two days at 60 °C. After cooling at room temperature, the solvent was removed and the crude residue was purified by SiO_2 gel column chromatography to afford a mixture of products (**5.9** and **5.10**) as brown solid (92 mg, 85%). ^{1}H NMR (300 MHz, $CDCl_3$) δ 7.50 – 7.30 (m, 6H, Ph, H-2'), 7.08 (s, 1H, H-5'), 5.32 (d, *J* = 11.9 Hz, 1H, H-1a''), 5.18 (d, *J* = 11.9 Hz, 1H, H-1b''), 4.57 (dd, *J* = 12.7, 6.7 Hz, 1H, H-2), 3.88 (s, 3H, H-1' isomer **5.9**), 3.85 (s, 3H, H-3' isomer **5.10**), 3.77 – 3.68 (m, 1H, H-3a isomer **5.9**), 3.53 (dd, *J* = 12.7, 4.7 Hz, 1H, H-3b isomer **5.9**), 3.43 (dd, *J* = 12.7, 6.7 Hz, 2H, H-3a isomer **5.10**), 3.29 (dd, *J* = 12.7, 6.7 Hz, 2H, H-3b isomer **5.10**), 1.42 (s, 9H, Boc).

***Tert*-butyl (*S*)-4-(2-((*tert*-butoxycarbonyl)amino)-3-methoxy-3-oxopropyl)-1*H*-imidazole-1-carboxylate (5.12)[18]**

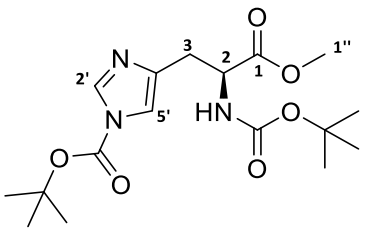

To a mixture of THF:H_2O (1:1, 20 mL) were added histidine methyl ester dihydrochloride (1.5 g, 6.20 mmol), $NaHCO_3$ (1.3 g, 15.5 mmol) and $(Boc)_2O$ (2.84 g, 13.02 mmol) at room temperature. The resulting homogenous reaction mixture was allowed to stir at room temperature for 19 hr (TLC monitoring). Solvent was removed to dryness and a mixture of H_2O:EtOAc (1:1, 50 mL) was added to the residue. Organic layer was retained and the aqueous phase was extracted with EtOAc (3 x 25 mL). Combined organic layers were washed with brine (10 mL), dried over $MgSO_4$ and flash SiO_2 chromatography afforded *tert*-butyl (*S*)-4-(2-((*tert*-butoxycarbonyl)amino)-3-methoxy-3-oxopropyl)-1*H*-imidazole-1-carboxylate **(5.12)** as a colourless solid (2.20 g, 96%). ^{1}H NMR (300 MHz, $CDCl_3$) δ 8.00 (s, 1H, H-2'), 7.12 (s, 1H, H-5'), 5.67 (br.s, 1H, NH), 4.62 – 4.38 (m, 1H, H-2), 3.68 (s, 3H, OCH_3), 3.03 (dd, *J* = 17.1, 6.9 Hz, 2H, H-3), 1.56 (s, 9H, Boc ^{Im}), 1.38 (s, 9H, Boc); ^{13}C NMR (75 MHz, $CDCl_3$) δ 172.2 (C-1), 155.4 (C=O (Boc)), 146.8 (C=O (Boc ^{Im})), 138.2 (C-4'), 136.6 (C-2'), 114.6 (C-5'), 85.6 (C (Boc ^{Im})), 79.9 (C (Boc)), 52.9 (C-2), 52.3 (O**C**H_3), 30.2 (C-3), 28.3 (3C (Boc ^{Im})), 27.8 (3C (Boc)).

Methyl N^{α}-(*tert*-butoxycarbonyl)-N^{π}-methyl-*L*-histidinate (5.13) and N^{α}-(*tert*-butoxycarbonyl)-N^{τ}-methyl-*L*-histidinate (5.14)

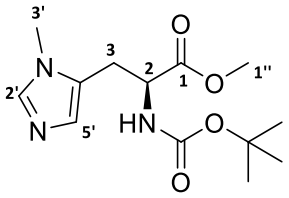

5.13

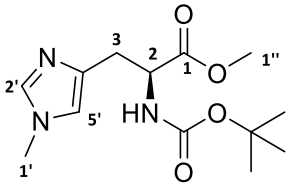

5.14

To a solution of *tert*-butyl (*S*)-4-(2-((*tert*-butoxycarbonyl)amino)-3-methoxy-3-oxopropyl)-1*H*-imidazole-1-carboxylate **(5.12)** (1.19 g, 3.22 mmol) in THF (5 mL) was added iodomethane (914 mg, 400 µL, 6.44 mmol) and the resulting reaction mixture was allowed to stir at room temperature for two days. Solvent was removed and the residue purified by SiO_2 column chromatography to afford a mixture of product (**5.13** and **5.14**) as yellow solid (200 mg, 21%). ^{1}H NMR (300 MHz, $CDCl_3$) δ 9.84 (s, 1H, H-2'), 7.17 (s, 1H, H-5'), 5.59 (br.s, 1H, NH), 4.56 (m, 1H, H-2), 4.00 (s, 3H, H-1' isomer **5.14**), 3.96 (s, 3H, H-3' isomer **5.13**), 3.80 (s, 3H, H-1''), 3.28 (dd, *J* = 15.8, 5.0 Hz, 1H, H-3a), 3.17 (dd, *J* = 15.8, 7.7 Hz, 1H, H-3b), 1.41 (s, 9H, Boc).

Methyl N^{α},N^{τ}-dibenzyl-*L*-histidinate (5.16)

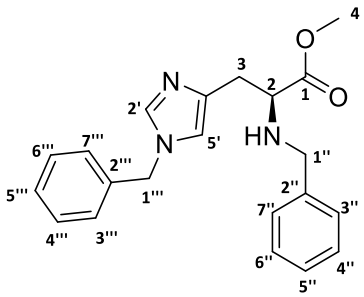

To a mixture of THF:H_2O (1:2, 6 mL) were added histidine methyl ester dihydrochloride (700 mg, 2.90 mmol), NaOH (255 mg, 6.38 mmol) and benzyl bromide (1.09 g, 0.8 mL, 6.38 mmol) rapidly. The resulting solution was allowed to stir at room temperature for 24 hr. The solvent was removed to dryness and to the residue was added H_2O (10 mL). The aqueous layer was extracted with EtOAc (4 x 20 mL), organic layers were washed with brine (10 mL), dried over $MgSO_4$, and the residue was triturated several times with Et_2O to afford pure methyl N^{α},N^{c}-dibenzyl-*L*-histidinate **(5.16)** as a colourless solid (800 mg, 81%), without the need of any SiO_2 column chromatography. ^{1}H NMR (400 MHz, $CDCl_3$) δ 10.38 (s, 1H, NH), 7.30 – 7.27 (m, 5H, Ph ^{imidazole}), 7.29 (overlapped, s, 1H, H-2'), 7.15 – 7.08 (m, 5H, Ph), 6.42 (s, 1H, H-5'), 5.43 (q, *J* = 14.5 Hz, 2H, H-1$'''$), 3.79 (s, 3H, H-4), 3.72 (d, *J* = 13.7 Hz, 1H, H-1a''), 3.54 (dd, *J* = 6.2, 8.7 Hz, 1H, H-2), 3.51 (d, *J* = 13.7 Hz, 1H, H-1b''), 2.67 (dd, *J* = 16.3, 6.2 Hz, 1H, H-3a), 2.60 (dd, *J* = 16.3, 8.7 Hz, 1H, H-3b), ^{13}C NMR (101 MHz, $CDCl_3$) δ 170.9 (C-1), 137.7 (C-2'), 133.1 (C-4'), 132.0 (C-2''' C-2''), 129.4 (C-7''' C-7'' C-3''' C-3''), 128.7 (C-6''' C-6'' C-4''' C-4''), 127.8 (C-5''' C-5''), 119.8 (C-5'), 58.6 (C-2), 54.9 (C-1'''), 53.4 (C-1''), 51.0 (C-4), 33.5 (C-3).

(*S*)-1-benzyl-4-(2-(benzylamino)-3-methoxy-3-oxopropyl)-3-methyl-1*H*-imidazol-3-ium (5.17)

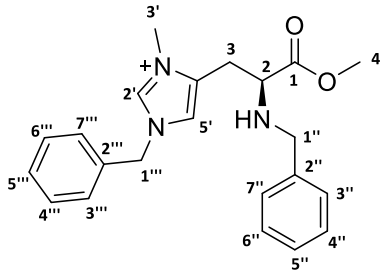

In dry DMF (2 mL) were added methyl N^{α},N^{c}-dibenzyl-*L*-histidinate **(5.16)** (280 mg, 0.80 mmol) and Me_2SO_4 (151 mg, 110 µL, 1.2 mmol). The resulting reaction mixture was allowed to stir at room temperature for 1-2 days. The reaction was quenched by the addition of HCl (5%, 10 mL) and extracted with EtOAc (3 x 20 mL). Combined organic layers were washed successively by H_2O, HCl 5% and brine, dried over $MgSO_4$ and purified by SiO_2 gel column chromatography (EtOAc 100% to EtOAc/MeOH 80:20) to afford (*S*)-1-benzyl-4-(2-(benzylamino)-3-methoxy-3-oxopropyl)-3-methyl-1*H*-imidazol-3-ium **(5.17)** as a yellow oil (211 mg, 72%). ^{1}H NMR (300 MHz, $CDCl_3$) δ 9.81 (s, 1H, NH), 7.15 – 7.05 (m, 5H, $Ph^{Imidazole}$), overlapped 7.11 (s, 1H, H-2'), 6.97 – 6.86 (m, 5H, Ph), 6.35 (s, 1H, H-5'), 5.20 (d, *J* = 2.6 Hz, 2H, H-1'''), 3.61 (s, 3H, H-4), 3.54 (s, 3H, H-3'), 3.36 (dd, *J* = 6.2, 8.7 Hz, 1H, H-2), 3.32 (dd, *J* = 14.3, 6.2 Hz, 2H, 1''), 2.65 – 2.57 (m, 2H, H-3); ^{13}C NMR (101 MHz, $CDCl_3$) δ 171.1 (C-1), 138.3 (C-2'), 133.4 (C-4'), 132.2 (C-2''' C-2''), 129.5 (C-7''' C-7'' C-3''' C-3''), 129.0 (C-6''' C-6'' C-4''' C-4''), 127.8 (C-5''' C-5''), 120.0 (C-5'), 58.8 (C-2), 54.9 (C-1'''), 53.4 (C-1''), 51.9 (C-3'), 51.1 (C-4), 24.6 (C-3); LRMS (EI^+) *m/z* calculated for $C_{22}H_{26}N_3O_2$ 364.2 found 364.2 ($[M]^+$; 1%), calculated for $C_{21}H_{22}N_3O_2$ 348.2 found 348 ($[M\text{-}CH_3\text{-}H]^+$; 100%)

Methyl N^{c}-benzyl-N^{α}-(*tert*-butoxycarbonyl)-*L*-histidinate[19]

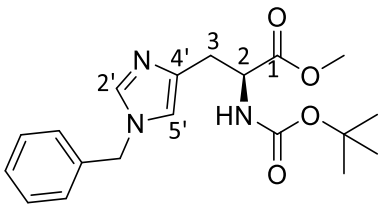

In acetone (6 mL) were added methyl (*tert*-butoxycarbonyl)-*L*-histidinate (165, 0.613 mL), Cs_2CO_3 (402 mg, 1.23 mmol) and bromide benzyl (105 mg, 70 µL, 0.613 mmol) at room

temperature. The resulting reaction mixture was allowed to stir overnight at room temperature. Undesired inorganic salts were removed by filtration, the solvent removed to dryness, the residue obtained was purified by SiO_2 gel column chromatography to afford methyl N^{c}-benzyl-N^{α}-(*tert*-butoxycarbonyl)-*L*-histidinate as a yellow sticky oil (218 mg, 99%). ^{1}H NMR (300 MHz, $CDCl_3$) δ (major rotamer) 7.43 (s, 1H, H-2'), 7.33 – 7.29 (m, 5H, **Ph**), 7.12 (d, *J* = 7.7 Hz, 1H, H-5'), 5.91 (br.s, 1H, NH), 5.46 (s, 2H, -C**H$_2$**-Ph), 4.45 – 4.30 (m, 1H, H-2), 3.60 (s, 3H, OC**H$_3$**), 3.05 (dd, *J* = 6.5, 3.7 Hz, 2H, H-3), 1.32 (s, 9H, Boc); ^{13}C NMR (101 MHz, $CDCl_3$) δ (major rotamer) 170.8 (C-1), 155.3 (C=O), 133,1 (**C**(Ph)), 132.7 (C-4'), 131.8 (C-2'), 129.5 (2 x **C**H(Ph meta)), 129.0 (2 x **C**H(Ph orto)), 128.2 (**C**H (Ph para)), 120.6 (C-5'), 80.6 (C(Boc)), 53.5 (O**C**H$_3$), 52.2 (C-2), 51.3 (-**C**H$_2$-Ph), 29.9 (C-3), 28.4 (3C, Boc).

7.2. Total Protein extraction and Purification from *Mycobacterium smegmatis.*[1]

7.2.1. Mc^{2}155 (*M. smegmatis*) growth conditions.

M. smegmatis cultures (800 mL) were grown to exponential phase, and dried to obtain 10 g of dry cells. The obtained pellets of *M. smegmatis* cells were thereafter stored at -80°C until it was required.

7.2.2. Total protein extraction.

M.smeg cells was sonicated for 35 min at 4°C (25 pulses), followed by the addition of potassium phosphate buffer (60 mL; pH 7). The solution was allowed to stir at 4°C for 10 min and thereafter centrifuged at 3000 rpm for 20 min. The supernatant was collected, measured

and the appropriate amount of ammonium sulfate was gradually added while stirring at 4 °C overnight to obtain 60-70% saturation.[20] After precipitation of total protein the suspension was centrifuged at 4°C at 3000 rpm for 20 min and stored at -20°C. A tablet of complete ultra-tablets, EDTA-free, glass vials (Roche ©) containing a cocktail of protease inhibitors was added to preserve the enzymatic activities of the crude enzyme preparation after cell lysis.

7.2.3. Total protein purification.

The total protein ammonium complex salt precipitates were resuspended in a buffer mixture (20 mL, pH 7) containing pyridoxal phosphate (10 mL, 20µM), potassium phosphate buffer (8 mL, 50 mM; pH 7) and (2 mL, 1mM EDTA).

7.2.4. Protein calibration curve

In order to determine the total protein concentration, the protein Dc assay and the Bradford assays were used. The calculated *M. smegmatis* total protein concentration was determined by Bradford assay and was found to be 10.33 µg/µL.

7.3. HPLC –ESI/MS (QTOF) analysis.

Analyses were carried out with a UHPLC Agilent 1290 Infinity Series (Germany), accurate mass spectrometer Agilent 6530 Quadrupole Time Of Flight (QTOF) equipped with an Agilent jet stream ionization source (positive ionization mode) (ESI^+) and column (Polaris 3 C_{18} Ether 100 X 2 mm, particle size 3 µm, Agilent, Germany).

15 µL of concentrate samples were injected into the LCMS. Analyte separation was attempted in 0.1% formic acid in milli-Q water (solvent A) and mixture of 90% acetonitrile, 0.1% formic acid, 10% milli-Q water (solvent B) as mobile phase in an isocratic flow rate of 0.3 mL/min. The system was controlled with the software packages Mass Hunter workstation software (Qualitative and Quantitative version B.05.00; Build 5.0.519.0, Agilent 2011, Germany).

7.4. *In vitro* reconstituted biosynthesis of ergothioneine in *Mycobacterium smegmatis*.[1,21]

The experiments were performed in triplicate, repeated several times (more than three times) and these results were reproducible.

7.4.1. Enzymatic reactions using *M. smegmatis* cell-free lysate enzyme preparation

100 µL reactions containing 20 mM Tris HCl pH= 7.4, 20 mM NaCl, 0.2 mM $FeSO_4.7\ H_2O$, 0.5 mM mercaptoethanol, 83 µL of crude enzymes and 50 mM of the substrates. The crude enzyme reactions were incubated for 1 day at 37 °C. The reaction was stopped by heating the mixture at 90 °C for 2 min followed by lyophilisation and subsequent reconstitution in LC buffer before analysis by LC/MS.

7.4.2. Non-enzymatic cleavage of the C-S bond catalysed by PLP

100 µL reactions containing 20 mM Tris HCl pH= 7.4, and 50 mM of the substrates, and 50 mM of PLP. The non-enzymatic reactions were incubated for 1 day at 37 °C, followed by lyophilisation and subsequent reconstitution in LC buffer before analysis by LC/MS.

7.5. *Mycobacterium smegmatis* Ergothioneine enzymes inhibition by *S*-(β-amino-β-carboxyethyl)ergothioneine sulfone (3.16).

Reactions (100 µL) containing 20 mM Tris HCl pH= 7.4, 20 mM NaCl, 0.2 mM $FeSO_4.7\ H_2O$, 0.5 mM mercaptoethanol, 66 µL of crude enzymes and 50 mM of substrates and *S*-(β-amino-β-carboxyethyl)ergothioneine sulfone **3.16**. The reaction was stopped by heating the mixture at 90 °C for 2 min followed by lyophilisation. The crude enzyme reactions were incubated for 1 day at 37 °C. The reaction was stopped by heating the mixture at 90 °C for 2 min followed by lyophilisation and subsequent reconstitution in LC buffer before analysis by LC/MS.

7.6. Determination of the Minimum Inhibitory Concentration (MIC) (Broth micro-dilution method)[22]

A two-fold serial dilution of the drug was performed across a V-bottom 96 well plate (Lasec) in a volume of 50 µL. An equal volume of exponential mycobacterial culture diluted to 104 CFU/mL was aliquoted in every well except the first row of wells, which serve as the negative control. After incubation for 3-4 days, growth was assessed visually by looking for a white

pellet at the bottom of the well, and 10 µL of 0.02% Resazurin or Alamar blue staining (Sigma Aldrich) was added in every well, as it becomes pink in a reduced environment (caused by oxygen depletion). The MIC is reported as the range between the concentration of the well where 99% of the growth is inhibited and the well just before it (where growth was detected). Results are representatives of at least three biological replicates.

7.7. UV-vis spectroscopy monitoring of the oxidation of thiols in presence of NBS/DMF

7.7.1. Preparation of solutions

A stock solution of phosphate-buffered saline (PBS) 0.01 M, pH 7.4 was freshly prepared and stored at 4 °C until use. Thiol solutions of either cysteine (1 mM) or γ-glutamylcysteine (1 mM) were prepared by dilution in PBS buffer and immediately analyzed by UV-vis spectrophotometer.

To DMF (1 mL) was added NBS (36 mg, 0.2 mmol) in one portion and the resulting solution was allowed to stir at room temperature. An aliquoted 30 µL of the resulting solution was diluted with PBS buffer to reach the final volume of 3 mL solution of NBS/DMF (100x dilution) and was analyzed by UV-vis spectrophotometer. (Control)

7.7.2. Detection of free thiols

To a solution of NBS/DMF (1 mL) prepared as described above, was added the thiol, either cysteine (10 mg, 0.09 mmol) or γ-glutamylcysteine (25 mg, 0.09 mmol) depending on the case. One drop of 1 mM DTNB was added to 30 µL of aliquoted reaction mixture and the resulting solution was diluted with PBS buffer to reach the final volume of 3 mL which was analyzed by UV-vis spectrophotometer at the specific time.

7.7.3. Reduction of disulfides by DTT subsequently followed by free thiols detection.

To 1 mL of a solution of NBS/DMF/cysteine or NBS/DMF/γ-glutamylcysteine prepared as described above, was added 1 mM DTT and the resulting reaction mixture was allowed to stir at room temperature. 5 min or one hr later, one drop of 1 mM DTNB was added and the resulting reaction mixture was diluted with PBS buffer to reach a final volume of 3 mL which was analyzed by UV-vis spectrophotometer.

7.8. References

1 Khonde, P. L. & Jardine, A. Improved synthesis of the super antioxidant, ergothioneine, and its biosynthetic pathway intermediates. *Organic & biomolecular chemistry* **13**, 1415-1419, doi:10.1039/c4ob02023e (2015).

2 Rostami, A., Hassanian, F., Ghorbani-Choghamarani, A. & Saadati, S. Selective Oxidation of Sulfides to Sulfoxides using H_2O_2Catalyzed by p-Toluenesulfonic Acid (p-TsOH) Under Solvent-Free Conditions. *Phosphorus, Sulfur, and Silicon and the Related Elements* **188**, 833-838, doi:10.1080/10426507.2012.710681 (2013).

3 Rostami, A. & Akradi, J. A highly efficient, green, rapid, and chemoselective oxidation of sulfides using hydrogen peroxide and boric acid as the catalyst under solvent-free conditions. *Tetrahedron Letters* **51**, 3501-3503, doi:10.1016/j.tetlet.2010.04.103 (2010).

4 Fukushima, N. *et al.* Synthesis of a photocontrollable hydrogen sulfide donor using ketoprofenate photocages. *Chemical communications* **50**, 587--589 doi:10.1039/c3cc47421f (2014).

5 Miroslav Trampota. Process for the synthesis of L-(+)-ergothioneine US 7,767,826 B2 (**2010**).

6 Yadan, J. C. & Jinzhu Xu, J. Process for the preparation of ergothioneine US005438151A (**1995**).

7 Erdelmeier, I., Daunay, S., Lebel, R., Farescour, L. & Yadan, J.-C. Cysteine as a sustainable sulfur reagent for the protecting-group-free synthesis of sulfur-containing amino acids: biomimetic synthesis of l-ergothioneine in water. *Green Chemistry* **14**, 2256, doi:10.1039/c2gc35367a (2012).

8 Jardine, M. A. & Khonde, L. P. Process for synthesizing ergothioneine and related compounds WO 2016/046618 A1 (**2016**).

9 Reinhold, V. N., Ishikawa, Y. & Melville, D. B. Synthesis of α-N-methylated histidines. *Journal of medicinal chemistry* **11**, 258 (1968).

10 Song, H., Leninger, M., Lee, N. & Liu, P. Regioselectivity of the Oxidative C-SBond Formation in Ergothioneine and Ovothiol Biosyntheses. *Organic letters* **15, No. 18**, 4854–4857 (2013).

11 Fattori, D. *et al.* Design and Synthesis of Novel Sulfonamide-Containing Bradykinin hB2 Receptor Antagonists. 2. Synthesis and Structure-Activity Relationships of r,r-Cycloalkylglycine Sulfonamides. *Journal of medicinal chemistry* **50**, 550 (2007).

12 Crosignani, S., White, P. D. & Linclau, B. Polymer-Supported O-Alkylisoureas: Useful Reagents for the O-Alkylation of Carboxylic Acids. *Journal of Organic Chemistry* **69**, 5897-5905 (2004).

13 Lidia, L. D., Giacomelli, G. & Porcheddu, A. An Efficient Route to Alkyl Chlorides from Alcohols Using the Complex TCT/DMF. *Organic letters* **4**, 553-555 (2002).

14 Jia, Y. *et al.* The synthesis and biological evaluation of novel Danshensu-cysteine analog conjugates as cardiovascular-protective agents. *European journal of medicinal chemistry* **55**, 176-187, doi:10.1016/j.ejmech.2012.07.016 (2012).

15 Maldonado, P. D. *et al.* Role of allyl group in the hydroxyl and peroxyl radical scavenging activity of S-allylcysteine. *The journal of physical chemistry. B* **115**, 13408-13417, doi:10.1021/jp208233f (2011).

16 Hooper, K. C., Rydon, H. N., Schofield J. A. & S., H. G. Polypeptides. Part 11. The Preparation of Some Protected Peptides of Cysteine and Glycine. *Journal of Chemical Society*, 3148-3156 (1956).

17 Mirzahosseini, A., Sándor Hosztafi, S., Tóth, G. & Noszála, B. A cost-effective synthesis of enantiopure ovothiol A from L-histidine, its natural precursor. *ARKIVOC* **vii**, 1 (2014).

18 Abdo, M. R. *et al.* Brucella suis histidinol dehydrogenase: synthesis and inhibition studies of a series of substituted benzylic ketones derived from histidine. *Bioorganic & medicinal chemistry* **15**, 4427-4433, doi:10.1016/j.bmc.2007.04.027 (2007).

19 Halland, N. An Atom-Efficient Direct Regioselective N(τ)-Allylation of Histidine Derivatives. *Synlett* **23,** , 2969–2971, doi:10.1055/s-0032-1317669 (2012).

20 El-Sayed, A. S. Purification and characterization of a new L-methioninase from solid cultures of Aspergillus flavipes. *Journal of microbiology* **49**, 130-140, doi:10.1007/s12275-011-0259-2 (2011).

21 Seebeck, F. P. In Vitro Reconstitution of Mycobacterial Ergothioneine Biosynthesis. *Journal of American Chemical Society* **132**, 6632 (2010).

22 Wallace, J. R., Nash, R. D., Steele, C. L. & Steingrube, V. Susceptibility Testing of Slowly Growing Mycobacteria by a Microdilution MIC Method with 7H9 Broth. *Journal of Clinical Microbiology* **24**, 976-981 (1986).